



## Durham E-Theses

---

### *A study of transition metal compounds in liquid hydrogen chloride*

Symon, David Allen

#### How to cite:

---

Symon, David Allen (1972) *A study of transition metal compounds in liquid hydrogen chloride*, Durham theses, Durham University. Available at Durham E-Theses Online: <http://etheses.dur.ac.uk/9115/>

#### Use policy

---

The full-text may be used and/or reproduced, and given to third parties in any format or medium, without prior permission or charge, for personal research or study, educational, or not-for-profit purposes provided that:

- a full bibliographic reference is made to the original source
- a [link](#) is made to the metadata record in Durham E-Theses
- the full-text is not changed in any way

The full-text must not be sold in any format or medium without the formal permission of the copyright holders.

Please consult the [full Durham E-Theses policy](#) for further details.

To Tina

## INDEX

PREFACE	i
ACKNOWLEDGEMENTS	ii
SUMMARY	iii
CHAPTER I INTRODUCTION	1
1.1.1 Non-Aqueous Solvents	1
1.1.2 History	2
1.1.3 Theory of the Solvent	9
1.2 Protonation of neutral transition metal complexes	14
1.2.1 History	14
CHAPTER 2 EXPERIMENTAL TECHNIQUES	18
2.1 The Vacuum System	18
2.2 Apparatus	23
2.3 Inert Atmosphere Glove Box Techniques	29
2.4 Determination of physical properties	30
2.4.1 Infrared spectra	30
2.4.2 <sup>1</sup> H Nuclear Magnetic resonance studies	42
2.4.3 Ultra violet/visible spectra	45
2.4.4 <sup>57</sup> Fe Mossbauer studies	45
2.4.5 Electron spectroscopy studies	45
2.5 Analytical techniques	46
2.5.1 Estimation of carbon, hydrogen and nitrogen	46
2.5.2 Estimation of chlorine, bromine and iodine	46
2.5.3 Estimation of iron	47
2.5.4 Estimation of phosphorus	47
2.6 Preparation and purification of reagents	47
2.6.1 Hydrogen chloride	47
2.6.2 Boron trichloride	49

## CHAPTER 2

2.6.3 Phosphorus pentafluoride	49
2.6.4 Chlorine	50
2.6.5 Nitrosyl chloride	51
2.6.6 Deuterium Chloride	51
2.6.7 Sulphur dioxide	51
2.6.8 Bis( $\pi$ -cyclopentadienyldicarbonyl iron (I))	52
2.6.9 $\pi$ -cyclopentadienyldicarbonyl iron(II) chloride	53
2.6.10 $\pi$ -cyclopentadienyldicarbonyl iron(II) bromide	53
2.6.11 $\pi$ -cyclopentadienyldicarbonyl iron(II) iodide	53
2.6.12 $\pi$ -cyclopentadienyltricarbonyl iron(II) chloride	54
2.6.13 $\pi$ -cyclopentadienyldicarbonyl iron $\sigma$ -methyl	54
2.6.14 Tetrakis( $\pi$ -cyclopentadienylcarbonyl iron(I))	55
2.6.15 Tetracarbonyl iron dibromide	57
2.6.16 Tetracarbonyl iron di-iodide	61

## CHAPTER 3 REACTIONS OF BIS( $\pi$ -CYCLOPENTADIENYLDICARBONYL IRON(I)) IN LIQUID HYDROGEN CHLORIDE

3.1 Introduction	62
3.2 Results and Discussion	62
3.3 Experimental	77

## CHAPTER 4 REACTIONS OF $\pi$ -CYCLOPENTADIENYLDICARBONYL IRON(II) HALIDES (CHLORIDE, BROMIDE AND IODIDE) AND OF $\pi$ -CYCLOPENTADIENYLTRICARBONYL IRON(II) CHLORIDE IN LIQUID HYDROGEN CHLORIDE

4.1 Results and Discussion	85
4.2 Experimental	90

CHAPTER 5	REACTIONS OF TETRAKIS( $\pi$ -CYCLOPENTADIENYLCARBONYL IRON(I))	99
	5.1 Results and Discussion	99
	5.2 Experimental	114
CHAPTER 6	STUDIES ON THE $\pi$ -CYCLOPENTADIENYLDICARBONYL IRON - $\mu$ -HALOGEN $\pi$ -CYCLOPENTADIENYLDICARBONYL IRON CATIONS, [ $(\pi\text{-C}_5\text{H}_5\text{)Fe(CO)}_2$ ] $_2\text{X}^+$ , X = Cl, Br, or I.	120
	6.1 Results and Discussion	120
	6.2 Experimental Section	138
CHAPTER 7	ELECTRON SPECTROSCOPY AND $^{57}\text{Fe}$ MOSSBAUER SPECTROSCOPY	140
	7.1 Electron spectroscopy	140
	7.1.1 Introduction	140
	7.1.2 Results and discussion	151
	7.2 $^{57}\text{Fe}$ Mossbauer Spectroscopy	168
	7.2.1 Introduction	168
	7.2.2 Results and discussion	171
CHAPTER 8	FAR INFRARED SPECTRAL STUDIES	186
	8.1 Introduction	186
	8.1.1 Advantages of interferometry over conventional spectroscopic techniques	187
	8.1.2 Theory	191
	8.1.3 Instrumentation	196
	8.1.4 Computation	197
	8.2 Results and discussion	201
	8.2.1 Examination of water vapour spectrum	201
	8.2.2 Metal carbonyl halides	212
	8.2.3 $\pi$ -cyclopentadienylcarbonyl iron complexes	223

CHAPTER 9	CONCLUSIONS AND FUTURE WORK	231
9.1	Acid-base reactions	231
9.2	Oxidation reactions	232
9.3	Structure of the $\pi$ -cyclopentadienyldicarbonyl iron- $\mu$ -halogeno $\pi$ -cyclopentadienyldicarbonyl iron cations.	232
9.4	Techniques available	
9.4.1	Infrared spectroscopy	233
9.4.2	<sup>57</sup> Fe Mossbauer Spectroscopy	234
9.4.3	uv/visible spectroscopy	234
APPENDIX A.	Computer program for storing data from paper tapes obtained from FS-720	236
	Fourier transform program	239
	Graph Plotter program	269
APPENDIX B.	ESTIMATION OF PHOSPHORUS	277
APPENDIX C.	MAGNETO CHEMISTRY OF THE TETRAKIS( $\pi$ -CYCLOPENTADIENYL CARBONYL IRON) CATION	280
REFERENCES		283
PRELIMINARY X-RAY CRYSTAL STRUCTURE DATA		290

## INDEX OF ILLUSTRATIONS

Figure	2.1	The Vacuum System	19
Plate	2.1	The Vacuum System	20
Figure	2.2	Rotaflo TF6/13 ampoules	24
Figure	2.3	Reaction Vessel	24
Figure	2.4	Rotaflo TF6/24 Reaction Vessel	24
Figure	2.5	Silica Ampoule	26
Figure	2.6	Ampoule Breaker	26
Figure	2.7	Ampoule Breaker in use	26
Figure	2.8	Conductivity Cells	28
Figure	2.9	Infrared Gas Cell	31
Figure	2.10	Disc Press	33
Plate	2.2	Disc Press	33
Plate	2.3A	Isolation Cell (Assembled View)	35
Plate	2.3B	Isolation Cell (Exploded View)	36
Plate	2.4	Isolation Cell	37
Plate	2.5A	Low Temperature Cell (Assembled View)	38
Plate	2.5B	Low Temperature Cell (Exploded View)	39
Figure	2.11	Low Temperature Cell	40
Figure	2.12	Silica nmr tubes	43
Plate	2.6	Organometallic compounds in liquid HCl	44
Spectrum	2.1	Bis( $\pi$ -cyclopentadienyldicarbonyl iron(I))	58
Spectrum	2.2	Bis( $\pi$ -cyclopentadienyldicarbonyl iron(I))	58
Spectrum	2.3	Bis( $\pi$ -cyclopentadienyldicarbonyl iron(I))	59
Spectrum	2.4	Bis( $\pi$ -cyclopentadienyldicarbonyl iron(I))	59
Spectrum	2.5	Bis( $\pi$ -cyclopentadienyldicarbonyl iron(I)) (Photolysis intermediate)	60

Spectrum	2.6	Tetrakis( $\pi$ -cyclopentadienylcarbonyl iron(I))	60
Figure	3.1	Conductimetric titration of Bis( $\pi$ -cyclopentadienyldicarbonyl iron(I)) with Boron trichloride	65
Spectrum	3.1	$\pi$ -cyclopentadienyldicarbonyl iron- $\mu$ -hydrogen $\pi$ -cyclopentadienyldicarbonyl iron tetrachloroborate	68a
Spectrum	3.2	$\pi$ -cyclopentadienyldicarbonyl iron- $\mu$ -hydrogen $\pi$ -cyclopentadienyldicarbonyl iron hexafluorophosphate	68a
Spectrum	3.3	$\pi$ -cyclopentadienyltricarbonyl iron(II) hexafluorophosphate	68b
Structures	I-VIII	Structures of the $[(\pi\text{-C}_5\text{H}_5)\text{Fe}(\text{CO})_2]_2\text{X}^+$ cations (X - H, Cl, Brand I).	71
Figure	3.2	Decomposition of $\pi$ -cyclopentadienyldi- carbonyl iron- $\mu$ -hydrogen $\pi$ -cyclopentadienyldi- carbonyl iron hexafluorophosphate	72
Figure	4.1	Conductimetric titration of $\pi$ -cyclopentadienyldi- carbonyl iron chloride with boron trichloride	86
Spectrum	4.1	$\pi$ -cyclopentadienyldicarbonyl iron- $\mu$ - chloro $\pi$ -cyclopentadienyldicarbonyl iron hexafluorophosphate	86
Spectrum	4.2	$\pi$ -cyclopentadienyldicarbonyl iron(II) chloride in sulphuric acid	91
Spectrum	4.3	$\pi$ -cyclopentadienyldicarbonyl iron(II) bromide in sulphuric acid	92
Spectrum	4.4	$\pi$ -cyclopentadienyldicarbonyl iron (II) iodide in sulphuric acid	93a
Spectrum	4.5	$\pi$ -cyclopentadienyltricarbonyl iron(II) tetrachloroborate	93b
Figure	5.1	Conductimetric titration of Tetrakis ( $\pi$ -cyclopentadienylcarbonyl iron(I)) with boron trichloride	

Spectrum	5.1	Tetrakis ( $\pi$ -cyclopentadienylcarbonyl iron(I)) dihydrogen Tetrachloroborate	103a
Spectrum	5.2	Tetrakis( $\pi$ -cyclopentadienylcarbonyl iron(I)) bis(boron trichloride)	
Spectrum	5.3	Tetrakis( $\pi$ -cyclopentadienylcarbonyl iron(I)) hexafluorophosphate	111b
Spectrum	5.4	Tetrakis( $\pi$ -cyclopentadienylcarbonyl iron(I)) tribromide	111b
Spectrum	5.5	Tetrakis( $\pi$ -cyclopentadienylcarbonyl iron(I)) heptaiodide	
Spectrum	6.1	$\pi$ -cyclopentadienyldicarbonyl iron- $\mu$ -chloro $\pi$ -cyclopentadienyldicarbonyl iron hexafluorophosphate	123
Spectrum	6.2	$\pi$ -cyclopentadienyldicarbonyl iron- $\mu$ -chloro $\pi$ -cyclopentadienyldicarbonyl iron hexafluorophosphate	124
Spectrum	6.3	$\pi$ -cyclopentadienyldicarbonyl iron- $\mu$ -bromo $\pi$ -cyclopentadienyl dicarbonyl iron hexafluorophosphate	125
Spectrum	6.4	$\pi$ -cyclopentadienyldicarbonyl iron- $\mu$ -bromo $\pi$ -cyclopentadienyl dicarbonyl iron hexafluorophosphate	126
Spectrum	6.5	$\pi$ -cyclopentadienyldicarbonyl iron- $\mu$ -iodo $\pi$ -cyclopentadienyl dicarbonyl iron hexafluorophosphate	127
Spectrum	6.6	$\pi$ -cyclopentadienyldicarbonyl iron- $\mu$ -iodo $\pi$ -cyclopentadienyldicarbonyl iron hexafluorophosphate	128
Spectrum	6.7	$\pi$ -cyclopentadienyldicarbonyl iron- $\mu$ -chloro $\pi$ -cyclopentadienyldicarbonyl iron hexafluorophosphate	133

Spectrum	6.8	Thermal decomposition product of $\pi$ -cyclopentadienyldicarbonyl iron- $\mu$ -chloro $\pi$ -cyclopentadienyl dicarbonyl iron hexafluorophosphate	133
Spectrum	6.9	$\pi$ -cyclopentadienyldicarbonyl iron- $\mu$ -bromo- $\pi$ -cyclopentadienyl dicarbonyl iron hexafluorophosphate	134
Spectrum	6.10	Thermal decomposition product of $\pi$ -cyclopentadienyl dicarbonyl iron- $\mu$ -bromo $\pi$ -cyclopentadienyl dicarbonyl iron hexafluorophosphate	134
Spectrum	6.11	$\pi$ -cyclopentadienyldicarbonyl iron- $\mu$ -iodo $\pi$ -cyclopentadienyl dicarbonyl iron hexafluorophosphate	135
Spectrum	6.12	Thermal decomposition product of $\pi$ -cyclopentadienyl dicarbonyl iron- $\mu$ -iodo $\pi$ -cyclopentadienyl dicarbonyl iron hexafluorophosphate	135
Figure	7.1	Basic processes in electron Spectroscopy	142
Figure	7.2	Photo ionisation of an electrical insulator	144
Figure	7.3	Electron relaxation	145
Spectrum	7.1	Bis( $\pi$ -cyclopentadienyldicarbonyl iron(I))	160
Spectrum	7.2	$\pi$ -cyclopentadienyldicarbonyl iron(II) chloride	161
Spectrum	7.3	$\pi$ -cyclopentadienyldicarbonyl iron(II) iodide	162
Spectrum	7.4	$\pi$ -cyclopentadienyldicarbonyl iron- $\mu$ -chloro- $\pi$ -cyclopentadienyldicarbonyl iron hexafluorophosphate	163
Spectrum	7.5	$\pi$ -cyclopentadienyldicarbonyl iron- $\mu$ -bromo $\pi$ -cyclopentadienyl dicarbonyl iron hexafluorophosphate	164
Spectrum	7.6	$\pi$ -cyclopentadienyldicarbonyl iron- $\mu$ -iodo $\pi$ -cyclopentadienyldicarbonyl iron hexafluorophosphate	165

Spectrum	7.7	Tetrakis( $\pi$ -cyclopentadienylcarbonyl iron(1))	166
Spectrum	7.8	Tetrakis( $\pi$ -cyclopentadienylcarbonyl iron) hexafluoro-phosphate	167
Spectrum	7.9	$\pi$ -cyclopentadienyl dicarbonyl iron- $\mu$ -hydrogen $\pi$ -cyclopentadienyldicarbonyl iron hexafluoro-phosphate	179
Spectrum	7.10	$\pi$ -cyclopentadienyldicarbonyl iron- $\mu$ -chloro $\pi$ -cyclopentadienyl dicarbonyl iron hexafluoro-phosphate	180
Spectrum	7.11	$\pi$ -cyclopentadienyldicarbonyl iron- $\mu$ -bromo $\pi$ -cyclopentadienyl dicarbonyl iron hexafluoro-phosphate	181
Spectrum	7.12	$\pi$ -cyclopentadienyldicarbonyl iron- $\mu$ -iodo $\pi$ -cyclopentadienyl dicarbonyl iron hexafluoro-phosphate	182
Spectrum	7.13	Tetrakis( $\pi$ -cyclopentadienyl carbonyl iron) hexafluorophosphate	183
Spectrum	7.14	Tetrakis( $\pi$ -cyclopentadienylcarbonyl iron) hexafluorophosphate	184
Spectrum	7.15	Tetrakis( $\pi$ -cyclopentadienyl carbonyl iron(1))	185
Figure	8.1	Efficiencies of beam splitters	189
Spectrum	8.1	FS-720 Instrumental background	202
Spectrum	8.2	Water vapour	203
Spectrum	8.3	Water vapour	204
Spectrum	8.4	Water vapour	205
Spectrum	8.5	Water vapour	206
Spectrum	8.6A	Water vapour	207
Spectrum	8.6B	Water vapour	208
Spectrum	8.7A	Water vapour	209
Spectrum	8.7B	Water vapour	210
Spectrum	8.7C	Water vapour	211

Spectrum	8.8	Tetracarbonyldibromo iron(II)	215
Spectrum	8.9	Tetracarbonyldi-iodo iron(II)	216
Spectrum	8.10	$\pi$ -cyclopentadienyldicarbonyl iron(II) chloride	217
Spectrum	8.11	$\pi$ -cyclopentadienyldicarbonyl iron(II) bromide	218
Spectrum	8.12	$\pi$ -cyclopentadienyldicarbonyl iron(II) iodide	219
Spectrum	8.13	$\pi$ -cyclopentadienyl dicarbonyl iron- $\mu$ -chloro $\pi$ -cyclopentadienyl dicarbonyl iron hexafluoro- phosphate	220
Spectrum	8.14	$\pi$ -cyclopentadienyldicarbonyl iron- $\mu$ -bromo $\pi$ -cyclopentadienyldicarbonyl iron hexafluoro- phosphate	221
Spectrum	8.15	$\pi$ -cyclopentadienyldicarbonyl iron- $\mu$ -iodo $\pi$ -cyclopentadienyldicarbonyl iron hexafluoro- phosphate	222
Spectrum	8.16	Bis( $\pi$ -cyclopentadienyl dicarbonyl iron(I))	226
Spectrum	8.17	Tetrakis( $\pi$ -cyclopentadienylcarbonyl iron(I))	227
Spectrum	8.18	Tetrakis( $\pi$ -cyclopentadienylcarbonyl iron) hexafluorophosphate	228
Spectrum	8.19	Tetrakis( $\pi$ -cyclopentadienylcarbonyl iron) hepta-iodide	229
Spectrum	8.20	Tetrakis( $\pi$ -cyclopentadienylcarbonyl iron) tribromide	230

PREFACE

The work described in this thesis is original, except in those portions where it is specifically stated to the contrary. It has not been submitted, either wholly, or in part, for a degree at this, or at any other university.

David . H. Symon

### ACKNOWLEDGEMENTS

The author wishes to thank Professor T.C. Waddington for his supervision, advice and encouragement throughout the course of the work. The author also appreciated the assistance provided by the Members of the Department, Technical staff, and Members of the Computer Unit, especially to Dr. C.J. Ludman for his valuable advice and interest in the work and to Mr. J. Dunn for all his practical assistance.

Thanks are also due to the Universities of Warwick and Durham for maintenance grants.

SUMMARY

The behaviour of some transition metal compounds in liquid hydrogen chloride has been examined. Previous work has established that both protonation and oxidation studies can be carried out in the solvent. The present work has shown that  $\pi$ -cyclopentadienylcarbonyl metal compounds can act as bases in the solvent. The structure of the products isolated was deduced from infrared,  $^{57}\text{Fe}$  Mossbauer and other spectroscopic techniques.

Hydrogen chloride and other volatile compounds were handled in a conventional vacuum system and reactions were carried out in detachable glass cells or in sealed silica ampoules. The reactions were followed by conductimetric techniques where possible. Characterisation of the products obtained was by chemical analysis, by the change of weight occurring during the reaction and by spectroscopic techniques.

Bis( $\pi$ -cyclopentadienyldicarbonyl iron(I)) had previously been shown to act as a base in sulphuric acid. Reaction with boron trichloride and phosphorus pentafluoride in the solvent resulted in isolation of the  $\pi$ -cyclopentadienyldicarbonyl iron- $\mu$ -hydrogen  $\pi$ -cyclopentadienyldicarbonyl iron cation as its tetrachloroborate and hexafluorophosphate salts respectively. In the presence of light over prolonged periods hydrogen chloride was observed to add to the iron-iron bond in bis( $\pi$ -cyclopentadienyldicarbonyl iron(I)). Oxidations with chlorine resulted in mixtures of cyclopentadienylcarbonyl iron halides and other products being obtained.

$\pi$ -cyclopentadienyldicarbonyl iron(II) chloride was observed to act as a base towards boron trichloride to give  $\pi$ -cyclopentadienyldicarbonyl iron- $\mu$ -chloro  $\pi$ -cyclopentadienyldicarbonyl iron tetrachloroborate.  $\pi$ -cyclopenta-



dienyldicarbonyl iron(II) bromide and  $\pi$ -cyclopentadienyldicarbonyl iron(II) iodide dissolved in liquid hydrogen chloride without solvolysis taking place.

Tetrakis( $\pi$ -cyclopentadienylcarbonyl iron(I)) dissolved in hydrogen chloride and in the presence of boron trichloride two protons were taken up. Phosphorus pentafluoride oxidised the complex to the mono-cation. This was the first observation of phosphorus pentafluoride acting as an oxidant in hydrogen chloride.

The  $\pi$ -cyclopentadienyldicarbonyl iron- $\mu$ -halogeno  $\pi$ -cyclopentadienyldicarbonyl iron cations (halogeno = chloro, bromo or iodo) were prepared by two new routes, and an examination of their infrared,  $^{57}\text{Fe}$  Mossbauer and electron spectra carried out in order to deduce information about their structure. The compounds were found to have symmetrical Fe-X-Fe (X = Cl, Br and I) bonds which were bent. The two iron atoms were found to be in identical chemical environments. The far infrared spectra of the compounds were examined and asymmetric metal halogen stretching frequencies assigned.

The tetrakis( $\pi$ -cyclopentadienylcarbonyl iron) compound were also examined by several physical techniques and structures suggested for the products observed. Evidence from  $^{57}\text{Fe}$  Mossbauer studies showed that the iron atoms remained equivalent on oxidation and protonation.

A STUDY OF TRANSITION METAL COMPOUNDS  
IN LIQUID HYDROGEN CHLORIDE

by

DAVID ALLEN SYMON, A.R.I.C.  
Graduate Society

A thesis submitted in part fulfilment of the requirements  
for the degree of Doctor of Philosophy in the University of Durham

July 1972



## CHAPTER 1

### INTRODUCTION

The work described in this thesis has been divided into two main sections. The first section deals with studies of the reactions of transition metal organometallic compounds when dissolved in liquid hydrogen chloride. The second section deals with the examination of the products formed in the liquid hydrogen chloride studies using several physical techniques, for example  $^{57}\text{Fe}$  Mossbauer spectroscopy, fourier transform far infrared spectroscopy and electron spectroscopy. Far infrared spectroscopy was found to be an extremely useful technique when examining compounds containing a metal-halogen bond. Related compounds were also studied in order that adsorption bands could be assigned with some degree of certainty.

#### 1.1.1. Non-Aqueous Solvents

After a rather late beginning and an unsteady development the study of non-aqueous solvent systems has now become a well established branch of inorganic chemistry. Many of the earlier studies attempted to show the similarities and differences between the chemistry of aqueous and non-aqueous solutions. Although the results of these studies have shown that all solvent systems have fundamental similarities, water is outstanding in its solvent properties. Although some work is still being carried out in an attempt to understand the modes of ionisation of some solvents the majority of current research has as its main aim the utilization of this extremely useful and powerful preparative technique.

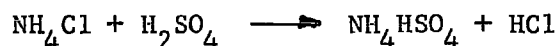
Non-aqueous solvent systems have been reviewed by several authors including Addison (1), Audrieth and Kleinberg (2), Drago and Purcell (3),



Emeleus and Anderson (4), and Gutmann (5). The theory of how dissociation and self-ionization phenomena in non-aqueous solvents should be interpreted are discussed by Drago (6) and Gutmann (7). Introductory texts to non-aqueous solvent chemistry by Waddington (8) and Jander and Lafrenz (9) give the newcomer an excellent background but for the established worker the collection of reviews giving a modern critical assessment of selected solvents by Waddington (10) is to be highly recommended.

### 1.1.2. History

The solvent properties of liquid hydrogen chloride were first studied by Gore (11) over a century ago. Gore prepared the hydrogen chloride used in his studies in an enclosed system from the reaction of ammonium chloride and sulphuric acid.



The experiments that Gore carried out were confined to observing visually any reaction between the liquid hydrogen chloride and mainly simple inorganic materials. Only ten materials of the sixty six examined dissolved and Gore concluded that "liquid hydrogen chloride has but a feeble solvent power for solid bodies in general". It was not until after 1900 that any systematic work on the liquid hydrogen chloride solvent system was carried out. The low temperatures required for handling the solvent (about  $-100^\circ\text{C}$ ) severely restricted the work since only limited supplies of liquid air and solid carbon dioxide were available. The results of the experiments are summarised and discussed in a lengthy paper (12) which is divided into four sections each complete in itself. The paper describes work meticulously carried out under very difficult practical conditions. The first section describes

the physical and thermodynamic properties of the hydrogen halides. Solubility, conductivity and ebullioscopic studies are dealt with in the second section. The third section deals with transport numbers in liquid hydrogen bromide. Hydrogen bromide was chosen because of the relative ease of maintaining a temperature where the solvent had less than one atmosphere pressure and was in the liquid state. For these studies a slurry of solid carbon dioxide and ether was used which gives a temperature of  $-81^{\circ}\text{C}$ . The final section sets out the results but the authors were unable to correlate dissolving power, dielectric constant, conductivity and deviations in molecular weight determinations.

Research in this solvent ceased after 1912, except for a few isolated experiments, until 1958 when Klanberg and Waddington (13)-(17) started a systematic study. These authors had a tremendous advantage over previous workers due to the facts that vacuum techniques and cryogenics were readily available; also considerable experience and knowledge of the handling of volatile, low dielectric solvents with rigorous exclusion of moisture had been gained in the previous two or three decades. The initial studies consisted of an examination of the conductance of various materials, primarily the halides of Groups III, IV and V in the solvent (15). Classification of the materials soluble in the solvent was put into three categories:

(i) Strong solvo bases, e.g. tetramethylammonium chloride and phosphorus pentachloride.

(ii) Medium strong solvo bases, e.g. acetyl chloride and tetraethylammonium chloride.

(iii) Weak solvo acids, e.g. boron trichloride and chlorosulphonic acid.

together with neutralisation reactions which had been followed conductimetrically were reported in a second paper (16). At about this time hydrogen bromide and hydrogen iodide were also being investigated as non-aqueous solvents (18,19). Comparisons were made between them and hydrogen chloride and hydrogen fluoride. The reactions studied in the higher hydrogen halides were mainly restricted to the acid-base type, information being obtained from conductimetric titrations and from infrared spectroscopy.

Conductimetric techniques were extensively utilised by Peach and Waddington in their studies of elements of Groups IV, V and VI (20); and compounds containing multiple bonds as solvo bases (21). An extension of the work on sulphur compounds, along with the examination of some selenium and tellurium compounds has recently been published (22).

Fuoss and Kraus (23) found that for solvents of low dielectric constant a plot of  $\log \Lambda$  against  $\log C$  showed a minimum which moved to higher concentration as the dielectric constant of the medium increased. For aqueous solutions this minimum occurred at too high a concentration to be observed. Archibald, McIntosh and Steele's work on the variation of equivalent conductivity with concentration (12) was extended (19,24) and the Fuoss and Kraus theory applied to the solvent. The theory of Fuoss and Kraus predicts a minimum at  $2 \times 10^{-2} M$  for a solvent of dielectric constant 9. Peach and Waddington (24) found that the minimum occurred at about  $10^{-2} M$  for liquid hydrogen chloride solutions; liquid hydrogen chloride has a dielectric constant of 9.3.

Non-metallic fluorides were examined in the solvent (25) and were divided into four categories based upon the type of reaction observed:

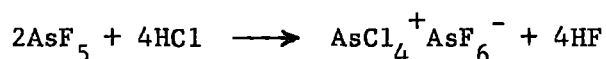
(i) no reaction e.g. silicon tetrafluoride and phosphorus trifluoride

(ii) total solvolysis e.g. arsenic trifluoride and antimony trifluoride

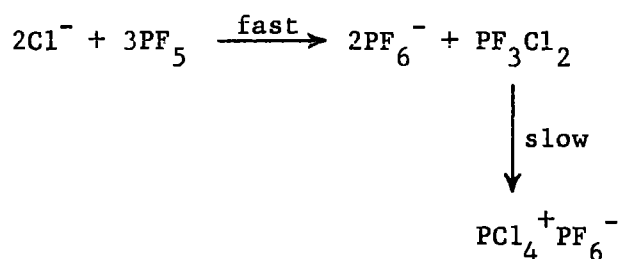
(iii) disproportionation e.g. phosphorus pentafluoride and arsenic pentafluoride

(iv) chlorofluoro anion formation e.g. boron trifluoride.

In category (iii) the reaction of arsenic pentafluoride gives tetrachloroarsonium hexafluoroarsenate thus:



whereas phosphorus pentafluoride disproportionates only in the presence of strong bases and does not produce free hydrogen fluoride thus:

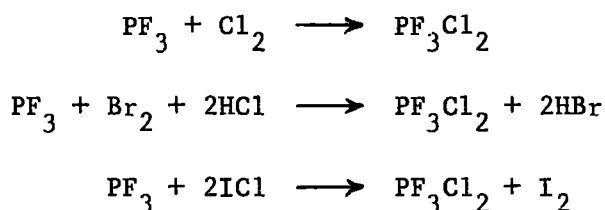


Conductimetric titrations using phosphorus pentafluoride as an acid show a break at the 1.5:1 (acid:base) molar ratio when salt formation occurs but at the 1:1 molar ratio when an adduct is produced. This enables salt formation and adduct formation to be readily distinguished.

Work in the solvent was then extended to include studies of oxidation-reduction systems. The first study consisted of an examination of the reaction of halogens with halide ions (26), polyhalide ions of the type  $\text{AB}_2^-$  being produced. The only exception being the reaction of chlorine

with iodine gave the  $\text{ICl}_4^-$  as the final product.

Phosphorus (III) compounds were shown to be oxidised to phosphorus(V) compounds by chlorine, bromine and iodine monochloride (27). The ions  $\text{PCl}_3\text{Br}^+$  and  $(\text{C}_6\text{H}_5)_3\text{PCl}^+$  were formed and stabilized as the tetrachloroborate salts. In the studies on phosphorus trifluoride, the final product of oxidation by chlorine, bromine and iodine monochloride was dichlorotrifluorophosphorane:

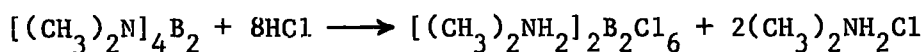


Dichlorotrifluorophosphorane slowly changes from the molecular form to the ionic form when dissolved in the solvent.



The above reactions were studied visually in cases where both the starting material and the resultant product were molecular species, and hence could not be followed by conductimetric techniques.

The work previously carried out on boron compounds (15,16) was extended (28). This work assessed the relative Lewis acidity of several boron compounds. Diborontetrachloride was shown to form the hexachlorodiborate ion,  $\text{B}_2\text{Cl}_6^{2-}$  quantitatively and some evidence for the formation of the trichloromethylborate ion,  $\text{CH}_3\text{BCl}_3^-$  was reported. Diborane, triethylboron and dimethylboron chloride failed to act as solvo acids in the solvent, and tetra(dimethylamino)diboron was solvolysed.

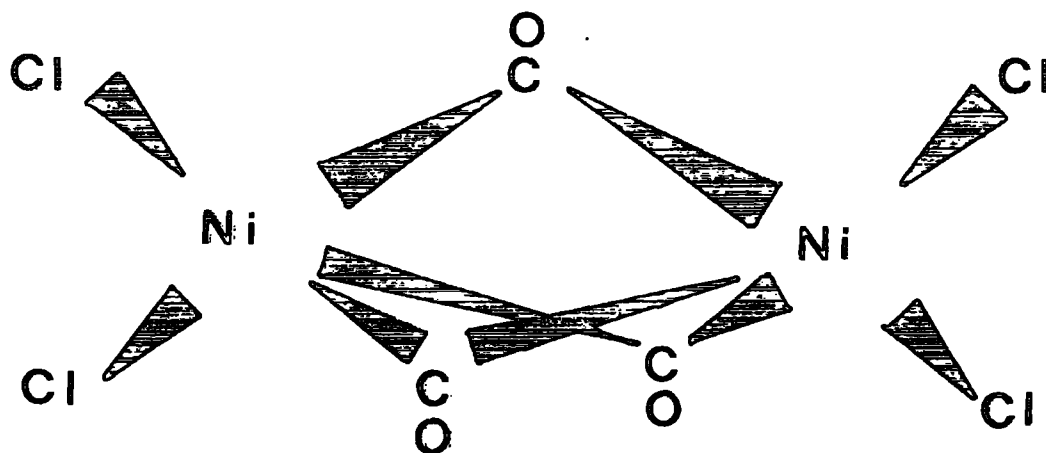


The work in liquid hydrogen chloride had been concerned with the main group elements and the logical extension was to examine the behaviour of some transition metal compounds in the solvent. Iron pentacarbonyl had been examined in sulphuric acid and in  $\text{BF}_3 \cdot \text{H}_2\text{O} - \text{CF}_3\text{CO}_2\text{H}$  solution and evidence for the formation of an Fe-H bond was obtained from  $^1\text{H}$  nuclear magnetic resonance studies (29). No solid products were obtained. In the case of iron pentacarbonyl dissolved in sulphuric acid a green solution was observed which decomposed violently.

Iqbal and Waddington (30) investigated the behaviour of iron pentacarbonyl in liquid hydrogen chloride and found that iron pentacarbonyl dissolved readily, without loss of carbon monoxide, to give a conducting solution. Reaction with the solvo acids boron trichloride and phosphorus pentafluoride gave the tetrachloroborate and hexafluorophosphate salts respectively of the hydrogen pentacarbonyl iron cation,  $\text{Fe}(\text{CO})_5\text{H}^+$ . The salts formed were observed to decompose fairly rapidly at room temperature. Oxidation of solutions of iron pentacarbonyl in the solvent with chlorine, bromine and nitrosyl chloride resulted in the formation of the cations  $\text{Fe}(\text{CO})_5\text{X}^+$ , where X is Cl, Br and NO respectively.

The  $\text{Fe}(\text{CO})_5\text{X}^+$  ions (X = Cl, Br and NO) were all diamagnetic and belonged to point groups  $\text{C}_{4v}$ . The infrared and uv/visible data reported are consistent with the cations containing  $\text{Fe}^{2+}$  and  $\text{X}^-$  (X = Cl, Br and NO). Formation of a species containing an iron atom in the +1 oxidation state was not reported, although breaks in the conductimetric titrations of iron pentacarbonyl with chlorine and bromine were observed at the 0.5:1 and 1:1 (oxidant:reductant) molar ratios. The conductivity was observed to increase with addition of halogen suggesting formation of an ionic intermediate.

Nickel tetracarbonyl dissolved in liquid hydrogen chloride, without loss of carbon monoxide, and formed an adduct with phosphorus pentafluoride (31). No solid products were obtained at room temperature after reaction with either boron trichloride or phosphorus pentafluoride. Oxidation of nickel tetracarbonyl solutions in the solvent with chlorine resulted in the isolation of a compound with an empirical formula  $\text{Ni}_2(\text{CO})_3\text{Cl}_4$  which was assigned the structure (I) on the basis of its infrared and magnetic properties.



(I)

STRUCTURE OF  $\text{Ni}_2(\text{CO})_3\text{Cl}_4$

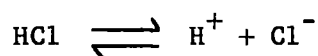
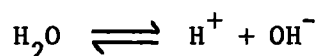
Oxidation of nickel tetracarbonyl with bromine gave nickelous bromide and with nitrosyl chloride a compound of empirical formula  $\text{Ni}(\text{NO})_2\text{Cl}_2$  was formed. The structure of  $\text{Ni}(\text{NO})_2\text{Cl}_2$  was assigned as tetrahedral based on the infrared and magnetic data.

Tricarbonylnitrosylcobalt dissolved in the solvent without evolution of carbon monoxide. Reaction with phosphorus pentafluoride resulted in the formation of a 1:1 adduct which disproportionated on warming to room temperature. Oxidation of solutions of tricarbonylnitrosyl cobalt in the solvent with chlorine and nitrosyl chloride gave cobaltic chloride (31).

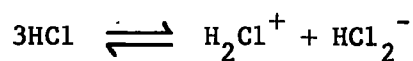
### 1.1.3 Theory of the Solvent

The properties of all protonic solvents are affected to greater or lesser extents by hydrogen bonding. Hydrogen bonding occurs to such an extent in hydrogen fluoride that the solid consists of zig-zag chains of hydrogen bonded polymers. In the lower hydrogen halides the solid consists of a molecular lattice showing clearly that hydrogen bonding is only of secondary importance. Hydrogen chloride, bromide and iodide are mutually miscible but all three are insoluble in liquid hydrogen fluoride.

The conductivity of liquid hydrogen chloride is in the region of  $0.35 \times 10^{-8} \text{ ohm}^{-1} \text{ cm}^{-1}$  at  $-85^\circ\text{C}$  (32), which is very similar to the value of  $5 \times 10^{-8} \text{ ohm}^{-1} \text{ cm}^{-1}$  at  $18^\circ\text{C}$  observed for pure water (33). These values are usually explained by assuming that self ionisation occurs.



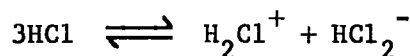
The ions produced will be solvated so that a more accurate representation is probably the equilibrium given below.



The exact degree of solvation is unknown. The postulated  $\text{H}_2\text{Cl}^+$  ion has been detected in the gas phase (34) and may exist in the explosive  $\text{HCl}\cdot\text{HClO}_4$  and in  $\text{HCl}\cdot\text{H}_2\text{SO}_4$  which could not be isolated as a solid (35). The only well documented  $\text{H}_2\text{Hal}^+$  ion observed in solution is  $\text{H}_2\text{F}^+$ , which has been detected by conductivity measurements, and Raman and infrared spectra of the hydrogen fluoride antimony pentafluoride system (36).

The  $\text{HCl}_2^-$  anion has been well established as the solvated anion in the liquid hydrogen chloride solvent system. It has been known for many years that co-ordination of more than one molecule of hydrogen chloride can occur with some large organic molecules (37). The hydrogen dichloride anion was suggested as an intermediate in several organic reactions in nitrobenzene (38), and later it was characterised as its tetramethylammonium salt (39). The infrared data is consistent with a linear  $[\text{Cl-H-Cl}]^-$  ion (39). Similar hydrogen dihalide anions have been established in liquid hydrogen bromide (19, 40-42) and in liquid hydrogen iodide (18,41,43). Evidence for the existence of  $[\text{Cl}(\text{HCl})_2]^-$ ,  $[\text{Br}(\text{HCl})_2]^-$ ,  $[\text{I}(\text{HCl})_2]^-$ ,  $[\text{Br}(\text{HBr})_2]^-$  and  $[\text{I}(\text{HBr})_2]^-$  as well as for the mixed hydrogen dihalides  $[\text{HBrCl}]^-$ ,  $[\text{HClI}]^-$  has been observed (44).

If ionisation of liquid hydrogen chloride can be represented by the equation:



it is clear that two definitions of acids and bases are applicable. Acids can be defined either as proton donors or chloride ion acceptors, and bases as proton acceptors or chloride ion donors. This arises from the fact that the primary step in the equilibrium can be regarded either as proton or chloride ion transfer. The two definitions arise not from a difference of principle but from a difference of emphasis. Hydrogen

chloride may be expected to show characteristics both of a chloridotropic solvent, such as  $\text{AsCl}_3$  (5),  $\text{SbCl}_3$  (45),  $\text{ICl}$  (5,46),  $\text{POCl}_3$  (5) and of a protonic solvent such as  $\text{HF}$  (2),  $\text{H}_2\text{SO}_4$  (47,48) and  $\text{CH}_3\text{COOH}$  (2). Hydrogen chloride is a simpler system to understand than sulphuric acid as sulphonation reaction occur as side effects (47).

The physical constants of the hydrogen halides and of water are given in Table 1.1. Water and hydrogen fluoride, both which have a long liquid range and large dielectric constants tend to dissolve a large number of substances, including many inorganic salts (2,49-53). In these cases the solvation energy is greater than the lattice energy. For the higher hydrogen halides which have short liquid ranges and low dielectric constants, materials having large lattice energies will tend to be insoluble e.g. sodium chloride. Lattice energies depend approximately on  $\frac{1}{r^+ + r^-}$  for ionic compounds, therefore a large cation chloride will tend to be soluble e.g. tetramethylammonium chloride. Also if the anion is small solvation of the anion will occur also favouring solubility.

In aqueous acid solutions, and in sulphuric acid the mechanism of conductance is thought to involve "proton jumping". It has been postulated that in liquid hydrogen chloride that the analogous phenomenon of "chloride ion transfer" could explain the mechanism of conductance in basic solutions. If this postulate was true all univalent bases would have virtually the same molar conductivity at infinite dilution. Unfortunately it has not been possible to measure these conductivities accurately (24).

Table 1.1  
Physical Properties of Water and the Hydrogen Halides

	H <sub>2</sub> O	HF	HCl	HBr	HI
Molecular Weight	18.0	20.0	36.5	80.9	127.9
M.p. (°C)	0.0	-83.0	-114.6	-88.5	-50.9
B.p. (°C)	100.0	19.5	-84.1	-67.0	-35.0
Liquid Range (°C)	100.0	102.5	30.5	21.5	15.9
Density of Liquid (gm/ml near m.p.)	1.0 (0°)	1.2 (-80°)	1.2 (-114°)	2.6 (-84°)	2.9 (-47°)
Molecular Volume (ml)	18.0	16.7	30.4	31.1	44.1
Latent Heat:Fusion (cals/mole)	1440	1094	476	600	686
: Vaporization	9720	7230	3860	4210	4724
Trouton's Constant	26.0	24.7	20.4	20.4	19.8
Dielectric Constant of Liquid	84.2 (0°)	175 (-73°)	9.3 (-95°)	7.0 (-85°)	3.4 (-50°)

contd./

Table 1.1 (contd.)

	H <sub>2</sub> O	HF	HCl	HBr	HI
Viscosity (centipoises)	1.00 (22 <sup>0</sup> )	0.24 (0 <sup>0</sup> )	0.51 (-95 <sup>0</sup> ) (14)	0.83 (-67 <sup>0</sup> ) (14)	1.35 (-35.4 <sup>0</sup> ) (14)
Spec. Conductivity ( $\mu\text{ohm}^{-1} \text{cm}^{-1}$ )	0.05 (18 <sup>0</sup> ) (44)	0.1 (-80 <sup>0</sup> ) (45)	0.0035 (85 <sup>0</sup> ) (43)	0.00014 (-84 <sup>0</sup> ) (27)	0.00085 (-45 <sup>0</sup> ) (246)
H-Hal Stretching Frequency, gas ( $\text{cm}^{-1}$ )	3568* (240)	3961 (233)	2886 (233)	2558 (233)	2230 (233)
Electronegativity (192)	3.5	4.0	3.0	2.8	2.5
Dipole Moment (D)	1.87	1.92	1.08	0.78	0.38

\* Value for the OH radical

The values quoted in this Table are taken either from Mellor (137) or from the Handbook of Chemistry and Physics (74) unless a specific reference is given.

## 1.2. Protonation of neutral transition metal complexes

Protonation of the central metal atom in a neutral transition metal complex was first demonstrated in 1955 by Birmingham and Wilkinson (54). Since then many transition metal complexes with strongly pi-bonded ligands have been shown to act as bases in strongly acidic media (29, 55-67). In a number of these studies the acidic media used was based on the sulphuric acid solvent system (29, 63, 65, 67). Sulphuric acid has two serious disadvantages; the first being that studies are limited to solution techniques since it is very difficult to isolate solid products, and secondly sulphuric acid is a sulphonating (47) and a oxidising agent as well as being a strong acid. Many of the transition metal complexes studied contain transition metal atoms in the 0, +1 or +2 oxidation states. In an attempt to enable the isolation of solid products and to study oxidation in a controlled manner in a protonic solvent, the use of hydrogen chloride as the acidic medium was thought to satisfy many of the requirements.

### 1.2.1. History

The demonstration that hydridodi- $\pi$ -cyclopentadienylrhodium acted as a base by Birmingham and Wilkinson (54) and Green et al (68) was soon followed by reports of the protonation of the biscyclopentadienyl-dihydrides of molybdenum and tungsten (57). Studies on ferrocene (55,56), ruthenocene (56) and osmocene (56) in the boron trifluoride solvent system also showed that protonation of the central metal atom has occurred. In 1962 Davison et al (29) reported the results of their studies of the behaviour of sixty four transition metal carbonyl complexes in several acidic mediums. Of the compounds examined ten were shown to be protonated in sulphuric acid. Isolation of the protonated

product was only achieved for two compounds; bis( $\pi$ cyclopentadienyl-dicarbonyl iron(1)) and  $\pi$ -cyclopentadienylheptacarbonyl iron manganese. Only four compounds of those investigated proved to be insoluble. Almost all of the evidence which supported protonation of the central metal atom was obtained from proton nuclear magnetic resonance studies.

Of the eight types of chromium complexes examined none were protonated in sulphuric acid but two types (arene  $\text{Cr}(\text{CO})_3$  and  $\text{XC}_6\text{H}_4\text{Cr}(\text{CO})_3$ , where X is F or Cl) were protonated in  $\text{BF}_3:\text{H}_2\text{O}$  (1:1 mole ratio). In the examination of eight types of molybdenum complexes and seven types of tungsten complexes only the bis( $\pi$ cyclopentadienyltricarbonyl) dimetal complexes were found to be protonated.  $\pi$ -cyclopentadienylheptacarbonyl iron manganese was the only manganese compound protonated of the five types examined. Bis( $\pi$ -cyclopentadienyldicarbonyl iron(1)) and compounds of the types  $\text{Fe}(\text{CO})_4\text{L}$  and  $\text{Fe}(\text{CO})_3\text{L}_2$  ( $\text{L} = (\text{C}_6\text{H}_5)_3\text{P}$  and  $(\text{C}_6\text{H}_5)_3\text{As}$ ) were protonated of eight types of complex of iron which were examined. Neither of the rhenium complexes nor any of the cobalt and nickel complexes examined behaved as bases.

Those complexes which contained a sigma bonded methyl ligand usually decomposed with the evolution of methane, whilst those complexes which contained a halogen ligand very often evolved hydrogen halide.

For complexes which contain an alkene as one of the ligands protonation often occurred at the carbon-carbon double bond (58), to give a carbonium ion, bonded and stabilised by the metal carbonyl fragment of the complex. One notable exception is the case of norbornadiene-tricarbonyl iron (59) in which protonation of the central iron atom was observed.

Protonation of iron pentacarbonyl had been shown to occur in

$\text{BF}_3 \cdot \text{H}_2\text{O} - \text{CF}_3\text{COOH}$ , and that a violent decomposition occurred in sulphuric acid (29). The protonation and oxidation of iron pentacarbonyl using hydrogen chloride as the acidic medium (30) successfully demonstrated the superiority of hydrogen chloride over sulphuric acid. Compounds of the type  $\text{Fe}(\text{CO})_4\text{X}^+$  ( $\text{X} = \text{H}, \text{Cl}, \text{Br}$  and  $\text{NO}$ ) were isolated as solid salts. No discussion will be given here as it has been included in the section on non-aqueous solvents.

Laing and Roper (61) reported the protonation of tricarbonyl bis(triphenylphosphine)osmium(0) using strong acids in the presence of the bases water and ethanol. These authors reported the conductivities and showed that the molar conductivity values were typical for 1:1 electrolytes. Also reported were infrared frequencies for the carbonyl stretch and the osmium-hydrogen stretch and deformation modes. No evidence for the classification of the protonated complexes as osmium(II) compounds was given by the authors.

Oxidative addition of carboxylic acids to complexes of the type  $[\text{IrX}(\text{CO})\text{L}_2]$  ( $\text{X} = \text{Cl}, \text{Br}$  or  $\text{I}$ ,  $\text{L} =$  tertiary phosphine or tertiary arsine) was shown by Deeming and Shaw (69). These authors had used uv/visible spectroscopy to monitor the transition from Ir(I) to Ir(III); also shown was the increase in basicities of the complexes in the order  $\text{X} = \text{Cl} < \text{Br} < \text{I}$ ; and  $\text{L} = (\text{C}_6\text{H}_5)_3\text{P} < (\text{C}_6\text{H}_5)_3\text{As} < (\text{C}_6\text{H}_5)_2\text{PCH}_3 < (\text{C}_6\text{H}_5)\text{P}(\text{CH}_3)_2 < (\text{CH}_3)_3\text{P}$ . The consequence of the above results were discussed in terms of the ligands basicities and stereochemistry.

A second type of oxidative addition was reported by K. Kudo and co-workers (66), who studied the reaction of ethanolic hydrogen chloride with carbonyltris(triphenylphosphine) palladium(0) to give trans-hydrido-chlorobis(triphenylphosphine) palladium(II).

Proton nuclear magnetic resonance was used by Katz and Pedrotty (64) to demonstrate the increase in basicities was in the order  $\text{Cr} < \text{Mo} < \text{W}$  for the triphenylphosphonium(tricarbonylmetal) cyclopentadieneides of chromium, molybdenum and tungsten.

At about this period in time a new interest in protonation of polynuclear metal carbonyls occurred, and many of the workers returned to sulphuric acid as the acid medium (63,65). Two independent groups of workers reported their results on the protonation of triosmium dodecacarbonyl (63,65). The  $[\text{HOs}_3(\text{CO})_{12}]^+$  cation was isolated as the hexafluorophosphate salt, one group of workers also isolated  $[\text{HOs}(\text{CO})_5]^+$  as a decomposition product (63).

Rapid decomposition was observed when examination of tri-iron dodecacarbonyl, tris( $\pi$ cyclopentadienylcarbonyl rhodium),  $\pi$ cyclopentadienyl nonacarbonyl iron rhodium, tetracobalt dodecacarbonyl and tettrarhodium dodecacarbonyl was attempted in sulphuric acid (65). When tetrairidium dodecacarbonyl was dissolved in sulphuric acid diprotonation occurred (demonstrated by proton nuclear magnetic resonance) but attempts to isolate the diprotonated species failed (65).

In a period of ten years the study of protonation of neutral transition metal complexes had completed a full circle and the disadvantages of sulphuric acid solvent systems had been clearly shown. The fact that some complexes can be protonated in aqueous solutions clearly shows that some of these complexes are quite strong bases.

CHAPTER 2  
EXPERIMENTAL TECHNIQUES

2.1. The vacuum system

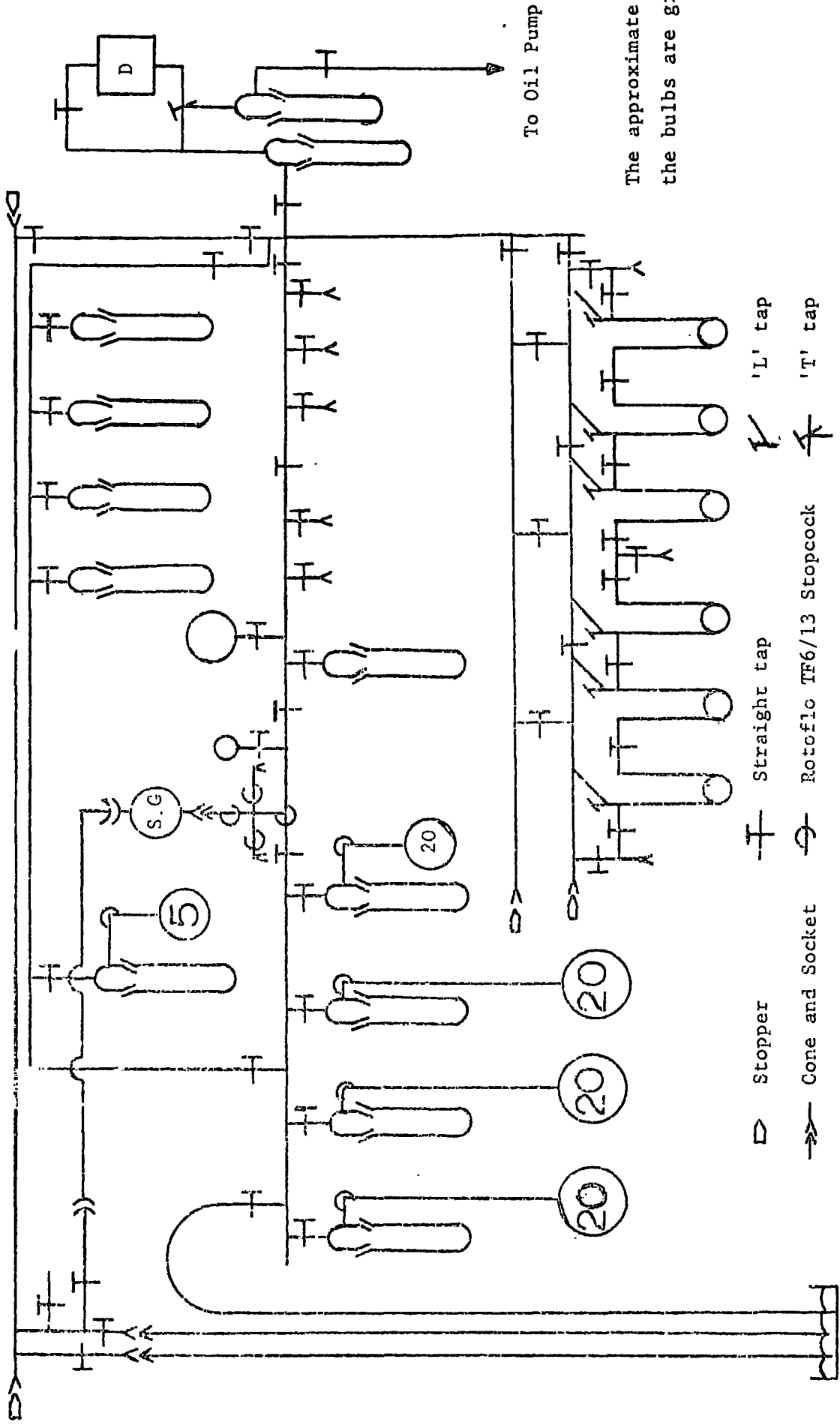
In all the experimental work described in this thesis, volatile materials were manipulated in a vacuum system constructed of pyrex glass; shown diagrammatically in Figure 2.1 and pictured in Plate 2.1. Similar systems have been used by previous workers for studying volatile non-aqueous solvents and as they have been described in detail elsewhere (18,70-72) only a brief description will be included here.

The vacuum was provided by a two stage mercury diffusion pump backed by a double stage rotary oil pump, enabling a pressure of  $10^{-4}$  mm Hg to be maintained. The pumps were protected by two traps immersed in liquid nitrogen. The trap situated between the mercury diffusion pump and the main section of the vacuum section also served to collect all the unwanted volatile materials from the vacuum system.

The pumping section was designed so that the mercury diffusion pump could be by-passed but still maintained the use of the two traps immersed in liquid nitrogen. This arrangement was of most use when large quantities of air or materials which readily attacked mercury e.g. chlorine, were being used.

All ground glass stopcocks were lubricated with Apiezon L, and standard Quickfit ground glass joints were lubricated with Apiezon M. The molecular weight section of the vacuum system was constructed using Quickfit Rotaflo TF6/13 teflon high vacuum stopcocks. Whenever possible handling of materials which readily attacked the Apiezon greases, e.g. chlorine and boron trichloride, were restricted to the molecular weight section of the vacuum system. All storage bulbs had Quickfit TF6/13 high

Figure 2.1  
The Vacuum System

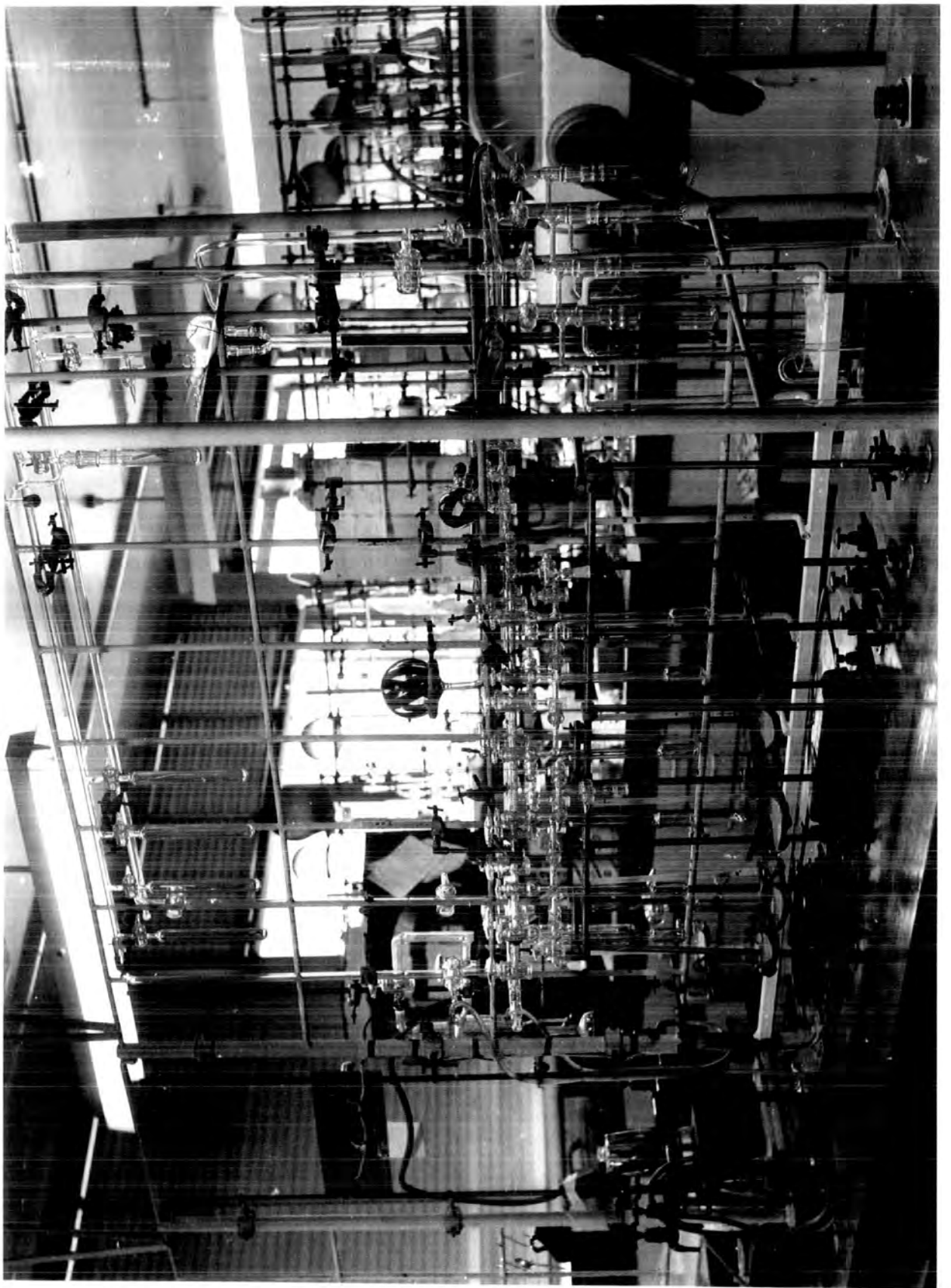


The approximate volumes of the bulbs are given in litres.

- ▷ Stopper
- ↔ Cone and Socket
- S.G. Spiral gauge
- + Straight tap
- ⊕ Rotoflo TF6/13 Stopcock
- D. Diffusion Pump
- ∩ 'L' tap
- ⊥ 'T' tap

Plate 2.1

The Vacuum System



vacuum stopcocks fitted thus eliminating the necessity for letting the storage bulbs up to atmospheric pressure for periodic re-greasing.

Volatile materials were purified in the fractionation train section of the vacuum system by trap to trap distillation at low temperatures and low pressures. The traps were cooled with liquid nitrogen, slurries of solid carbon dioxide in acetone or methylated spirits, or with melting organic compounds (slush baths). Low temperature baths were always contained in dewar vessels. The low temperature baths found most useful are listed in Table 2.1. Other low temperature baths are listed in a standard text book (73).

Materials with a vapour pressure in excess of five atmospheres at ambient temperature, were stored as gases in bulbs connected via traps to the vacuum system. Hydrogen chloride was stored, after purification, in three twenty litre bulbs; and chlorine after purification was stored in a five litre bulb. Materials with vapour pressures of less than five atmospheres at ambient temperatures e.g. boron trichloride and sulphur dioxide, were stored as liquids offline in pyrex glass ampoules fitted with Quickfit Rotaflo TF6/13 teflon stopcocks (Figure 2.2).

Phosphorus pentafluoride was stored frozen down on the vacuum system in a cold finger immersed in a liquid nitrogen bath.

Pressure measurements were carried out using a spiral gauge as a null point instrument; the sensitivity being such that a pressure change of 2 cm of Hg could be measured with an accuracy of one per cent. The spiral gauge was robust enough to withstand a pressure difference of one atmosphere.

An additional mercury manometer was connected to the main section of the vacuum system and was used primarily as a safety valve when dealing

Table 2.1  
Low Temperature Baths

Approximate Temperature	Solvent
-23°C	Carbon Tetrachloride slush
-45°C	Chlorobenzene slush
-64°C	Chloroform slush
-78°C	Ethanol/solid carbon dioxide slurry
-84°C	Ethyl Acetate slush Acetone/solid Carbon Dioxide slurry
-95°C	Toluene slush
-112°C	Carbon Disulphide slush
-126°C	Methyl Cyclohexane slush
-131°C	Pentane slush
-160°C	Isopentane slush
-196°C	Liquid Nitrogen

with conditions which might have lead to pressures in excess of one atmosphere being handled by the vacuum system. Conditions which were likely to give rise to a pressure in excess of one atmosphere were the purification of hydrogen chloride and when reaction ampoules were opened which might contain large quantities of hydrogen.

Two calibrated bulbs were attached to the vacuum system; the smaller bulb had a volume of about  $100 \text{ cm}^3$  and the larger bulb had a volume of about  $500 \text{ cm}^3$ . The volumes of these bulbs were calibrated by weighing them empty and then weighing them full of water. The volumes of the spiral gauge and molecular weight section of the vacuum system were calibrated by expanding dry nitrogen from a calibrated bulb into them, measuring the pressure change and assuming ideal gas behaviour.

## 2.2. Apparatus

Reactions in liquid hydrogen chloride were normally carried out in vessels which were connected to the vacuum system by a Quickfit B14 cone mounted horizontally and mated to the vertically mounted B14 socket take offs of the vacuum system by use of a B14 "elbow" adaptor. This arrangement allowed the vessel to be agitated in order to ensure complete mixing of the contents of the vessel. There were basically two types of reaction vessel used; the first type employed a conventional 4 mm bore ground glass stopcock which was used at less than one atmosphere pressure (Figure 2.3) and the second type employed a Quickfit Rotaflo TF6/24 teflon stopcock which was usable at pressures in excess of one atmosphere (Figure 2.4). Both of the reaction vessels described above were satisfactory for carrying out weight analyses. A weight analysis consisted of measuring the change of weight which occurred when a reaction was carried out. The result was expressed as a percentage increase or

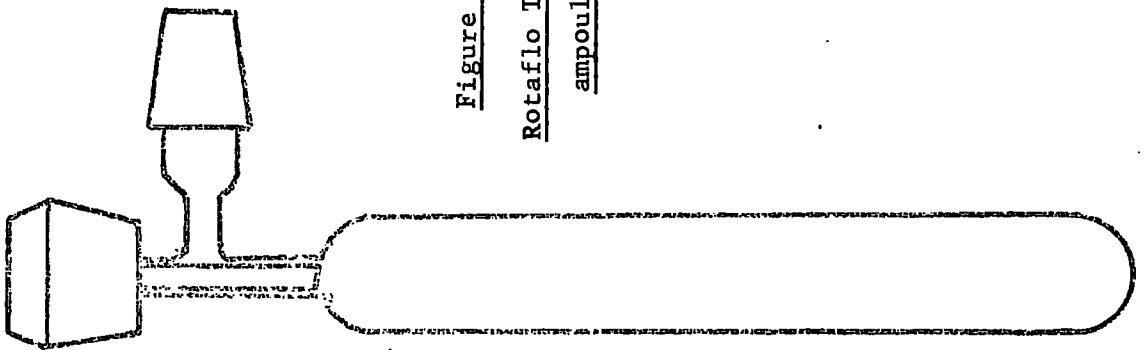


Figure 2.2

Rotaflo TF6/13  
ampoules

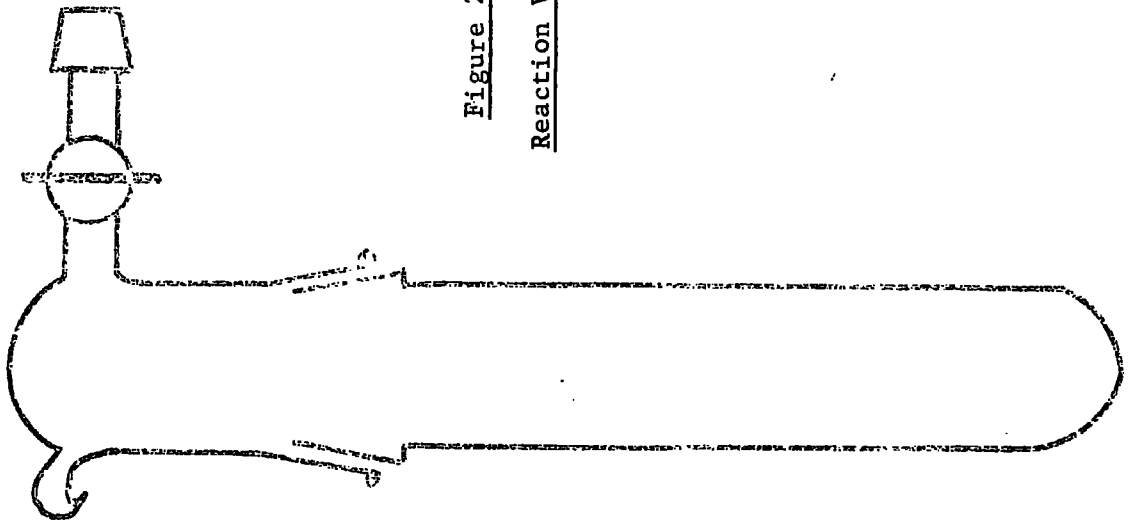


Figure 2.3

Reaction Vessel

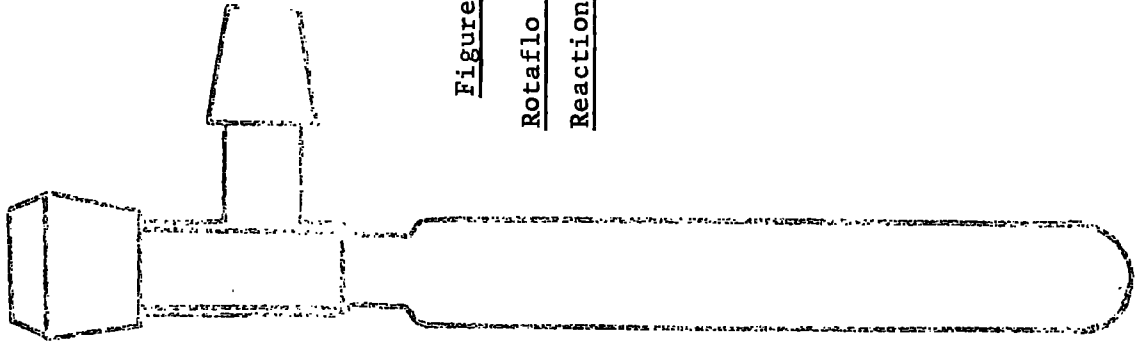


Figure 2.4

Rotaflo TF6/24  
Reaction Vessel

or loss based on the weight of the compound under investigation. Weight analyses were accurate provided care was taken and an increase (or loss) of 50 mg or more had occurred.

Hydrogen chloride has a vapour pressure of fourty atmospheres at  $17.8^{\circ}\text{C}$  (74); therefore reactions studied in liquid hydrogen chloride at room temperature were carried out in ampoules constructed of silica (Figure 2.5). After freezing down the ampoules in liquid nitrogen they were opened directly into the vacuum system using the technique outlined below. After freezing the ampoule to  $-196^{\circ}\text{C}$  (liquid nitrogen bath) a scratch was made just below the tip of the seal. The neck of the ampoule was then inserted into the ampoule breaker (shown in Figure 2.6) so that the scratch was positioned as shown in Figure 2.7. Apiezon black wax was used to join the ampoule breaker and the ampoule together in a vacuum tight joint. The ampoule breaker was then opened to the vacuum system and evacuated. After isolation of the section of the vacuum system in use the key of the ampoule breaker was rotated thus snapping the seal of the ampoule off. Any gases observed at this stage were examined by infrared spectroscopy. Volatile materials were then removed in vacuo prior to examination of the solid product. The above technique was also used for opening ampoules which had been used for storing volatile and/or hygroscopic materials, e.g. nitrosyl chloride and boron trichloride.

Conductivity cells were attached to the vacuum system in an identical manner to that described for the reaction vessels. Typical conductivity cells for low temperature non-aqueous solvent work have been fully described by previous workers (18,70-72). There are two basic types of conductivity cell, differing only in the materials used for the construction. The first type was constructed of pyrex glass and used



Figure 2.5  
Silica Ampoule

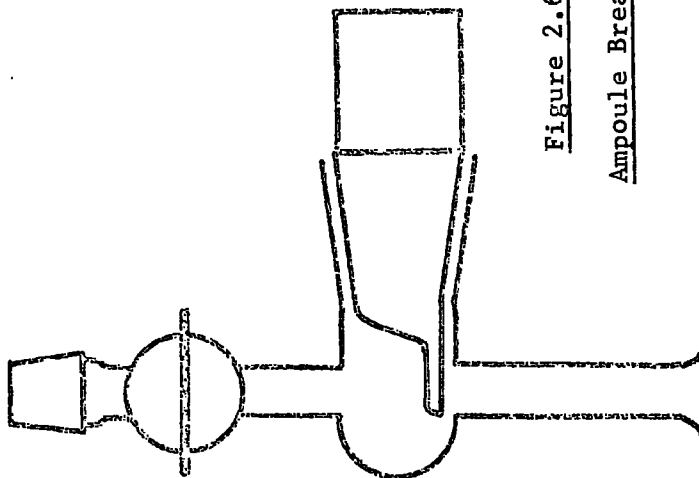


Figure 2.6  
Ampoule Breaker

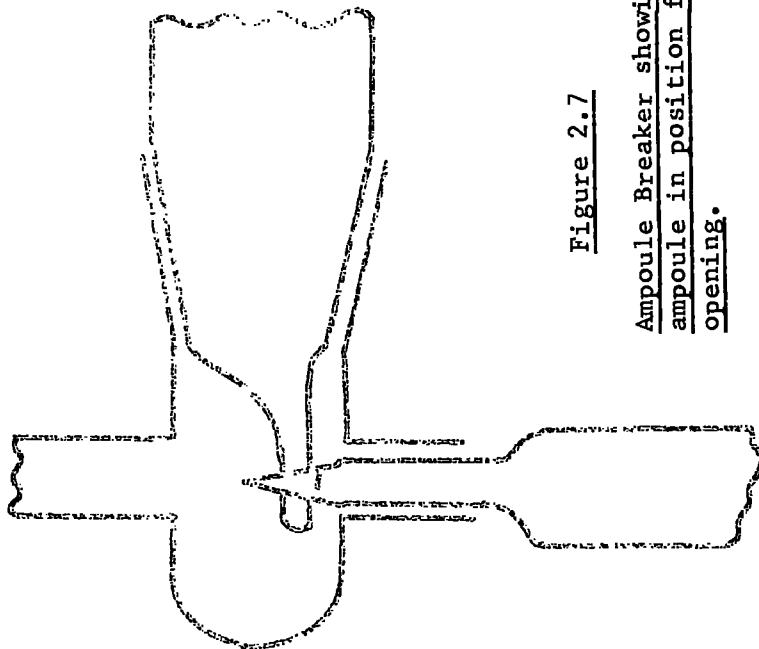


Figure 2.7  
Ampoule Breaker showing  
ampoule in position for  
opening.

tungsten junctions in the cell 'legs'. The second type used platinum junctions sealed in soda glass with the upper part of the cell legs joined via a soda-pyrex graded seal to the rest of the cell which was constructed in pyrex glass. The two types of conductivity cell are shown in Figure 2.8. The author preferred the cells constructed with platinum seals since it was much easier to maintain a good electrical contact at the copper mercury platinum junction than at the copper mercury tungsten of the all pyrex cell.

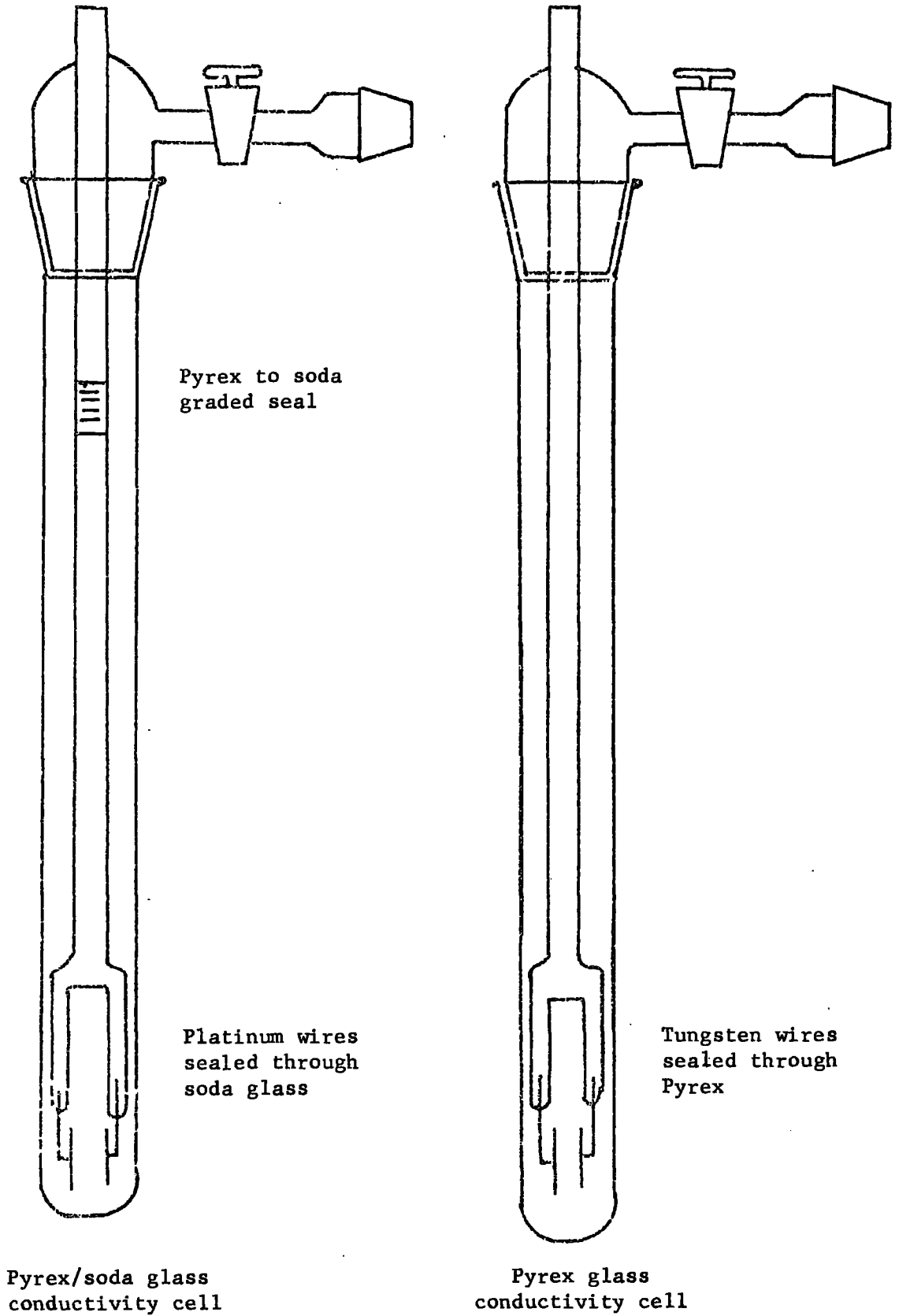
The conductivity cell and platinum electrodes were cleaned using organic solvents, aqua-regia and deionised water.

Conductance measurements were made using a Wayne Kerr Universal Bridge Model B224 which also allowed capacitance measurements to be carried out. The balance point was shown by minimum deflection of a needle from zero on an uncalibrated dial. The bridge had a range of  $1 \text{ n ohm}^{-1}$  -  $100 \text{ ohm}^{-1}$  with a 0.1% accuracy.

Conductimetric titrations were carried out by weighing 0.1-0.3 mmoles of the substance under investigation into the conductivity cell and degassing in vacuo. After cooling the cell to  $-196^{\circ}\text{C}$  (liquid nitrogen bath), hydrogen chloride (ca.  $7 \text{ cm}^3$ ; 0.25 mole) was condensed in from the gas phase. The solution was allowed to warm up to  $-111^{\circ}\text{C}$  (carbon disulphide slush bath) for titrations which involved phosphorus pentafluoride and  $-95^{\circ}\text{C}$  (toluene slush bath) for all the other titrations.

In all the conductimetric titrations portions of acid or oxidant were added from the gas phase, in known amounts, to the solution of the substance under investigation. The amount of titrant added was calculated from the temperature and pressure of the gas in a known volume assuming that the ideal gas laws were obeyed. The titrant was transferred to the

Figure 2.8



conductivity cell by cooling the cell to  $-196^{\circ}\text{C}$  (liquid nitrogen bath) and allowing the titrant to condense. The solution was warmed to either  $-111^{\circ}\text{C}$  (carbon disulphide slush bath) or  $-95^{\circ}\text{C}$  (toluene slush bath) and the conductivity recorded once a steady reading was observed. Each addition and conductance measurement took about one and a half hours. The author found that the titration must be completed during the same day, allowing the titration to stand overnight at  $-196^{\circ}\text{C}$  (liquid nitrogen bath) nearly always resulted in a break in the titre at that point. This break was thought to be caused by photochemical decomposition. After completion of the titration all volatile materials were removed in vacuo. The solid product obtained at room temperature was examined by infrared spectroscopy to confirm that it was the same product as that which was obtained from large scale preparations.

### 2.3. Inert atmosphere glove box techniques

The glove boxes used throughout these studies were flushed with dry nitrogen, obtained as the boil off from liquid nitrogen. Trays of phosphorus pentoxide were kept in the glove box and served two functions:

(a) a desiccant,

and (b) an indicator to the dryness of the glove box.

A recirculatory pump situated inside the glove box was used to circulate the glove box atmosphere through two traps connected in parallel. Both of the traps were immersed in liquid air and this method served to remove any solvent vapours from the glove box atmosphere. The general technique of working with a glove box is well established and no description will be given here.

All solids isolated from liquid hydrogen chloride solutions were always handled in the inert atmosphere glove box. The solid product was

purified wherever possible by washing free of any unreacted starting material with a dry solvent, usually methylene chloride. All volatile species were removed in vacuo before examination of the solid products by any of the physical techniques used.

## 2.4. Determination of physical properties

### 2.4.1. Infrared spectra

Infrared spectra were recorded on a Perkin-Elmer 621 or 457 double beam continuously recording spectrophotometers over the region 4000-250  $\text{cm}^{-1}$ . A Beckman-RIIC FS-720 interferometer was used to record the infrared spectra over the region 400-50  $\text{cm}^{-1}$ , the interferogram was recorded on eight track paper tape. Analysis of the interferogram was carried out using the IBM 360/67 computer jointly owned by the Universities of Durham and Newcastle. The computer programme used was based on the Cooley-Tukey Algorithm for calculation of complex fourier series (75). The computer programme is dealt with in more detail in Chapter 8 and is given in Appendix A.

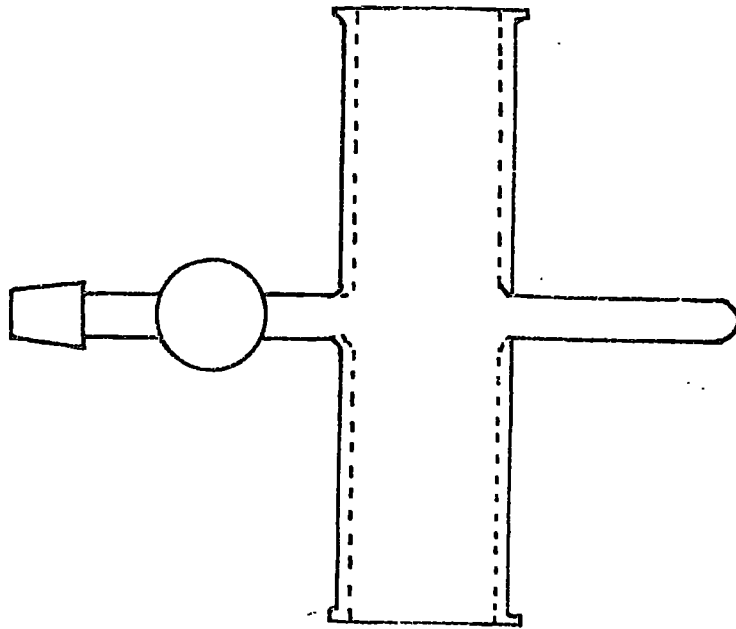
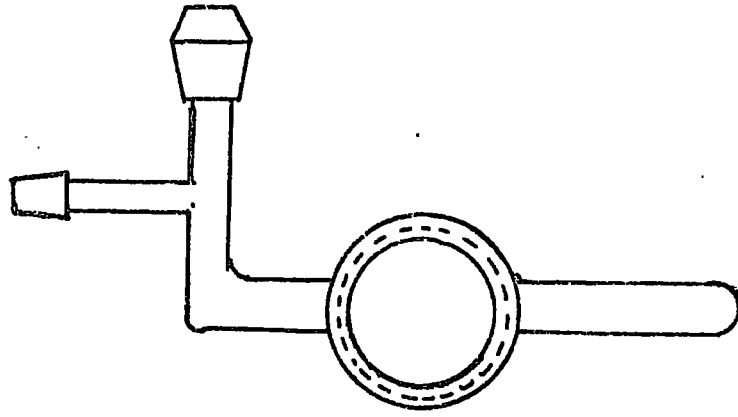
Infrared spectra of gaseous materials were carried out using 10 cm path length cells fitted with windows of the appropriate material (Figure 2.9). Infrared spectra of solids were carried out by grinding the solid in agate pestle and mortar then either being mulled with nujol and smeared between polished optics or ground with an alkali halide and pressed into a disc.

The problem of preparing alkali halide discs in an inert atmosphere was solved by the author who designed a press which could be used in an inert atmosphere glove box.

The design described below required the use of two spanners, the press and a locking plate fitted to the base of the inert atmosphere

Figure 2.9

Infrared Gas Cell for use in 4000-250  $\text{cm}^{-1}$  region



glove box. The work space required for use of the press was 60 cm long, 30 cm high and 25 cm wide. The press is shown in an exploded view form in Plate 2.2 and in section in Figure 2.10.

The main body of the press, 1, was tapped to receive the inner die, 2. The inner die, 2, was tapped to receive the screw, 3, which applied the pressure to the plates, 4 and 5, which sandwiched the material under investigation. After the press had been assembled it was evacuated before full pressure was applied. The whole press was made in stainless steel except the plates, 4 and 5, which were purchased from Beckman-RIIC Ltd., Sunley House, 4 Bedford Park, Croydon. In the initial work the plates, 4 and 5, were made of stainless steel but were found to be too soft and rapidly became damaged in use.

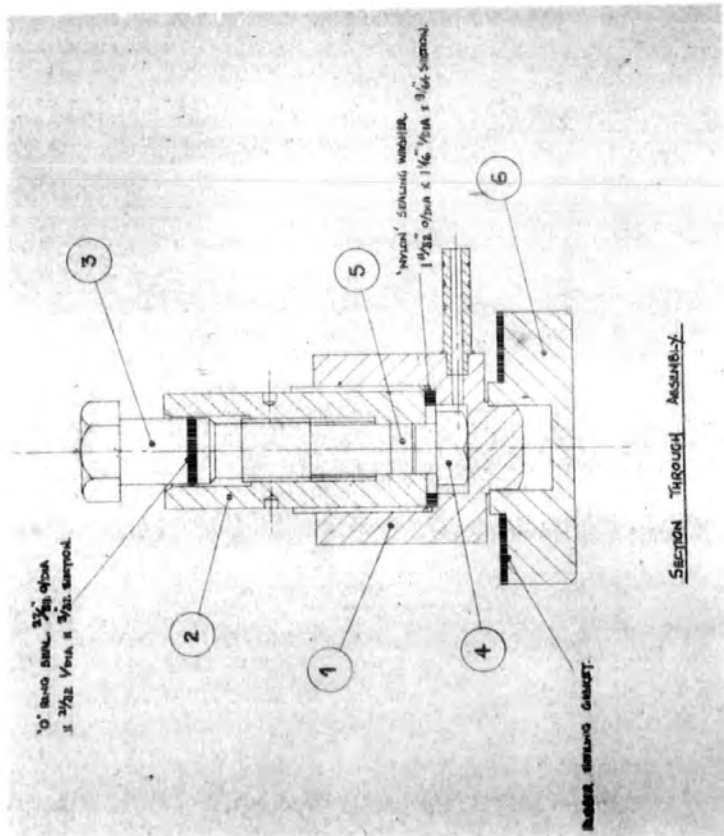
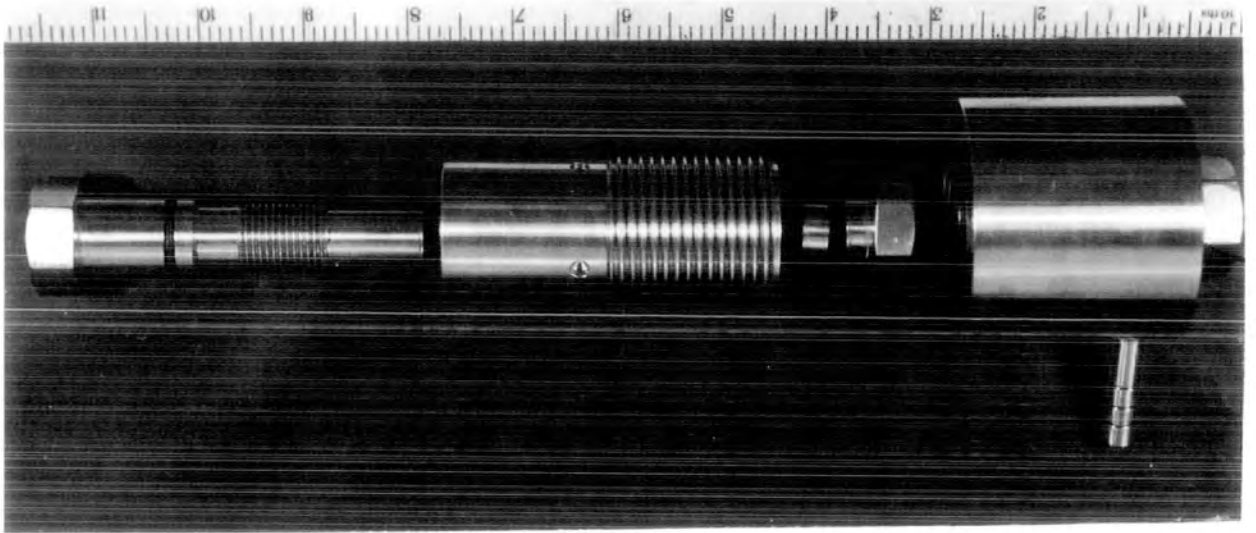
Best results from the press were obtained when the following procedure was used.

The sample was ground to a fine powder in an agate pestle and mortar before being ground with the alkali halide (usually potassium chloride) which was going to be used as the host matrix. The homogeneous powder was then loaded between plates, 4 and 5, whilst the inner die was held upside down. Rotation of the plate, 4, ensured a uniform layer before the main body of the press, 1, was screwed down onto the inner die, 2, until it seated on the nylon sealing washer. The screw was then tightened finger-tight before the press was inverted. The assembled press was then stood in the locking plate, 6, and the inner die, 2, tightened with a "C" spanner before the press was evacuated. Once the press had been evacuated the screw, 3, was tightened to a torque of 5-8 KgM, which resulted in a pressure of  $100 \text{ mNm}^{-2}$  (assuming 10% efficiency) being applied to the plates 4 and 5. After a period of about two minutes the vacuum was disconnected and the screw, 3, slackened prior to removal

A Press for Preparing Discs  
for Examination by Infrared Spectroscopy

Figure 2.10

Plate 2.2



of the inner die, 2, from the main body of the press, 1, whilst the press was held upside down. After the head of the screw, 3, had been inserted into the locking plate, 6, the inner die, 2, was screwed down until the pressed disc was proud of the inner die, 2. The disc was then removed and then mounted in an isolation cell whilst still in the glove box. Removal of the isolation cell from the glove box thus enabled infrared spectral examination to be carried out on a specimen which had only been exposed to the atmosphere of the glove box.

Discs using potassium chloride as the host matrix were examined in the  $4000-300\text{ cm}^{-1}$  using the isolation cell shown in Plate 2.3. This isolation cell consisted basically of the lower half of the low temperature cell with the Dewar arrangement omitted and then sealed as close to the ground glass joint as convenient. The windows used were polished cesium iodide. This isolation cell was also used for examination of nujol mulls and was usable either evacuated or containing an inert atmosphere. For examination of samples in the  $400-50\text{ cm}^{-1}$  region the disc was prepared using a host matrix of polythene and mounted in the isolation cell shown in Plate 2.4.

This isolation cell consisted of a polythene window sealed into a rectangular stainless steel plate. The inside of the plate was tapped to receive the front polythene window mounted in a stainless steel frame. The front window was screwed into the back plate until it seated on a viton B 'O' ring thus ensuring that the cell was vacuum tight. This isolation cell was also used for the examination of moisture sensitive materials as nujol mulls, the mull being made with a consistency of toothpaste and was smeared on one of the windows.

Low temperature infrared spectra were recorded using the low temperature cell shown in Plate 2.5 and in Figure 2.11. The cell

Plate 2.3A

Isolation Cell for Use in the 4000-250 cm<sup>-1</sup> region

Assembled View

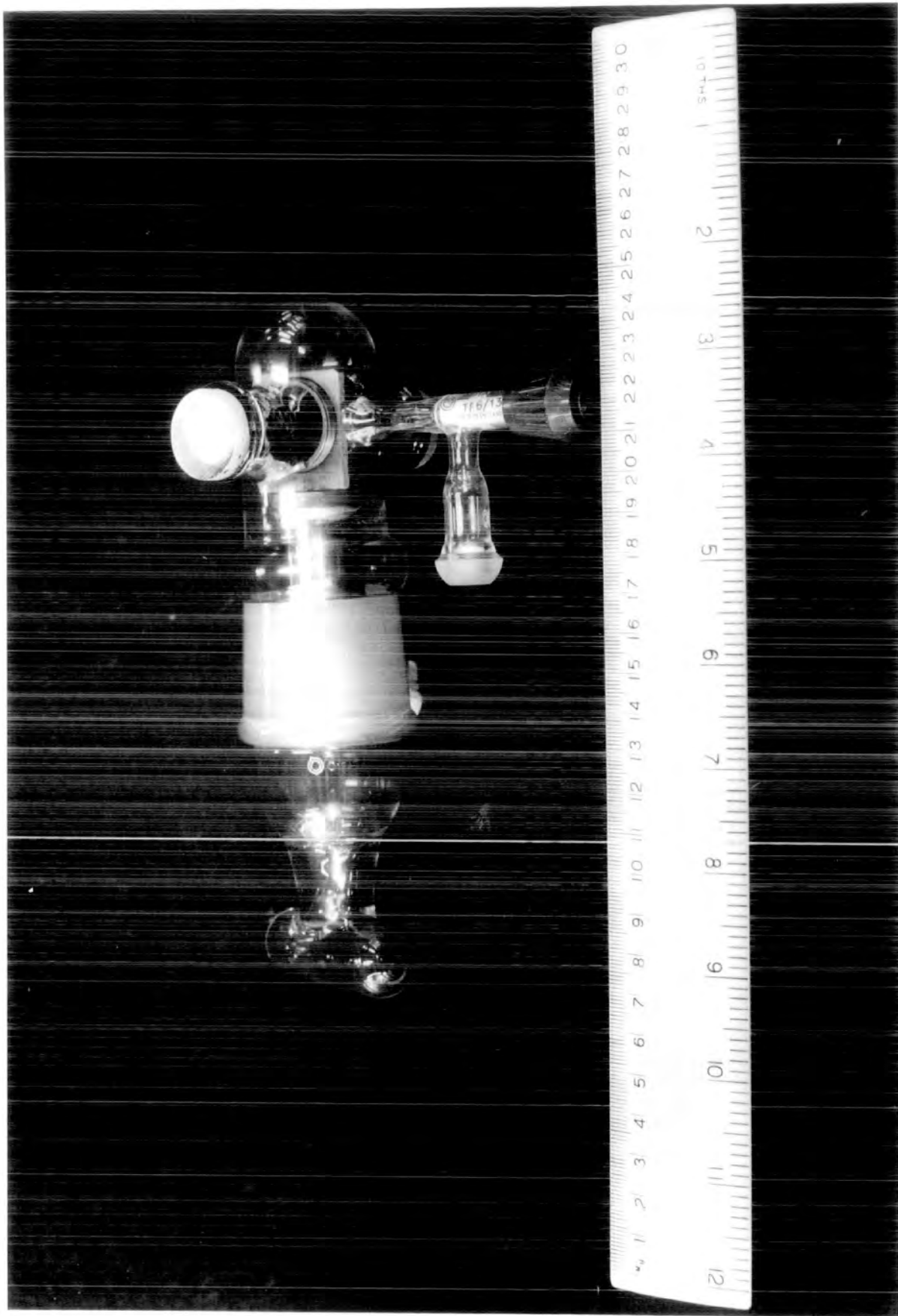
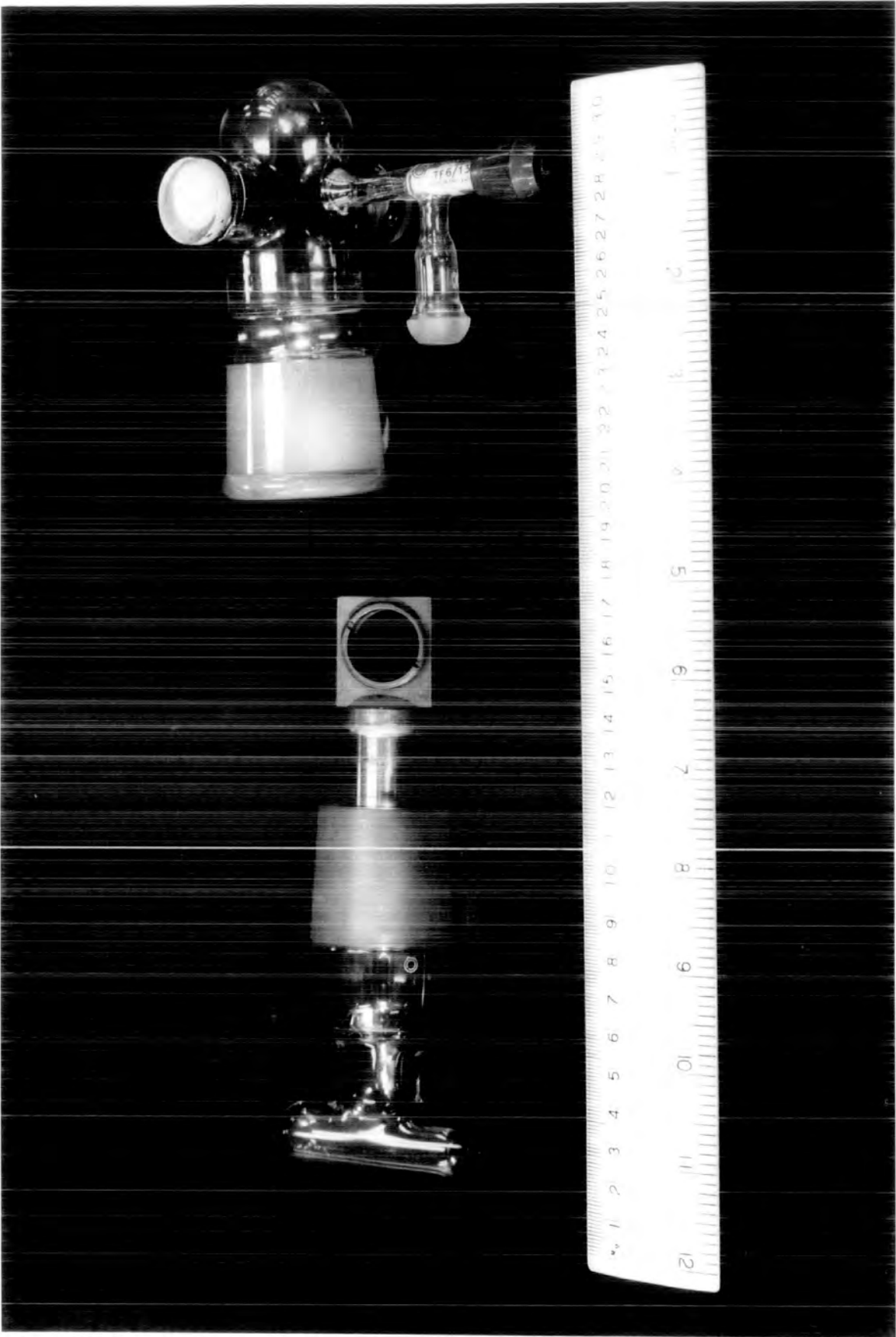


Plate 2.3B

Isolation Cell for Use in the 4000-250 cm<sup>-1</sup> region

Exploded View



Isolation Cell for use in the 400-50 cm<sup>-1</sup> region. Plate 2.4

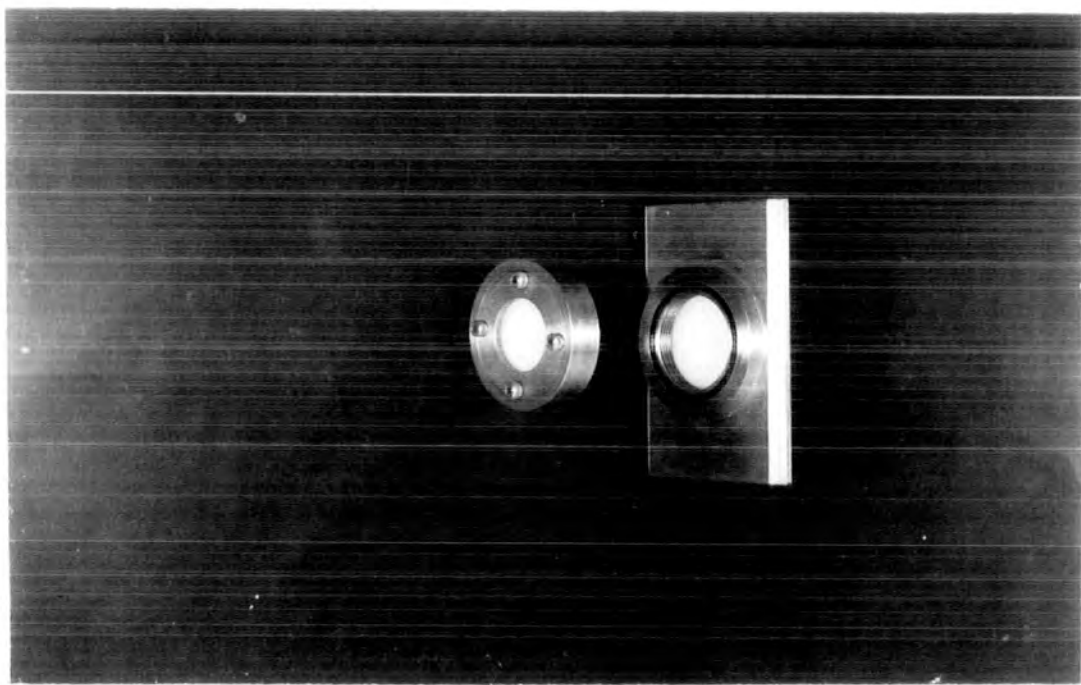
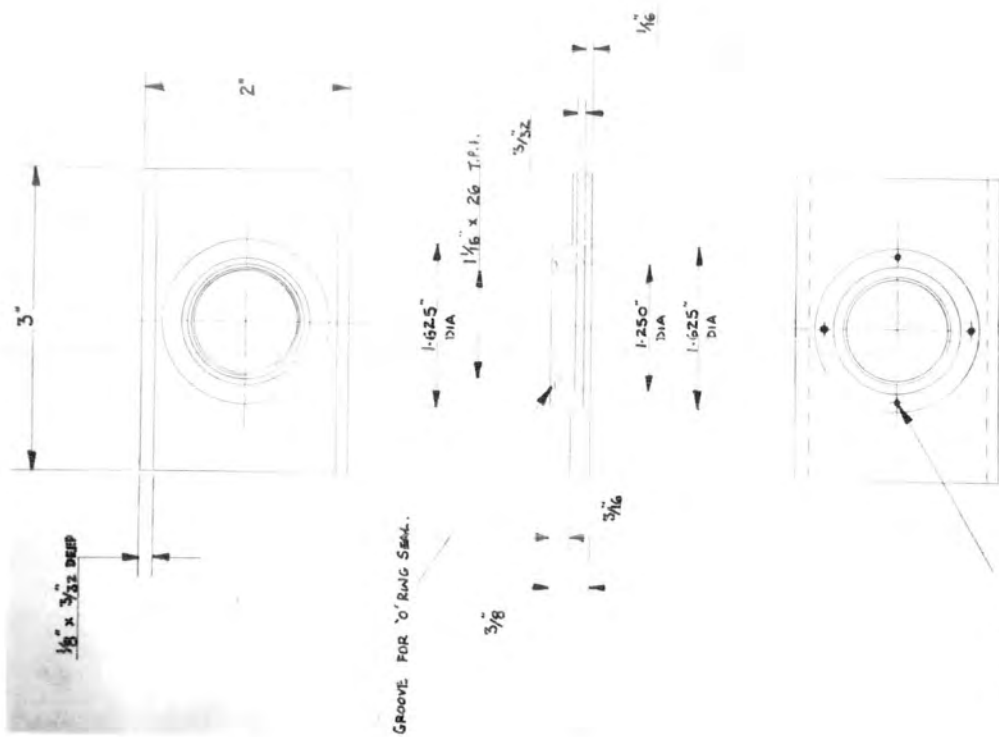


Plate 2.5A

Low Temperature Cell for use in the 4000-250 cm<sup>-1</sup> region

Assembled View



Plate 2.5B

Low Temperature cell for use in the 4000-250  $\text{cm}^{-1}$  region

Exploded View

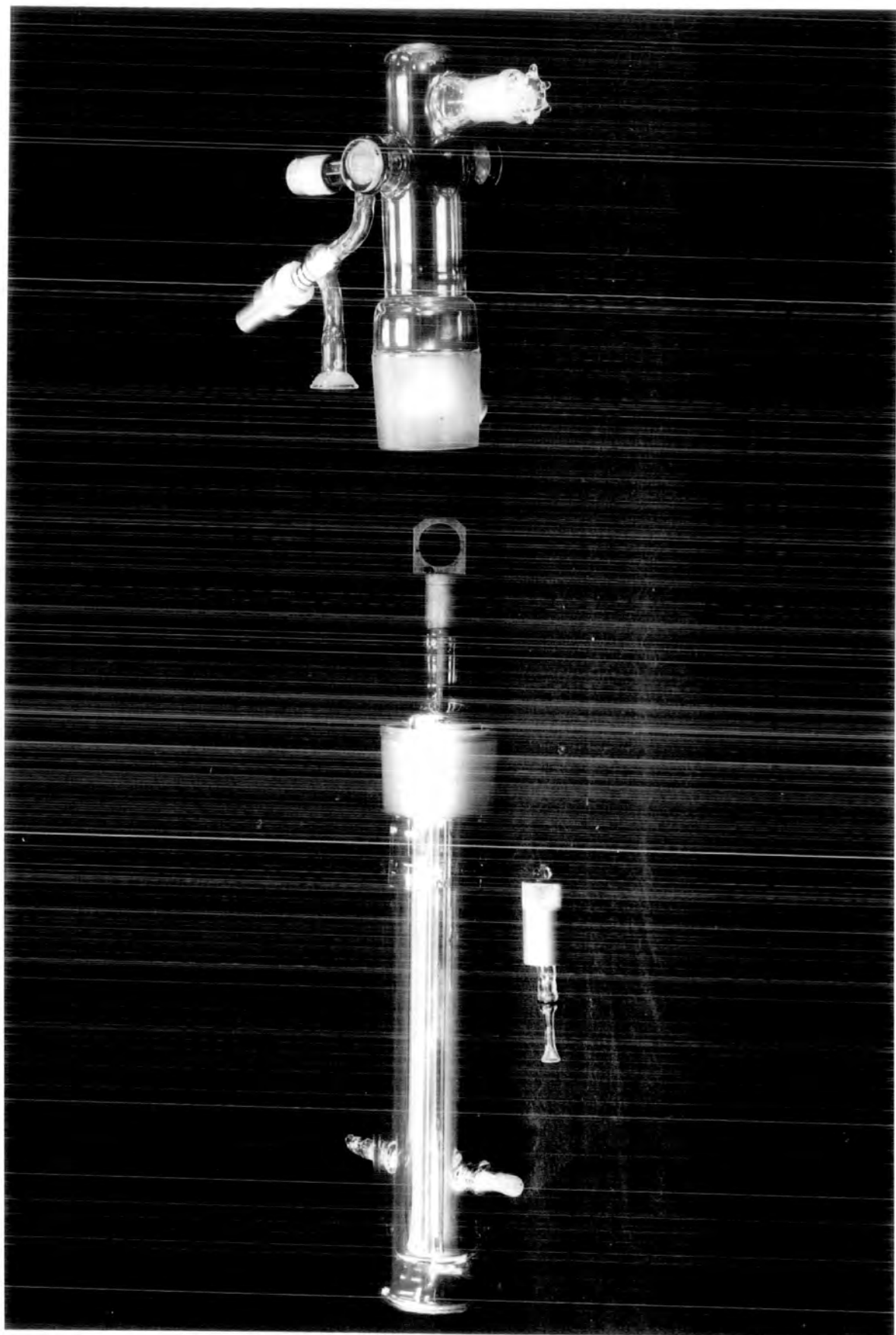
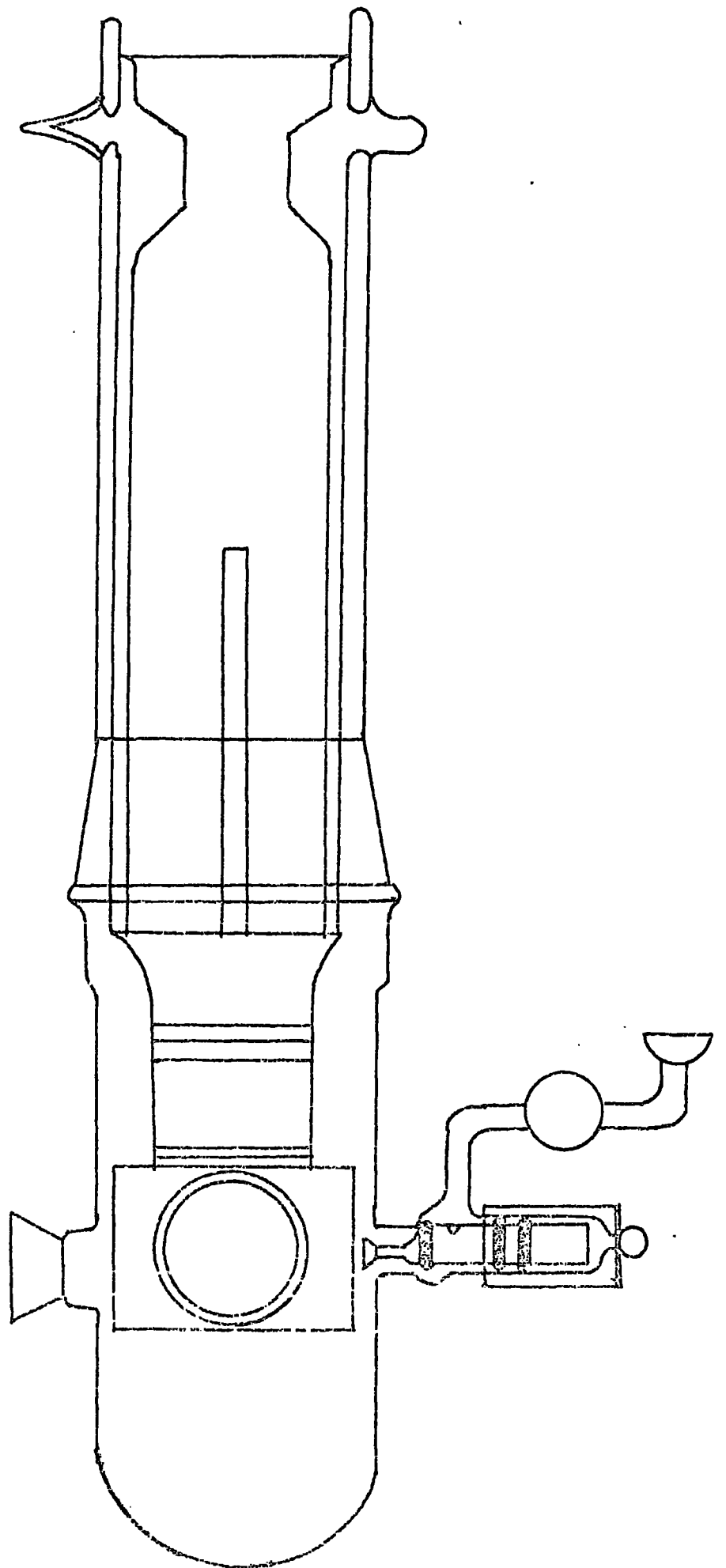


Figure 2.11

Low Temperature Infrared Cell for Use in the 4000-250 cm<sup>-1</sup> region



consisted of a copper block for support of the sample. The copper block had a copper rod extending upwards which would be immersed in the refrigerant when the cell was in use. The copper block was soft soldered into a glass to metal seal; the glass part being terminated in a silvered dewar. The dewar was surrounded by a glass envelope which terminated in a B55 socket at the lower end. The lower section of the low temperature cell consisted of a tube with a B55 cone fitted at one end and being sealed at the other end. Also fitted to the cells lower section were the two polished cesium iodide windows and two vacuum take-offs. One of the vacuum take offs could be used for spraying a volatile material on to a frozen window whilst the other take off was employed for evacuating the low temperature cell. The cell was not evacuated until the mull had frozen, since evacuation of the liquid mull was always accompanied by degassing and subsequent loss in uniformity of the mull.

Nujol was always dried by heating in vacuo with sodium until the sodium became molten and no further evolution of gas was observed. The nujol was then transferred to a dropping bottle containing clean sodium.

Potassium chloride was ground and sieved through a 200 mesh sieve before heating to  $350^{\circ}\text{C}$  in vacuo for a period of 12-18 hours. After the potassium chloride had cooled to room temperature, it was transferred to small ampoules which were either sealed in vacuo or stored in the glove box. Infrared spectral examination failed to show any absorption bands due to OH.

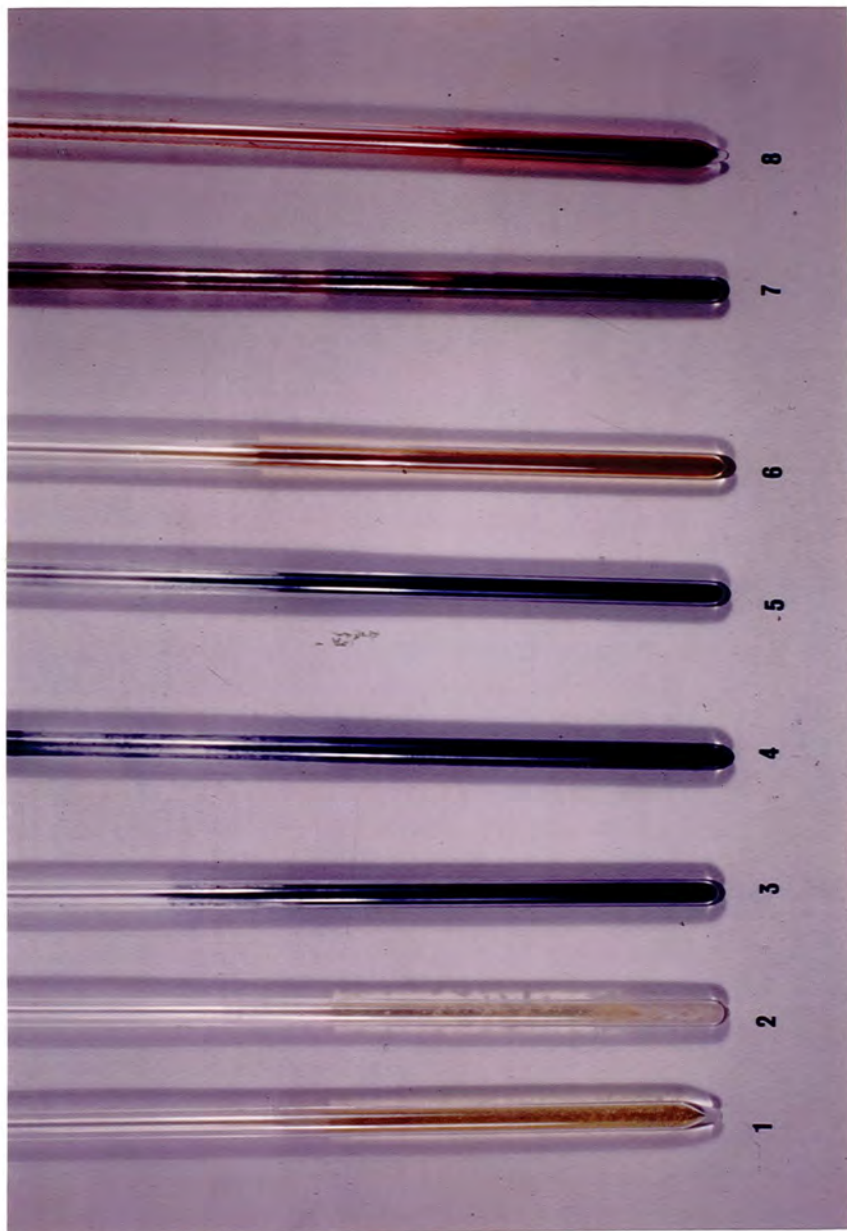
Polythene powder was dried by pumping overnight at a pressure of about  $10^{-4}$  mm Hg.

#### 2.4.2. $^1\text{H}$ Nuclear magnetic resonance studies

Proton nuclear magnetic resonance studies were carried out using either a Perkin-Elmer R10 or Varian A56/60 spectrometer, both instruments operated at 60 MHz. The Varian instrument was preferred since the probe used 5.00 mm tubes and silica tubing of this diameter was available. (The Perkin-Elmer R10 required tubes of 4.64 mm and this meant that 4 mm tubes of silica had to be used without spinning). Silica tubing was essential when proton nuclear magnetic resonance studies were carried out in liquid hydrogen chloride, due to the high vapour pressure of the solvent at ambient temperatures. The tubes, shown in Figure 2.12, were first loaded with a finely ground sample of the material under investigation before being degassed in vacuo overnight. After cooling the tube to  $-196^\circ\text{C}$  (liquid nitrogen bath) hydrogen chloride was condensed into a depth of about 2 cms, and then about 0.5 mmoles of tetramethylsilane was condensed into the tube as internal reference. The tube was sealed under vacuo, and then immersed in a solid carbon dioxide/acetone slurry ( $-84^\circ\text{C}$ ). It was at this stage that the tube was most likely to explode, but this only happened on a few occasions. Explosions at this stage are most likely due to the expansion of the solid. Once the hydrogen chloride had liquified the tube was immersed in a chlorobenzene slush bath ( $-45^\circ\text{C}$ ) for about ten minutes before immersing in a carbon tetrachloride slush bath ( $-23^\circ\text{C}$ ) and then allowed to warm to ambient temperature. In order to reduce the possibility of an explosion in the nmr probe spectra were recorded using a probe temperature of  $0^\circ\text{C}$  as soon after warming the tube to ambient temperature as was possible. The spectra were recorded in an identical manner to that used when recording nuclear magnetic resonance spectra using a more conventional solvent e.g. chloroform, and deuteriochloroform. Typical tubes are shown in Plate 2.6.

Figure 2.12

Silica Tubes for Containing Hydrogen Chloride  
for Nuclear Magnetic Studies



1. Iron pentacarbonyl
2. Di-iron nonacarbonyl
3. Tri-iron dodecacarbonyl
4. Ferrocene
5. Tetrakis( $\pi$ -cyclopentadienylcarbonyl iron (I))
6.  $\pi$ -Methylcyclopentadienyltricarbonyl manganese (I)
7. Bis( $\pi$ -cyclopentadienylcarbonyl nickel (I))
8. Bis( $\pi$ -cyclopentadienyldicarbonyl iron (I))



All other  $^1\text{H}$  nuclear magnetic resonance studies were carried out using sealed tubes which had had the solvent distilled in thus moisture and air were always excluded.

#### 2.4.3. Ultra violet/visible spectra

Ultra violet/visible spectra were recorded over the range 40,000-14,000  $\text{cm}^{-1}$  (250-700 nm) on a Pye-Unicam SP800. Extinction coefficients were calculated on the assumption that the Beer-Lambert Law was obeyed.

#### 2.4.4. $^{57}\text{Fe}$ Mossbauer studies

$^{57}\text{Fe}$  Mossbauer spectra were provided initially by Dr. Johnson and then during the later stages of the authors work by Dr. Dale of the Physio Chemical Measurements Unit, Harwell. All computer fits of the  $^{57}\text{Fe}$  Mossbauer spectra were carried out by Dr. Dale, and the author would like to express his thanks to Dr. Dale for all the help and assistance provided. The  $^{57}\text{Fe}$  Mossbauer studies are dealt with in Chapter 7.

#### 2.4.5. Electron spectroscopy studies

X-ray photoelectron spectra were recorded on an A.E.I. ES100 electron spectrometer, and were provided by Mr. D. Adams and Dr. D.T. Clark at this department.

Ultra violet photoelectron spectra were kindly provided by Perkin-Elmer. The results of the electron spectroscopy studies are dealt with in Chapter 7.

## 2.5. Analytical techniques

### 2.5.1. Estimation of carbon, hydrogen and nitrogen

Carbon, hydrogen and nitrogen were estimated by microcombustion on a Perkin-Elmer 240 elemental analyser. Air sensitive materials were loaded into a tared aluminium capsule in the inert atmosphere glove box, the capsule being sealed using a mechanical press situated in the glove box. The sealed aluminium capsule was then reweighed before placing in the Perkin-Elmer 240 elemental analyser and the analysis was then carried out using the normal techniques. Secondary analytical standards were analysed before and after unknown samples as checks. This was necessary as frequent trouble was experienced with the microswitches of the elemental analyser. If either of the reference standards analysed incorrectly the unknown sample would be resubmitted. This service was provided by this department's micro-analytical laboratory.

In some cases the analyses obtained for moisture sensitive materials were somewhat inaccurate but it must be taken into account that these materials are extremely hygroscopic and the sample weights involved were only 1-2 mg.

### 2.5.2. Estimation of chlorine, bromine and iodine

Chlorine, bromine and iodine were estimated using standard potentiometric techniques (76). Before the estimation was carried out the sample was fused with either sodium peroxide or sodium carbonate, the melt dissolved in a small quantity of distilled water and acidified with nitric acid.

### 2.5.3. Estimation of iron

The iron content of the samples was estimated by atomic absorption spectroscopy using an Eel 140 or Perkin-Elmer 403 instrument. The sample was wet oxidised using concentrated sulphuric and nitric acids prior to carrying out the iron estimation.

### 2.5.4. Estimation of phosphorus

Phosphorus was determined spectrophotometrically as the vanadomolybdophosphoric acid complex using a Pye-Unicam SP500 single beam ultra violet/visible spectrophotometer. Full details of the analytical method are given in Appendix B.

The halide, iron and phosphorus analyses were carried out by the author during his work at Warwick University, but were performed by the analytical laboratory of this department.

## 2.6. Preparation and purification of reagents

### 2.6.1. Hydrogen chloride

During the early stages of the author's work, hydrogen chloride was prepared from ammonium chloride and sulphuric acid in a Kipp's apparatus. The Kipp's apparatus was connected directly to the vacuum system using standard Quickfit ground glass joints lubricated with Apiezon M grease. All connections were evacuated before the tap on the Kipp's apparatus was opened and the hydrogen chloride allowed to pass through a trap immersed in a bath at  $-84^{\circ}$  (solid carbon dioxide/acetone slurry) into a trap immersed in a bath at  $-196^{\circ}\text{C}$  (liquid nitrogen).

When the trap immersed in liquid nitrogen was about half full (ca.  $15\text{ cm}^3$ ) the flow of hydrogen chloride was stopped and the traps isolated. Any non-condensable gas, mainly air which had been trapped in

the ammonium chloride lumps and carried over with the hydrogen chloride, was pumped away from the solid hydrogen chloride. The hydrogen chloride was then liquified by warming to  $-95^{\circ}\text{C}$  (toluene slush bath), refrozen to  $-196^{\circ}\text{C}$  (liquid nitrogen bath) and then pumped on; this process was repeated until no further non-condensable gas was released from the hydrogen chloride. The hydrogen chloride was then purified by distillation through two traps connected in tandem and cooled to  $-95^{\circ}\text{C}$  (toluene slush bath) into a third trap cooled to  $-196^{\circ}\text{C}$  (liquid nitrogen bath). The above process was repeated until the purified hydrogen chloride was water white and showed no turbidity in the liquid state ( $-95^{\circ}\text{C}$ , toluene slush bath). The infrared spectrum of the purified hydrogen chloride showed no absorption bands due to common impurities such as water and carbon dioxide (77).

For conductimetric studies the hydrogen chloride was further purified by distillation from a trap cooled to  $-131^{\circ}\text{C}$  (n-pentane slush bath) to a trap immersed in a liquid nitrogen bath ( $-196^{\circ}\text{C}$ ). Previous workers (32) have prepared hydrogen chloride in a high state of purity and found a specific conductivity of  $0.0035 \mu\text{mho cm}^{-1}$  at  $-85^{\circ}\text{C}$ . The specific conductivity of the hydrogen chloride prepared by the above technique was in the region of  $0.05 \mu\text{mho cm}^{-1}$  at  $-95^{\circ}\text{C}$  and was considered pure enough for the majority of experiments.

During the later stages of the authors work hydrogen chloride was obtained from British Drug Houses ( $\frac{1}{2}$  pound lecture bottles) and British Oxygen Company (20 pound cylinders) with a purity of 99.99%. Purification of the hydrogen chloride obtained commercially was carried out in an identical manner to that used for the purification of the hydrogen chloride prepared from the reaction of ammonium chloride and sulphuric acid in a Kipp's apparatus.

At  $-95^{\circ}\text{C}$  (toluene slush bath) hydrogen chloride is a clear colourless liquid when pure; any water impurity present is evident as a white turbidity (15). No samples of purified hydrogen chloride that were used in these studies ever showed signs of any turbidity.

The purified hydrogen chloride was stored as a gas in the three twenty litre bulbs mentioned previously, at pressures up to one atmosphere.

#### 2.6.2. Boron trichloride

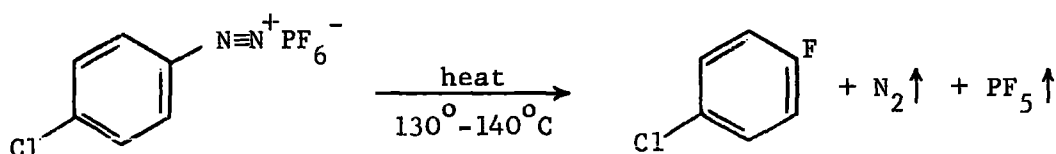
Boron trichloride was obtained from British Drug Houses and any chlorine impurity was removed by storing over mercury in a rotaflo ampoule (Figure 2.2) for twenty four hours. The boron trichloride was then purified by distillation from a trap maintained at  $-45^{\circ}\text{C}$  (chlorobenzene slush bath) into a trap maintained at  $-131^{\circ}\text{C}$  (n-pentane slush bath), any hydrogen chloride being collected in a third trap which was immersed in a liquid nitrogen bath ( $-196^{\circ}\text{C}$ ).

The purified boron trichloride was then transferred to a rotaflo ampoule for storage until required.

#### 2.6.3. Phosphorus pentafluoride

Phosphorus pentafluoride was prepared by the thermal decomposition of p-chlorobenzene diazonium hexafluorophosphate (78) commercially available as 'Phosfluorogen A' from Messrs J. Sas Ltd. The 'Phosfluorogen A' was mixed with sand and small glass rings in order to maintain a good thermal contact and minimise the amount of powder being carried into the vacuum system. The mixture was pumped on overnight in vacuo ( $10^{-4}$  mm Hg) to remove any moisture, before being heated to  $130^{\circ}$ - $140^{\circ}\text{C}$  for about two hours. A pressure of about half an atmosphere was

maintained in the system. The gases evolved were passed through three traps in tandem, the first two were cooled to  $-84^{\circ}\text{C}$  (solid carbon dioxide/acetone slurry) to remove the p-chlorofluorobenzene by-product. The third trap was cooled to  $-196^{\circ}\text{C}$  (liquid nitrogen bath) where the phosphorus pentafluoride was collected. The crude product was then purified by distillation from a trap maintained at  $-131^{\circ}\text{C}$  (n-pentane slush bath) into a trap immersed in a liquid nitrogen bath ( $-196^{\circ}\text{C}$ ). This process was repeated until the purified product showed no infrared absorption bands which were attributable to phosphorus trifluoride or phosphoryl fluoride (79). The purified phosphorus pentafluoride was finally transferred to a cold finger where it was stored frozen down ( $-196^{\circ}\text{C}$ , liquid nitrogen bath). Phosphorus pentafluoride was always used as soon after purification as possible to minimise hydrolysis from surface moisture on the glass.



#### 2.6.4. Chlorine

Chlorine was obtained from Imperial Chemical Industries and was purified by fractional distillation. After degassing the sample at  $-196^{\circ}\text{C}$  (liquid nitrogen bath) in a manner identical to that used for hydrogen chloride, the sample was warmed to  $-95^{\circ}\text{C}$  (toluene slush bath) and was pumped on for two or three minutes. The chlorine was then fractionally distilled from a trap cooled to  $-64^{\circ}\text{C}$  (chloroform slush bath) through a trap cooled to  $-78^{\circ}\text{C}$  (solid carbon dioxide/methylated spirits slurry) and collected in a trap cooled to  $-131^{\circ}$  (n-pentane slush bath).

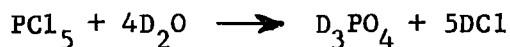
The purified chlorine was then stored in the five litre bulb mentioned previously at pressures of up to one atmosphere.

#### 2.6.5. Nitrosyl chloride

Nitrosyl chloride was obtained from British Drug Houses and was purified by fractional distillation. The sample was first cooled down to  $-84^{\circ}\text{C}$  (solid carbon dioxide/acetone slurry) and pumped on in vacuo for about ten minutes. After warming the sample to  $-45^{\circ}\text{C}$  (chlorobenzene slush bath) and distilled into a trap cooled to  $-84^{\circ}\text{C}$  (solid carbon dioxide/acetone slurry) discarding the last fraction. This process was repeated twice before the purified nitrosyl chloride was transferred to a rotaflo ampoule for storage until required. Infrared spectroscopic examination of the purified nitrosyl chloride showed that it was pure (80,81).

#### 2.6.6. Deuterium chloride

Deuterium chloride was kindly supplied by Dr. C.J. Ludman. The deuterium chloride had been prepared by the reaction of deuterium oxide with phosphorus pentachloride. Purification of the crude product was carried out in an identical manner to that used for the purification of hydrogen chloride.



Infrared spectra of the purified product showed a small amount of hydrogen chloride, estimated at less than five per cent (77).

#### 2.6.7. Sulphur dioxide

Sulphur dioxide was obtained from British Drug Houses and was poured into a rotaflo ampoule containing phosphorus pentoxide. The ampoule was cooled to  $-196^{\circ}\text{C}$  (liquid nitrogen bath), evacuated, and then

degassed by warming to  $-64^{\circ}\text{C}$  (chloroform slush bath) then cooling down to  $-196^{\circ}\text{C}$  (liquid nitrogen bath) in the manner described for hydrogen chloride. The ampoule was allowed to warm to ambient temperature and agitated regularly over a period of twenty four hours. After being cooled to  $-45^{\circ}\text{C}$  (chlorobenzene slush bath) the sulphur dioxide was distilled into a second ampoule which contained fresh phosphorus pentoxide. The ampoule was allowed to stand at ambient temperature with frequent agitation for a second period of twenty four hours. The ampoule was immersed in a chlorobenzene slush bath ( $-45^{\circ}\text{C}$ ) and the sulphur dioxide distilled into a trap cooled to  $-84^{\circ}\text{C}$  (solid carbon dioxide/acetone slurry). The sulphur dioxide was then degassed as described previously, before a final fractionation from  $-45^{\circ}\text{C}$  (chlorobenzene slush bath) to  $-84^{\circ}\text{C}$  (solid carbon dioxide/acetone slurry). The pure sulphur dioxide was then transferred to a rotaflo ampoule for storage until required.

Infrared spectra of the purified product only showed absorption bands attributable to sulphur dioxide (81).

#### 2.6.8. Bis( $\pi$ cyclopentadienyldicarbonyl iron(I))

Bis( $\pi$ cyclopentadienyldicarbonyl iron(I)) was obtained from Alfa Inorganics. The commercial product was dissolved in hot methylene chloride and hexane added dropwise until precipitation just occurred. On standing a pure product crystallised out. Found: C,47.39; H,2.84; Fe,31.43;  $\text{C}_{14}\text{H}_{10}\text{Fe}_2\text{O}_4$  requires C,47.51; H,2.85; Fe,31.56. The infrared spectra of the purified product was in agreement with that reported in the literature (82-84) for bis( $\pi$ cyclopentadienyldicarbonyl iron(I)).

2.6.9.  $\pi$ cyclopentadienyldicarbonyl iron(II) chloride

$\pi$ cyclopentadienyldicarbonyl iron(II) chloride was prepared from bis( $\pi$ cyclopentadienyldicarbonyl iron(I)) by the passage of oxygen through an ethanolic/chloroform solution acidified with hydrochloric acid as described by Piper et al (85). Found: C,39.66; H,2.36; Cl,17.1;  $C_7H_5ClFeO_2$  requires C,39.58; H,2.37; Cl,16.69. The infrared spectrum of the purified product agreed with that reported for  $\pi$ cyclopentadienyldicarbonyl iron(II) chloride by A.R. Manning (86).

2.6.10.  $\pi$ cyclopentadienyldicarbonyl iron(II) bromide

$\pi$ cyclopentadienyldicarbonyl iron(II) bromide was prepared by the addition of a solution of bromine in methylene chloride to a solution of bis( $\pi$ -cyclopentadienyldicarbonyl iron(I)) in methylene chloride (87). After evaporation of the solvent in vacuo, hexane was added dropwise to precipitate the product. The crude product was dissolved in hot methylene chloride and hexane added dropwise until precipitation just occurred. On standing a pure product crystallised out. Found: C,32.81; H,2.00; Br,31.5;  $C_7H_5BrFeO_2$  requires C,32.73; H,1.96; Br,31.11. The infrared spectra of the purified product agreed with that reported in the literature (86).

2.6.11.  $\pi$ -cyclopentadienyldicarbonyl iron(II) iodide

To a solution of bis( $\pi$ -cyclopentadienyldicarbonyl iron(I)) in methylene chloride was added a saturated solution of iodine in methylene chloride (88). The volume of solution was reduced in vacuo and hexane added to precipitate the product. The crude product was dissolved in hot methylene chloride and hexane added dropwise until precipitation just occurred. On standing a pure product crystallised out. Found: C,27.59; H,1.71; I,41.80;  $C_7H_5FeIO_2$  requires C,27.67; H,1.66; I,41.76.

The infrared spectrum of the purified product agreed with that reported in the literature (86).

#### 2.6.12. $\pi$ -cyclopentadienyltricarbonyl iron (II) chloride

$\pi$ -cyclopentadienyltricarbonyl iron(II) chloride was prepared from the reaction of sodium cyclopentadienyldicarbonyl iron (prepared from bis( $\pi$ -cyclopentadienyldicarbonyl iron(I)) and excess one per cent sodium amalgam) with ethyl chloroformate in tetrahydrofuran (89). After the reaction had been allowed to proceed for ten hours the solvent was removed in vacuo. The solid product was then extracted with five twenty  $\text{cm}^3$  portions of benzene. After filtering the benzene extracts, hydrogen chloride was passed through the solution for about twenty minutes. The pale yellow precipitate was filtered off and washed with ether. The crude product was dissolved in water and reprecipitated by the addition of acetone. After filtration the pale yellow solid was washed with acetone, ether and finally pentane and dried in vacuo. Found: C, 39.07; H, 2.14; Cl, 14.99;  $\text{C}_8\text{H}_5\text{ClFeO}_3$  requires C, 39.97; H, 2.10; Cl, 14.74. The infrared spectra of the purified material showed two carbonyl stretching absorptions at 2121 and 2068  $\text{cm}^{-1}$  in good agreement with those published for the  $\pi$ -cyclopentadienyltricarbonyl iron(II) cation (89).

#### 2.6.13. $\pi$ -cyclopentadienyldicarbonyl iron $\sigma$ -methyl

$\pi$ -cyclopentadienyldicarbonyl iron  $\sigma$ -methyl was prepared by treatment of a tetrahydrofuran solution of sodium  $\pi$ -cyclopentadienyldicarbonyl iron with excess methyl iodide (90). After removal of the solvent in vacuo the product was sublimed in vacuo. The product was sublimed immediately prior to use. The infrared spectra of the purified product agreed with that reported in the literature (86) for  $\pi$ -cyclopentadienyldicarbonyl iron  $\sigma$ -methyl.

#### 2.6.14. Tetrakis( $\pi$ -cyclopentadienylcarbonyl iron(I))

Tetrakis( $\pi$ -cyclopentadienylcarbonyl iron(I)) was first prepared by King (91) by the pyrolysis of bis( $\pi$ -cyclopentadienyldicarbonyl iron(I)) in refluxing xylene. When preparations were carried out in this laboratory using King's method (91) the yields were much lower than reported, however increased yields were obtained using the improved preparation given below.

Bis( $\pi$ -cyclopentadienyldicarbonyl iron(I)) (56.8 g., 0.16 mole) in xylene (500 cm<sup>3</sup>) was refluxed in a nitrogen atmosphere in a pyrex glass apparatus. The refluxing solution was irradiated using a 500 watt mercury discharge lamp placed about 10-15 cm from the apparatus.

Samples were taken from reaction mixture periodically, and after removal of the solvent in vacuo, the solid was examined by infrared spectroscopy. In this manner the disappearance of the carbonyl stretching absorptions of bis( $\pi$ -cyclopentadienyldicarbonyl iron(I)) and the appearance of the carbonyl stretching absorption of tetrakis( $\pi$ -cyclopentadienylcarbonyl iron(I)) was monitored. During the course of the reaction additional carbonyl stretching absorptions appeared and then finally disappeared. These carbonyl stretching absorptions were thought to be due to  $\pi$ -cyclopentadienyldicarbonyl iron  $\sigma$ -xylene. Isolation of this intermediate was carried out and is described later.

When no carbonyl stretching absorptions were observed in the sample taken from the reaction mixture, the reaction was allowed to cool, and the mercury discharge lamp switched off. This was usually after a period of five to eight days. The cold reaction mixture was filtered, and the residue washed with three twenty cm<sup>3</sup> portions of xylene and finally with hexane until the washings were colourless. Ferrocene was recovered from the filtrate in yields of up to about ten per cent.

The moist residue was transferred to the thimble of a soxhlet apparatus and extracted with methylene chloride until the washings were colourless or very pale green (this usually occurred after about twenty four hours). On cooling a pure product crystallised out. After reduction of the bulk of the filtrate in vacuo addition of hexane gave a second crop of pure crystals. Found: C,48.10; H,3.40; Fe, 37.50;  $C_{24}H_{20}Fe_4O_4$  requires C,48.38; H,3.38; Fe,37.49. The infrared spectrum of the pure product agreed with that reported by King (91). The yields of 5 reactions using the above procedure are given in Table 2.2. The above procedure required about nine days and gave yields of the order of forty two per cent compared with the literature preparation which required nineteen days and gave a yield of fourteen per cent.

Table 2.2.

Yields\* of Photolysis of  $[(\pi-C_5H_5)Fe(CO)_2]_2$

Expt. No.	Yield %	Reaction Time (days)
1	32	$8\frac{1}{2}$
2	44	$7\frac{1}{2}$
3	29	9
4	56	7
5	49	7

\* Yield based on  $[(\pi-C_5H_5)Fe(CO)_2]_2$

The major disadvantage of the photolysis method is that it is important to stop the irradiation at the earliest possible moment because over-irradiation was found to decrease the yield of tetrakis( $\pi$ -cyclopentadienylcarbonyl iron(I)) and increase the amount of ferrocene produced.

Isolation of the intermediate formed in the preparation of tetrakis( $\pi$ -cyclopentadienylcarbonyl iron(I)) was carried out as outlined below.

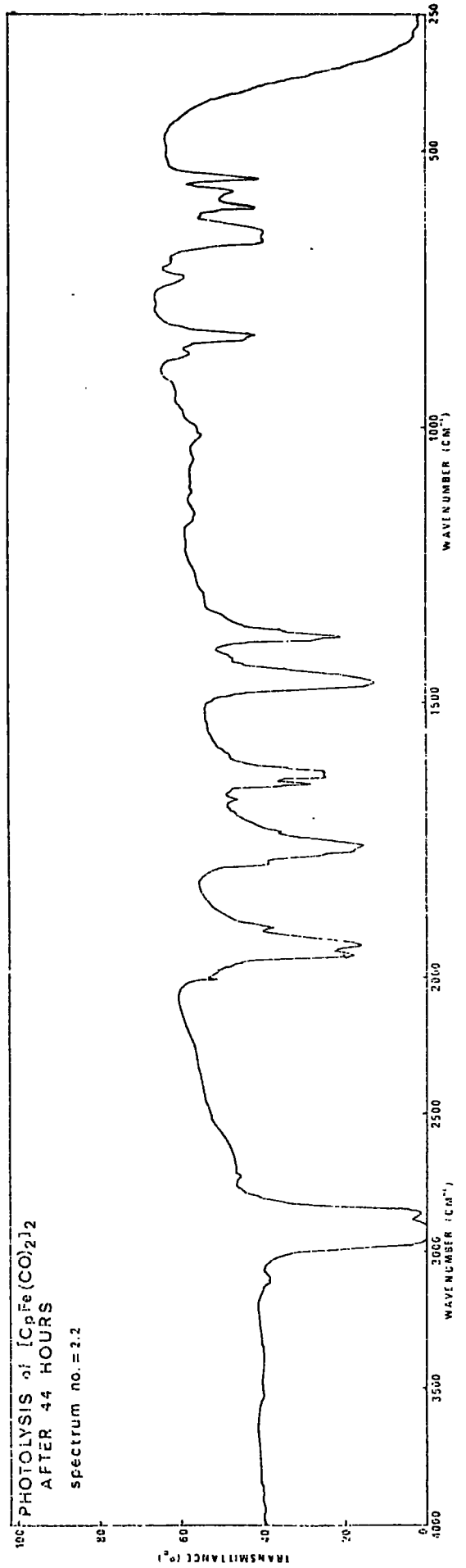
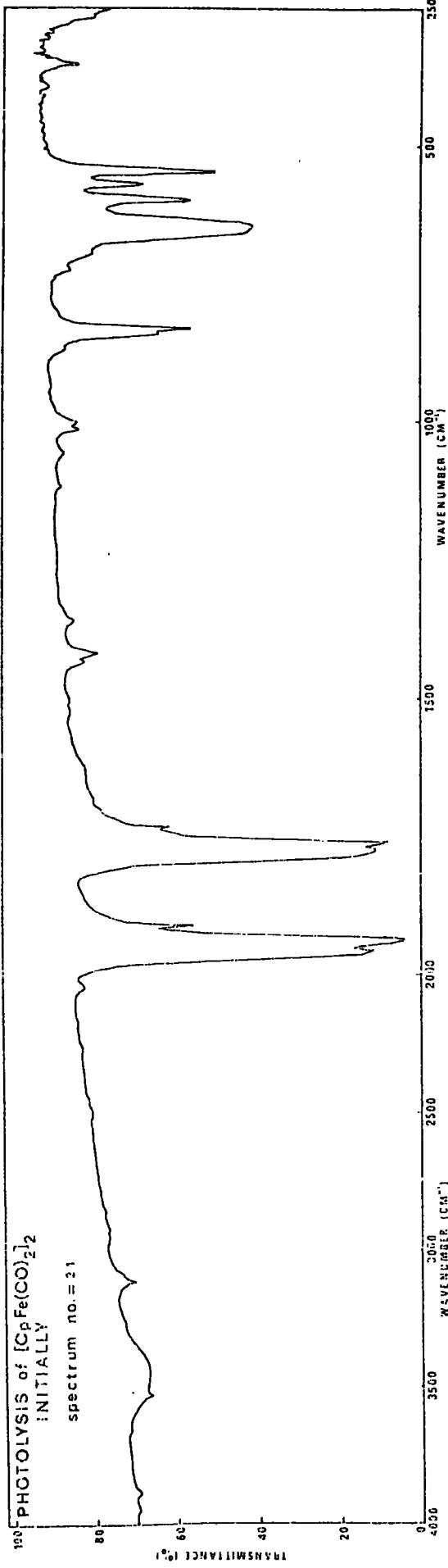
The preparation was carried out and monitored as described previously, except that the reaction was terminated when the intensity of the new carbonyl stretching absorption was at a maximum (after about two days). The cold reaction mixture was filtered washed with three twenty  $\text{cm}^3$  portions of xylene and finally hexane. The filtrate was then evaporated to dryness in vacuo, then the solid was extracted with hexane. After the volume of hexane had been reduced in vacuo, the components were separated by column chromatography on a polythene powder column. Removal of the solvent gave a pale yellow waxy solid with carbonyl absorptions at 1990 and 1940  $\text{cm}^{-1}$ . Found: C, 71.04; H, 6.76. Typical infrared spectra obtained whilst monitoring the reaction, of the intermediate product and of tetrakis( $\pi$ -cyclopentadienylcarbonyl iron(I)) are shown in spectra 2.1-2.4, 2.5 and 2.6 respectively.

#### 2.6.15. Tetracarbonyl iron dibromide

Tetracarbonyl iron dibromide was kindly supplied by Dr. M. Kilner and had been prepared by treatment of a solution of pentacarbonyl iron in hexane with a solution of bromine in hexane. Reduction of the bulk of the solution in vacuo followed by chilling yielded a pure crystalline product (92).

Photolysis of  $[\text{CpFe}(\text{CO})_2]_2$  Initially  
Spectrum number = 2.1

Photolysis of  $[\text{CpFe}(\text{CO})_2]_2$  After 44 hours  
Spectrum number = 2.2

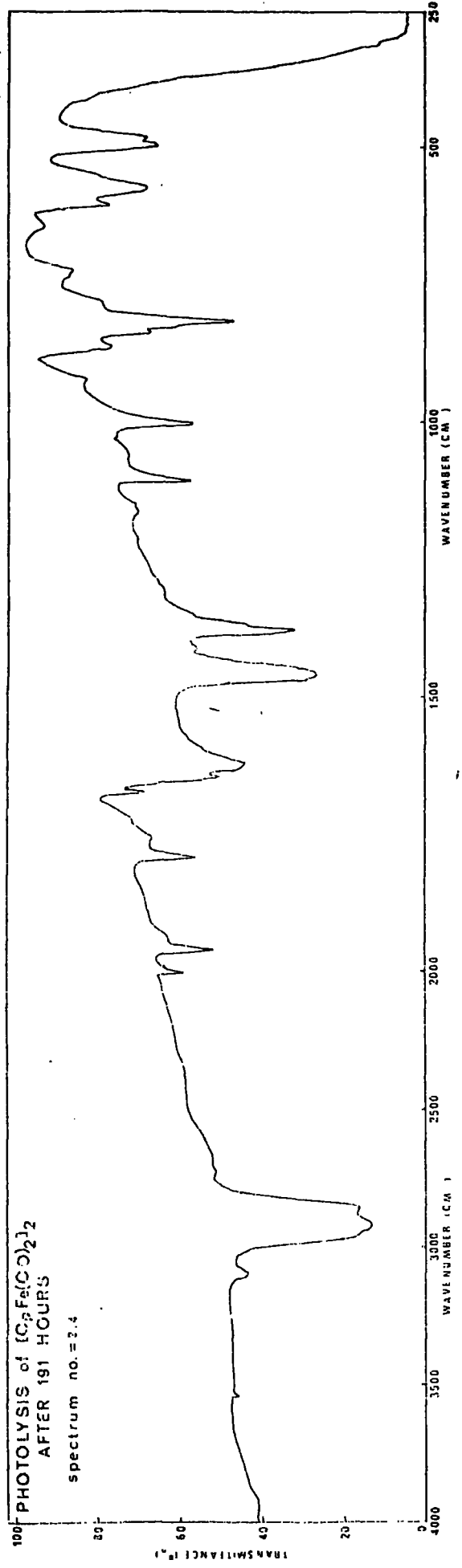
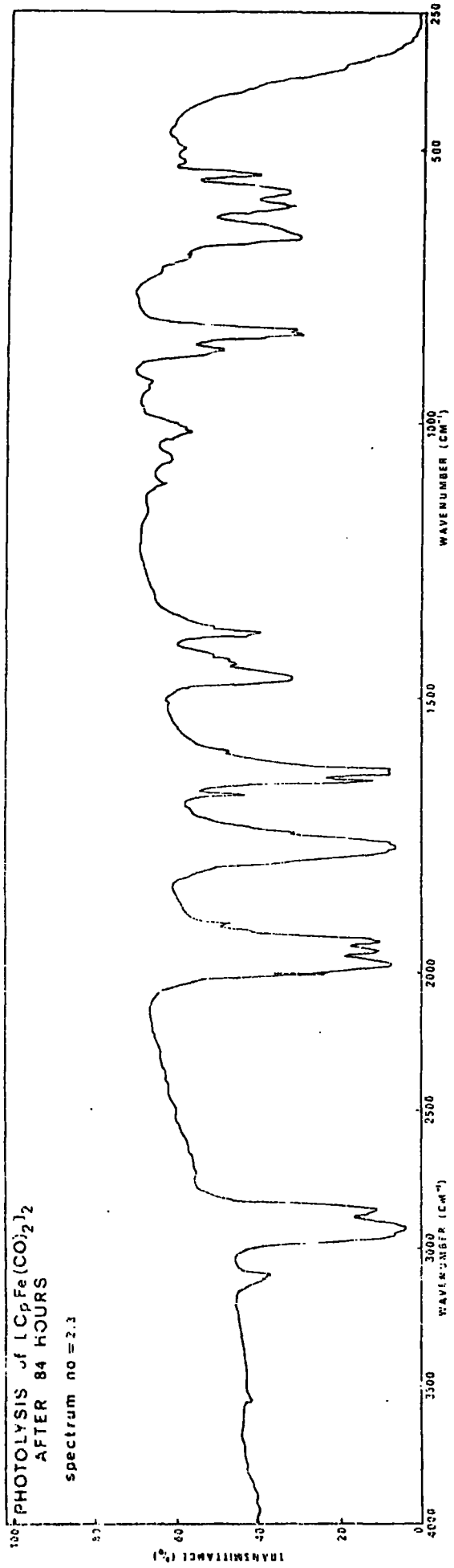


Photolysis of  $[\text{CpFe}(\text{CO})_2]_2$  After 84 hours

Spectrum number = 2.3

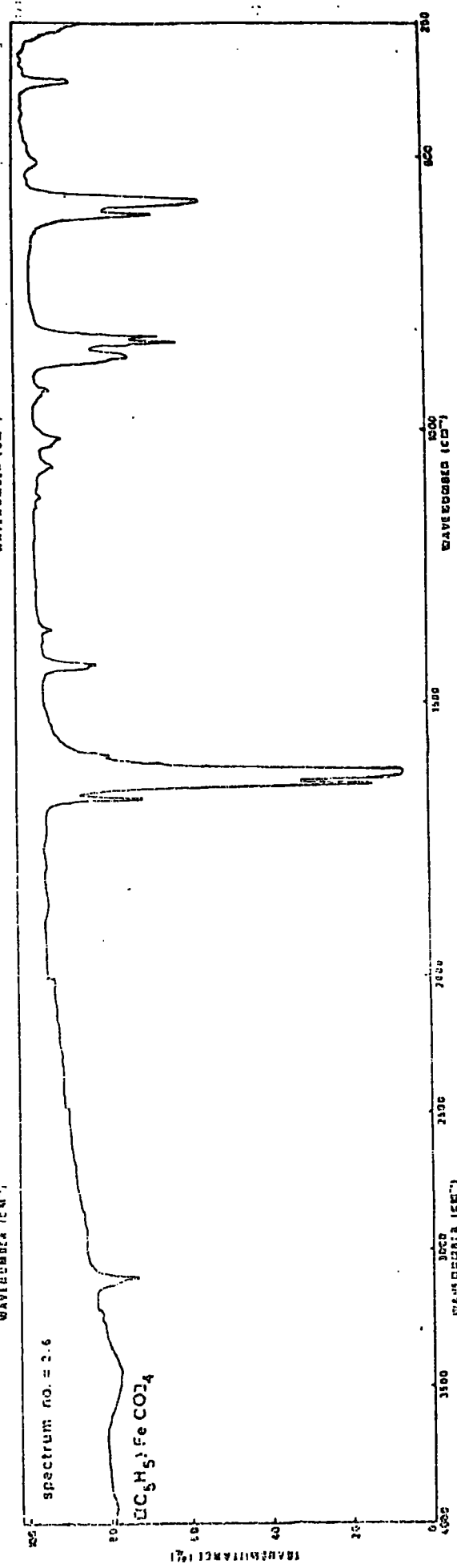
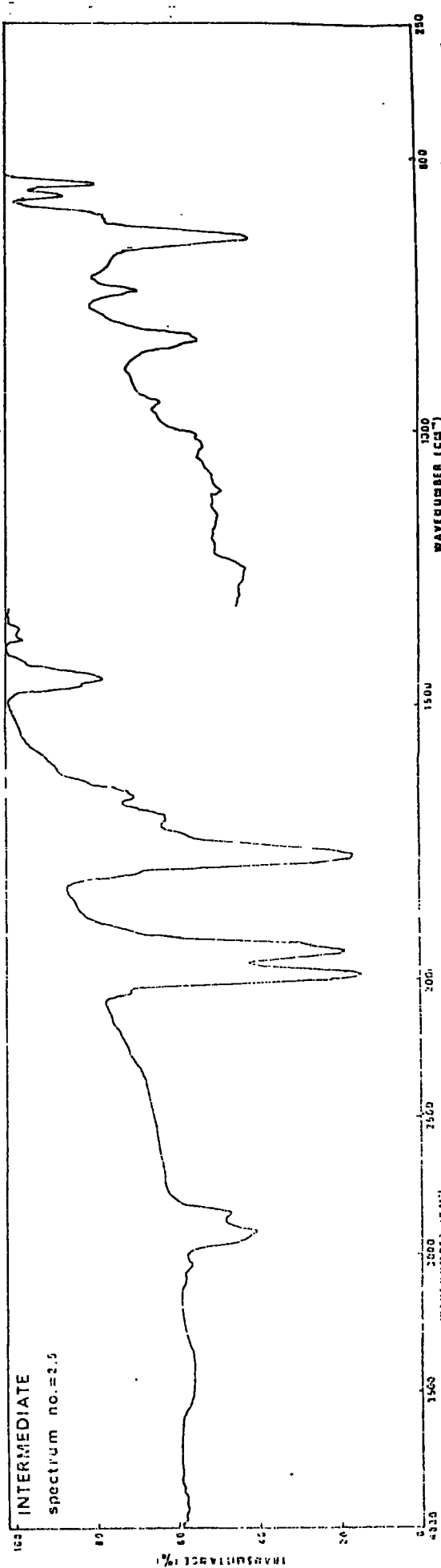
Photolysis of  $[\text{CpFe}(\text{CO})_2]_2$  After 191 hours

Spectrum number = 2.4



Photolysis of  $[\text{CpFe}(\text{CO})_2]_2$  Intermediate  
Spectrum number = 2.5

$[(\text{C}_5\text{H}_5)\text{Fe}(\text{CO})]_4$   
Spectrum number = 2.6



2.6.16. Tetracarbonyl iron di-iodide .

Tetracarbonyl iron di-iodide was kindly supplied by Dr. M. Kilner and had been prepared by treatment of a solution of pentacarbonyl iron in hexane with a saturated solution of iodine in hexane. Reduction of the bulk of the solution in vacuo followed by chilling yielded a pure crystalline product (92).

### CHAPTER 3

#### REACTIONS OF BIS( $\pi$ -CYCLOPENTADIENYLDICARBONYL IRON(I)) IN LIQUID HYDROGEN CHLORIDE

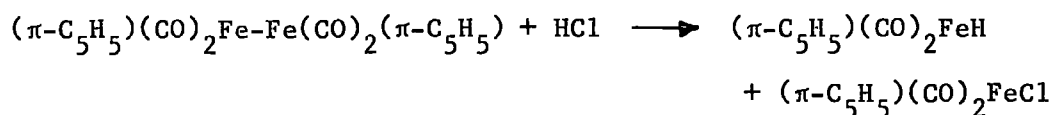
##### 3.1. Introduction

Bis( $\pi$ -cyclopentadienyldicarbonyl iron(I)) has been shown to be monobasic in sulphuric and trifluoroacetic acids (29). However, the published data for the  $\nu$  carbonyl stretching modes of bis( $\pi$ -cyclopentadienyldicarbonyl iron(I)) when dissolved in sulphuric acid was markedly different to those published for  $\pi$ -cyclopentadienyldicarbonyl iron(I)- $\mu$ -hydrogen  $\pi$ -cyclopentadienyldicarbonyl iron(I) hexafluorophosphate. Problems often encountered when sulphuric acid is used as the acidic medium are the difficulty in isolation of a solid product and that only solution techniques can be applied. Concentrated sulphuric acid is an oxidising agent and the possibility of oxidation of the neutral transition metal complexes is a real possibility. The study of the behaviour of bis( $\pi$ -cyclopentadienyldicarbonyl iron(I)) in liquid hydrogen chloride would not only enable protonation and oxidation to be studied independently but would also enable solid products to be obtained.

##### 3.2. Results and Discussion

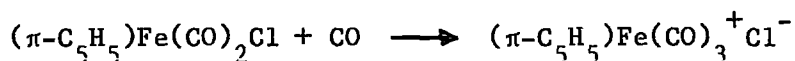
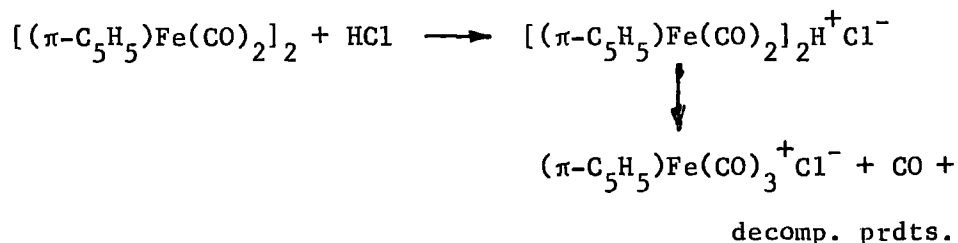
Bis( $\pi$ -cyclopentadienyldicarbonyl iron(I)) dissolved in liquid hydrogen chloride at  $-95^{\circ}\text{C}$  without loss of a measurable amount of carbon monoxide. The infrared spectra of the material recovered from the liquid hydrogen chloride solution showed weak absorptions at 2047 and  $1984\text{ cm}^{-1}$ , which were thought to be attributable to a small amount of  $\pi$ -cyclopentadienyldicarbonyl iron(II) chloride. The main proportion of the material recovered was unchanged starting material.

Bis( $\pi$ -cyclopentadienyldicarbonyl iron(I)) when dissolved in hydrogen chloride at ambient temperatures was observed to give two layers; a lower dark layer and an upper pale orange layer. No change occurred whilst the solution was stored in the absence of light, but in the presence of light a large amount of solid was deposited from the solution over a period of about eight days. After isolation of the solid material examination over the 2200-1900  $\text{cm}^{-1}$  region by infrared spectroscopy showed absorption bands at 2119s, 2070vs, 2043s and 1993s  $\text{cm}^{-1}$ . These results are consistent with the formation of  $\pi$ -cyclopentadienyldicarbonyl iron(II) chloride and  $\pi$ -cyclopentadienyltricarbonyl iron(II) chloride. The reaction was thought to occur by the addition of hydrogen chloride to the iron-iron bond in bis( $\pi$ -cyclopentadienyldicarbonyl iron(I)) to give  $\pi$ -cyclopentadienyldicarbonyl iron hydride and  $\pi$ -cyclopentadienyldicarbonyl iron(II) chloride.  $\pi$ -cyclopentadienyldicarbonyl iron hydride then reacts with a further molecule of hydrogen chloride to give  $\pi$ -cyclopentadienyldicarbonyl iron chloride and hydrogen gas (which was detected when the reaction ampoule was opened).



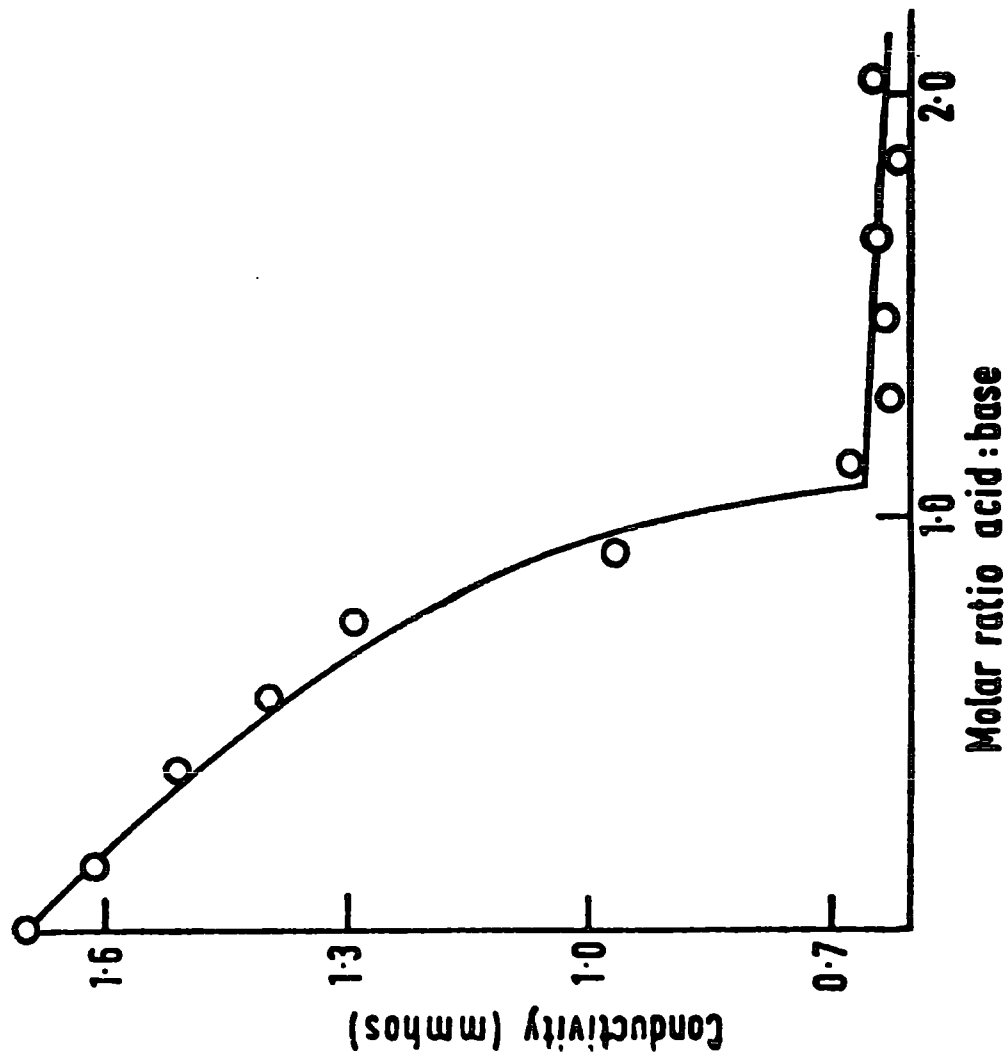
$\pi$ -cyclopentadienyldicarbonyl iron(I)- $\mu$ -hydrogen  $\pi$ -cyclopentadienyldicarbonyl iron chloride,  $[(\pi\text{-C}_5\text{H}_5)\text{Fe}(\text{CO})_2]_2\text{H}^+\text{Cl}^-$  would also be present in solution, formed by direct protonation of the starting material. Compounds of the type  $[(\pi\text{-C}_5\text{H}_5)\text{Fe}(\text{CO})_2]_2\text{X}^+\text{Y}^-$  (X = H, Cl, Br and I; Y =  $\text{PF}_6$ ,  $\text{BCl}_4$  and  $\text{ClO}_4$ ) are known to be thermally sensitive (from other studies carried out and discussed later) and decompose to give the

$\pi$ -cyclopentadienyltricarbonyl iron(II) cation,  $(\pi\text{-C}_5\text{H}_5)\text{Fe}(\text{CO})_3^+$ , as the only carbonyl compound. Carbon monoxide was also formed during the reaction of bis( $\pi$ -cyclopentadienyldicarbonyl iron(I)) with hydrogen chloride, and it has been reported in the literature (93) that  $\pi$ -cyclopentadienyldicarbonyl iron chloride reacts with carbon monoxide under pressure to give the  $\pi$ -cyclopentadienyltricarbonyl iron(II) cation. The  $\pi$ -cyclopentadienyltricarbonyl iron(II) chloride formed in the reaction of bis( $\pi$ -cyclopentadienylcarbonyl iron(I)) with hydrogen chloride could have been produced by either of the two routes mentioned above and it is probable that both routes gave rise to the observed product.



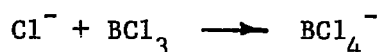
A solution of bis( $\pi$ -cyclopentadienyldicarbonyl iron(I)) in liquid hydrogen chloride has a molar conductance of  $40 \text{ cm}^2 \text{ ohm}^{-1} \text{ mole}^{-1}$  for a 0.015M solution, which is of the same order as that observed for a solution of tetramethylammonium chloride in hydrogen chloride (molar conductance for a 0.14 molar solution  $31.1 \text{ cm}^2 \text{ ohm}^{-1} \text{ mole}^{-1}$  (15)). A conductimetric titration with boron trichloride shows a break at a molar ratio 1:1 (Fig.3.1). Although a break at the 1:1 molar ratio can indicate either salt or adduct formation, the facts that the conductance had fallen with the addition of boron trichloride and that

Figure 3.1

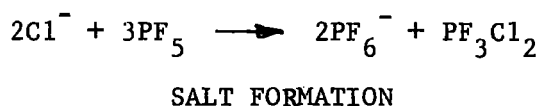
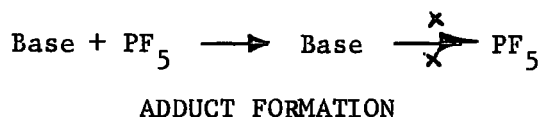


The conductimetric titration of  $\text{BCl}_3$  against  $[(\pi\text{-C}_5\text{H}_5)\text{Fe}(\text{CO})_2]_2$  in liquid hydrogen chloride

even after the 1:1 molar ratio the conductance was still fairly high supported the formation of a salt rather than an adduct. The fall in conductivity is consistent with replacement of a more mobile ion with a less mobile ion (i.e. replacement of a chloride ion with a tetrachloroborate ion).



During the later stages of the titration precipitation was also observed which would also tend to reduce the conductivity. Conductimetric titrations using phosphorus pentafluoride as the acid failed to react to completion during the time scale used. Hence the fact that the end point occurs at 1:1 molar ratios for adduct formation and at 1.5:1 molar ratio (acid:base) for salt formation could not be utilised.



Infrared spectra of the purified products obtained from reaction of bis( $\pi$ -cyclopentadienyldicarbonyl iron(I)) with the Lewis acids and boron trichloride and phosphorus pentafluoride in liquid hydrogen chloride showed absorption bands characteristic of the tetrachloroborate (691, 659  $\text{cm}^{-1}$ ) (17) and hexafluorophosphate (845, 555  $\text{cm}^{-1}$ ) (94) ions respectively. No absorption band in the infrared spectrum could be assigned to a Fe-H stretching mode, although previous workers (29) had suggested a weak band observed at 1767  $\text{cm}^{-1}$  as possibly the Fe-H stretching mode. A weak band was also observed in a sample of  $\pi$ -cyclopentadienyldicarbonyl iron- $\mu$ -deuterium- $\pi$ -cyclopentadienyldicarbonyl iron hexafluorophosphate and was assigned as a  $\nu$  C-O stretching mode of

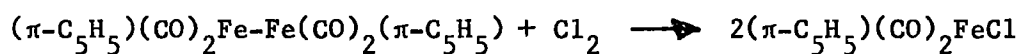
the bis( $\pi$ -cyclopentadienyldicarbonyl iron(I)) starting material. Infrared spectroscopic examination of the decomposition of  $\pi$ -cyclopentadienyldicarbonyl iron- $\mu$ -hydrogen  $\pi$ -cyclopentadienyldicarbonyl iron hexafluorophosphate showed that the band at  $1767\text{ cm}^{-1}$  increased with time confirming that it was not a Fe-H stretching mode.

The infrared spectrum of the  $\pi$ -cyclopentadienyldicarbonyl iron- $\mu$ -hydrogen  $\pi$ -cyclopentadienyldicarbonyl iron cation is shown in spectra 3.1 and 3.2 as the tetrachloroborate and hexafluorophosphate salts respectively.

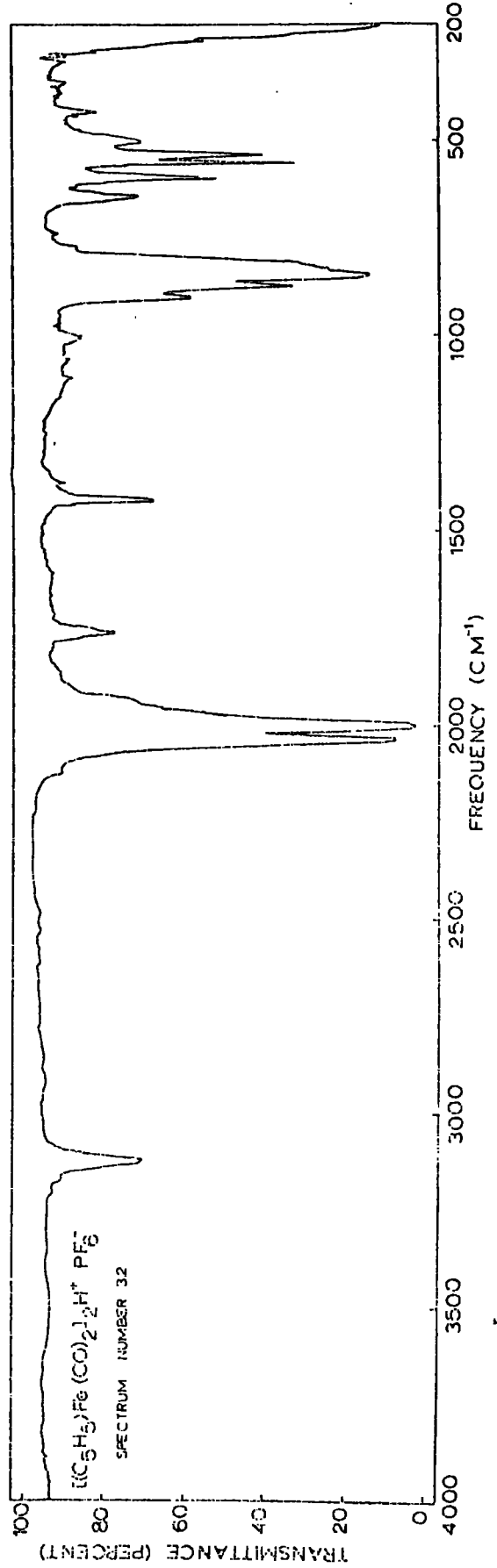
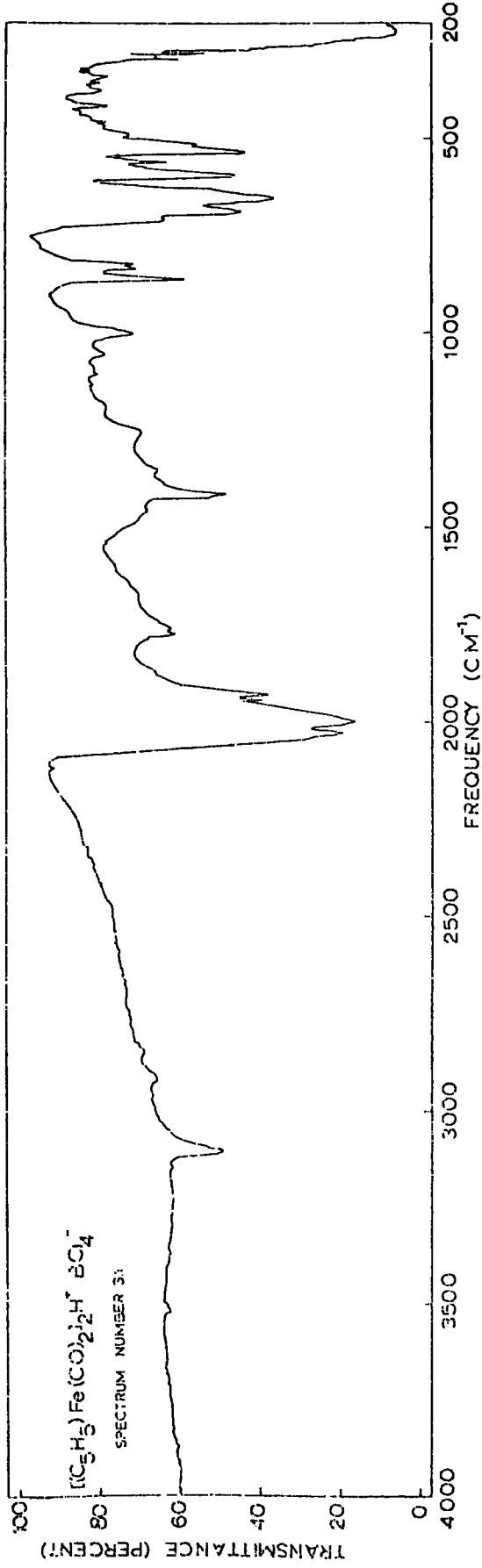
Reaction of bis( $\pi$ -cyclopentadienyldicarbonyl iron(I)) with the oxidising agents nitrosyl chloride and chlorine could not be followed conductimetrically since the reactions gave mixtures of products and individual conductances were time variable and not reproducible.

Reaction of nitrosyl chloride with a solution of bis( $\pi$ -cyclopentadienyldicarbonyl iron(I)) in hydrogen chloride gave  $\pi$ -cyclopentadienyldicarbonyl iron chloride as the only identifiable products. All attempts to identify a green paramagnetic solid soluble in acetone and insoluble in methylene chloride failed.

The reaction of chlorine with a solution of bis( $\pi$ -cyclopentadienyldicarbonyl iron(I)) in hydrogen chloride caused extensive decomposition with the formation of some  $\pi$ -cyclopentadienyldicarbonyl iron chloride and  $\pi$ -cyclopentadienyltricarbonyl iron chloride. The  $\pi$ -cyclopentadienyldicarbonyl iron chloride was formed by the addition of one molecule of chlorine to the iron-iron bond in the starting material.



The  $\pi$ -cyclopentadienyltricarbonyl iron chloride may have been formed either directly by the action of chlorine on bis( $\pi$ -cyclopentadienyl-



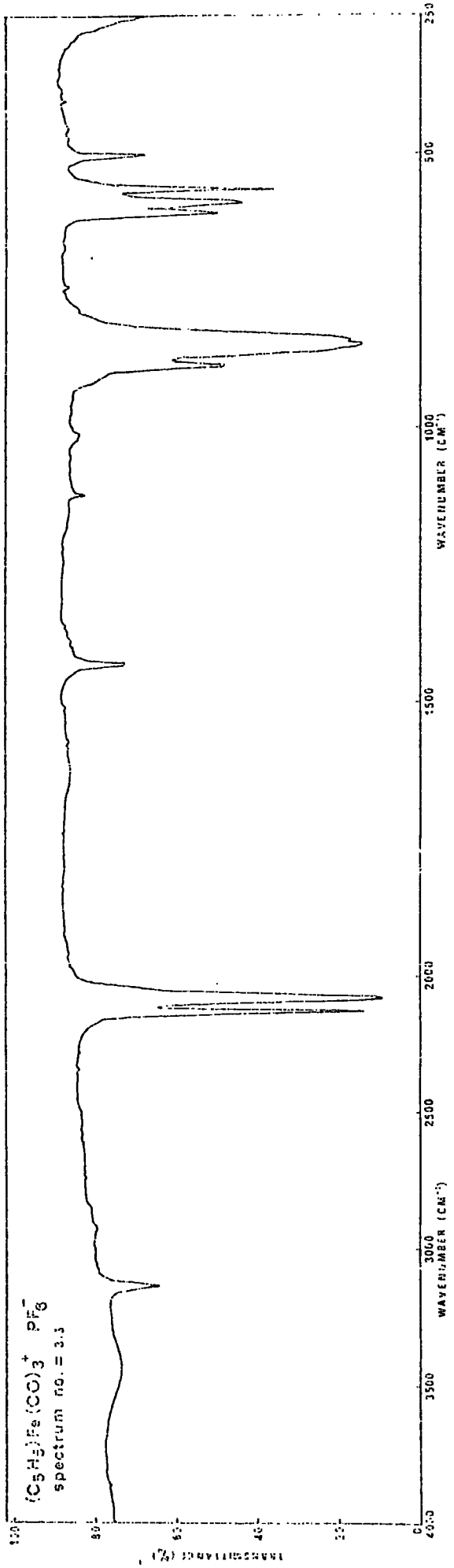
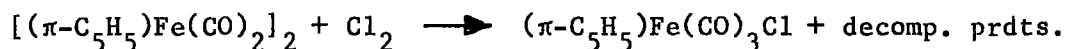


Table 3.1

Infrared of the  $\pi$ -cyclopentadienyldicarbonyl iron- $\mu$ -hydrogen  
 $\pi$ -cyclopentadienyldicarbonyl iron cations in the 4000-300  $\text{cm}^{-1}$  region

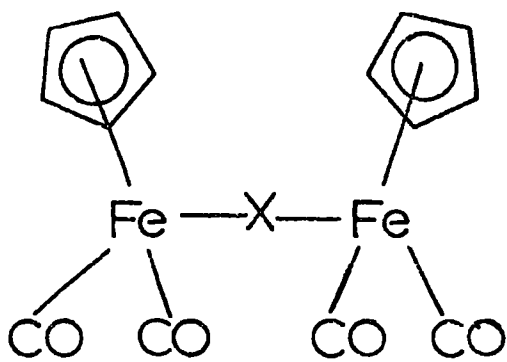
Assignment	$[(\pi\text{-C}_5\text{H}_5)\text{Fe}(\text{CO})_2]_2\text{H}^+\text{BCl}_4^-$	$[(\pi\text{-C}_5\text{H}_5)\text{Fe}(\text{CO})_2]_2\text{H}^+\text{PF}_6^-$
C-H Stretch	3110w	3110w
$\nu\text{C-O}$	2030s 2000s	2032s 2002s
C-C Stretch	1420m	1420m
		1112vw
	1060w	1060w
	1010w	1010w
	1000w	1000w
$\nu_3 \text{PF}_6^-$		905m 874m 845s 820sh
	862m	
$\nu_3 \text{BCl}_4^-$	691s	
$\nu_1 + \nu_4 \text{BCl}_4^-$	659s	
		645m
	593s	595s
$\nu_4 \text{PF}_6^-$		555s
	532s	536s
		496w
	416w	420w

dicarbonyl iron(I)) or from the reaction of  $\pi$ -cyclopentadienyldicarbonyl iron chloride with carbon monoxide, which had been evolved during the reaction. It is perhaps significant that in the reaction using nitrosyl chloride as oxidant no  $\pi$ -cyclopentadienyltricarbonyl iron chloride was formed although carbon monoxide was present.

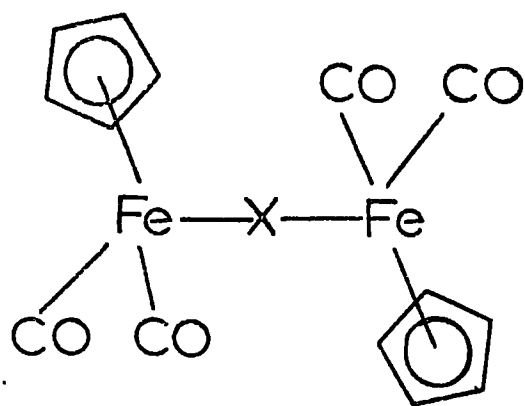


$\nu$  C-O stretching modes have been extensively used as probes into the structure and environment of carbonyl containing compounds (95). In a large proportion of carbonyl compounds only the symmetry of the carbonyl groups around the metal atom need be considered, rather than consideration of the overall symmetry of the carbonyl compound, e.g.  $(\pi\text{-CH}_3\text{C}_5\text{H}_4)\text{Mn}(\text{CO})_3$   $C_{3v}$ .

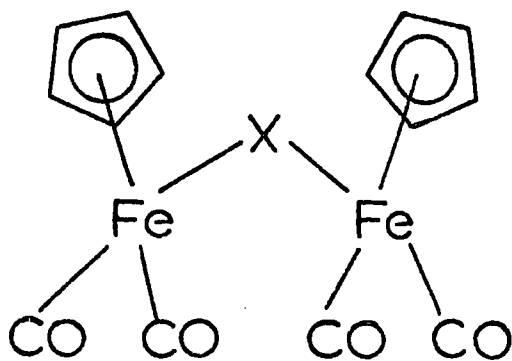
For compounds of the type  $[(\pi\text{-C}_5\text{H}_5)\text{Fe}(\text{CO})_2]_2\text{X}^+$ , (X = H, Cl, Br and I) the structures (I)-(VIII) are possible. Structures (I) and (II) contain a symmetrical linear Fe-X-Fe bond and are related by cis/trans isomerism. Structures (III) and (IV) contain a symmetrical bent Fe  Fe bond and are related by cis/trans isomerism. Four other analogous structures are also possible, which have asymmetric Fe-X-Fe bonds and are intermediate between structures (I)-(IV) and structures (V)-(VIII). The latter four structures contain a Fe-X bond, the atom X being bonded first to one iron atom and then to the other iron atom. Consideration of structures (I) to (IV), two carbonyl absorptions would be expected, a symmetric and asymmetric stretching mode. If coupling from one  $(\pi\text{-C}_5\text{H}_5)\text{Fe}(\text{CO})_2$  unit to the other  $(\pi\text{-C}_5\text{H}_5)\text{Fe}(\text{CO})_2$  unit occurs or the solid contains a mixture of cis and trans isomers four carbonyl stretching absorptions would be expected. For all other expected structures



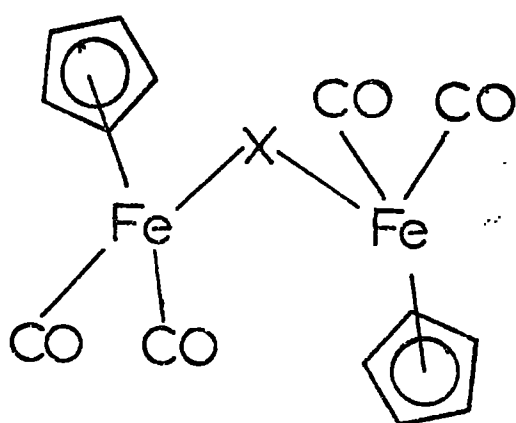
I



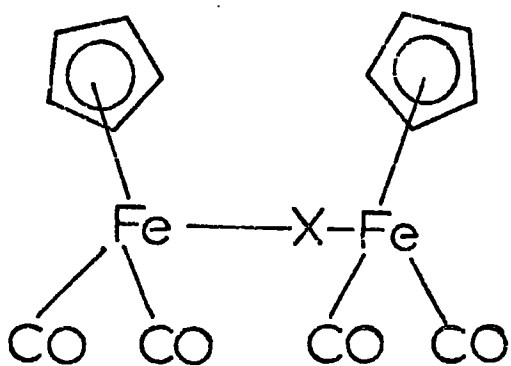
II



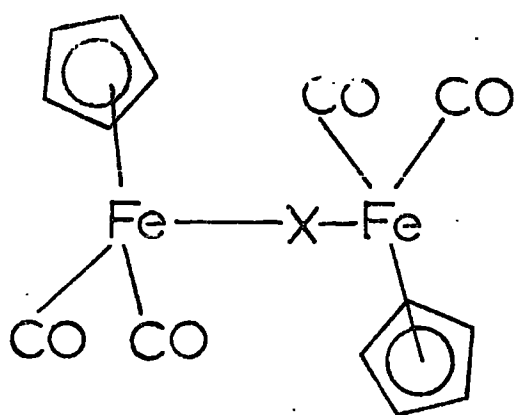
III



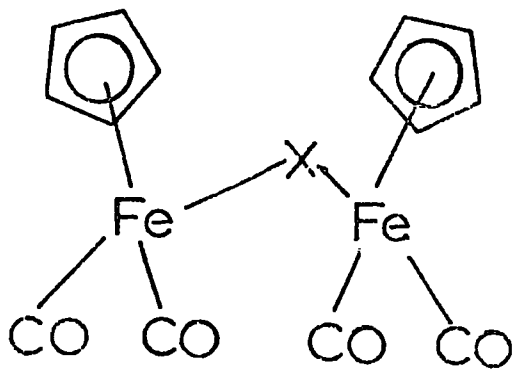
IV



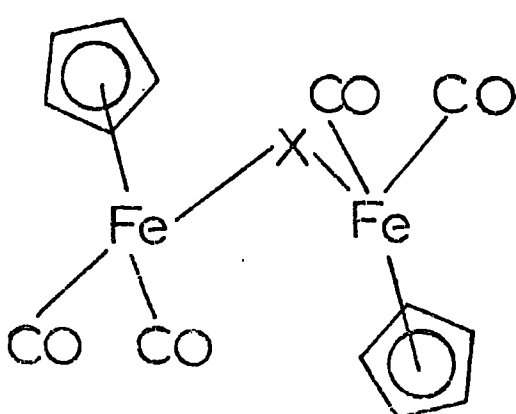
V



VI

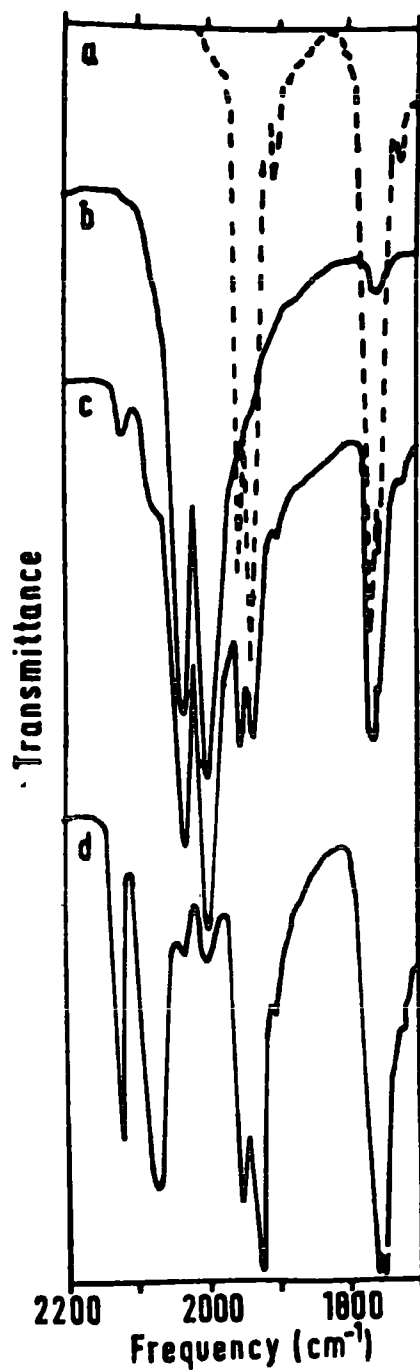


VII



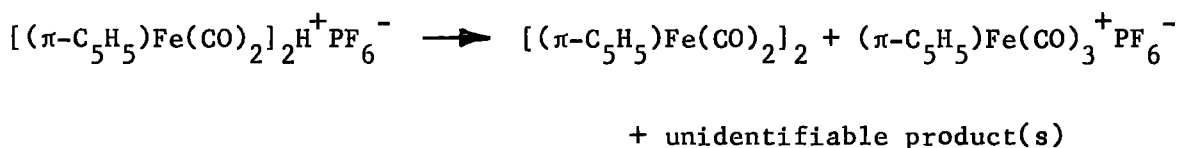
VIII

Figure 3.2



The i.r. spectrum of  $[(\pi\text{-C}_5\text{H}_5)\text{Fe}(\text{CO})_2]_2\text{H}+\text{PF}_6^-$  in the carbonyl region as a function of time. a,  $[(\pi\text{-C}_5\text{H}_5)\text{Fe}(\text{CO})_2]_2$ , b,  $[(\pi\text{-C}_5\text{H}_5)\text{Fe}(\text{CO})_2]_2\text{H}+\text{PF}_6^-$  initially, c, the same after 2 h in the i.r. beam, and d, the same after 18 h in the i.r. beam

i.e. (V) to (VIII) and those containing an asymmetric Fe-X-Fe bond four carbonyl absorptions would be expected. The fact that three carbonyl absorptions have been reported for species of the type  $[(\pi\text{-C}_5\text{H}_5)\text{Fe}(\text{CO})_2]_2\text{X}^+\text{Y}^-$  ( $\text{X} = \text{H}, \text{Cl}, \text{Br}$  and  $\text{I}$ ,  $\text{Y} = \text{BF}_4, \text{PF}_6, \text{B}(\text{C}_6\text{H}_5)_4, \text{I}_3$ ) (29, 96-101) and that for the case where  $\text{X} = \text{H}$  a shift of up to  $54 \text{ cm}^{-1}$  was observed on going from a nujol mull of the hexafluorophosphate salt to a solution in sulphuric acid (29) warranted further investigation. The infrared spectrum of  $\pi$ -cyclopentadienyldicarbonyl iron- $\mu$ -hydrogen  $\pi$ -cyclopentadienyldicarbonyl iron hexafluorophosphate reported by Davies et al (29) shows  $\nu$  carbonyl stretching absorptions at 2138s, 2068sh, 2050vs and  $2018\text{vs cm}^{-1}$ . The sample of  $\pi$ -cyclopentadienyldicarbonyl iron- $\mu$ -hydrogen  $\pi$ -cyclopentadienyldicarbonyl iron hexafluorophosphate prepared by the author only showed  $\nu$  carbonyl stretching absorptions at 2032s and  $2002\text{s cm}^{-1}$  when examined in a KCl pressed disc.  $\nu$  carbonyl stretching absorptions at 2120m,  $2070\text{s cm}^{-1}$  as well as the  $\nu$  carbonyl absorptions attributable to bis( $\pi$ -cyclopentadienyldicarbonyl iron(I)) were observed to appear with time indicating formation of  $\pi$ -cyclopentadienyltricarbonyl iron cation ( $\nu$  CO 2122s and  $2070 \text{ vs cm}^{-1}$ ) (89) as well as deprotonation (Fig.3.2).



Solutions of bis( $\pi$ -cyclopentadienyldicarbonyl iron(I)) in anhydrous acids were examined over the region  $2200\text{-}1700 \text{ cm}^{-1}$  by infrared spectroscopy. The results are shown in Table 3.2. Deprotonation was eliminated since excess acid was always present and the results confirmed that the  $\pi$ -cyclopentadienyl tricarbonyl iron cation was the only

Table 3.2

Infrared spectra of  $\pi$ -cyclopentadienyl iron dicarbonyl dimer in anhydrous acids in the region 2200-1700  $\text{cm}^{-1}$ . (Mulls between polythene plates)

Mulling Agent	$\nu_{\text{CO}}$ frequencies $\text{cm}^{-1}$	Remarks
$\text{H}_2\text{SO}_4$	2122* 2066* 2035† 2012†	Ref.2 2068(ms), 2045(vs), 2022(vs).
$\text{H}_2\text{SO}_4/20\% \text{SO}_3$	2124* 2068* 2039† 2013†	
$\text{CH}_3\text{SO}_3\text{H}$	2122* 2062* 2040† 2010†	
$\text{HSO}_3\text{Cl}$	2123* 2068* 2034† 2012†	
$\text{CF}_3\text{COOH}^\ddagger$	2125 2063	Poor mull, solvent evaporated, 2063 band very broad
$\text{H}_2\text{PO}_3\text{F}^\ddagger$	2124 2070 2037 2015	
$\text{HPO}_2\text{F}_2^\ddagger$	2123 2068 2040 2019	

\* Bands increasing in intensity with time

† Bands decreasing in intensity with time

‡ Effect of time not studied

carbonyl compound formed. The formation of the  $\pi$ -cyclopentadienyltricarbonyl iron cation was confirmed by isolation as the hexafluorophosphate salt from a methane sulphonic acid solution of bis( $\pi$ -cyclopentadienyl-dicarbonyl iron(I)). The product isolation was identical with that described in the literature (89) and its infrared spectrum is shown in spectrum 3.3.

A kinetic study following the appearance of the absorption band at  $2122 \text{ cm}^{-1}$  showed that the reaction of bis( $\pi$ -cyclopentadienyl-dicarbonyl iron(I)) with methanesulphonic acid was first order with a half life of fifteen minutes and a rate constant of  $4.6 \times 10^{-2} \text{ min}^{-1}$  at about  $40^\circ\text{C}$ .

The appearance of only two carbonyl absorption bands in the infrared spectrum of the  $\pi$ -cyclopentadienyl-dicarbonyl iron- $\mu$ -hydrogen  $\pi$ -cyclopentadienyl-dicarbonyl iron cation suggests that the two  $\pi$ -cyclopentadienyl-dicarbonyl iron groups are identical and are related by a centre of symmetry.

The results of  $^1\text{H}$  nuclear magnetic resonance studies in various strong anhydrous acids are given in Table 3.3. The occurrence of the Fe-H resonance indicates that the proton experiences more deshielding than is normal when attached to a single iron atom. In  $(\pi\text{-C}_5\text{H}_5)_2\text{FeH}^+$  the Fe-H resonance is observed at  $\tau$  11.89-12.10 (56) and in  $(\pi\text{-C}_5\text{H}_5)\text{Fe}(\text{CO})_2\text{H}$ , the Fe-H is observed at  $\tau$  21.91 (102). The Fe-H absorption is sharp and occurs at the same position in all three acids investigated suggesting that exchange with the solvent must be slow. Confirmation of this comes from the fact that preparation of  $[(\pi\text{-C}_5\text{H}_5)\text{Fe}(\text{CO})_2]_2\text{D}^+\text{PF}_6^-$  could not be carried out by an exchange reaction using  $[(\pi\text{-C}_5\text{H}_5)\text{Fe}(\text{CO})_2]_2\text{H}^+\text{PF}_6^-$  and  $\text{DCl}$ .

Davison et al (29) also studied the ions  $[(\pi\text{-C}_5\text{H}_5)\text{Mo}(\text{CO})_3]_2\text{H}^+$ ,  $[(\pi\text{-C}_5\text{H}_5)\text{W}(\text{CO})_3]_2\text{H}^+$  and  $[(\pi\text{-C}_5\text{H}_5)_2\text{MoW}(\text{CO})_6]\text{H}^+$ . The isotope  $^{183}\text{W}$  has a

Table 3.3

<sup>1</sup>H Nuclear Magnetic Resonance of Bis( $\pi$ -cyclopentadienyldicarbonyl Iron(I)) in Anhydrous Acids  
 (at 60 Mc/sec., relative intensities in parentheses)

Solvent	Absorptions		Notes
	$\tau(\pi\text{-C}_5\text{H}_5)$	$\tau\text{FeH}$	
H <sub>2</sub> SO <sub>4</sub>	4.76 (10)	36.30 (1)	* Measured at 56.45 Mc/sec.
CF <sub>3</sub> COOH	4.76 (10)	36.30 (1)	* Measured at 56.45 Mc/sec.
CF <sub>3</sub> COOH	4.77 (10)	36.60 (0.95)	Measured on P.E., R10
HCl	4.77 (10)	36.6 (0.87)	Measured on P.E., R10
HCl	4.76 (10)	36.6 (0.91)	Varian A56/60D

\* A. Davison, W. McFarlane, L. Pratt and G. Wilkinson, J. Chem. Soc., 1962, 3653.

spin of  $\frac{1}{2}$  and can therefore couple directly with the proton to give rise to satellite structure of the W-H absorption. Unfortunately the sensitivity of the instrument was not sufficient to observe all the expected satellite bands it was however possible to show that the proton was associated with both tungsten atoms. Examination of the hydrides  $[M_2H(CO)_{10}]^-$  (M = Cr, Mo and W) was carried out by Hayter (103) using infrared,  $^1H$  nuclear magnetic resonance and X-ray diffraction techniques. Hayter concluded that a linear M-H-M bond fitted the evidence best. Similar environments for the hydrogen atom in  $[(\pi-C_5H_5)W(CO)_3]_2H^+$  and  $[W_2H(CO)_{10}]^-$  would be expected since the  $^1H$  nuclear magnetic resonance data for the W-H resonance is similar. The  $[(\pi-C_5H_5)Fe(CO)_2]_2H^+$  ion would also be expected to be very similar to the chromium group compounds and the  $^1H$  nuclear magnetic resonance studies show a marked similarity to those for the tungsten compounds previously described.

### 3.3. Experimental

#### 3.3.1. Reaction of bis( $\pi$ -cyclopentadienyldicarbonyl iron(I)) with liquid hydrogen chloride

##### (a) at $-95^\circ C$

Bis( $\pi$ -cyclopentadienyldicarbonyl iron(I)) (0.0425 g., 0.120 mmoles) was degassed overnight in vacuo ( $10^{-4}$  mm Hg). Hydrogen chloride (7 cm<sup>3</sup>, 0.25 mole) was condensed on to the solid cooled to  $-196^\circ C$  (liquid nitrogen bath), on warming to  $-95^\circ C$  (toluene slush bath) a homogeneous solution was obtained. The reaction was allowed to proceed for one hour before cooling to  $-196^\circ C$  (liquid nitrogen bath), no detectable amount of carbon monoxide or hydrogen had been evolved. All volatile materials were removed at low temperatures before warming to room temperature. No increase

in weight was observed and the infrared spectra of the product showed that it was primarily starting material with a trace of  $\pi$ -cyclopentadienyldicarbonyl iron(II) chloride.

(b) at ambient temperatures

Bis( $\pi$ -cyclopentadienyldicarbonyl iron(I)) (1.05 g., 0.003 moles) was degassed in vacuo overnight. Hydrogen chloride (8 cm<sup>3</sup>, 0.30 moles) was distilled into the silica ampoule cooled to -196°C (liquid nitrogen bath) before being sealed. At room temperature two layers were evident; a lower dark layer and a pale orange upper layer. No apparent change was observed over a period of three weeks while the ampoule was stored in the absence of light. Ten days exposure to sunlight caused a large amount of precipitate to be deposited. After cooling to -196°C (liquid nitrogen bath) the ampoule was opened into the vacuum system. Infrared spectra of the gas showed the presence of carbon monoxide. Hydrogen was also assumed to be present due to the fact that the pressure of gas evolved was about 24 cm Hg in 80 cm<sup>3</sup> (carbon monoxide has a vapour pressure of 10 cm at -196°C (74)). All volatile materials were removed at low temperature in vacuo before warming to ambient temperature and transferring to the glove box. Infrared spectra of the solid showed  $\nu_{C-O}$  absorptions at 2049, 1947, 2120 and 2069 cm<sup>-1</sup> suggesting that  $\pi$ -cyclopentadienyldicarbonyl iron(II) chloride and  $\pi$ -cyclopentadienyltricarbonyl iron(II) chloride were the only two carbonyl compounds present. No other products were identified.

3.3.2.  $\pi$ -cyclopentadienyldicarbonyl iron- $\mu$ -hydrogen  $\pi$ -cyclopentadienyldicarbonyl iron tetrachloroborate,  $[(\pi-C_5H_5)Fe(CO)_2]_2H^+BCl_4^-$

Bis( $\pi$ -cyclopentadienyldicarbonyl iron(I)) (0.7 g., 0.002 mole) was

weighed into a rotaflo TF6/24 ampoule and degassed in vacuo overnight. After cooling the sample to  $-196^{\circ}\text{C}$  (liquid nitrogen bath), hydrogen chloride ( $7\text{ cm}^3$ , 0.25 mole) was distilled in, and dissolution effected by warming to  $-95^{\circ}\text{C}$  (toluene slush bath). The solution was cooled to  $-196^{\circ}\text{C}$  (liquid nitrogen bath) and boron trichloride (4 mmole) was distilled into the ampoule. The mixture was allowed to react at  $-84^{\circ}\text{C}$  (solid carbon dioxide/acetone slurry) and an immediate red-brown precipitate was observed. All volatile materials were removed at low temperature in vacuo. The solid obtained on warming to room temperature was washed with methylene chloride (freshly distilled from phosphorus pentoxide) to yield a red brown solid which decomposed slowly with the evolution of hydrogen chloride and boron trichloride. Found: % increase in weight on the bis( $\pi$ -cyclopentadienyldicarbonyl iron(I)) 43.4; C, 31.8; H, 2.1; Cl, 27.0; Fe, 20.9;  $\text{C}_{14}\text{H}_{11}\text{BCl}_4\text{Fe}_2\text{O}_4$  requires % increase in weight on the bis( $\pi$ -cyclopentadienyldicarbonyl iron(I)) 41.4; C, 33.1; H, 2.2; Cl, 27.9; Fe, 22.0%.

3.3.3.  $\pi$ -cyclopentadienyldicarbonyl iron- $\mu$ -hydrogen  $\pi$ -cyclopentadienyl-dicarbonyl iron hexafluorophosphate,  $[(\pi\text{-C}_5\text{H}_5)\text{Fe}(\text{CO})_2]_2\text{H}^+\text{PF}_6^-$

Bis( $\pi$ -cyclopentadienyldicarbonyl iron(I)) (0.7 g., 2 mmole) was weighed into an ampoule and degassed under high vacuum overnight. The sample was cooled to  $-196^{\circ}\text{C}$  (liquid nitrogen bath), hydrogen chloride (ca.  $7\text{ cm}^3$ ; 0.25 mole) was distilled in and dissolution effected by warming the mixture to  $-95^{\circ}$  (toluene slush bath). The solution was cooled to  $-196^{\circ}\text{C}$  (liquid nitrogen bath) and phosphorus pentafluoride (6 mmoles) was distilled into the ampoule. The mixture was allowed to react at  $-84^{\circ}\text{C}$  (solid carbon dioxide/acetone slurry) overnight. All volatile materials were removed in vacuo. The resulting solid at room

temperature was washed with methylene chloride (freshly distilled from phosphorus pentoxide) to give a red-brown solid. Found: C,33.4; H,2.15; Fe,22.1; P,6.05.  $C_{14}H_{11}F_6Fe_2O_4P$  requires C,33.65; H,2.2; Fe,22.35; P,6.20%.

3.3.4.  $\pi$ -cyclopentadienyldicarbonyl iron- $\mu$ -deuterium  $\pi$ -cyclopentadienyl-dicarbonyl iron hexafluorophosphate,  $[(\pi-C_5H_5)Fe(CO)_2]_2D^+PF_6^-$  was prepared in an identical manner to that described above except that deuterium chloride was used in place of hydrogen chloride.

3.3.5. Reaction of bis( $\pi$ -cyclopentadienyldicarbonyl iron(I)) with nitrosyl chloride in liquid hydrogen chloride

Bis( $\pi$ -cyclopentadienyldicarbonyl iron(I)) (0.7 g., 0.002 mole) was weighed into an ampoule and degassed overnight in vacuo. After cooling to  $-196^\circ C$  (liquid nitrogen bath), hydrogen chloride (ca. 7 cm<sup>3</sup>; 0.25 mole) was distilled into the ampoule. Nitrosyl chloride (25 mmoles) was also added from the vapour phase and the mixture allowed to react at  $-84^\circ$  (solid carbon dioxide/acetone slurry) for eighteen hours. An infrared spectrum of the gaseous fraction at  $-95^\circ C$  showed the presence of carbon monoxide, nitric oxide, nitrosyl chloride and hydrogen chloride. All volatile materials were removed in vacuo.

The solid product obtained at room temperature was washed with methylene chloride, on evaporation the filtrate gave a red solid whose infrared spectrum was identical with that of an authentic sample of  $\pi$ -cyclopentadienyldicarbonyl iron(II) chloride. (Found: C,40.4; H,2.25; Cl,17.1;  $C_7H_5ClFeO_2$  requires C,39.6; H,2.4; Cl,16.7%). The residue was washed with acetone, on evaporation the filtrate yielded a green paramagnetic solid which could not be identified (Found: C,24.8; H,1.67;

Cl, 30.32; Fe, 25.3; N, 1.15). The residue was a pale yellow solid which had  $\nu_{\text{C-O}}$  absorptions at 2122 and 2071  $\text{cm}^{-1}$  in the infrared and was probably  $\pi$ -cyclopentadienyldicarbonyl iron(II) chloride contaminated with other decomposition products (Found: C, 44.24; H, 5.63; Cl, 19.31; Fe, 1.43; N, 9.43).

3.3.6. Reaction of bis( $\pi$ -cyclopentadienyldicarbonyl iron(I)) with chlorine in liquid hydrogen chloride

Bis( $\pi$ -cyclopentadienyldicarbonyl iron(I)) (0.7 g., 2 mmoles) was weighed into an ampoule and degassed in vacuo. After cooling the ampoule to  $-196^{\circ}\text{C}$  (liquid nitrogen bath), hydrogen chloride (10  $\text{cm}^3$ ; 0.38 mole) was distilled in and solution effected by warming the mixture to  $-95^{\circ}\text{C}$  (toluene slush bath). After cooling to  $-196^{\circ}\text{C}$  (liquid nitrogen bath) chlorine (1 mmole) was distilled into the ampoule. The reaction was allowed to proceed for four hours at  $-84^{\circ}\text{C}$  (solid carbon dioxide/acetone slurry) before cooling down to  $-196^{\circ}$  (liquid nitrogen bath). Infrared spectra of the volatile fraction showed absorption bands attributable to carbon monoxide. All volatile materials were then removed in vacuo. Examination by infrared spectroscopy of the solid obtained at room temperature showed the presence of  $\pi$ -cyclopentadienyldicarbonyl iron(II) chloride and  $\pi$ -cyclopentadienyltricarbonyl iron(II) chloride ( $\nu_{\text{CO}}$  2120s, 2066vs and 2048, 1987  $\text{cm}^{-1}$  respectively) in addition to the  $\nu_{\text{CO}}$  absorptions of unreacted bis( $\pi$ -cyclopentadienyldicarbonyl iron(I)).

3.3.7.  $\pi$ -cyclopentadienyltricarbonyl iron(II) hexafluorophosphate,  
 $(\pi\text{-C}_5\text{H}_5)\text{Fe}(\text{CO})_3^+ \text{PF}_6^-$

Bis( $\pi$ -cyclopentadienyldicarbonyl iron(I)) (0.67 g., 1.90 mmoles) was warmed to  $50^{\circ}\text{C}$  with methane sulphonic acid (5  $\text{cm}^3$ ) in vacuo and the amount of gas evolved measured. When no further increase in pressure was

observed, the solution was diluted with water ( $20 \text{ cm}^3$ ) and then potassium hexafluorophosphate solution added dropwise until no further precipitation occurred. After filtering at the pump, the pale yellow solid was washed with water, ethanol and finally ether, and dried in vacuo. Found: C, 27.40; H, 1.43; Fe, 15.91; P, 8.79;  $\text{C}_8\text{H}_5\text{F}_6\text{FeP}$  requires C, 27.46; H, 1.44; Fe, 15.96; P, 8.85. Infrared spectra of the product was identical with that of a authentic sample of  $(\pi\text{-C}_5\text{H}_5)\text{Fe}(\text{CO})_3^+ \text{PF}_6^-$  which had been prepared according to the method described in the literature (89). 1.0 mmoles of gas was evolved during the reaction, the infrared of which only showed absorption bands attributable to carbon monoxide.

### 3.3.8. Infrared spectra of bis( $\pi$ -cyclopentadienyldicarbonyl iron(I)) in some anhydrous strong acids

Bis( $\pi$ -cyclopentadienyldicarbonyl iron(I)) was degassed in vacuo overnight. Most acids used in this study (sulphuric, methanesulphonic, chlorosulphonic and trifluoroacetic) were degassed before use. Solutions of bis( $\pi$ -cyclopentadienyldicarbonyl iron(I)) in the acids were prepared under a nitrogen shield; it was not practical to make the solutions up in a glove box since the solution decomposed fairly readily. The solution was smeared between polythene sheets and the infrared spectrum recorded over the region  $2200\text{-}1700 \text{ cm}^{-1}$  against a reference of two identical polythene sheets smeared with nujol.

The  $\nu_{\text{C-O}}$  absorption bands observed are given in Table 3.2.

3.3.9.  $^1\text{H}$  nuclear magnetic resonance studies of bis( $\pi$ -cyclopentadienyl-dicarbonyl iron(I)) in anhydrous acids

Bis( $\pi$ -cyclopentadienyldicarbonyl iron(I)) was finely powdered and transferred to a nmr tube with a ground glass joint attached and degassed in vacuo overnight. The acid being used was then vacuum distilled into the sample tube, as was the 0.5 mmol of tetramethylsilane used as internal standard. The tube was then sealed in vacuo. The results are given in Table 3.3.

3.3.10. Conductimetric titrations of bis( $\pi$ -cyclopentadienyldicarbonyl iron(I))

(i) with boron trichloride in liquid hydrogen chloride

Bis( $\pi$ -cyclopentadienyldicarbonyl iron(I)) (31.5 mg., 0.09 mmoles) was weighed into a conductivity cell and hydrogen chloride (7 cm<sup>3</sup>, 0.25 mole) condensed in at -196°C (liquid nitrogen bath). Aliquots of boron trichloride were then added and the reaction followed conductimetrically. Precipitation occurred very early on in the titration, but a clean break in the titration curve was observed at a mole ratio of 1:1 (acid:base). The conductivity curve is shown in Figure 3.1.

(ii) with phosphorus pentafluoride in liquid hydrogen chloride

Bis( $\pi$ -cyclopentadienyldicarbonyl iron(I)) (31.5 mg., 0.09 mmoles) was weighed into a conductivity cell and hydrogen chloride (7 cm<sup>3</sup>, 0.25 mole) condensed in at -196°C (liquid nitrogen bath). Aliquots of phosphorus pentafluoride were added and the reaction followed conductimetrically. The conductance measurements were observed to fluctuate with time and no meaningful end point could be detected. After removal of all the volatiles in vacuo examination of the solid

product obtained on warming to room temperature by infrared spectroscopy showed the presence of considerable amounts of unreacted bis( $\pi$ -cyclopentadienyldicarbonyl iron(I)) ( $\nu_{C-O}$  absorptions at 1954s, 1937s, 1767s and 1755s).

(iii) with nitrosyl chloride in liquid hydrogen chloride

Bis( $\pi$ -cyclopentadienyldicarbonyl iron(I)) (31.5 mg., 0.09 mmoles) was weighed into the conductivity cell and hydrogen chloride (7 cm<sup>3</sup>, 0.25 mole) was condensed in at -196°C (liquid nitrogen bath). Aliquots of nitrosyl chloride were added from the vapour phase and the reaction followed conductimetrically. The conductance measurements were observed to vary markedly with time even after thermostating for up to three hours, and no satisfactory end point could be seen in the range 0-4:1 mole ratio (oxidant:sample).

(iv) with chlorine in liquid hydrogen chloride

Bis( $\pi$ -cyclopentadienyldicarbonyl iron(I)) dimer (31.5 mg., 0.09 mole) was weighed into a conductivity cell and hydrogen chloride (7 cm<sup>3</sup>, 0.25 mole) was condensed in at -196°C (liquid nitrogen bath). Aliquots of chlorine were added from the vapour phase and the reaction followed conductimetrically. The conductance measurements were observed to vary markedly with time and no satisfactory end point could be seen in the range 0-2:1 mole ratio (oxidant:sample).

## CHAPTER 4

REACTIONS OF  $\pi$ -CYCLOPENTADIENYLDICARBONYL IRON(II) HALIDES (CHLORIDE, BROMIDE AND IODIDE) AND OF  $\pi$ -CYCLOPENTADIENYLTRICARBONYL IRON(II) CHLORIDE IN LIQUID HYDROGEN CHLORIDE

4.1. Results and Discussion

$\pi$ -Cyclopentadienyldicarbonyl iron(II) chloride dissolved readily in liquid hydrogen chloride, without evolution of carbon monoxide, and gave an orange red solution of low conductivity. Conductimetric titration using boron trichloride as an acid showed a break at the 1:0.5 (base:acid) molar ratio (Figure 4.1). Characterisation of the product obtained after warming to ambient temperatures showed it to be  $\pi$ -cyclopentadienyl-dicarbonyl iron- $\mu$ -chloro  $\pi$ -cyclopentadienyldicarbonyl iron tetrachloroborate,  $[(\pi-C_5H_5)Fe(CO)_2]_2Cl^+BCl_4^-$ , and its infrared spectrum is given in spectra 4.1.

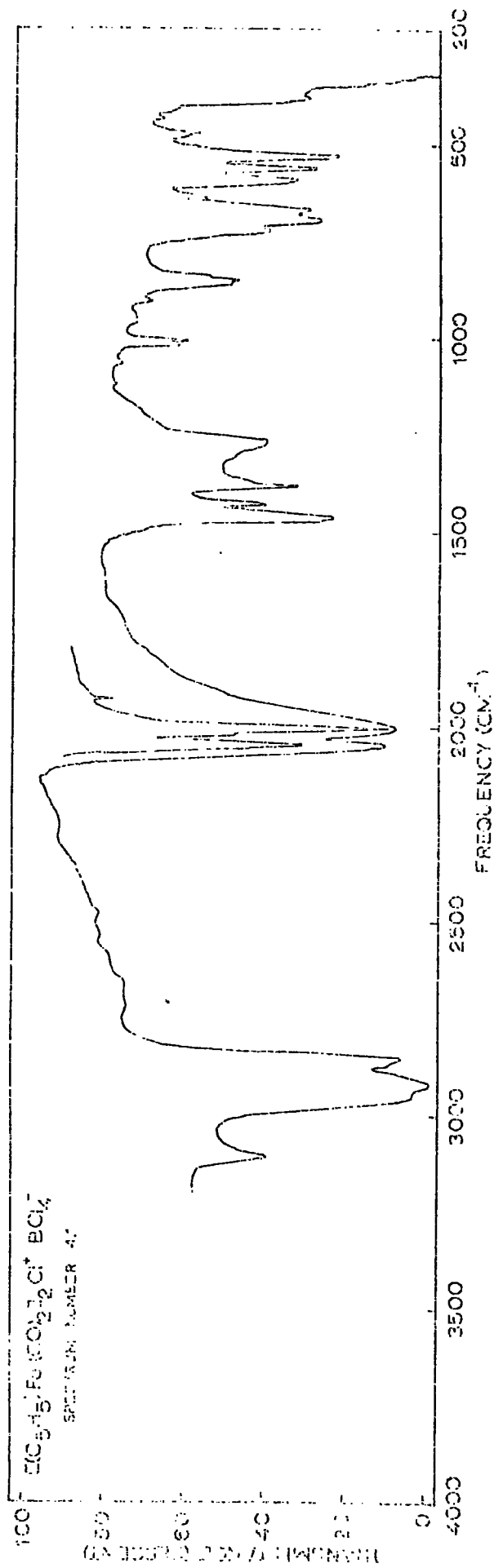
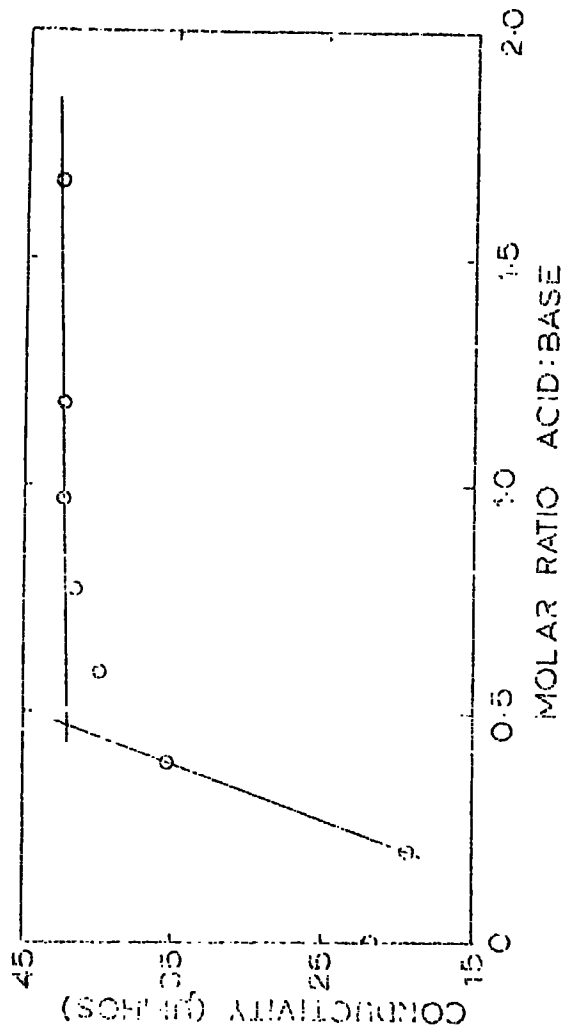


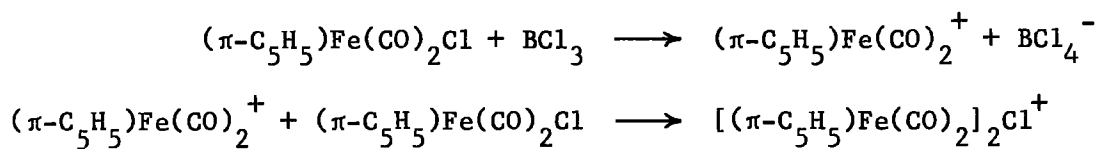
No evidence for the formation of the  $\pi$ -cyclopentadienyldicarbonyl iron(II) cation was observed, suggesting that the  $\pi$ -cyclopentadienyldicarbonyl iron(II) cation is a stronger chloridotropic acid than is boron trichloride. From the conductivity titration curve (Figure 4.1) it is seen that the addition of boron trichloride increased the conductivity of solution suggesting an increase in the number of ions in solution. The mechanism for the formation of the  $\pi$ -cyclopentadienyldicarbonyl iron- $\mu$ -chloro  $\pi$ -cyclopentadienyldicarbonyl iron cation could either have involved abstraction of a chloride ion from the  $\pi$ -cyclopentadienyldicarbonyl iron(II) chloride with the resultant cation attacking at the chlorine atom of a second  $\pi$ -cyclopentadienyldicarbonyl iron chloride molecule thus:

Figure 4.1

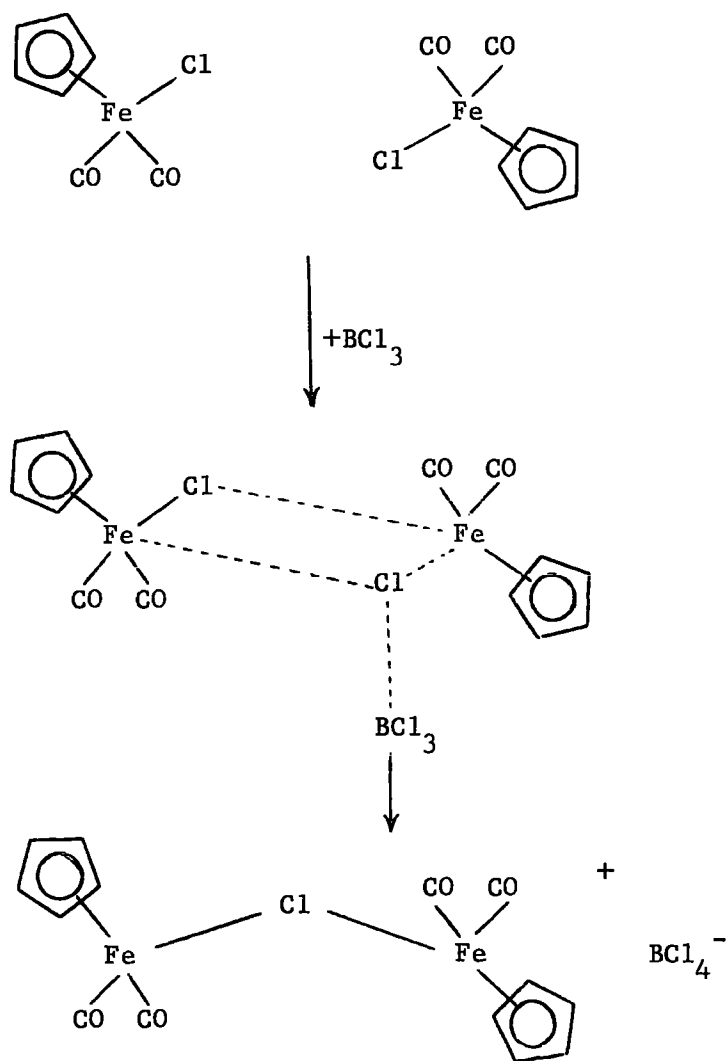
Conductimetric titration of  $\pi$ -cyclopentadienyldicarbonyl iron  
chloride with boron trichloride

Spectrum Number = 4.1





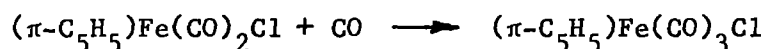
or the chloride ion might be abstracted simultaneously from two molecules of the  $\pi$ -cyclopentadienyldicarbonyl iron(II) chloride thus:



[N.B. Only the trans isomer is shown but any of the possible structures or a mixture of them may exist].

The failure of phosphorus pentafluoride to react with  $\pi$ -cyclopentadienyldicarbonyl iron(II) chloride demonstrates that phosphorus pentafluoride is a weaker chloridotropic acid than is boron trichloride. Previous workers (25) report that phosphorus pentafluoride only formed hexafluorophosphates in the presence of strong bases. Attempts to prepare salts of the  $\text{PF}_5\text{Cl}^-$  anion in liquid hydrogen chloride have always resulted in solvolysis to  $\text{PF}_6^-$  salts and  $\text{PF}_3\text{Cl}_2$  (25,44). This suggests that  $\text{PF}_6^-$  is the thermodynamically more stable product. The failure of phosphorus pentafluoride to react with weak bases may not be due to thermodynamic reasons but to kinetic reasons.

$\pi$ -Cyclopentadienyldicarbonyl iron(II) chloride did not react with the oxidising agent nitrosyl chloride, and reaction with chlorine caused extensive decomposition and resulted in the isolation of a brown tar at ambient temperatures. An infrared spectrum of the brown tar shows absorption bands at 2120s, 2070vs, 2053vs and 2018s  $\text{cm}^{-1}$  in the  $\nu_{\text{C-O}}$  stretching region. The absorption bands at 2120s and 2070vs  $\text{cm}^{-1}$  were thought to be attributable to  $\pi$ -cyclopentadienyltricarbonyl iron(II) chloride while those at 2053vs and 2018  $\text{cm}^{-1}$  were due to unreacted  $\pi$ -cyclopentadienyldicarbonyl iron(II) chloride. Carbon monoxide under pressure is known to react with  $\pi$ -cyclopentadienyldicarbonyl iron(II) chloride to give  $\pi$ -cyclopentadienyltricarbonyl iron(II) species (93) and this type of reaction was thought to give rise to the observed product in the case of the hydrogen chloride solutions.



$\pi$ -Cyclopentadienyldicarbonyl iron(II) bromide and  $\pi$ -cyclopentadienyldicarbonyl iron(II) iodide both dissolved in liquid hydrogen chloride to give orange-red solutions of very low conductance. Neither compound acted as a base towards boron trichloride and were recovered unchanged after removal of all volatiles in vacuo. Solvolysis of the  $\pi$ -cyclopentadienyldicarbonyl iron(II) bromide and iodide to the corresponding chloride could not have occurred since no  $\pi$ -cyclopentadienyldicarbonyl iron- $\mu$ -chloro- $\pi$ -cyclopentadienyldicarbonyl iron tetrachloroborate was formed.

Previous workers (29) demonstrated that  $\pi$ -cyclopentadienyldicarbonyl iron(II) chloride dissolved in sulphuric acid with evolution of hydrogen chloride. Examination of the reaction of the  $\pi$ -cyclopentadienyldicarbonyl iron(II) halides (halide = chloride, bromide and iodide) with sulphuric acid showed that evolution of the corresponding hydrogen halide occurred, and that a bright cherry red solution was also produced. The infrared spectra of these bright cherry red solutions recorded over the range 2200-1800  $\text{cm}^{-1}$  are given in Table 4.1 and shown in spectra 4.2-4.4. In the case of the  $\pi$ -cyclopentadienyldicarbonyl iron(II) chloride solution two rather broad (width at half height 25  $\text{cm}^{-1}$ ) absorptions were observed. For the solution of  $\pi$ -cyclopentadienyldicarbonyl iron(II) bromide in sulphuric acid three absorption bands are observed. The solution of  $\pi$ -cyclopentadienyldicarbonyl iron(II) iodide in sulphuric acid also exhibited three absorption bands but the lower frequency band had a shoulder on its low frequency side. These spectra are very similar to those exhibited by the  $\pi$ -cyclopentadienyldicarbonyl iron- $\mu$ -halogeno  $\pi$ -cyclopentadienyldicarbonyl iron cations (96-99) and these cations were isolated from the sulphuric acid solutions as their hexafluorophosphate salts. These spectra suggest that compounds of the type

Table 4.1

Infrared Spectra of the Sulphuric Acid Solutions of  $\pi$ -Cyclopentadienyl-dicarbonyl iron(II) Halides (halide = chloride, bromide and iodide) in the 2200-1900  $\text{cm}^{-1}$  region

Compound	$\nu_{\text{CO}} \text{ cm}^{-1}$
$(\pi\text{-C}_5\text{H}_5)\text{Fe}(\text{CO})_2\text{Cl}$	2075s, 2055sh, 2029s
$(\pi\text{-C}_5\text{H}_5)\text{Fe}(\text{CO})_2\text{Br}$	2071s, 2059s, 2023s
$(\pi\text{-C}_5\text{H}_5)\text{Fe}(\text{CO})_2\text{I}$	2063s, 2049s, 2017s, 2003sh

$[(\pi\text{-C}_5\text{H}_5)\text{Fe}(\text{CO})_2]_2\text{X}^+$  (X = Cl, Br and I) exhibit  $4\nu_{\text{C-O}}$  stretching modes which are not completely resolved. The interpretation of these spectra and a more detailed examination are reported in Chapter 6.

$\pi$ -Cyclopentadienyltricarbonyl iron(II) chloride dissolved in liquid hydrogen chloride, without evolution of carbon monoxide, to give a pale yellow solution. Boron trichloride reacted in the solution to give the expected  $\pi$ -cyclopentadienyltricarbonyl iron(II) tetrachloroborate (Spectrum 4.5).

#### 4.2 Experimental

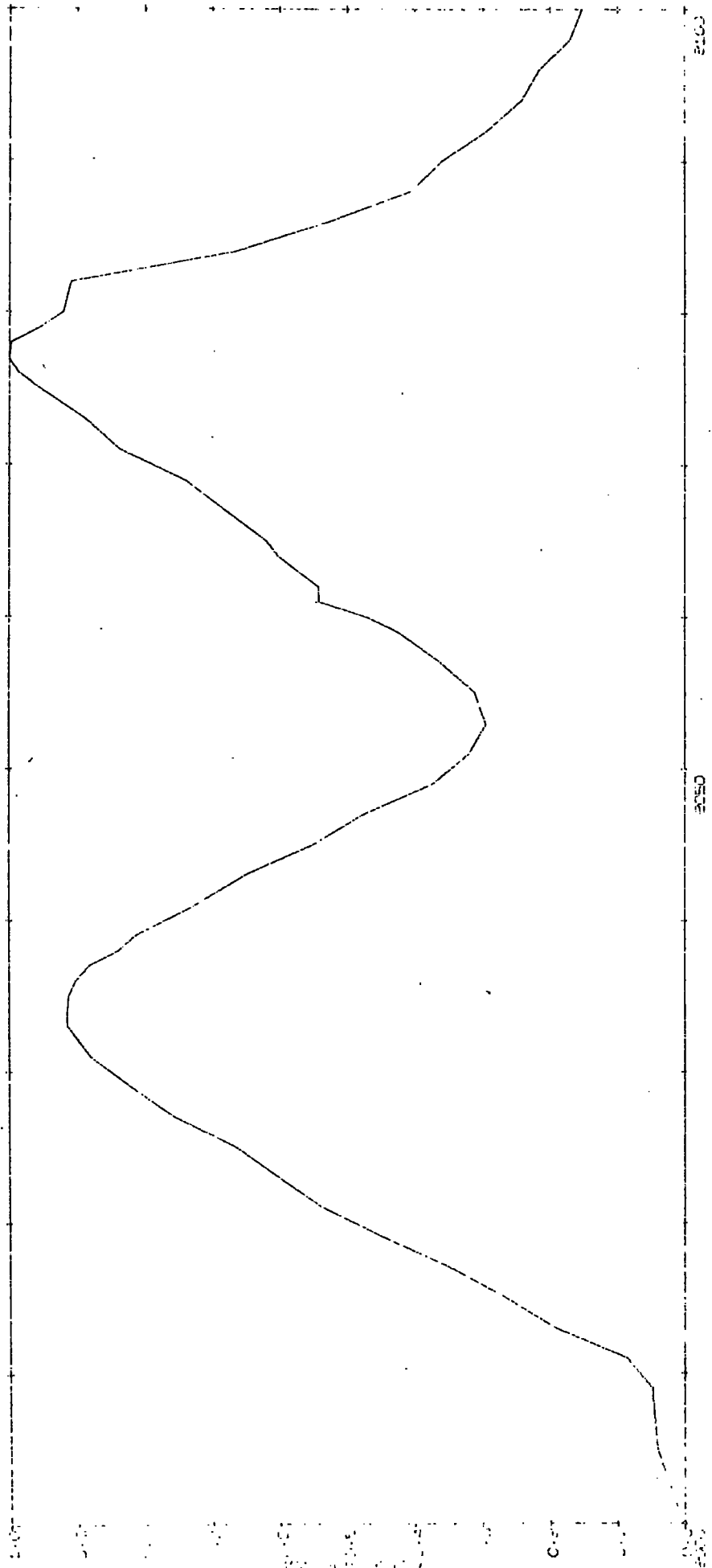
##### 4.2.1. $\pi$ -Cyclopentadienyldicarbonyl iron- $\mu$ -chloro $\pi$ -cyclopentadienyldicarbonyl iron tetrachloroborate, $[(\pi\text{-C}_5\text{H}_5)\text{Fe}(\text{CO})_2]_2\text{Cl}^+\text{BCl}_4^-$

$\pi$ -Cyclopentadienyldicarbonyl iron(II) chloride (0.42 g., 0.002 mole) was weighed into an ampoule and degassed overnight in vacuo. The sample was cooled to  $-196^\circ\text{C}$  (liquid nitrogen bath) and hydrogen chloride (12  $\text{cm}^3$ , 0.43 mole) was distilled in, solution was effected by warming the

Spectrum Number = 4.2

$\pi$ -cyclopentadienyldicarbonyl iron(II)  
chloride in sulphuric acid

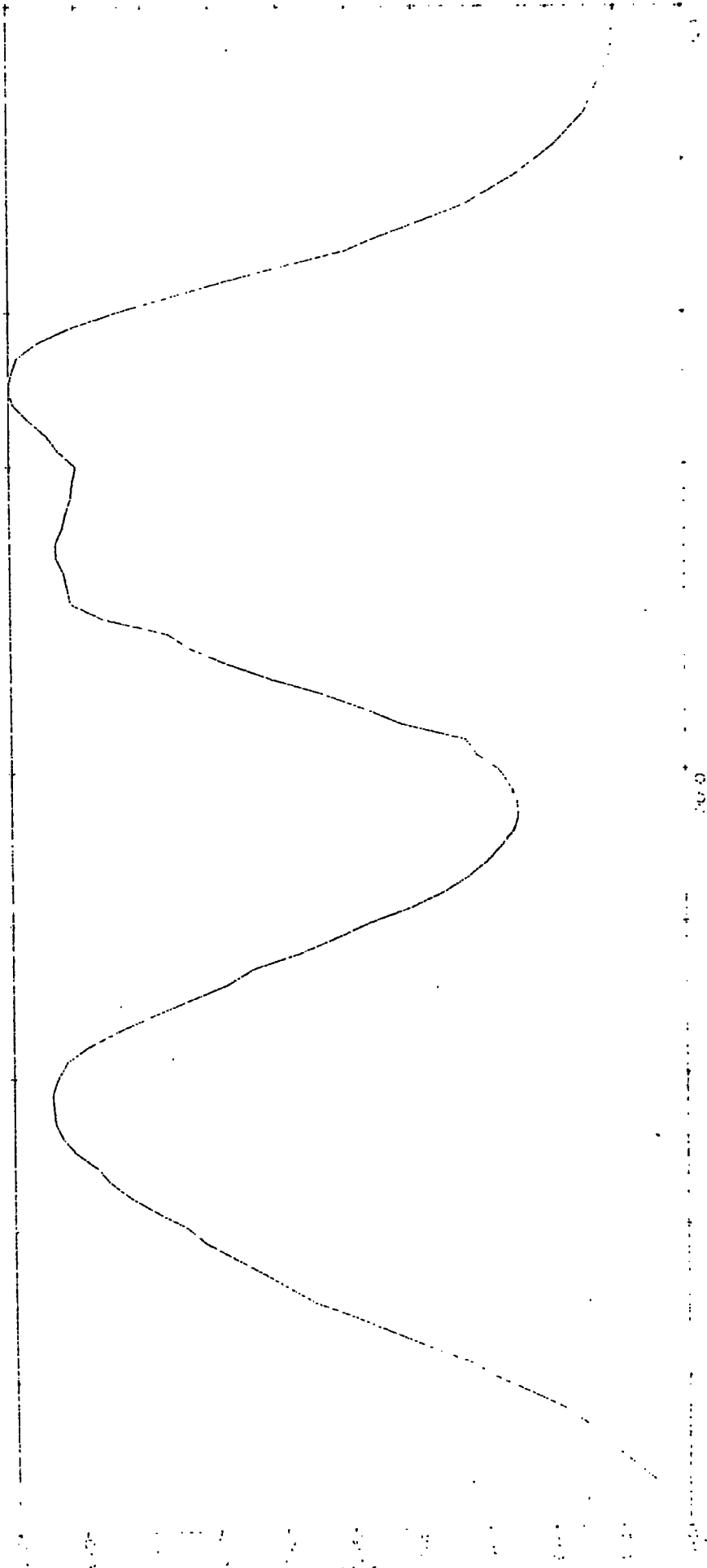
(CH<sub>3</sub>)<sub>2</sub>FE(CO)<sub>2</sub> CL



Spectrum Number = 4.3

$\pi$ -cyclopentadienyldicarbonyl iron(II)  
bromide in sulphuric acid

(C-144) FE (CO)E BR

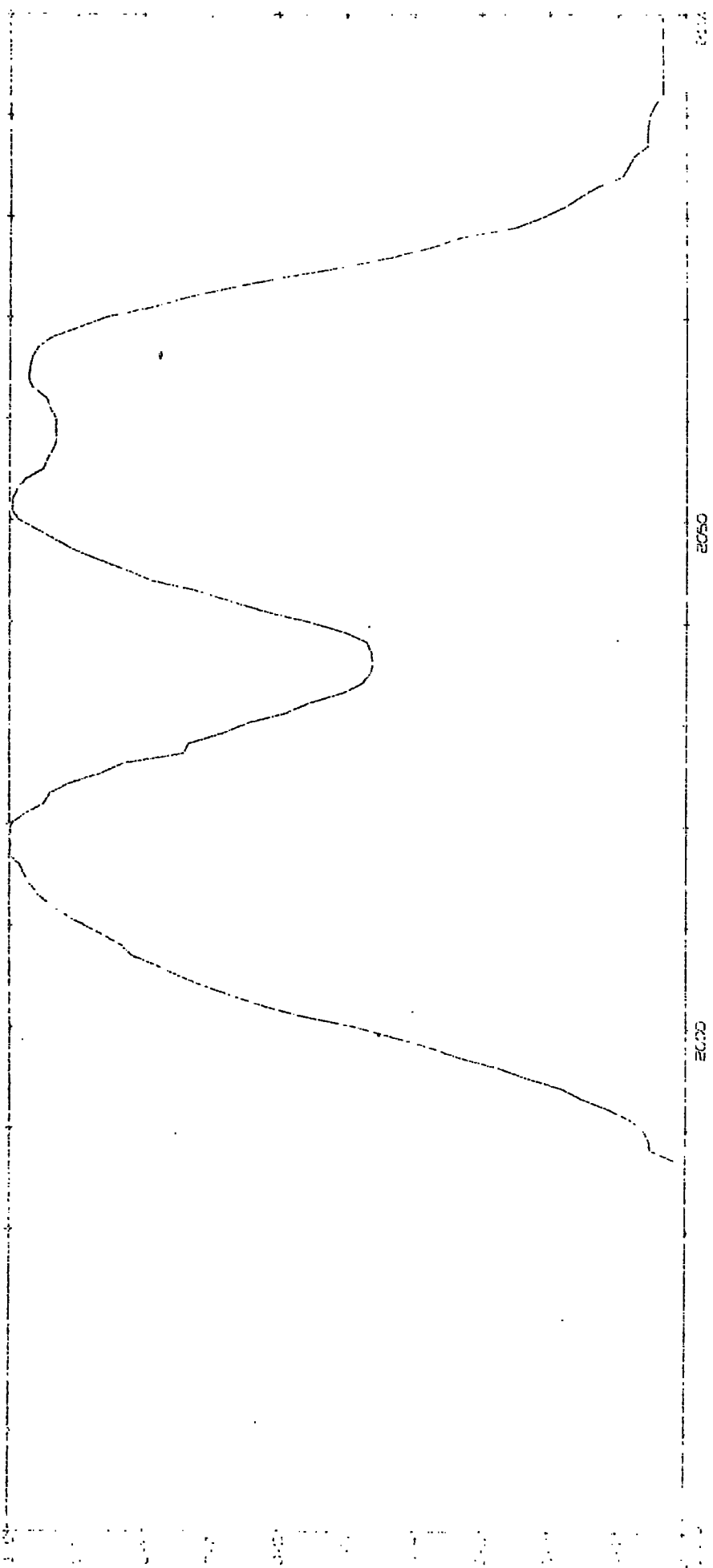


RAVEN HESTER 11M

Spectrum Number = 4.4

$\eta$ -cyclopentadienyldicarbonyl iron(II)  
iodide in sulphuric acid

(CANE) FE (CO) 1



WAVENUMBER CM⁻¹

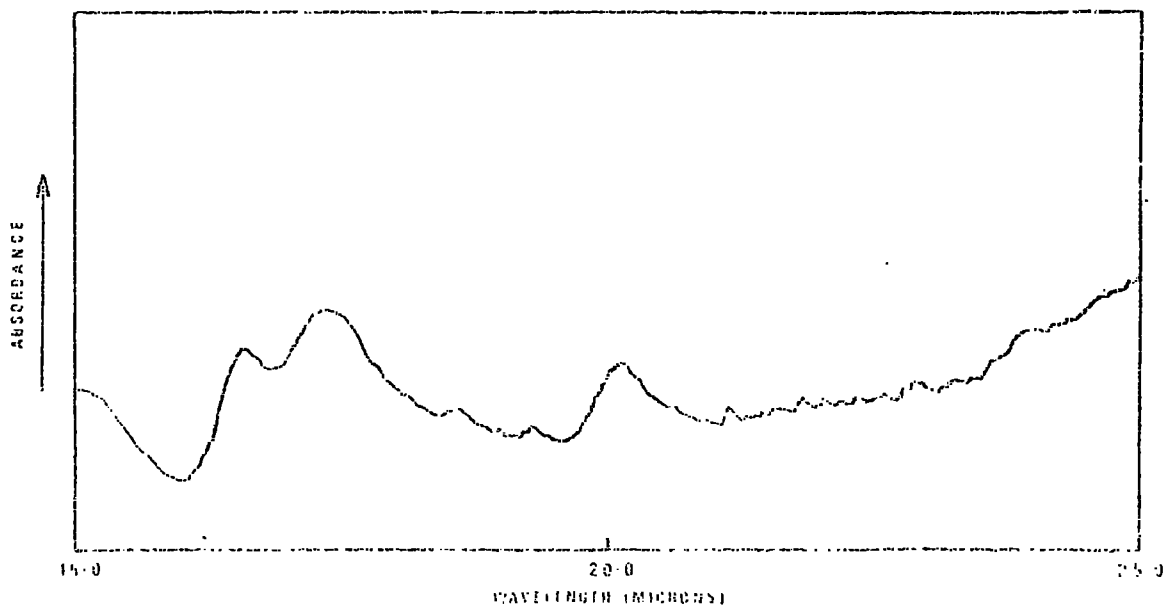
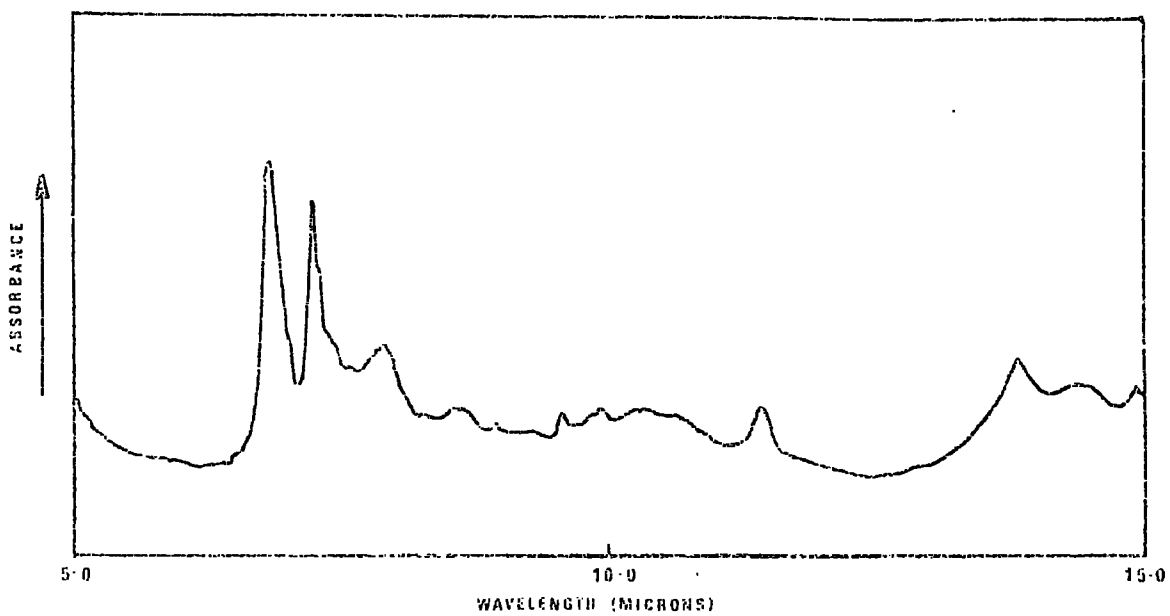
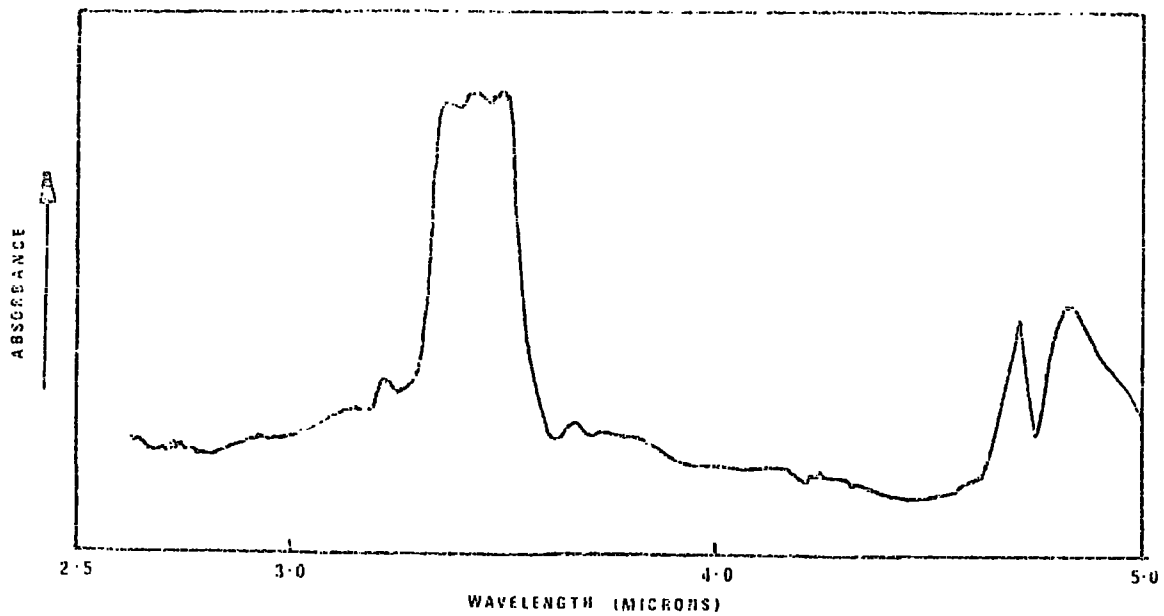
2000

2050

2100

Spectrum Number = 4.5

$\pi$ -cyclopentadienyltricarbonyl iron(II)  
tetrachloroborate



mixture to  $-95^{\circ}\text{C}$  (toluene slush bath). The solution was cooled to  $-196^{\circ}\text{C}$  (liquid nitrogen bath) and boron trichloride (0.005 mole) distilled into the ampoule. The mixture was allowed to react at  $-84^{\circ}$  (solid carbon dioxide/acetone slurry) for twenty four hours before removing all volatiles in vacuo at low temperature. The red-brown solid obtained at room temperature dissociated slowly into  $\pi$ -cyclopentadienyldicarbonyl iron(II) chloride and boron trichloride. Found: % increase in weight in  $\pi$ -cyclopentadienyldicarbonyl iron(II) chloride 29.9; C,30.1; H,1.82; Cl,31.7;  $\text{C}_{14}\text{H}_{10}\text{BCl}_5\text{Fe}_2\text{O}_4$  requires % increase in weight on the chloride 27.6; C,31.02; H,1.86; Cl,32.71.

4.2.2. Action of phosphorus pentafluoride on a solution of  $\pi$ -cyclopentadienyldicarbonyl iron(II) chloride in liquid hydrogen chloride

$\pi$ -Cyclopentadienyldicarbonyl iron(II) chloride (0.101 g., 0.00048 mol) was weighed into an ampoule and degassed overnight in vacuo. The sample was cooled to  $-196^{\circ}\text{C}$  (liquid nitrogen bath) and hydrogen chloride ( $10\text{ cm}^3$ , 0.38 mol) condensed in. Solution was effected by warming the mixture to  $-95^{\circ}$  (toluene slush bath). The sample was then cooled to  $-196^{\circ}$  (liquid nitrogen bath) and phosphorus pentafluoride (0.0015 mol) condensed in. The mixture was allowed to stand for twelve hours at  $-84^{\circ}\text{C}$  (solid carbon dioxide/acetone slurry) before volatiles were removed in vacuo at low temperature. Examination of the product isolated at room temperature by infrared spectroscopy showed it to be  $\pi$ -cyclopentadienyldicarbonyl iron(II) chloride, no increase in weight was observed.

4.2.3. Action of nitrosyl chloride on a solution of  $\pi$ -cyclopentadienyldicarbonyl iron(II) chloride in liquid hydrogen chloride

$\pi$ -Cyclopentadienyldicarbonyl iron(II) chloride (0.486 g., 0.00229 mol) was weighed into an ampoule and degassed overnight in vacuo. The sample was cooled to  $-196^{\circ}\text{C}$  (liquid nitrogen bath) and hydrogen chloride ( $8\text{ cm}^3$ , 0.28 mol) and nitrosyl chloride (0.005 mol) distilled in. The mixture was allowed to stand at  $-84^{\circ}\text{C}$  (solid carbon dioxide/acetone slurry) for twenty four hours before removing volatiles in vacuo at low temperature. No increase in weight was observed and the infrared spectrum of the product isolated at room temperature showed it to be  $\pi$ -cyclopentadienyldicarbonyl iron(II) chloride.

4.2.4. Reaction of chlorine with a solution of  $\pi$ -cyclopentadienyldicarbonyl iron(II) chloride in liquid hydrogen chloride

$\pi$ -Cyclopentadienyldicarbonyl iron(II) chloride (0.329 g., 0.00136 mol) was weighed into an ampoule and degassed in vacuo overnight. The sample was cooled to  $-196^{\circ}\text{C}$  (liquid nitrogen bath) and hydrogen chloride ( $7\text{ cm}^3$ , 0.25 mol) and chlorine (0.002 mol) condensed in. Within a few minutes of warming the mixture to  $-84^{\circ}\text{C}$  (solid carbon dioxide/acetone slurry) a precipitate was observed. After cooling the mixture to  $-196^{\circ}\text{C}$ , an infrared spectrum of the volatile fraction showed it to be carbon monoxide. All volatiles were removed in vacuo at low temperature. On warming to room temperature the product was observed to darken rapidly. Infrared spectra of the product in the  $\nu_{\text{C-O}}$  region showed absorption bands at 2120s, 2070vs, 2053vs, and 2018s  $\text{cm}^{-1}$ .

4.2.5. Action of boron trichloride on a solution of  $\pi$ -cyclopentadienyldicarbonyl iron(II) bromide in liquid hydrogen chloride

$\pi$ -Cyclopentadienyldicarbonyl iron(II) bromide (0.577 g., 0.00225 mol) was degassed in vacuo overnight. The sample was cooled to  $-196^{\circ}\text{C}$  (liquid

nitrogen bath), hydrogen chloride ( $8 \text{ cm}^3$ ,  $0.28 \text{ mol}$ ) and boron trichloride ( $0.006 \text{ mol}$ ) were then distilled into the ampoule. The mixture was allowed to stand at  $-84^\circ\text{C}$  (solid carbon dioxide/acetone slurry) for sixteen hours before removal of all volatiles in vacuo at low temperature. No increase in weight was observed and an infrared spectrum of the product showed it to be  $\pi$ -cyclopentadienyldicarbonyl iron(II) bromide.

4.2.6. Action of boron tribromide with a solution of  $\pi$ -cyclopentadienyldicarbonyl iron(II) bromide in liquid hydrogen chloride

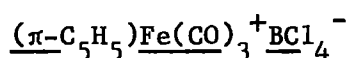
$\pi$ -Cyclopentadienyldicarbonyl iron(II) bromide ( $0.457 \text{ g.}$ ,  $0.00178 \text{ mol}$ ) was weighed into an ampoule and degassed overnight in vacuo. The sample was cooled to  $-196^\circ\text{C}$  (liquid nitrogen bath), hydrogen chloride ( $10 \text{ cm}^3$ ,  $0.38 \text{ mol}$ ) and boron tribromide ( $0.005 \text{ mol}$ ) were then distilled into the ampoule. The mixture was allowed to stand at  $-84^\circ\text{C}$  (solid carbon dioxide/acetone slurry) before removal of volatiles in vacuo at low temperature. No increase in weight was observed and the infrared spectrum of the solid isolated at room temperature showed it to be  $\pi$ -cyclopentadienyldicarbonyl iron(II) bromide. Infrared spectra of the volatiles showed boron trichloride to be present, and boron tribromide to be absent.

4.2.7. Action of boron trichloride on a solution of  $\pi$ -cyclopentadienyldicarbonyl iron(II) iodide

$\pi$ -Cyclopentadienyldicarbonyl iron(II) iodide ( $0.617 \text{ g.}$ ,  $0.0020 \text{ mol}$ ) was weighed into an ampoule and degassed in high vacuo overnight. After cooling the sample to  $-196^\circ\text{C}$  (liquid nitrogen bath), hydrogen chloride ( $8 \text{ cm}^3$ ,  $0.28 \text{ mol}$ ) and boron trichloride ( $0.005 \text{ mol}$ ) was distilled into the ampoule. The ampoule was allowed to stand at  $-84^\circ\text{C}$  (solid carbon

dioxide/acetone slurry) for twenty hours before removal of volatiles in vacuo at low temperature. No increase in weight was observed and the infrared spectrum of the solid obtained at room temperature showed it to be  $\pi$ -cyclopentadienyldicarbonyl iron iodide.

4.2.8.  $\pi$ -Cyclopentadienyltricarbonyl iron(II) tetrachloroborate,



$\pi$ -Cyclopentadienyltricarbonyl iron(II) chloride (0.38 g., 0.0016 mol) was weighed into an ampoule and degassed in vacuo overnight. The sample was then cooled to  $-196^\circ\text{C}$  (liquid nitrogen bath) and hydrogen chloride (12 cm<sup>3</sup>, 0.43 mol) condensed in. Solution was effected by warming to  $-95^\circ\text{C}$  (toluene slush bath); the solution was cooled to  $-196^\circ\text{C}$  (liquid nitrogen bath) and boron trichloride (0.005 mol) condensed into the ampoule. On warming the mixture to  $-84^\circ\text{C}$  (solid carbon dioxide/acetone slurry) a pale yellow solid was precipitated from solution. After removal of all volatiles in vacuo at low temperature a yellow solid remained. Found: C, 26.1; H, 1.7; Cl, 38.2;  $\text{C}_8\text{H}_5\text{BCl}_4\text{FeO}_3$  requires C, 26.9; H, 1.4; Cl, 39.7%.

4.2.9. The infrared spectra of  $\pi$ -cyclopentadienyldicarbonyl iron(II) halide (halide = chloride, bromide and iodide) were recorded as sulphuric acid solutions over the region 2200-1900 cm<sup>-1</sup>, the results are given in Table 4.1.

4.2.10. Conductimetric Study

Conductimetric titration of  $\pi$ -cyclopentadienyldicarbonyl iron(II) chloride with boron trichloride in liquid hydrogen chloride.

Cyclopentadienyldicarbonyl iron(II) chloride (0.0275 g., 0.00013 mol) was weighed into a conductivity cell and degassed in vacuo. After

cooling the sample to  $-196^{\circ}\text{C}$  (liquid nitrogen bath) hydrogen chloride (5 ml., 0.17 mol) was condensed into the cell. The conductivity of the solution was measured at  $-95^{\circ}\text{C}$  (toluene slush bath). The solution was then cooled to  $-196^{\circ}\text{C}$  (liquid nitrogen bath) and boron trichloride (0.000025 mol) condensed in. The mixture was allowed to warm to  $-95^{\circ}\text{C}$  (toluene slush bath) before the conductivity was determined. Further aliquots of boron trichloride were introduced in the same manner and the conductivity determined after each addition. A break in the conductivity was observed at about the 1.0:0.5 molar ratio (acid:base). (Fig.4.1).

## CHAPTER 5

### REACTIONS OF TETRAKIS( $\pi$ -CYCLOPENTADIENYLCARBONYL IRON(I))

#### 5.1 Results and Discussion

Tetrakis( $\pi$ -cyclopentadienylcarbonyl iron(I)) was first prepared in 1966 by King (91). Bromine was shown to oxidise the carbonyl to give the tribromide salt of the unipositive cation,  $[(\pi\text{-C}_5\text{H}_5)\text{Fe}(\text{CO})]_4^+\text{Br}_3^-$ . The paramagnetic susceptibility was consistent with one unpaired electron per four iron atoms. No metal-hydrogen resonance in trifluoroacetic acid in the range 10-200 $\tau$  was observed.

Tetrakis( $\pi$ -cyclopentadienylcarbonyl iron(I)) was observed to be soluble in liquid hydrogen chloride at  $-95^\circ$  without loss of a measurable amount of carbon monoxide, and could be recovered unchanged at room temperature.

The solution of tetrakis( $\pi$ -cyclopentadienylcarbonyl iron(I)) in liquid hydrogen chloride has a molar conductance of  $20 \text{ cm}^2 \text{ ohm}^{-1} \text{ mole}^{-1}$  for a 0.015M solution, which is about half that observed for a solution of bis( $\pi$ -cyclopentadienyldicarbonyl iron(I)) in hydrogen chloride (molar conductance for a 0.015M solution  $40 \text{ cm}^2 \text{ ohm}^{-1} \text{ mole}^{-1}$ ). The above facts suggest that tetrakis( $\pi$ -cyclopentadienylcarbonyl iron(I)) is less basic than bis( $\pi$ -cyclopentadienyldicarbonyl iron(I)). A base can be defined as an electron donor, and the more readily the electrons are donated the stronger is the base. In both the dimeric and tetrameric compounds each iron atom is in the +1 oxidation state and has a pi bonded cyclopentadienyl ligand. The basic strength of the compounds would therefore depend on how readily a positive charge can be delocalised. Clearly the compound with the two carbon monoxide ligands per iron atom can delocalise any positive charge more effectively than the compound with one carbon monoxide ligand per iron atom. The above argument assumes

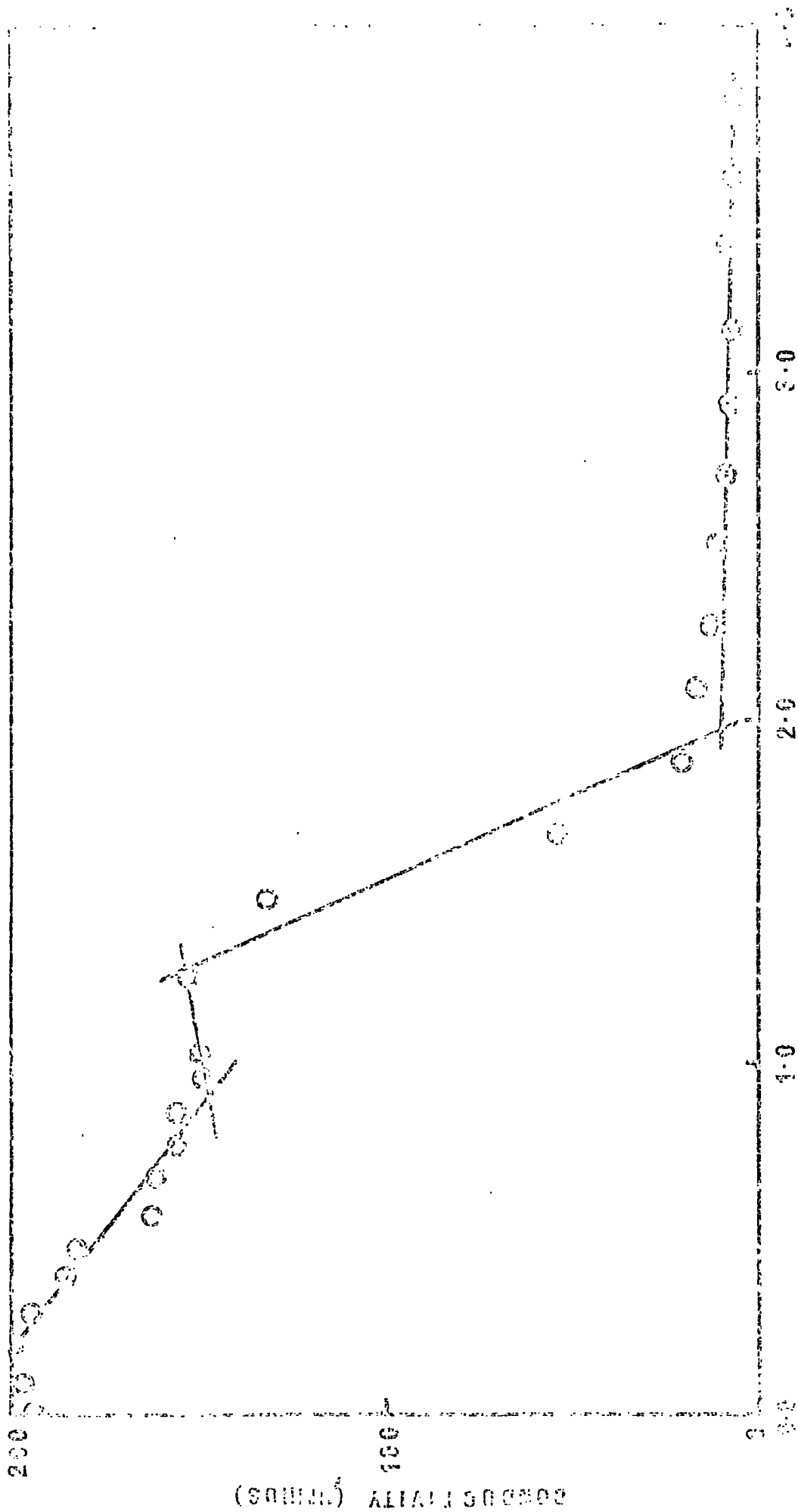
that the proton would be present in the same ratio to the iron atoms in both compound i.e. monoprotection in the dimeric compound and diprotection in the tetrameric compound. If mono protonation of each compound occurs there are four carbon monoxide ligands which can delocalise the charge, thus similar basicities might be expected. In the tetrameric compound the carbon monoxide ligands attempt to delocalise +5 charges (4, +1 iron atoms and a proton) in the dimeric compound only +3 charges have to be delocalised (two +1 iron atoms and a proton), suggesting the dimeric compound as the strongest base even in the case of monoprotection. Low spin iron compounds attempt to achieve the iron atom with an essentially neutral overall charge, so the carbon monoxide ligands try to donate electron density to reduce the +1 on the iron to zero, hence we must consider the iron atom charges and not only the addition of one extra positive charge. In all the discussion the  $\pi$ -cyclopentadienyl ligand has been assumed to play little or no part in the stabilisation of the cations, this is borne out by the fact that very little change in the spectroscopic properties of the ligand occur in a very wide range of compounds.

A conductimetric study of the reaction of boron trichloride with tetrakis( $\pi$ -cyclopentadienylcarbonyl iron(I)) in liquid hydrogen chloride showed that addition of boron trichloride reduced the conductance of the solution with breaks in the curve at the 1:1 and 2:1 molar ratios (acid:base) (Figure 5.1). The final conductance's were very low; the decrease in conductance can be due to adduct formation or by replacement of a more mobile ion by a less mobile ion or by precipitation of conducting material out of solution. During the conductimetric titration no clear indication of when precipitation started was observed but at the completion of the titration a green precipitate and an almost

Figure 5.1

Conductimetric titration of Tetrakis( $\eta$ -cyclopentadienylcarbonyl  
iron(I)) with boron trichloride

BRITISH LIBRARY  
28 SEP 1972  
LIBRARY



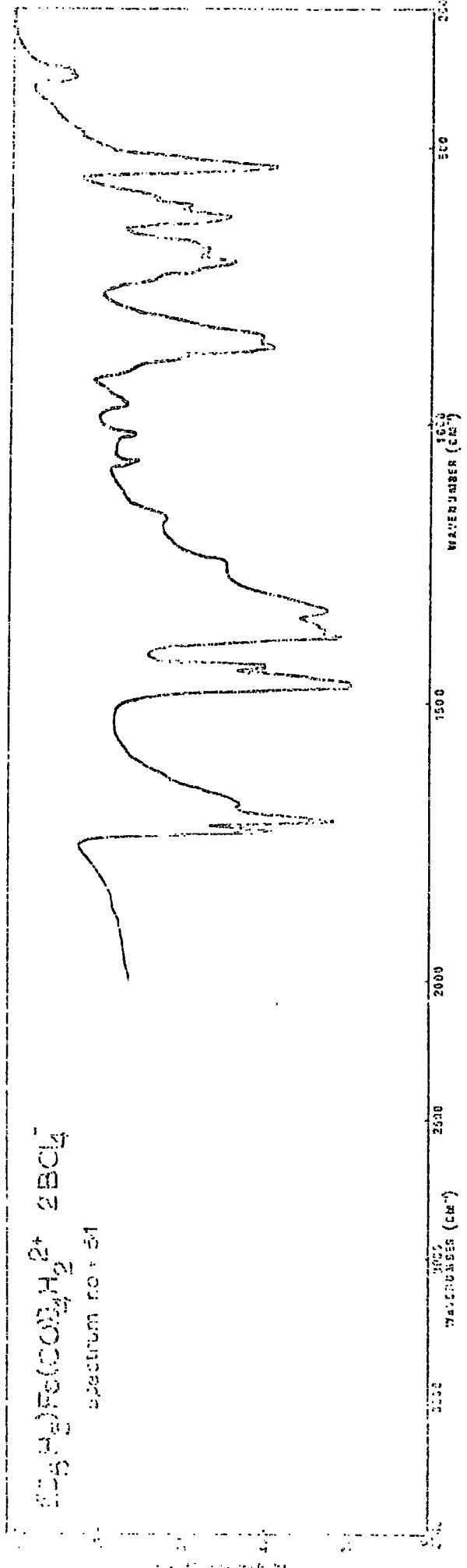
colourless solution was observed. The increase in weight was consistent with the addition of two moles of  $\text{HBCl}_4$  rather than two moles of  $\text{BCl}_3$  and the infrared spectrum showed absorption bands at 698 and  $673 \text{ cm}^{-1}$  characteristic of the tetrachloroborate ion,  $\text{BCl}_4^-$  (17). The tetrakis( $\pi$ -cyclopentadienylcarbonyl iron) dihydrogen tetrachloroborate was observed to lose hydrogen chloride readily at room temperature to give tetrakis( $\pi$ -cyclopentadienylcarbonyl iron) bis(boron trichloride) which exhibits bands at 806 and  $749 \text{ cm}^{-1}$  attributable to co-ordinated boron trichloride. The infrared spectrum of the tetrachloroborate and boron trichloride adduct are shown in spectrum 5.1 and 5.2 respectively.

Attempts to distinguish between adduct and salt formation using phosphorus pentafluoride as the acid in a conductimetric titrations were unsuccessful since complete reaction was never observed. Isolation of a pure hexafluorophosphate salt was achieved however which was found to be paramagnetic. This was the first example of a reaction in hydrogen chloride where phosphorus pentafluoride acted as an oxidising agent.



The studies of Ferguson and Meyer (104) showed that tetrakis( $\pi$ -cyclopentadienylcarbonyl iron(I)) could be electrochemically oxidised to the monocation and dication with potentials of  $+0.32\text{v}$  and  $+1.07\text{v}$  respectively.

The first example of a doubly protonated neutral metal complex obtained by dissolution in acid was recently reported (105) but isolation of a solid salt from the sulphuric acid solution proved impossible. The only report concerning the basic strength of tetrakis( $\pi$ -cyclopentadienylcarbonyl iron(I)) was in reaction with aluminium triethyl, which showed that each terminal carbon monoxide ligand bonded via the oxygen atom to the aluminium of the aluminium triethyl (106). This was the



Spectrum Number = 5.2

Tetrakis( $\pi$ -cyclopentadienylcarbonyl iron(I)) bis(boron trichloride)

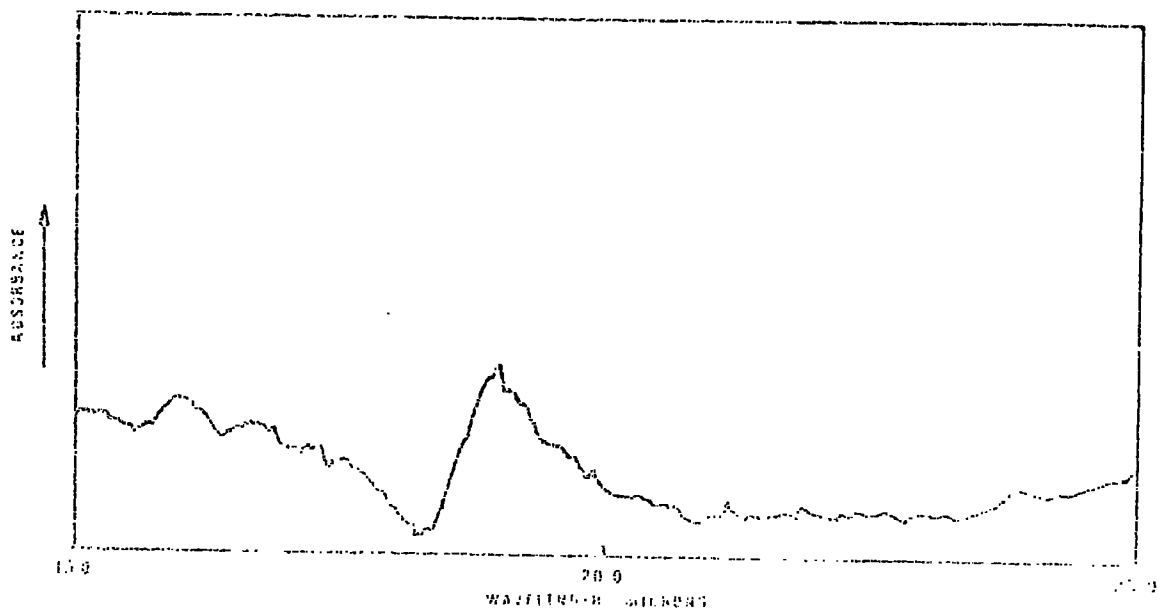
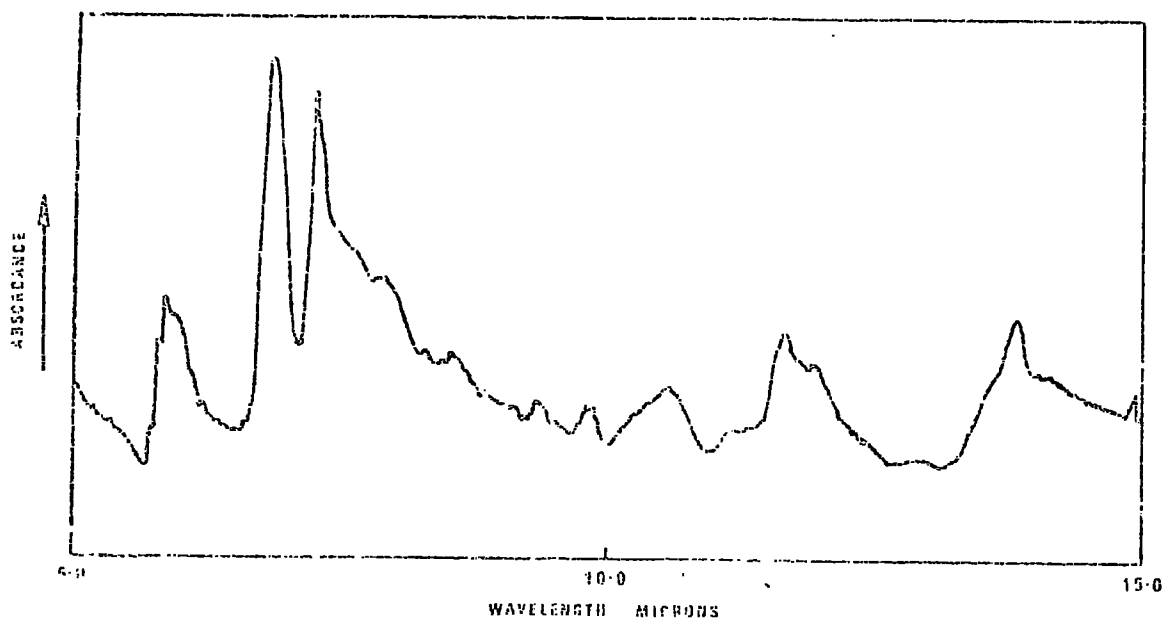
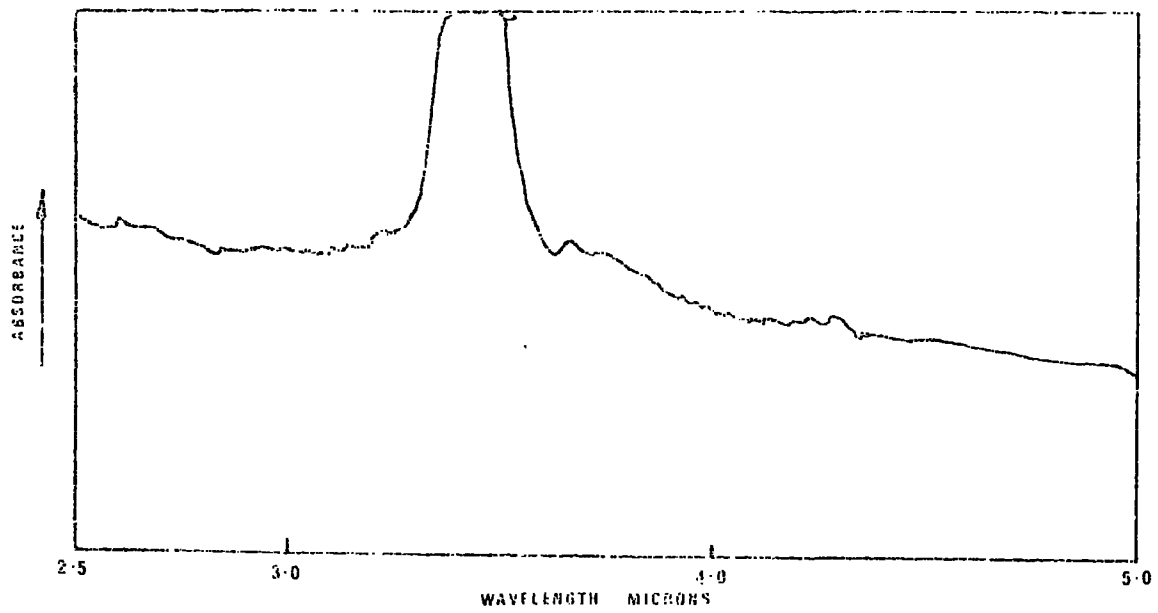


Table 5.1

Infrared Spectra of the Tetrakis( $\pi$ -cyclopentadienylcarbonyl iron)  
Compounds in the 4000-250  $\text{cm}^{-1}$  Region

Assignment	Compound	
	$[(\pi-C_5H_5)Fe(CO)]_4$	$[(\pi-C_5H_5)Fe(CO)]_4H_2^{2+} \cdot 2BCl_4^-$
C-H Stretch	3108sh 3096w	3115w
$\nu_{CO}$	1673w 1656w.sh 1644ms 1629s 1619s 1591w.sh	1726m 1706s 1700m.sh 1684m
C-C Stretch	1431sh 1426m  1360w	
	1064w	1060w
	1026w 1018w 1010w	1016w 1006sh
		958w 950sh
	933sh 920w	935sh
		891sh
$\nu_3 PF_6^-$	870sh 864m	870m.sh
		850s 831s
	836m 826m	
B-Cl		
$\nu_3 BCl_4^-$		738w.sh 716m.sh 698s
$\nu_1 + \nu_4 BCl_4^-$		673s
		618s 600s
	598m	
	574ms	584sh
$\nu_4 PF_6^-$		528s 516msh
	506w	
		470w 440w.sh 368m
	355m	356m.sh

Assignment	Compound	
	$[(\eta^5\text{C}_5\text{H}_5)\text{Fe}(\text{CO})]_4 \cdot 2\text{BCl}_3$	$[(\pi\text{-C}_5\text{H}_5)\text{Fe}(\text{CO})]_4^+ \text{PF}_6^-$
C-H Stretch	3109w	3113w
$\nu_{\text{CO}}$	1706m 1667s	1738w, sh 1719m, sh 1702s 1693s
C-C Stretch		1431w <del>1424m</del> 1358vw 1120vw
	1065w	1062w
	1015m	1016w 1006w
	962w	951w
	883m	
$\nu_3 \text{PF}_6^-$	848s 834s	856s 838s 824s
B-Cl	806s 749m, sh 741w, sh 721w, sh	
$\nu_3 \text{BCl}_4^-$ $\nu_1 + \nu_4 \text{BCl}_4^-$	629s, sh 619s 600s	
	581m, sh	
$\nu_4 \text{PF}_6^-$		556s
		498m 478m
		356m

Assignment	Compound	
	$[(\pi\text{-C}_5\text{H}_5)\text{Fe}(\text{CO})]_4^+\text{Br}_3^-$	$[(\pi\text{-C}_5\text{H}_5)\text{Fe}(\text{CO})]_4^+\text{I}_7^-$
C-H Stretch	3113w	3108w
$\nu_{\text{CO}}$	1728w.sh 1700m.sh 1690s 1681s.sh	1734m 1704s.sh 1694s 1664w.sh
C-C Stretch	1430m 1424m	1426w 1356vw 1120vw
	1066w	1061w
	1016w 1006w	1006w
	940w	938w
	887m	
	870m	874m
$\nu_3 \text{PF}_6^-$	848m	846m
	826sh	
B-Cl		
$\nu_3 \text{BCl}_4^-$ $\nu_1 + \nu_4 \text{BCl}_4^-$		
$\nu_4 \text{PF}_6^-$		
	480m	495m.sh 476m
	358m	356m

first example of a carbon monoxide being co-ordinated through both carbon and oxygen. Apart from the proton nuclear magnetic resonance study carried out by King (91) no protonation studies on tetrakis( $\pi$ -cyclopentadienylcarbonyl iron(I)) have been reported. The fact that no Fe-H resonance was observed in the trifluoroacetic solution could be due to either no protonation occurring in solution or that the exchange rate was such that the Fe-H resonance was time averaged with the trifluoroacetic acid signal and broadened out so that it was not observable.

The infrared spectra of tetrakis( $\pi$ -cyclopentadienylcarbonyl iron(I)) in some strong acids are given in Table 5.2.

Table 5.2  
Infrared Spectra of Tetrakis( $\pi$ -cyclopentadienylcarbonyl iron(I)) in acid mulls recorded over the 2200-1600  $\text{cm}^{-1}$  region

Acid	$\nu_{\text{CO}}$ absorptions ( $\text{cm}^{-1}$ )
$\text{H}_2\text{SO}_4$	1714s
$\text{H}_2\text{SO}_4/\text{SO}_3$	2127w, 2079m, 1686s
$\text{CH}_3\text{SO}_3\text{H}$	1708s
$\text{HSO}_3\text{Cl}$	2125m, 2075s, 2028m, 1714ms
$\text{CF}_3\text{COOH}$	1786s, * 1716m
$\text{HPF}_6$	1710s
$\text{H}_2\text{PO}_3\text{F}$	1716s

\*  $\nu_{\text{C-O}}$  of  $\text{CF}_3\text{COOH}$

In all cases a  $\nu_{\text{C-O}}$  absorption occurred at about  $1710 \text{ cm}^{-1}$ , which is a shift of about  $90 \text{ cm}^{-1}$  to higher frequencies from the  $\nu_{\text{C-O}}$  absorption observed for tetrakis( $\pi$ -cyclopentadienylcarbonyl iron(I)). The position of the  $\nu_{\text{C-O}}$  absorptions in the acid solutions is at a very similar position to that observed for the  $\nu_{\text{C-O}}$  absorption of the tetrakis( $\pi$ -cyclopentadienylcarbonyl iron cation) (91). Unchanged tetrakis( $\pi$ -cyclopentadienylcarbonyl iron(I)) could be obtained from solutions in sulphuric acid and trifluoroacetic acid by addition of water and by evaporation in vacuo, respectively, i.e., no oxidation had occurred. In the spectrum using oleum as the solvent decomposition to the  $\pi$ -cyclopentadienyltricarboxyl iron(II) cation was observed; and where chlorosulphonic acid was used as solvent  $\pi$ -cyclopentadienyldicarbonyl iron(II) chloride was produced in addition to the  $\pi$ -cyclopentadienyltricarboxyl iron(II) cation. The observed carbonyl absorption shift is much more than can be explained by a simple solvent shift and can only reasonably be explained by protonation of the iron atom(s).

The infrared spectrum of tetrakis( $\pi$ -cyclopentadienylcarbonyl iron) dihydrogen tetrachloroborate failed to show the presence of an absorption characteristic of a O-H group also suggesting that protonation of the iron atom(s) had occurred (spectrum 5.1).

The structure of the diprotonated tetrakis( $\pi$ -cyclopentadienylcarbonyl iron) cation has not been fully elucidated. Solid state infrared spectra of these tetrameric compounds show a very complicated series of carbonyl absorption bands. Attempts to examine these compounds in solution were unsuccessful as a solvent could not be found which did not decompose the protonated species on dissolution.  $^{57}\text{Fe}$  Mossbauer spectroscopy might be successful but isolation of a pure compound was found to be very difficult. By analogy with bis( $\pi$ -cyclopentadienyldicarbonyl iron(I)) and other

dinuclear compounds (29) the proton might be expected to lie along the iron-iron bonds (edge of the tetrahedron formed by the four iron atoms). The addition of two protons on opposite edges would result in a structure with  $S_4$  symmetry and only one  $\nu_{C-O}$  absorption would be expected. Mono protonation would have to position the proton inside the cage in order that only one carbonyl absorption would be observed. The  $^{57}\text{Fe}$  Mossbauer spectrum of a solution of tetrakis( $\pi$ -cyclopentadienylcarbonyl iron(I)) in trifluoroacetic acid showed clearly a change in electron density at the nucleus to that observed for tetrakis( $\pi$ -cyclopentadienylcarbonyl iron(I)). The results also show that the iron atoms are all equivalent and are diamagnetic. Although no evidence about the number of protons attached to the compound could be obtained from the Mossbauer studies; studies in hydrogen chloride clearly showed diprotonation occurred. The only structure which clearly fits in with the  $^{57}\text{Fe}$  Mossbauer evidence is one which has  $S_4$  symmetry and has all four iron atoms equivalent with a proton bridging two iron atoms on opposite edges of the tetrahedron.

Ferguson and Meyer (104) had shown that a mono- and di-cation of tetrakis( $\pi$ -cyclopentadienylcarbonyl iron(I)) could be produced electrochemically. In an attempt to isolate the tetrakis( $\pi$ -cyclopentadienylcarbonyl iron) dication an oxidation using chlorine in liquid hydrogen chloride was carried out. The reaction resulted in isolation of a mixture which contained a principle product which had a  $\nu_{C-O}$  absorption at  $1692\text{ cm}^{-1}$  and some  $\pi$ -cyclopentadienyltricarboxyl iron(II) chloride and  $\pi$ -cyclopentadienyldicarbonyl iron(II) chloride. The principle product was thought to be the monocation but all attempts to separate the components of the mixture produced impure products.

Preparation of the tetrakis( $\pi$ -cyclopentadienylcarbonyl iron) mono-cation as the hexafluorophosphate, tribromide and heptaiodide salts (spectra 5.3-5.5 respectively) were prepared by unambiguous routes. The ultra violet/visible spectra of the hexafluorophosphate salt of tetrakis ( $\pi$ -cyclopentadienylcarbonyl iron) prepared by phosphorus pentafluoride in hydrogen chloride and by the oxidation routes were recorded and showed no differences within the experimental error of the technique used (Table 5.3).

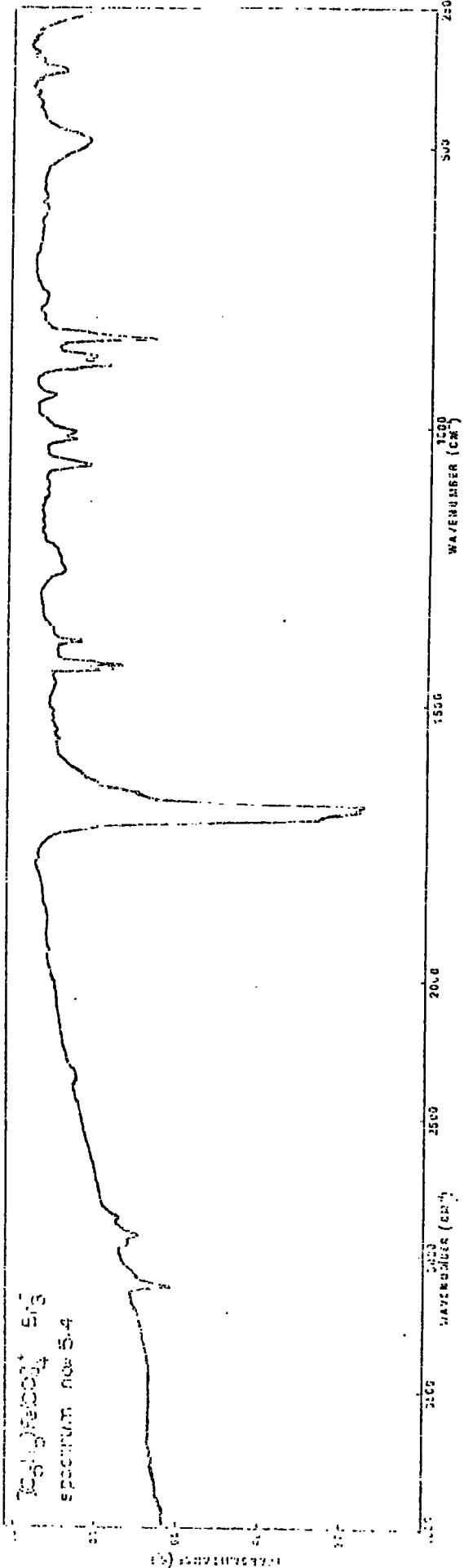
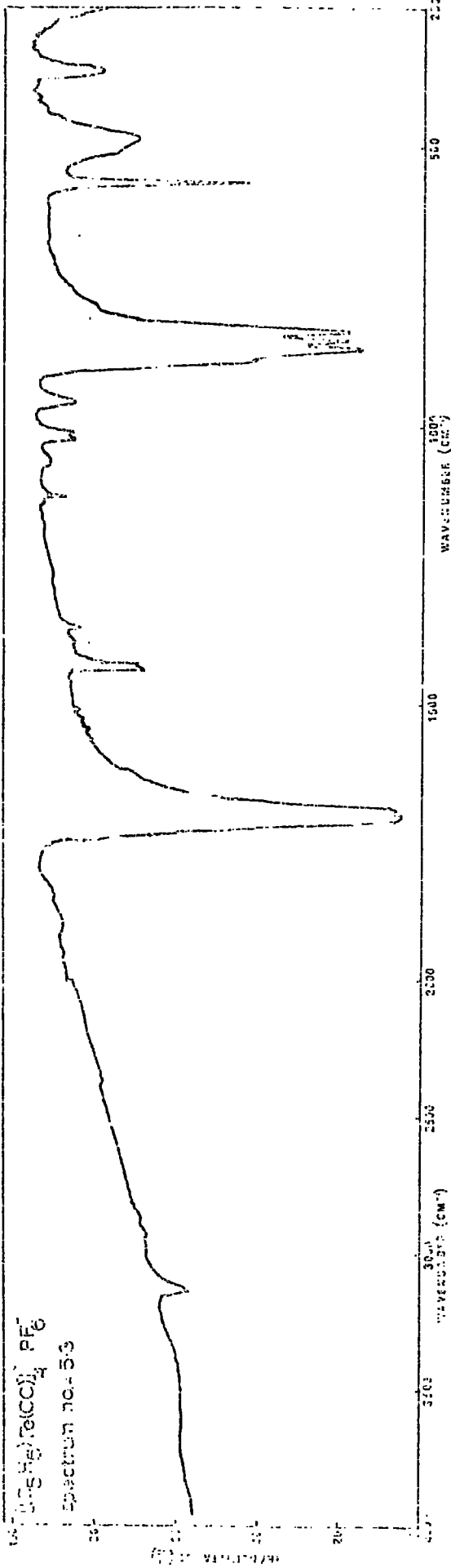
Table 5.3  
UV/Visible Spectra of Tetrakis( $\pi$ -cyclopentadienylcarbonyl  
iron) compounds

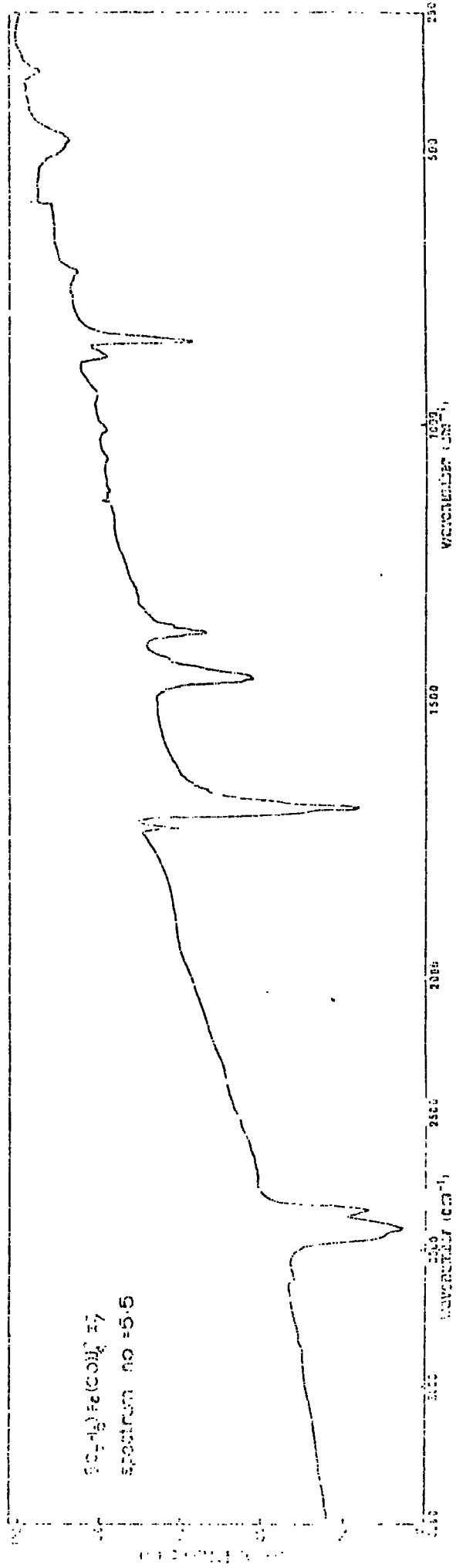
Compound	Solvent	Absorptions cm <sup>-1</sup>	Extinction Coeff.
$[(\pi\text{-C}_5\text{H}_5)\text{Fe}(\text{CO})]_4$	CH <sub>3</sub> CN	15,150 25,380sh 34,480sh	1,730 11,000 13,730
$[(\text{C}_5\text{H}_5)\text{Fe}(\text{CO})]_4^+ \text{PF}_6^- \dagger$	CH <sub>3</sub> CN	15,060 25,770 34,480	2,850 15,700 23,200
$[(\text{C}_5\text{H}_5)\text{Fe}(\text{CO})]_4^+ \text{PF}_6^- *$	CH <sub>3</sub> CN	15,110 25,770 34,480	2,900 17,000 21,800

† prepared from reaction of HCl/PF<sub>5</sub> and  $[(\pi\text{-C}_5\text{H}_5)\text{Fe}(\text{CO})]_4$

\* prepared from reaction of Bu<sub>4</sub>NPF<sub>6</sub> + Br<sub>2</sub> and  $[(\pi\text{-C}_5\text{H}_5)\text{Fe}(\text{CO})]_4$

The cation showed a marked increase in the extinction coefficients of the absorption bands although minimal change in the frequency of the absorption bands were observed.





Decomposition of the cation was followed by observing the disappearance of the  $\nu_{C-O}$  absorption band at ca.  $1700\text{ cm}^{-1}$  in the infrared spectrum. The heptaiodide was the most stable, then the hexafluorophosphate and finally the tribromide. The product from the chlorination of tetrakis( $\pi$ -cyclopentadienylcarbonyl iron) behaved differently from the above compounds (which showed a total disappearance of carbonyl absorptions) by reverting to tetrakis( $\pi$ -cyclopentadienylcarbonyl iron(I)). This reaction occurred relatively fast (about two days). The stability of the ionic species showed the correct type of trend for salts of a large cation. The most stable species would be expected when the cation and anion were of similar size, providing of course that the individual ions were themselves stable.

Magnetic studies on the tetrakis( $\pi$ -cyclopentadienylcarbonyl iron) cation as the hexafluorophosphate and heptaiodide salts were carried out in conjunction with Mr. J. Cope and Dr. J.J. Cox. The results of these studies are given in Appendix C.

$^{13}\text{C}$  Fourier magnetic resonance spectra of tetrakis( $\pi$ -cyclopentadienylcarbonyl iron(I)) and its hexafluorophosphate salt were carried out at Queen Mary College under the SRC sponsored research programme. Table 5.4 gives the results of these studies together with the values for some related compounds. The parent carbonyl shows a resonance attributable to the  $\pi$ -cyclopentadienyl ligand at  $+99.24\text{ ppm}$  which suggests a stronger  $\pi$  overlap with metal d orbitals than observed in the cases of  $\pi$ -cyclopentadienyldicarbonyl iron(II) halides. The spectra of the hexafluorophosphate salt showed a sharp  $\pi$ -cyclopentadienyl resonance at  $+206.99\text{ ppm}$ . The large shift is almost certainly due to the fact that the cation is paramagnetic (one unpaired electron per molecule). The fact

Table 5.4  
<sup>13</sup>C Nuclear Magnetic Resonance Spectra

Compound	Absorptions*		
	$\delta(\pi\text{-C}_5\text{H}_5)$	$\delta(\text{C-O})$	$\delta(\text{CH}_3)$
$[(\pi\text{-C}_5\text{H}_5)\text{Fe}(\text{CO})]_4$	99.24		
$[(\pi\text{-C}_5\text{H}_5)\text{Fe}(\text{CO})]_4^+ \text{PF}_6^-$	205.99		
$(\pi\text{-C}_5\text{H}_5)\text{Fe}(\text{CO})_2\text{Cl}^\dagger$	85.6	212.9	
$(\pi\text{-C}_5\text{H}_5)\text{Fe}(\text{CO})_2\text{Br}^\dagger$	85.4	213.2	
$(\pi\text{-C}_5\text{H}_5)\text{Fe}(\text{CO})_2\text{I}^\dagger$	84.8	213.8	
$(\pi\text{-C}_5\text{H}_5)\text{Fe}(\text{CO})_2\text{CH}_3^\dagger$	85.3	218.4	-23.5

\* Resonances taken relative to tetramethyl silane = 0.0 ppm

† L.F. Farnell, E.W. Randall and E. Rosenberg, J. Chem. Soc.(D), 1971, 1078.

that a sharp resonance could be readily obtained in the <sup>13</sup>C nmr, in contrast to <sup>1</sup>H nmr (where a broad line only was exhibited) may mean that paramagnetic complexes containing carbon may be examined by <sup>13</sup>C techniques. Magnetic measurements using nmr techniques may enable a very precise measurement of the paramagnetism of the complex and eliminate packing problems encountered in measurements using the Gouy technique (107). Current techniques using nmr to measure paramagnetism use a solvent containing an observer compound which exhibits a sharp resonant absorption. The shift of the signal of the observer from in the neat solvent to in the solution containing a paramagnetic species can then be related to the bulk susceptibility of the solution and thus to the paramagnetism of the complex. The use of fourier techniques enables much more precise shift measurements to be made and gives a much better signal to noise ratio,

hence enabling more accurate measurements to be carried out. The spectra recorded failed to show the  $^{13}\text{C}$  resonance attributable to the carbonyl ligands. Farnell and co-workers in their work on metal carbonyls (108) pointed out that the decay times for  $^{13}\text{C}$  varied according to their environment and that spectra with different pulse times were needed to record all the  $^{13}\text{C}$  resonances in the compounds. Further studies may provide the evidence for the resonance of the  $^{13}\text{C}$  in the carbonyl ligands but this technique seems to be less sensitive to changes in carbonyl bonding than infrared spectroscopy. Detecting small differences in the carbonyl ligands in attempts to assign the structure of the compounds was thought to be best accomplished by infrared spectroscopy.

## 5.2. Experimental

### 5.2.1. Dihydrogen Tetrakis( $\pi$ -cyclopentadienylcarbonyl iron(I)) tetrachloroborate, $[(\pi\text{-C}_5\text{H}_5)\text{Fe}(\text{CO})]_4\text{H}_2 \text{ } ^2+\text{ } ^-\text{ } 2\text{BCl}_4$

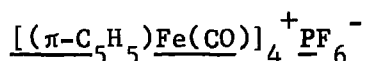
Tetrakis( $\pi$ -cyclopentadienylcarbonyl iron(I)) (0.3683 g., 0.618 mmoles) was degassed in vacuo overnight. Hydrogen chloride (10 cm<sup>3</sup>, 0.38 mole) was distilled into the ampoule cooled to  $-196^\circ\text{C}$  (liquid nitrogen bath), on warming to  $-95^\circ\text{C}$  (toluene slush bath) a homogeneous solution was obtained. The solution was cooled to  $-196^\circ\text{C}$  (liquid nitrogen bath) and boron trichloride (8 mmoles) was condensed in from the gas phase. The mixture was allowed to react at  $-84^\circ\text{C}$  (solid carbon dioxide/acetone slurry) overnight, a dark green solid being precipitated. After removing all volatiles in vacuo at temperatures below  $-84^\circ\text{C}$  the solid was allowed to warm to room temperature. Found: C, 32.34; H, 2.88; Cl, 28.8; % increase in weight on tetrakis( $\pi$ -cyclopentadienylcarbonyl iron(I)) 54.50.

$\text{C}_{24}\text{H}_{22}\text{B}_2\text{Cl}_8\text{Fe}_4\text{O}_4$  requires C, 31.84; H, 2.45; Cl, 31.33; % increase on tetrakis( $\pi$ -cyclopentadienylcarbonyl iron(I)), 51.9.

5.2.2. Tetrakis( $\pi$ -cyclopentadienylcarbonyl iron(I)) di(boron trichloride),

$[(\pi\text{-C}_5\text{H}_5)\text{Fe}(\text{CO})]_4 \cdot 2\text{BCl}_3$ , was prepared in an identical manner to that used for preparing dihydrogen tetrakis( $\pi$ -cyclopentadienylcarbonyl iron(I)) tetrachloroborate except that the product was pumped on at room temperature for about thirty minutes. Found: C,34.2; H,2.05; Cl,25.7; % increase in weight on tetrakis( $\pi$ -cyclopentadienylcarbonyl iron(I)) 38.95,  $\text{C}_{24}\text{H}_{20}\text{B}_2\text{Cl}_6\text{Fe}_4\text{O}_4$  requires C,34.73; H,2.43; Cl,25.62; % increase in weight on tetrakis( $\pi$ -cyclopentadienylcarbonyl iron(I)), 39.3.

5.2.3. Tetrakis( $\pi$ -cyclopentadienylcarbonyl iron) hexafluorophosphate,



Tetrakis( $\pi$ -cyclopentadienylcarbonyl iron(I)) (0.1280 g., 0.215 mmoles) was degassed in vacuo overnight. Hydrogen chloride (10 cm<sup>3</sup>, 0.38 mole) was condensed into the ampoule after cooling to -196°C (liquid nitrogen bath), on warming to -95°C (toluene slush bath) a homogeneous solution was obtained. The solution was cooled to -196°C (liquid nitrogen bath) and phosphorus pentafluoride (3 mmoles) was condensed in from the gas phase. The mixture was allowed to react at -84°C (solid carbon dioxide/acetone slurry) overnight before removing all volatiles in vacuo. After warming to room temperature the solid product was washed with methylene chloride to remove unreacted starting material to leave a insoluble green solid. Found: C,38.44; H,2.81; Fe,30.20; P,3.95;  $\text{C}_{24}\text{H}_{20}\text{F}_6\text{Fe}_4\text{O}_4\text{P}$  requires C,38.91; H,2.72; Fe,30.16; P,4.18.

Alternative preparation procedures for tetrakis( $\pi$ -cyclopentadienylcarbonyl iron) hexafluorophosphate,  $[(\pi\text{-C}_5\text{H}_5)\text{Fe}(\text{CO})]_4^+ \text{PF}_6^-$

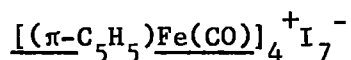
(A) Tetrakis( $\pi$ -cyclopentadienylcarbonyl iron(I)) (5.95 g., 0.01 mol) and tetra-n-butylammonium hexafluorophosphate (3.81 g., 0.01 mol) were dissolved in a minimum quantity of methylene chloride. After filtering

through a pad of filter aid to the filtrate was added dropwise a solution of bromine (0.8 g., 0.01 mol) in methylene chloride (200 cm<sup>3</sup>). After filtering off the precipitate it was dissolved in acetone and reprecipitated by the careful addition of hexane. Found: C,39.06; H,2.69; Fe,30.2; P,3.97; C<sub>24</sub>H<sub>20</sub>F<sub>6</sub>Fe<sub>4</sub>O<sub>4</sub>P requires C,38.91; H,2.72; Fe,30.16; P,4.18.

(B) To tetrakis( $\pi$ -cyclopentadienylcarbonyl iron(I)) (2.98 g., 0.005 mol) in methylene chloride (150 cm<sup>3</sup>) was added dropwise a solution of triphenyl methyl hexafluorophosphate (1.88 g., 0.005 mol) in a minimum quantity of methylene chloride. The triphenyl carbonium hexafluorophosphate was prepared immediately prior to use by dissolving triphenyl methyl carbinol (4.5 g., 0.017 mole) in proprionic anhydride (45 cm<sup>3</sup>, 0.35 moles). After cooling the solution to 10°C, hexafluorophosphoric acid (4.5 cm<sup>3</sup>, 65% solution) was added slowly ensuring that the temperature remained below 15°C. After allowing the yellow crystals to settle the supernatant liquor was decanted off and the solid washed quickly with four portions of cold dry diethyl ether (3 cm<sup>3</sup>) and the product finally dried in vacuo.

The solution of the iron compound was filtered at the pump, the residue dissolved in acetone and reprecipitated by the careful addition of hexane. Found: C,38.29; H,2.78; Fe,30.10; C<sub>24</sub>H<sub>20</sub>F<sub>6</sub>Fe<sub>4</sub>O<sub>4</sub>P requires C,38.91; H,2.72; Fe,30.16.

#### 5.2.4. Tetrakis( $\pi$ -cyclopentadienylcarbonyl iron) heptaiodide,



To tetrakis( $\pi$ -cyclopentadienylcarbonyl iron(I)) (5.95 g., 0.01 mole) in methylene chloride (250 cm<sup>3</sup>) was added dropwise iodine 8.9 g., 0.07 mole) dissolved in a minimum quantity of methylene chloride. After stirring the solution overnight it was filtered at the pump to yield a

pale green solid. Found: C, 19.40; H, 1.34; Fe, 15.60; I, 60.1;

$C_{24}H_{20}FeI_4O_4$  requires C, 19.41; H, 1.36; Fe, 15.05; I, 59.87.

5.2.5. Reaction of tetrakis( $\pi$ -cyclopentadienylcarbonyl iron(I)) with chlorine in liquid hydrogen chloride

Tetrakis( $\pi$ -cyclopentadienylcarbonyl iron(I)) (0.0777 g., 0.130 mmoles) was degassed in vacuo overnight. Hydrogen chloride (7 cm<sup>3</sup>, 0.25 mol) was condensed into the ampoule cooled to -196°C (liquid nitrogen bath), warming to -95°C (toluene slush bath) gave a homogeneous solution. After cooling the mixture to -196°C (liquid nitrogen bath) chlorine (0.17 mmole) was condensed in from the gas phase and the mixture was allowed to react at -95°C for about four hours. On cooling the mixture to -196°C (liquid nitrogen bath) some non-condensable gas was detected (ca. 6 mm. in 65 cm<sup>3</sup>, 0.03 mole), removal of all volatiles at low temperature in vacuo resulted in a green solid being isolated at room temperature. The infrared spectrum showed  $\nu_{C-O}$  absorptions at 2122w, 2074w, 2048m, 2002m, 1692s, 1623m. Attempts to separate the components were not successful also the products smelt of chlorocarbons suggesting chlorination of the  $\pi$ -cyclopentadienyl ring. A weight increase corresponding to addition of 1 mole of chlorine per mole of starting material was observed.

5.2.6. Conductimetric studies of tetrakis( $\pi$ -cyclopentadienylcarbonyl iron(I)) solutions in hydrogen chloride

(a) with boron trichloride

Tetrakis( $\pi$ -cyclopentadienylcarbonyl iron(I)) (0.0533 g., 0.0896 mmoles) was degassed in vacuo overnight. After cooling the conductivity cell to -196°C (liquid nitrogen bath), hydrogen chloride

(7 cm<sup>3</sup>, 0.25 mole) was condensed in from the gas phase. Aliquots of boron trichloride were added from the gas phase and the reaction followed conductimetrically. Breaks in the titration curve were observed at the 1:1 and 2:1 mole ratios (acid:base). The conductivity curve is shown in Figure 5.1.

(b) with chlorine

Tetrakis( $\pi$ -cyclopentadienylcarbonyl iron(I)) (0.0777 g., 0.130 mmoles) was degassed in vacuo overnight. After cooling to -196°C (liquid nitrogen bath), hydrogen chloride (7 cm<sup>3</sup>, 0.25 mole) was condensed in from the gas phase. Aliquots of chlorine were added from the gas phase and the reaction followed conductimetrically. A general increase in conductivity was observed but the individual conductivities were very variable, and since a mixture of products was obtained, no reliable evidence could be gleaned.

5.2.7. Infrared spectra of tetrakis( $\pi$ -cyclopentadienylcarbonyl iron(I)) in some strong anhydrous acids

Tetrakis( $\pi$ -cyclopentadienylcarbonyl iron) was degassed in vacuo overnight. The acids used in this study were degassed prior to use, solutions of the tetrakis( $\pi$ -cyclopentadienylcarbonyl iron(I)) were prepared under a nitrogen shield and were smeared between polythene sheets and examined in the 2200-1600 cm<sup>-1</sup> region by infrared spectroscopy. The  $\nu_{C-O}$  absorption bands are given in Table 5.2.

5.2.8. <sup>1</sup>H Nuclear magnetic resonance studies were carried out on solutions of tetrakis( $\pi$ -cyclopentadienylcarbonyl iron(I)) in hydrogen chloride and in trifluoroacetic acid. In the case of the hydrogen chloride solution insufficient sample dissolved to detect the protons

on the  $\pi$ -cyclopentadienyl ligand. The spectra in trifluoroacetic acid showed the  $\pi$ -cyclopentadienyl ring protons, no proton attached to a metal atom could be detected in the -20 to +100 ppm range.

CHAPTER 6

STUDIES ON THE  $\pi$ -CYCLOPENTADIENYLDICARBONYL IRON- $\mu$ -HALOGENO  $\pi$ -CYCLO-PENTADIENYLDICARBONYL IRON CATIONS,  $[(\pi\text{-C}_5\text{H}_5)\text{Fe}(\text{CO})_2]_2\text{X}^+$ , X = Cl, Br or I

6.1. Results and Discussion

Davis and co-workers (29) in their studies of the protonation of neutral transition metal complexes found that  $\pi$ -cyclopentadienyldicarbonyl iron(II) chloride reacted with sulphuric acid to liberate hydrogen chloride. No other reaction products were identified. The author noted that in addition to the evolution of hydrogen chloride a bright cherry red solution was formed when  $\pi$ -cyclopentadienyldicarbonyl iron(II) chloride reacted with sulphuric acid. Similarly bright cherry red solutions were obtained from the reactions of  $\pi$ -cyclopentadienyldicarbonyl iron(II) bromide and of  $\pi$ -cyclopentadienyldicarbonyl iron(II) iodide with sulphuric acid, hydrogen bromide and hydrogen iodide being evolved, respectively. Addition of hexafluorophosphoric acid to the cherry red solutions precipitated the  $\pi$ -cyclopentadienyldicarbonyl iron- $\mu$ -halogeno  $\pi$ -cyclopentadienyldicarbonyl iron hexafluorophosphates, halogeno = chloro, bromo and iodo. The preparation of the  $\pi$ -cyclopentadienyldicarbonyl iron- $\mu$ -halogeno  $\pi$ -cyclopentadienyldicarbonyl iron(II) cations had previously been reported by Fischer and Moser (96,97) who reacted aluminium trihalide with  $\pi$ -cyclopentadienyldicarbonyl iron(II) halide in liquid sulphur dioxide. The  $\pi$ -cyclopentadienyldicarbonyl iron- $\mu$ -iodo  $\pi$ -cyclopentadienyldicarbonyl iron(II) cation has been shown to be formed as an intermediate in the reaction of bis( $\pi$ -cyclopentadienyldicarbonyl iron(I)) with iodine to give  $\pi$ -cyclopentadienyldicarbonyl iron(II) iodide (99). The reaction of halogens with bis( $\pi$ -cyclopentadienyl-

dicarbonyl iron(I)) in the presence of tetraphenyl boron also gives  $\pi$ -cyclopentadienyldicarbonyl iron- $\mu$ -halogens  $\pi$ -cyclopentadienyldicarbonyl iron salts, in the case of the chlorination an equal quantity of  $\pi$ -cyclopentadienyltricarbonyl iron(II) chloride is also produced (100,101).

The structure of the  $\pi$ -cyclopentadienyldicarbonyl iron- $\mu$ -halogeno  $\pi$ -cyclopentadienyldicarbonyl iron(II) cations and the interpretation of the carbonyl stretching modes, in particular the occurrence of three and four bands in different salts has not been attempted.

A consideration of local symmetry, using the carbonyls as probes would predict either two or four carbonyl absorptions, no structure which would give rise to three carbonyl absorptions could be envisaged.

Careful examination of the sulphuric acid solutions of  $\pi$ -cyclopentadienyldicarbonyl iron(II) halides (halide = chloride, bromide or iodide) was carried out over the region  $1950-2200\text{ cm}^{-1}$  using infrared spectroscopy. The results are given in Table 6.1; and the spectra are shown on pages 91-93.

The band at higher wavenumbers is clearly split into two in the case of the  $\pi$ -cyclopentadienyldicarbonyl iron(II) bromide and  $\pi$ -cyclopentadienyldicarbonyl iron(II) iodide. In the case of the  $\pi$ -cyclopentadienyldicarbonyl iron(II) chloride however a slight shoulder occurs on the lower frequency side of the band. The lower frequency carbonyl absorption band is broad but distortion is only clearly shown in the case of  $\pi$ -cyclopentadienyldicarbonyl iron(II) iodide.

Results of the examination of the  $\pi$ -cyclopentadienyldicarbonyl iron- $\mu$ -halogeno  $\pi$ -cyclopentadienyldicarbonyl iron(II) hexafluorophosphates, halogeno = chloro, bromo or iodo in the  $2200-1950\text{ cm}^{-1}$  region using infrared spectroscopy are given in Table 6.1, and the spectra are shown in spectra 6.1-6.6.

Table 6.1

Infrared Spectra of the  $[(\pi\text{-C}_5\text{H}_5)\text{Fe}(\text{CO})_2]_2\text{X}^+$  cations, X = Cl, Br and I in the  $\nu_{\text{C-O}}$  region

Compound	Sample mode	$\nu_{\text{CO}} \text{ cm}^{-1}$
$(\pi\text{-C}_5\text{H}_5)\text{Fe}(\text{CO})_2\text{Cl}^*$	H <sub>2</sub> SO <sub>4</sub> soln.	2075s, 2055sh, 2029s
$(\pi\text{-C}_5\text{H}_5)\text{Fe}(\text{CO})_2\text{Br}^*$	H <sub>2</sub> SO <sub>4</sub> soln.	2071s, 2059s, 2023s
$(\pi\text{-C}_5\text{H}_5)\text{Fe}(\text{CO})_2\text{I}^*$	H <sub>2</sub> SO <sub>4</sub> soln.	2063s, 2049s, 2017s, 2003sh
$[(\pi\text{-C}_5\text{H}_5)\text{Fe}(\text{CO})_2]_2\text{Cl}^+\text{PF}_6^-$	KBr disc	2058sh, 2050s, 2013s, 2003sh, 2123s <sup>†</sup> , 2073s <sup>†</sup>
$[(\pi\text{-C}_5\text{H}_5)\text{Fe}(\text{CO})_2]_2\text{Cl}^+\text{PF}_6^-$	CH <sub>2</sub> Cl <sub>2</sub> soln.	2071s, 2064sh, 2025s <sup>**</sup>
$[(\pi\text{-C}_5\text{H}_5)\text{Fe}(\text{CO})_2]_2\text{Cl}^+\text{PF}_6^-$	Nujol mull	2057sh, 2050s, 2013s, 2000sh
$[(\pi\text{-C}_5\text{H}_5)\text{Fe}(\text{CO})_2]_2\text{Br}^+\text{PF}_6^-$	KBr disc	2057sh, 2043s, 2007sh, 2001s, 2027s <sup>†</sup> , 2074s <sup>†</sup>
$[(\pi\text{-C}_5\text{H}_5)\text{Fe}(\text{CO})_2]_2\text{Br}^+\text{PF}_6^-$	CH <sub>2</sub> Cl <sub>2</sub> soln.	2068s, 2058s, 2020s <sup>**</sup>
$[(\pi\text{-C}_5\text{H}_5)\text{Fe}(\text{CO})_2]_2\text{I}^+\text{PF}_6^-$	KBr disc	2047sh, 2040s, 2013sh, 2007s, 2129s <sup>†</sup> , 2079 <sup>†</sup>
$[(\pi\text{-C}_5\text{H}_5)\text{Fe}(\text{CO})_2]_2\text{I}^+\text{PF}_6^-$	CH <sub>2</sub> Cl <sub>2</sub> soln.	2063s, 2051s, 2017s <sup>**</sup>
$[(\pi\text{-C}_5\text{H}_5)\text{Fe}(\text{CO})_2]_2\text{Cl}^+\text{BCl}_4^-$	Nujol	2055sh, 2050s, 2013, 2003

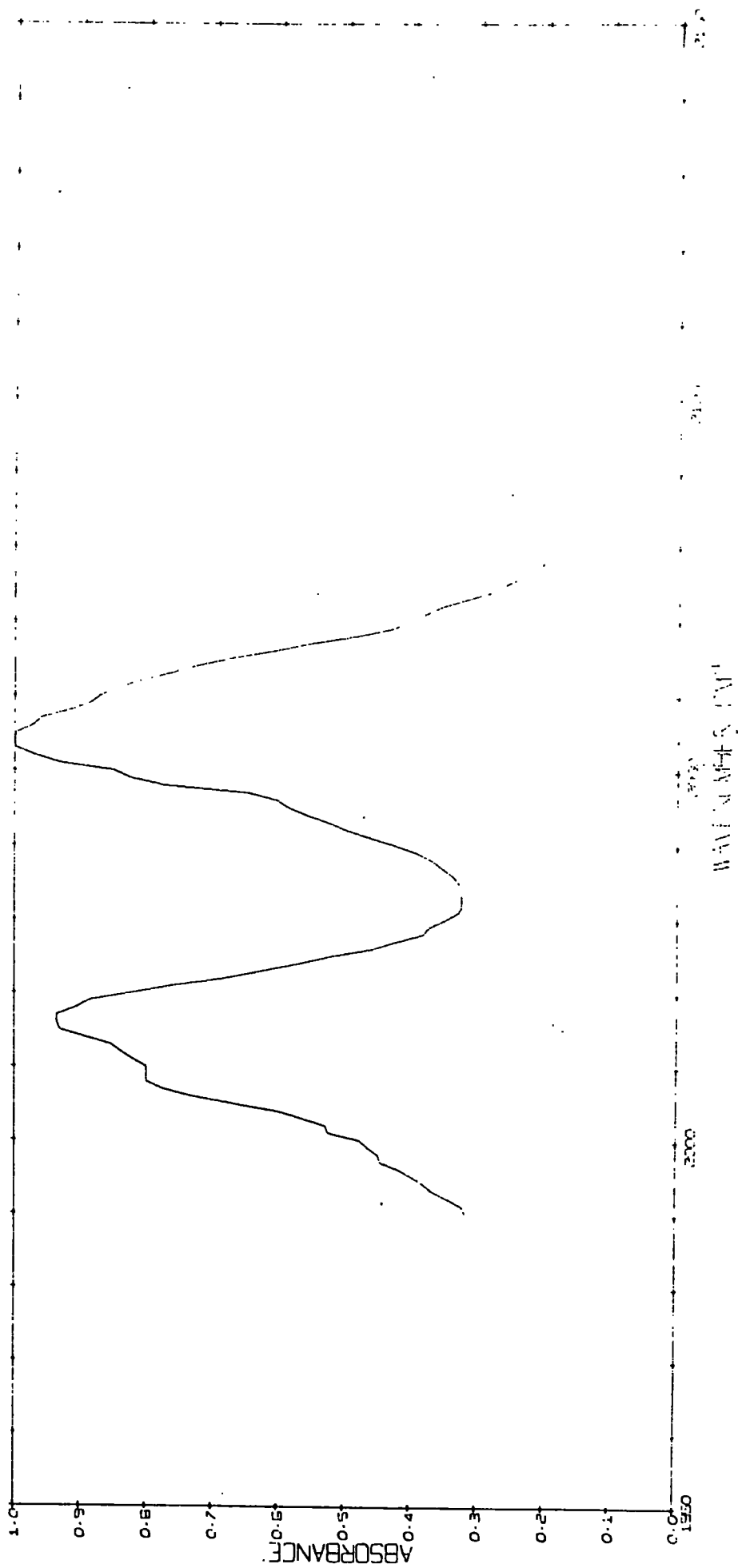
† Bands appeared with time

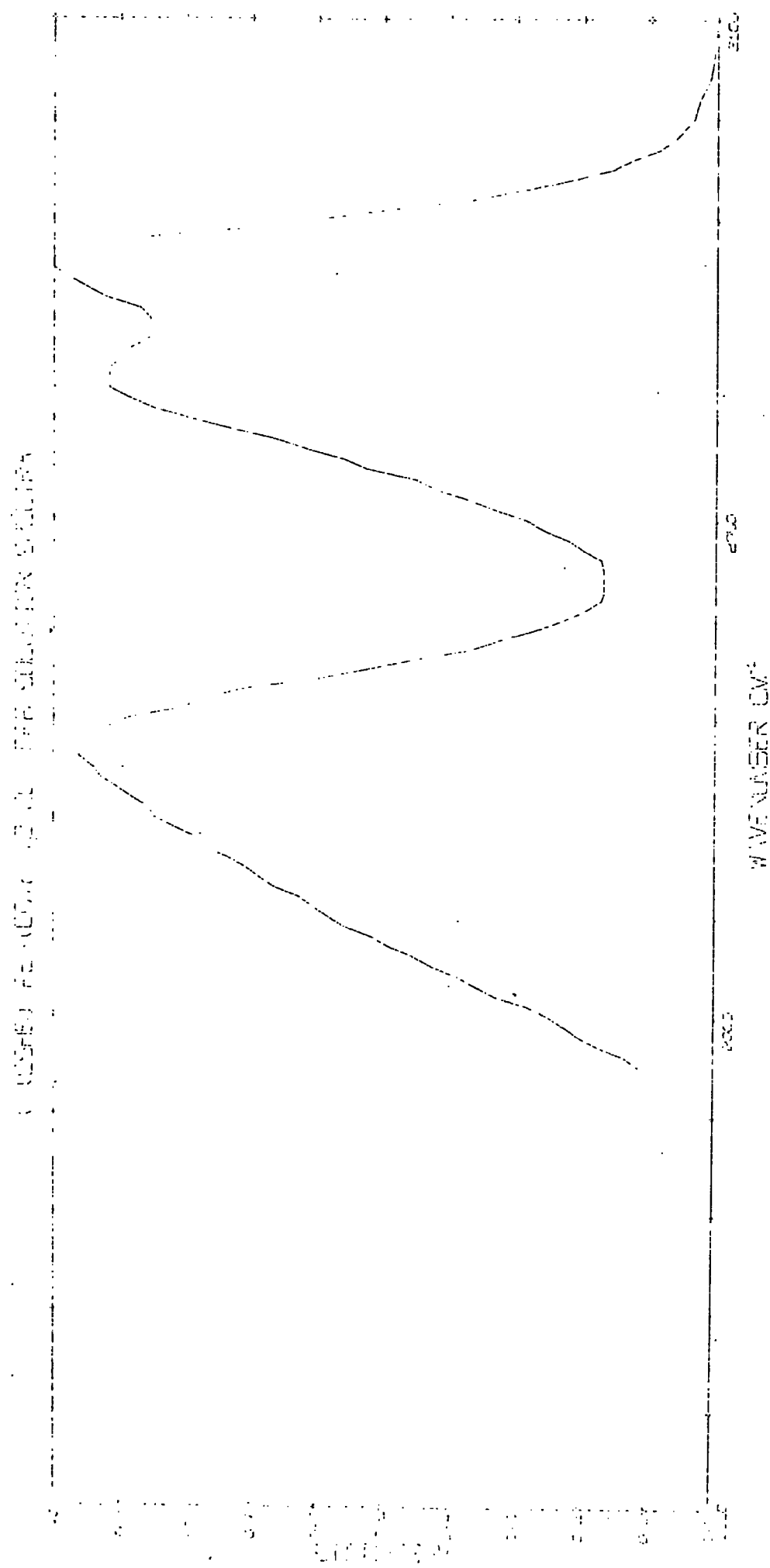
\* These compounds react with sulphuric acid to give the corresponding  $[(\pi\text{-C}_5\text{H}_5)\text{Fe}(\text{CO})_2]_2\text{X}^+$  cation

\*\* Bands asymmetric in shape

## Spectrum number 6.1

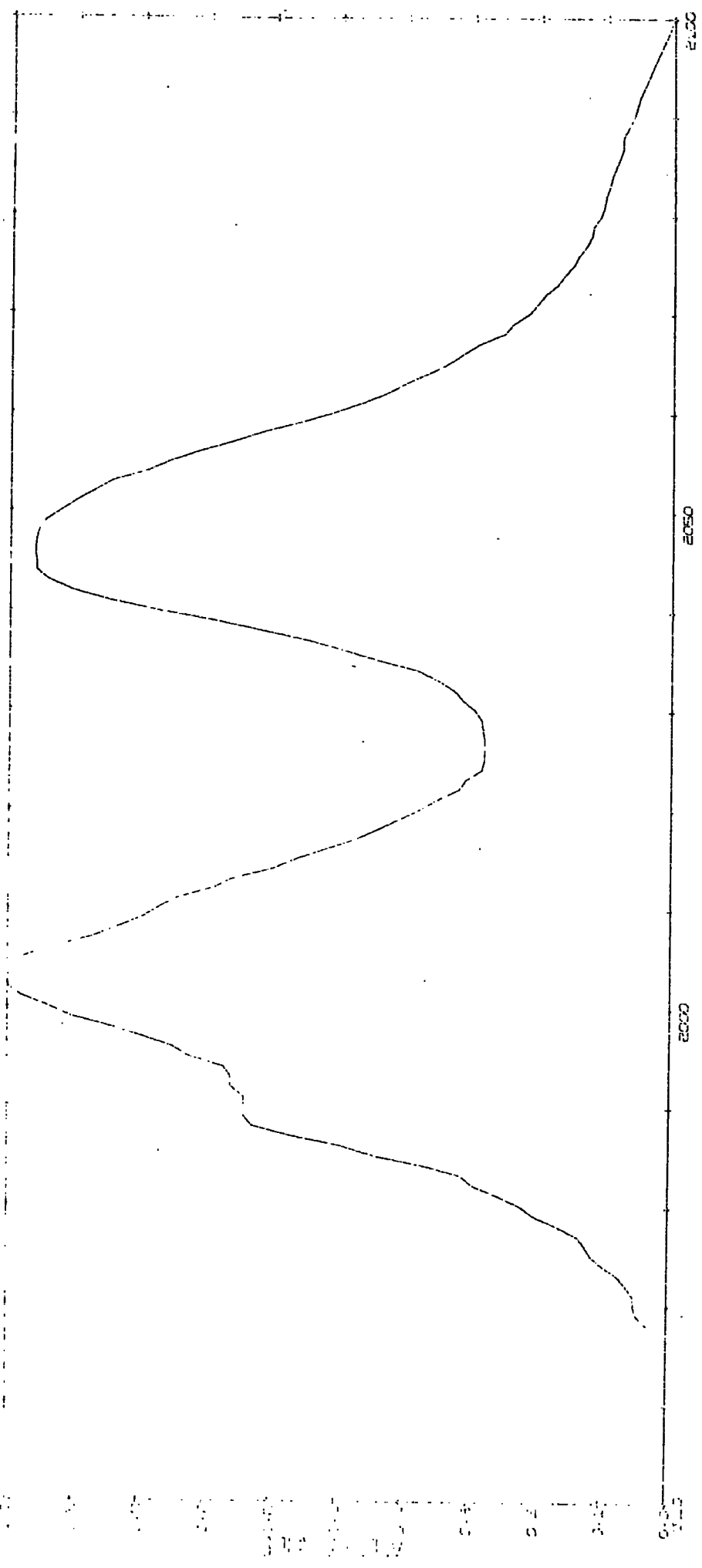
( (CS HS) FE (CO) 2 ) 2 CL PFE SOLID SPECTRA





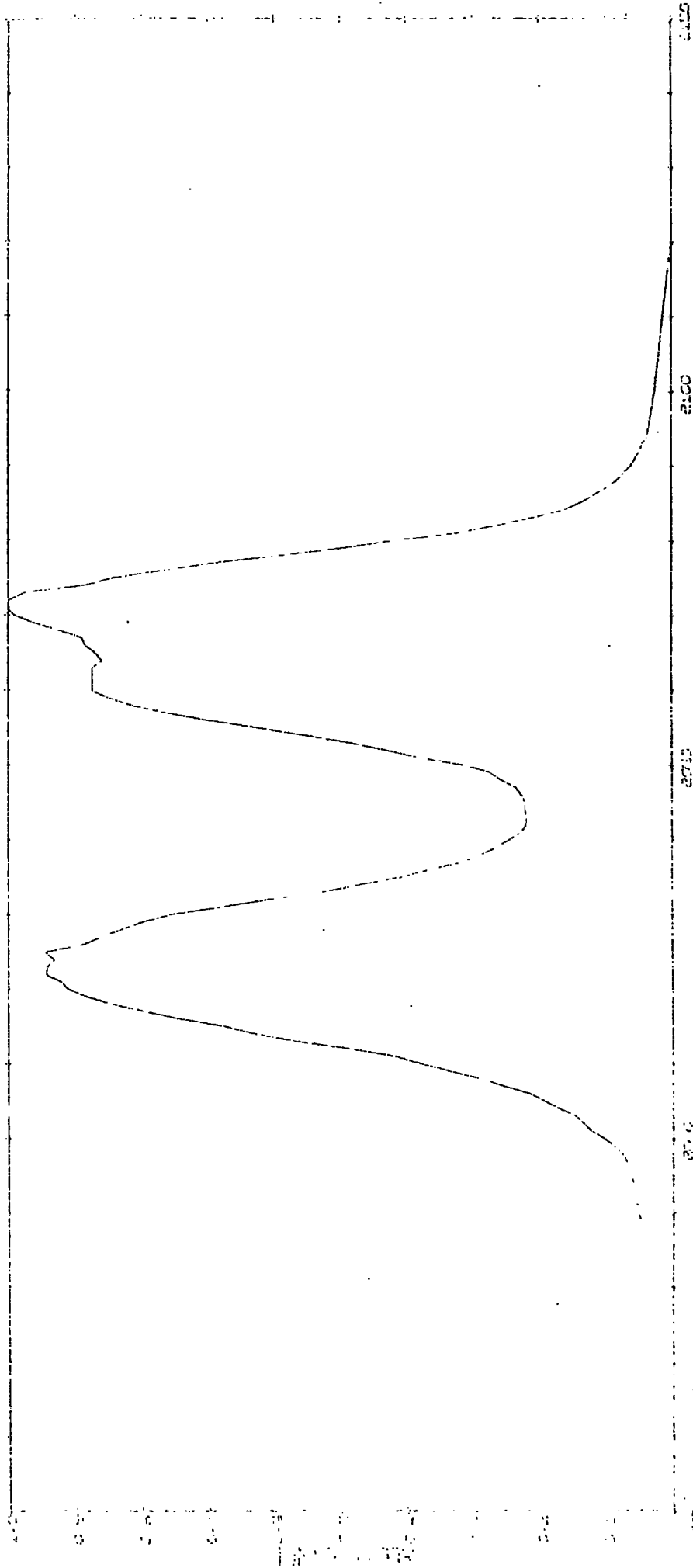
Spectrum Number = 6.2

1 (CS H<sub>2</sub>) FL (CON) 12 BR PFS SOLID SPECTRA



Spectrum Number = 6.3

( (CS HS) FE (CO)2.12 BR PF6 SOLUTION SPECTRA

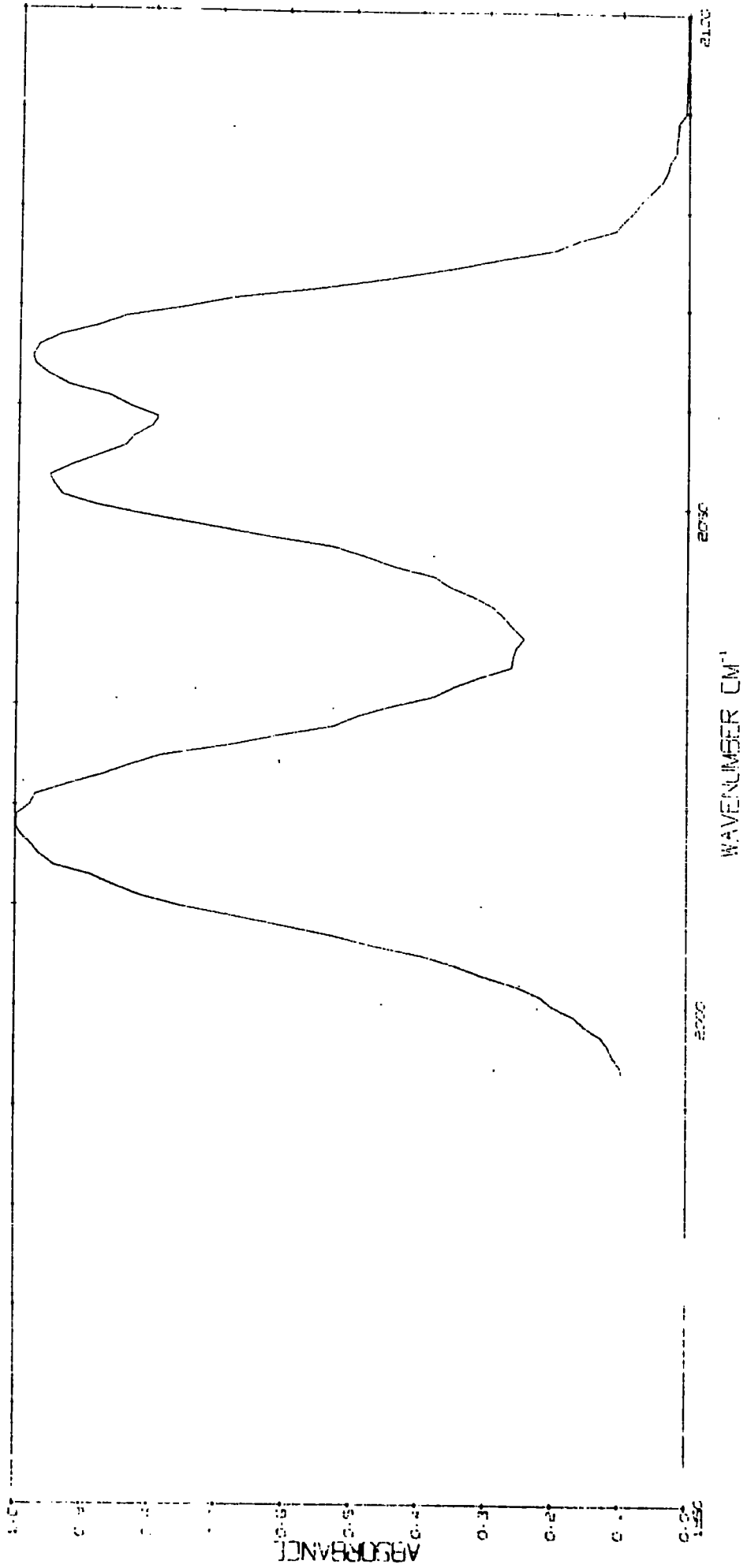


WAVELENGTH (nm)

Spectrum Number = 6.4

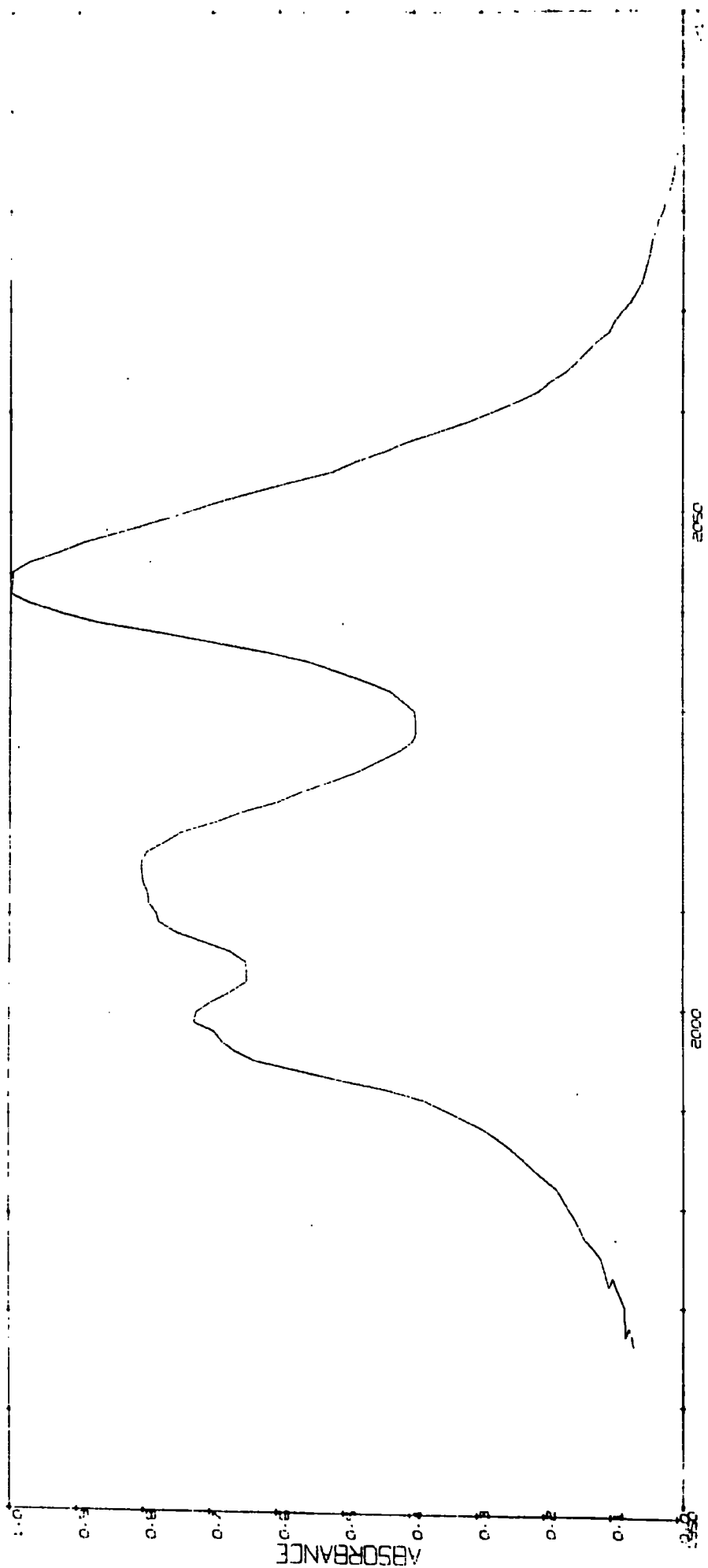
Spectrum Number 6.5

( (CSHS) FE (CO)2 ) 2 I PF6 SOLUTION SPECTRA



Spectrum Number 6.6

IR SPECTRUM OF POLYMER I PPS SOLID SPECTRA



The high frequency carbonyl absorption shows a definite splitting into two absorption bands in all  $\pi$ -cyclopentadienyldicarbonyl iron- $\mu$ -halogeno  $\pi$ -cyclopentadienyldicarbonyl iron(II) complexes when examined in methylene chloride solution or KBr discs. The methylene chloride solution spectra do not however show any splitting on the low frequency carbonyl absorption band, such as exhibited in the KBr disc spectra. The lower frequency carbonyl band has a half width of about  $14 \text{ cm}^{-1}$  which is about one and a half times the width of the low frequency carbonyl absorption band of the  $\pi$ -cyclopentadienyldicarbonyl iron(II) halides when recorded under identical instrumental and experimental conditions. This is suggestive that the lower frequency carbonyl absorption band may be composed of an unresolved doublet. The structure of the  $\pi$ -cyclopentadienyldicarbonyl iron- $\mu$ -halogeno  $\pi$ -cyclopentadienyldicarbonyl iron(II) cations is unknown but the structures (I) to (IV) shown on page 71 are likely. Conversion of the cis isomer into the trans isomer can be achieved by rotation of one of the  $\pi$ -cyclopentadienyldicarbonyl iron groups about the iron halogen bond. Both the cis and trans forms of the cations would be expected to give four carbonyl absorption bands all infrared active. However the carbonyl absorptions of the cis and trans forms would not be expected to occur at very different frequencies and would probably result in the observation of only four bands in a mixture of the isomers. The splitting of the lower frequency carbonyl absorption band in the KBr disc spectra may be due to solid state effects, or it might be due to the crystal form of the cations existing in the isomer which gives the maximum splitting of the carbonyl frequencies. The half-width of the carbonyl absorption bands observed in the KBr disc spectra are broader than those observed in the methylene chloride solution. The

possibility of reaction with the KBr was eliminated by recording the spectra as Nujol mulls which gave spectra with bands in the same position. The bands tended however to be broader and the spectra show more scatter, this was thought to be due to the fact that the  $\pi$ -cyclopentadienyldicarbonyl iron- $\mu$ -halogeno  $\pi$ -cyclopentadienyldicarbonyl iron(II) hexafluorophosphates are relatively soft and that grinding with nujol did not give such a finely ground sample as that obtained when grinding with potassium bromide. If the halogen in the cations is not symmetrically situated between the two iron atoms we would expect four carbonyl absorptions. For  $\pi$ -cyclopentadienyldicarbonyl iron(II) chloride the two carbonyl absorptions occur at 2050 and 2010  $\text{cm}^{-1}$  (85) and for  $\pi$ -cyclopentadienyldicarbonyl pyridine iron(II) hexafluorophosphate the two carbonyl absorptions occur at 2070 and 2025  $\text{cm}^{-1}$  (109), which suggests that any asymmetry in the iron-chlorine-iron bond probably would not result in a marked difference in the frequencies of the carbonyl absorptions of the two  $\pi$ -cyclopentadienyldicarbonyl iron groups.

In an attempt to determine whether or not the iron-halogen-iron bond in these cations are symmetrical we investigated the  $^{57}\text{Fe}$  Mossbauer spectra and the X-ray photoelectron spectra of the compounds. The results of our  $^{57}\text{Fe}$  studies and X-ray photoelectron studies are given in detail in Chapter 7. Neither of the above mentioned techniques could detect any difference in the two iron atoms, hence the evidence is strongly suggestive of a symmetrical iron-halogen-iron bond. The X-ray crystal structure of the  $\pi$ -cyclopentadienyldicarbonyl iron- $\mu$ -bromo  $\pi$ -cyclopentadienyldicarbonyl iron(II) hexafluorophosphate is now being determined in conjunction with Dr. N. Alcock at Warwick University.

The  $\pi$ -cyclopentadienyldicarbonyl iron- $\mu$ -hydrogen  $\pi$ -cyclopentadienyldicarbonyl cation has been observed to decompose readily on warming to

form the  $\pi$ -cyclopentadienyltricarbonyl iron cation. Similarly the  $\pi$ -cyclopentadienyldicarbonyl iron- $\mu$ -halogeno  $\pi$ -cyclopentadienyldicarbonyl iron cations were observed to decompose slowly on gentle heating. The decomposition was followed by monitoring 2200-1900  $\text{cm}^{-1}$  region using infrared spectroscopy. The stability of the  $[(\pi\text{-C}_5\text{H}_5)\text{Fe}(\text{CO})_2]_2\text{X}^+$  cations (X = H, Cl, Br and I) was found to increase with increasing atomic weight of the bridging atom, X. In the compounds where X was chlorine or bromine the only product of decomposition identified was the  $\pi$ -cyclopentadienyltricarbonyl iron(II) cation. In the case where X was iodine in addition to the formation of the  $\pi$ -cyclopentadienyltricarbonyl iron(II) cation,  $\pi$ -cyclopentadienyldicarbonyl iron(II) iodide was also formed. The case where X was hydrogen has been discussed previously in Chapter 3. Typical spectra of the  $\pi$ -cyclopentadienyldicarbonyl iron- $\mu$ -halogeno  $\pi$ -cyclopentadienyldicarbonyl iron hexafluorophosphate (halogeno = chloro, bromo or iodo) are given in spectra 6.7-6.12. The spectra of the decomposed samples were recorded after a period of heating at 80°C for six days

The far infrared spectra (400-50  $\text{cm}^{-1}$ ) of the  $\pi$ -cyclopentadienyldicarbonyl iron- $\mu$ -halogeno  $\pi$ -cyclopentadienyldicarbonyl iron hexafluorophosphates were recorded as nujol mulls. In all cases the Fe-X, (X = Cl, Br or I) of the parent  $\pi$ -cyclopentadienyldicarbonyl iron(II) halides was moved to lower frequencies in the  $[(\pi\text{-C}_5\text{H}_5)\text{Fe}(\text{CO})_2]_2\text{X}^+\text{PF}_6^-$  (X = Cl, Br or I) compounds. These results are considered in detail in Chapter 8.

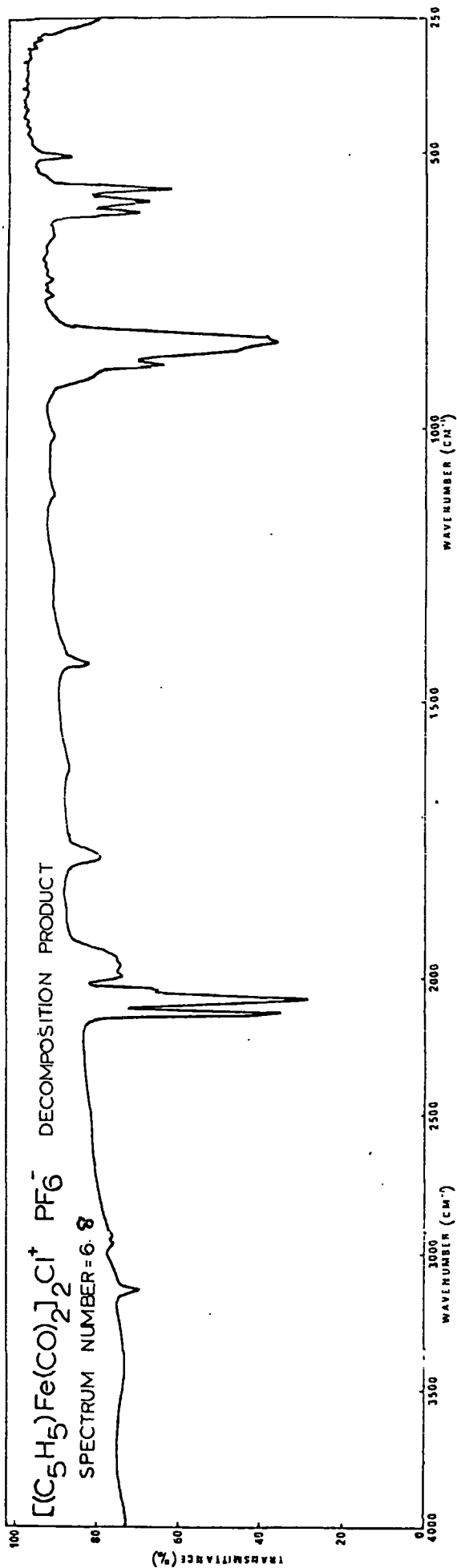
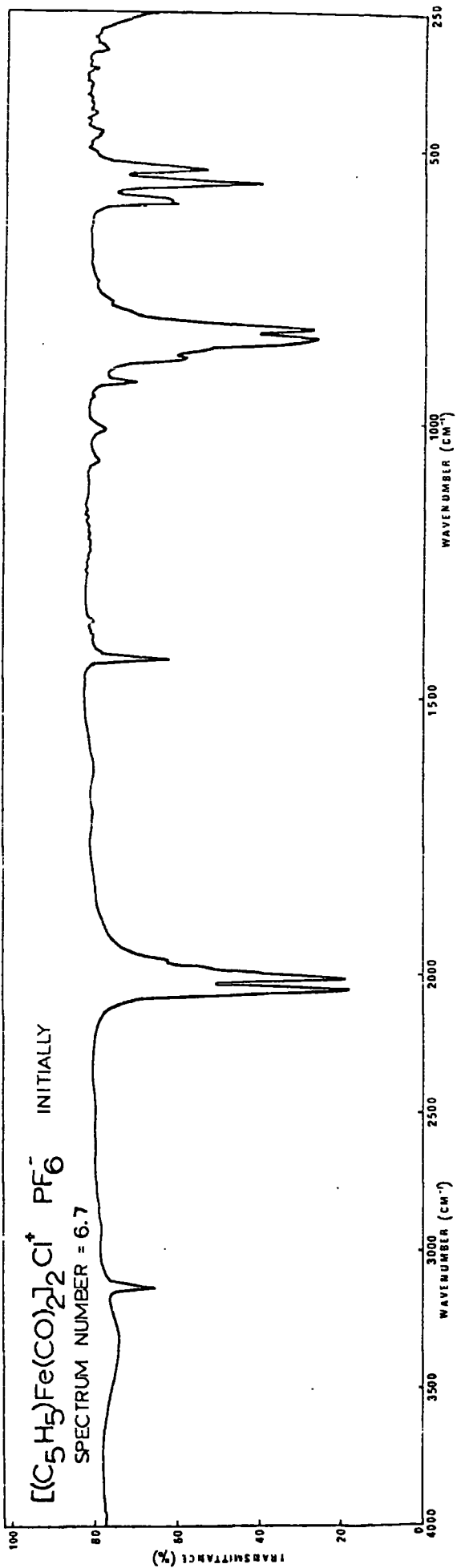
The ultra violet/visible absorption spectra of the  $\pi$ -cyclopentadienyldicarbonyl iron(II) halides and of the  $\pi$ -cyclopentadienyldicarbonyl iron- $\mu$ -halogeno  $\pi$ -cyclopentadienyldicarbonyl iron(II) hexafluorophosphates were recorded in methylene chloride solution (halide = chloride, bromide or iodide; halogeno = chloro, bromo or iodo). The results are given in

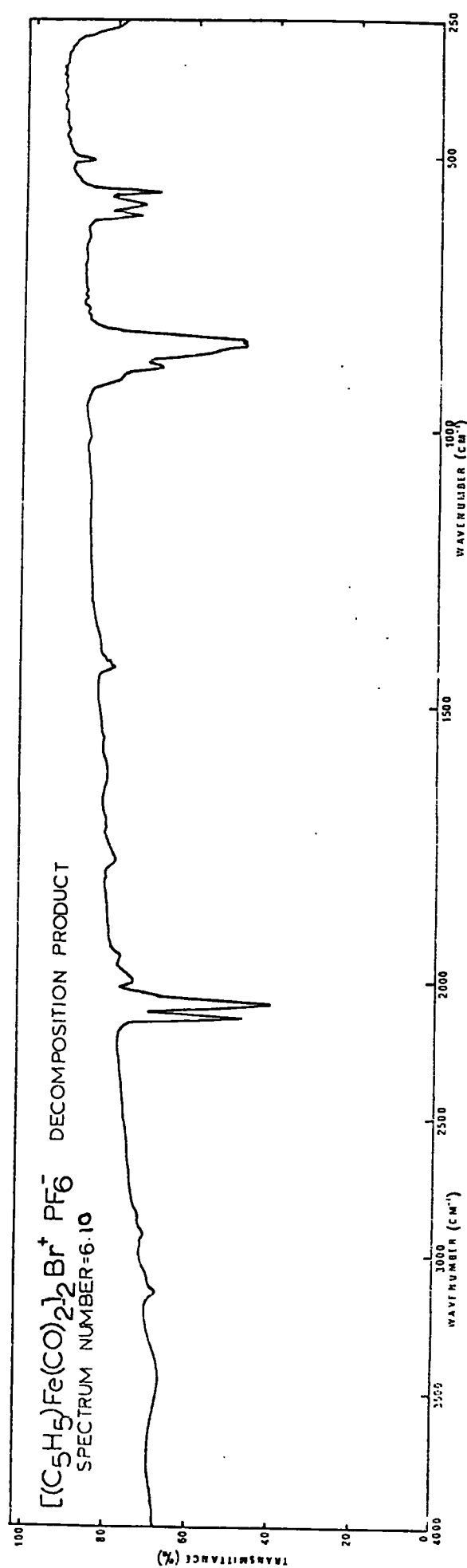
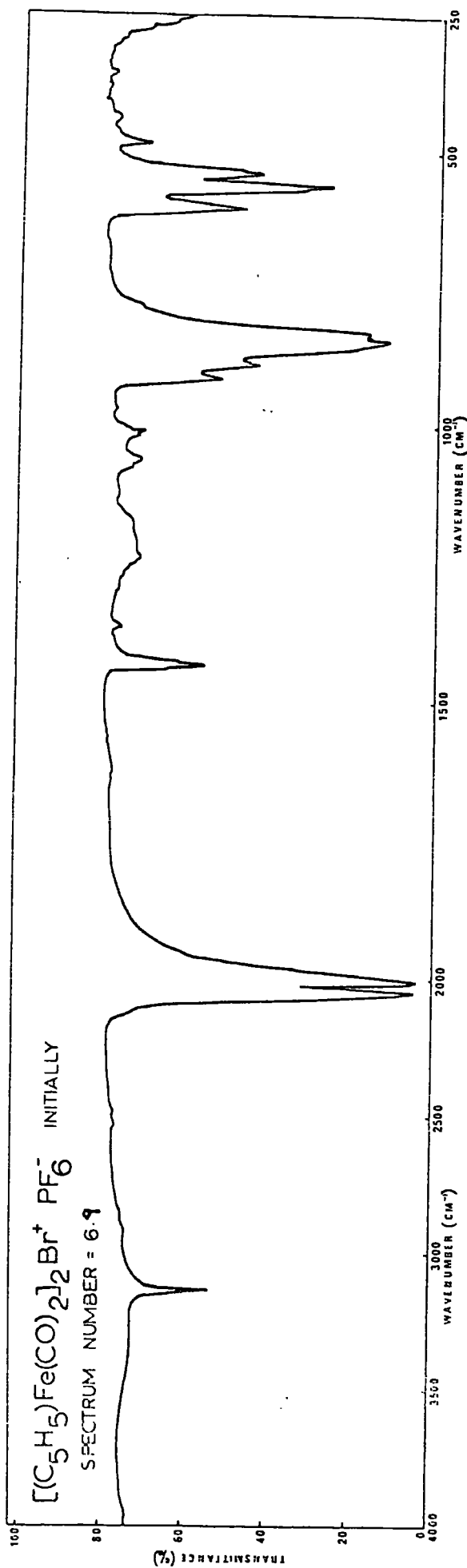
Table 6.2

Infrared Spectra of the  $\mu$ -Halo-bis( $\pi$ -cyclopentadienyldicarbonyl iron(II))  
hexafluorophosphates (halo = chloro, bromo, iodo) in 4000-250  $\text{cm}^{-1}$  region\*

Assignment	$[(\pi\text{-C}_5\text{H}_5)\text{Fe}(\text{CO})_2]_2\text{Cl}^+\text{PF}_6^-$	Compound $[(\pi\text{-C}_5\text{H}_5)\text{Fe}(\text{CO})_2]_2\text{Br}^+\text{PF}_6^-$	$[(\pi\text{-C}_5\text{H}_5)\text{Fe}(\text{CO})_2]_2\text{I}^+\text{PF}_6^-$
C-H stretch	3133w	3133w	3133w
$\nu$ CO	2058sh 2050s 2013s 2003sh	2056sh 2043s 2007sh 2001s	2047sh 2040s 2013sh 2007s
C-C stretch	1428m	1430m 1016w	1428m 1014w
C-H bend (11)	1010w 920 878	1006w 909m 881m	1005w 888m 864ms
$\nu_3 \text{PF}_6^-$	850s, b	850s, b	850s, b,
$\delta(\text{Fe-C-O})$	597m 562sh	597m 564sh	597m 567sh
$\nu_4 \text{PF}_6^-$	556ms	555ms 536m 530m	556ms 538m
$\nu(\text{Fe-CO})$	466m	480w	479w
$[(\pi\text{-C}_5\text{H}_5)\text{-Fe}]$ stretch	320w	350vw 311•3vw	363vw
$\nu(\text{Fe-X})?$	252m		

\* Samples run as KBr discs.





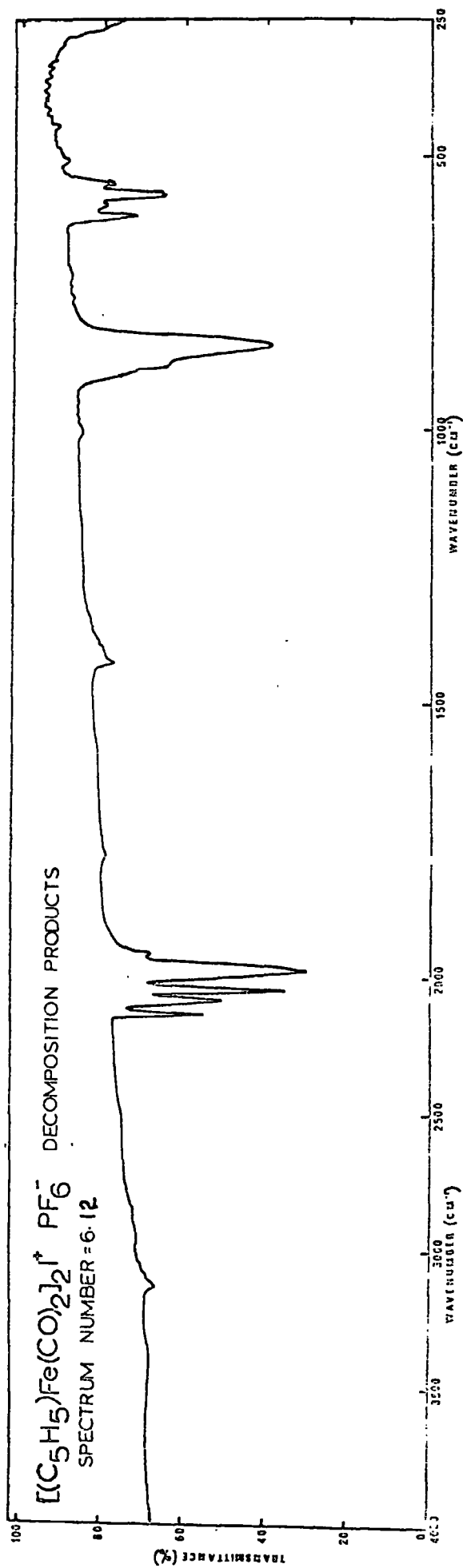
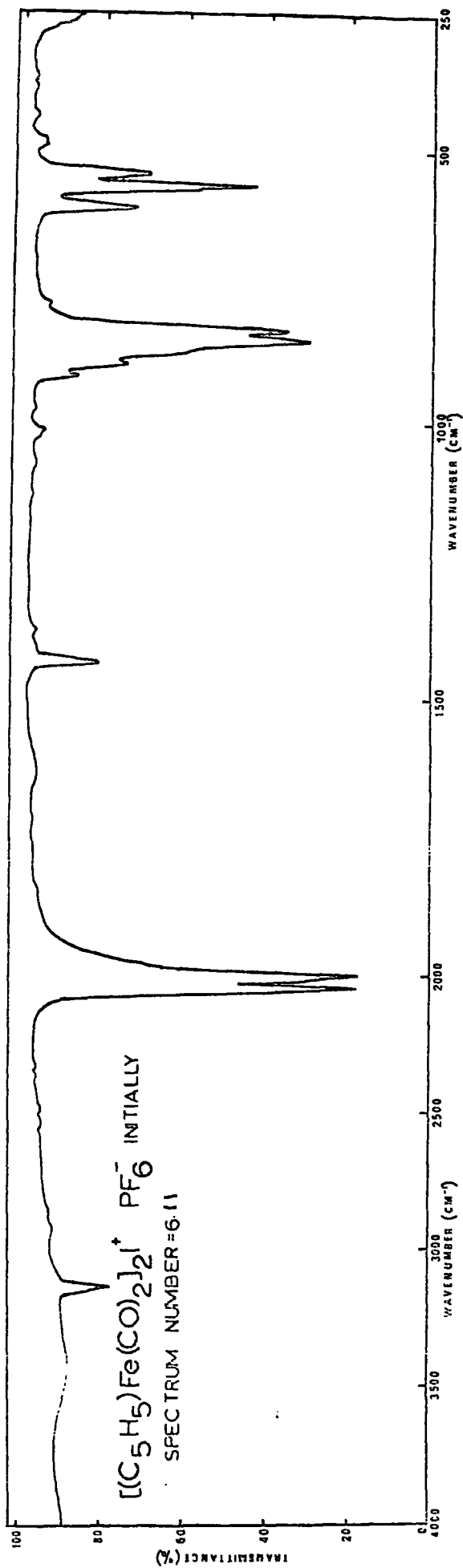


Table 6.3. The initial analysis of the spectra of the  $(\pi\text{-C}_5\text{H}_5)_2\text{Fe}(\text{CO})_2\text{X}$  shows them to be composed of a peak at about  $20,000\text{ cm}^{-1}$  which appears as a shoulder on the absorption edge of the lower frequency ultra violet band. This lower frequency ultra violet band occurs at about  $28,000\text{ cm}^{-1}$  and shows marked distortions suggesting that more than one transition is responsible. A further band at higher frequencies was observed which was distorted by the absorption edge of the solvent (methylene chloride). The intensity of all the absorption bands increased with increasing atomic weight of the halide. Examination of the ultra violet/visible absorption spectra of the  $\pi$ -cyclopentadienyldicarbonyl iron- $\mu$ -halogeno  $\pi$ -cyclopentadienyldicarbonyl iron(II) hexafluorophosphates (halogeno = chloro, bromo or iodo) shows that they follow similar trends to those exhibited by the  $\pi$ -cyclopentadienyldicarbonyl iron(II) halides (halide = chloride, bromide or iodide). The ultra violet region of the spectra shows clearly three distinct bands. Fe(II) has a  $d^6$  configuration and in the  $\pi$ -cyclopentadienyl compounds mentioned in this section the iron atom would be in a low spin state. Such an environment would be expected to give rise to two transitions,  ${}^1T_1 \leftarrow {}^1A_1$  and  ${}^1T_2 \leftarrow {}^1A_1$ . The absorption band at the lowest frequency (ca.  $20,000\text{--}21,000\text{ cm}^{-1}$ ) is probably  ${}^1T_1 \leftarrow {}^1A_1$  transition. The  ${}^1T_2 \leftarrow {}^1A_1$  transition is expected to give rise to an absorption at ca.  $27,000\text{ cm}^{-1}$ ; the absorption bands observed at  $25,000\text{--}30,000\text{ cm}^{-1}$  may be due to the  ${}^1T_2 \leftarrow {}^1A_1$  transition but the extinction coefficients are larger than expected. One explanation being that the  ${}^1T_2 \leftarrow {}^1A_1$  transition is obscured by charge transfer bands of the complexes. For complexes of iron with a  $d^6$  low spin environment the complexes of cis 1,2-bis(dimethylarsino)ethylene were chosen as a rough guide (110). Apart from some studies on

Table 6.3

Ultra Violet and Visible Spectra of the  $(\pi\text{-C}_5\text{H}_5)\text{Fe}(\text{CO})_2\text{X}$  and  $[(\pi\text{-C}_5\text{H}_5)\text{Fe}(\text{CO})_2]_2\text{X}^+\text{PF}_6^-$  Compounds (X = Cl, Br or I) over the region 38,000-14,000  $\text{cm}^{-1}$

Compound	Absorption Band $\text{cm}^{-1}$	Extinction Coefficient
$(\pi\text{-C}_5\text{H}_5)\text{Fe}(\text{CO})_2\text{Cl}$	21,050	155
	29,850	1,070
	35,590	2,055
$(\pi\text{-C}_5\text{H}_5)\text{Fe}(\text{CO})_2\text{Br}$	21,140	330
	28,740	1,330
	34,130	4,690
$(\pi\text{-C}_5\text{H}_5)\text{Fe}(\text{CO})_2\text{I}$	20,070	570
	29,150	2,330
	38,460	4,740
$[(\pi\text{-C}_5\text{H}_5)\text{Fe}(\text{CO})_2]_2\text{Cl}^+\text{PF}_6^-$	19,840	475
	25,550	2,630
	30,000	4,120
	35,340	5,750
$[(\pi\text{-C}_5\text{H}_5)\text{Fe}(\text{CO})_2]_2\text{Br}^+\text{PF}_6^-$	19,800	525
	25,640	3,230
	29,240	5,000
	35,840	5,265
$[(\pi\text{-C}_5\text{H}_5)\text{Fe}(\text{CO})_2]_2\text{I}^+\text{PF}_6^-$	20,410	740
	25,640	10,200
	28,820	12,800
	37,880	18,365

ferrocene (111,112) little work has been carried out on the electronic spectra of  $\pi$ -cyclopentadienyl iron complexes. No detailed assignment of the charge transfer bands of the complexes examined has been attempted. The assignment of the charge transfer bands requires more detailed information than is presented in this thesis and was considered to be outside the scope of this thesis.

The general trend of increasing intensity and reducing frequency of the absorption bands follows the expected trend in the series  $\text{Cl} < \text{Br} < \text{I}$  for both series of complexes examined.

## 6.2. Experimental Section

The  $\pi$ -cyclopentadienyldicarbonyl iron- $\mu$ -halogeno  $\pi$ -cyclopentadienyl-iron cations,  $[(\pi\text{-C}_5\text{H}_5)\text{Fe}(\text{CO})_2]_2\text{X}^+$ , (X = Cl, Br or I) were prepared by either of the two general methods given below.

### Method A

To  $\pi$ -cyclopentadienyldicarbonyl iron(II) halide (halide = chloride, bromide or iodide) (0.005 mole) was added ice cold sulphuric acid (2 cm<sup>3</sup>, sp.gr. 1.84) and a homogeneous solution effected. The solution was evacuated using a water pump until evolution of hydrogen halide almost ceased. After cooling the solution in ice cold water ice cold distilled water (6 cm<sup>3</sup>) was added and the solution filtered at the pump. To the filtrate was added hexafluorophosphoric acid (65% aqueous solution) spotwise until precipitation ceased. After filtering off at the pump the solid product was dissolved in acetone and reprecipitated by the addition of hexane to give a red crystalline solid.

### Method B

To a solution of  $\pi$ -cyclopentadienyldicarbonyl iron(II) halide (halide = chloride, bromide or iodide) (0.005 mole) in toluene (15 cm<sup>3</sup>) was

added a solution of silver hexafluorophosphate (0.0625 g., 0.0025 mole) in toluene (10 cm<sup>3</sup>). After allowing the reaction to proceed for thirty minutes the precipitate of silver halide was filtered off at the pump. The toluene was removed in vacuo to yield a red solid, which after dissolution in acetone and reprecipitation by the addition of hexane gave a red crystalline solid.

$\pi$ -Cyclopentadienyldicarbonyl iron- $\mu$ -chloro  $\pi$ -cyclopentadienyldicarbonyl iron hexafluorophosphate,  $[(\pi\text{-C}_5\text{H}_5)\text{Fe}(\text{CO})_2]_2\text{Cl}^+\text{PF}_6^-$  was prepared by both of the general methods to give a red crystalline solid. Found: C, 31.54; H, 1.90; Cl, 6.42; Fe = 20.6; P, 5.71;  $\text{C}_{14}\text{H}_{10}\text{ClF}_6\text{Fe}_2\text{O}_4\text{P}$  requires C, 31.47; H, 1.88; Cl, 6.63; Fe, 20.90; P, 5.80.

$\pi$ -Cyclopentadienyldicarbonyl iron- $\mu$ -bromo  $\pi$ -cyclopentadienyldicarbonyl iron hexafluorophosphate,  $[(\pi\text{-C}_5\text{H}_5)\text{Fe}(\text{CO})_2]_2\text{Br}^+\text{PF}_6^-$  was prepared by both of the general methods to give a red crystalline solid. Found: C, 29.03; H, 1.73; Fe, 19.27; P, 5.33;  $\text{C}_{14}\text{H}_{10}\text{BrF}_6\text{Fe}_2\text{O}_4\text{P}$  requires C, 29.05; H, 1.74; Fe, 19.30; P, 5.35.

$\pi$ -Cyclopentadienyldicarbonyl iron- $\mu$ -iodo  $\pi$ -cyclopentadienyldicarbonyl iron hexafluorophosphate,  $[(\pi\text{-C}_5\text{H}_5)\text{Fe}(\text{CO})_2]_2\text{I}^+\text{PF}_6^-$  was prepared by Method A to give a red crystalline solid. Found: C, 26.81; H, 1.47; Fe, 17.90; I, 20.31; P, 5.04;  $\text{C}_{14}\text{H}_{10}\text{F}_6\text{Fe}_2\text{I O}_4$  requires C, 26.87; H, 1.61; Fe, 17.85; I, 20.28; P, 4.95.

## CHAPTER 7

### ELECTRON SPECTROSCOPY AND <sup>57</sup>Fe MOSSBAUER SPECTROSCOPY

#### 7.1. Electron Spectroscopy

##### 7.1.1. Introduction

Electron spectroscopy is the latest technique to be developed by physicists to study the fundamental properties of matter and which chemists have recognised as a potentially invaluable chemical technique.

This technique involves the measurement of the energies of electrons which have been ejected from molecules irradiated with a mono-energetic beam of photons. The two types of exciting radiation used (X-rays and u.v. light) enable a convenient division of electron spectroscopy into two classes. Where the exciting radiation is high energy X-rays the technique is known as X-ray Photoelectron Spectroscopy (X.P.S.) or Electron Spectroscopy for Chemical Analysis (E.S.C.A.). The use of a beam of u.v. light as the exciting radiation is known as Photoelectron Spectroscopy (P.E.S.). Throughout this thesis the technique involving X-ray irradiation will be abbreviated to XPS and the technique involving u.v. irradiation will be abbreviated to PES. Electron spectroscopy (both XPS and PES) has a very significant and valuable role to play as a chemical tool. This is since it offers qualitative flexibility coupled with quantitative measurements.

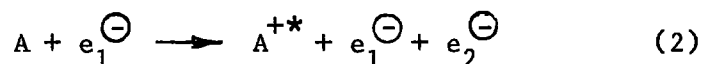
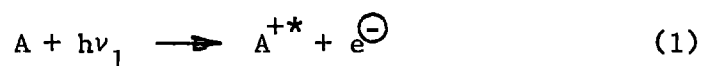
The foundations of electron spectroscopy were laid in 1946 (113) when the basic theory of a XPS instrument was described, a double focussing instrument was described a decade later (114). In 1958 the observations of chemical shifts for copper were first recorded (115), but the general applicability of these chemical shifts were not appreciated

until 1964 (116-118). Turner in 1962 first reported the utilization of PES for ionisation potential measurements (119).

The basic processes involved in electron spectroscopy (shown in block diagram form in Figure 7.1) are the impingement of ionising radiation on a sample causing ejection of electrons. After the electrons have been passed through a monochromator, their energy is measured and displayed as a signal proportional to the intensity of the electrons falling on the detector. The information obtained from electron spectroscopy depends on the exciting radiation and the resolution of the monochromator. High energy exciting radiation (for example X-rays) enables the ejection of core electrons. Conversely low energy exciting radiation (for example vacuum ultra violet photons) enables ejection of electrons from the valence shell.

Electron spectroscopy is a fairly recently developed technique so a brief introduction to the theory will be included here.

The two basic processes which cause the ejection of electrons are photoionisation (1) and electron bombardment (2).



The exciting irradiation ( $h\nu_1$ ) must, of course, have greater energy than the binding energy of the electron ejected. The relaxation of electrons occur by either X-ray emission (3) or Auger electron emission (4)

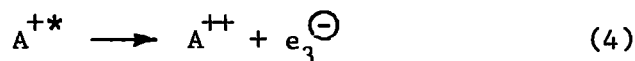
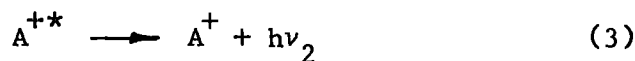
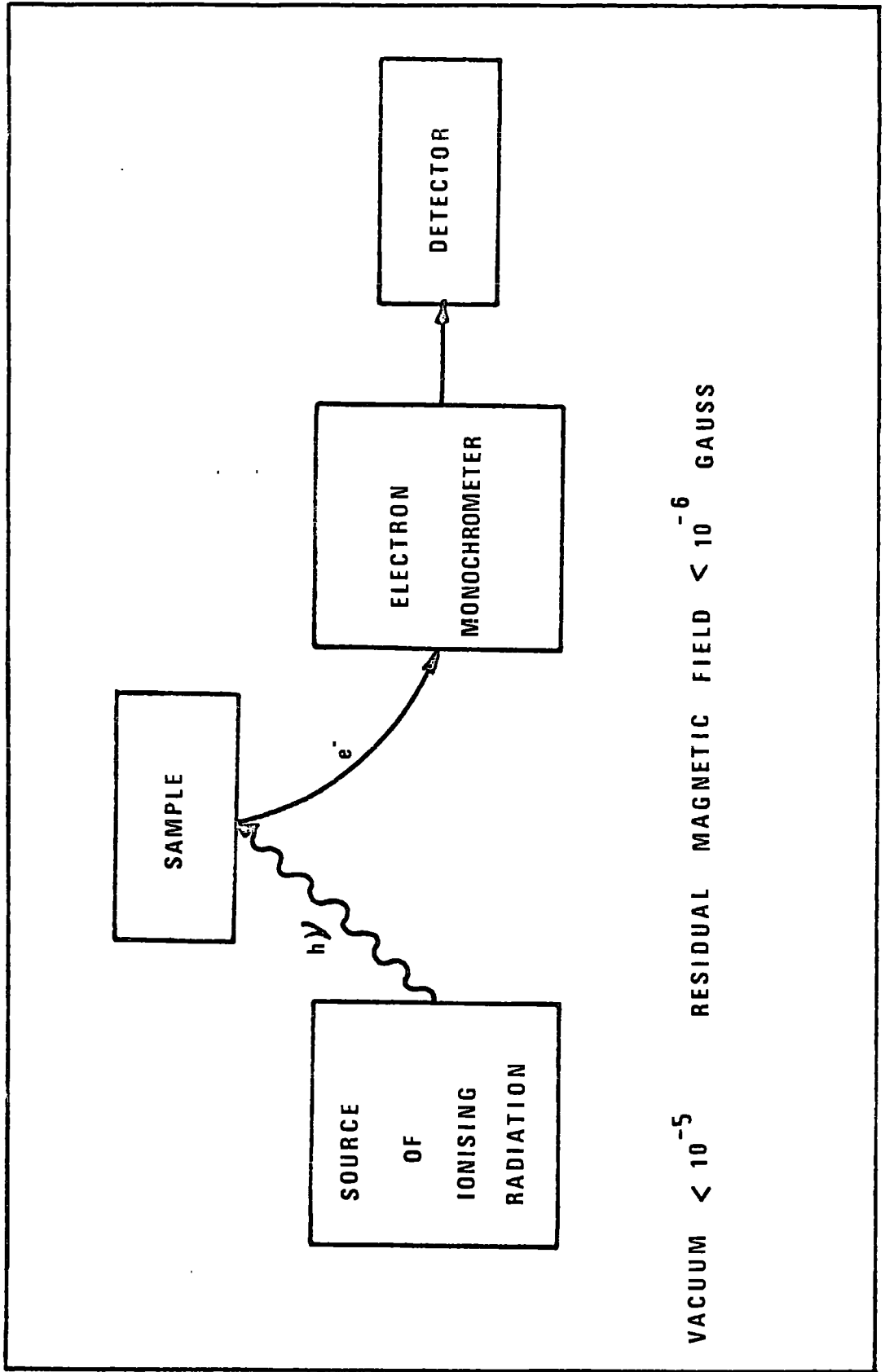


Fig. 7.1 Block diagram of basic processes in electron spectroscopy.



The probability of photoexcitation of an electron is inversely proportional to the square of the orbital radius. Thus photoexcitation is not equally probable for all electrons, or indeed for the same electron among different atoms. For light atoms the probability of excitation of a 1s electron will be about twenty times that for a 2s electron. This becomes less important for the core electrons as the atomic number of the element increases since the orbitals radius will decrease with increasing nuclear charge. The probability of excitation of a given electron varies as  $Z^3$  where  $Z$  is the nuclear charge, ie. considering a 1s electron of hydrogen and a 1s electron of iodine, the probability of excitation of the iodine 1s electron is 143,577 times that of the hydrogen 1s electron. The most intense photoelectron lines are, therefore, expected from the 1s electrons in elements of high atomic number. Excitation of core electrons has the highest probability, however, excitation of outer electrons occurs with a reasonable probability.

Photoionization for an electrical insulator is shown in Figure 7.2. The photo ejection of a 1s electron leaves a  $2s_{\frac{1}{2}}$  state vacant or a K hole. The electron must be ejected to the Free Electron Level, i.e. a position where the ejected electron no longer experience any forces due to the sample, before its binding energy can be determined. Promotion of the 2s electron to the conduction band is an excitation or promotion not a photo ejection, and is accompanied by absorption of a X-ray photon. The information obtained from binding energy studies is intrinsically contained in X-ray adsorption data, although it is much more difficult to extract from the X-ray absorption data.

After ejection of an electron, electron relaxation takes place and is summarised in Figure 7.3. Figure 7.3 shows electron relaxation for a

Fig. 7.2 Photo ionisation of an electrical insulator.

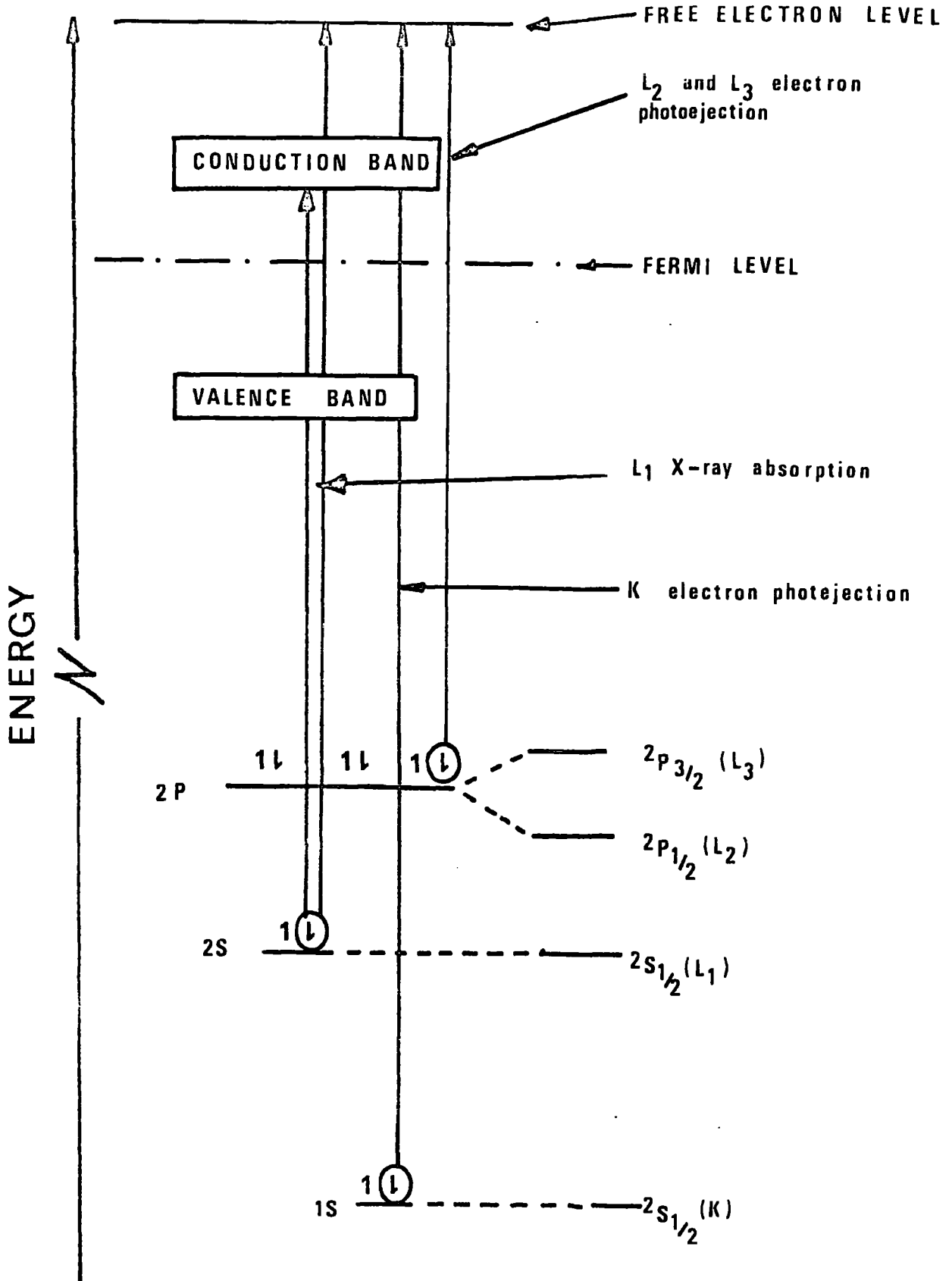
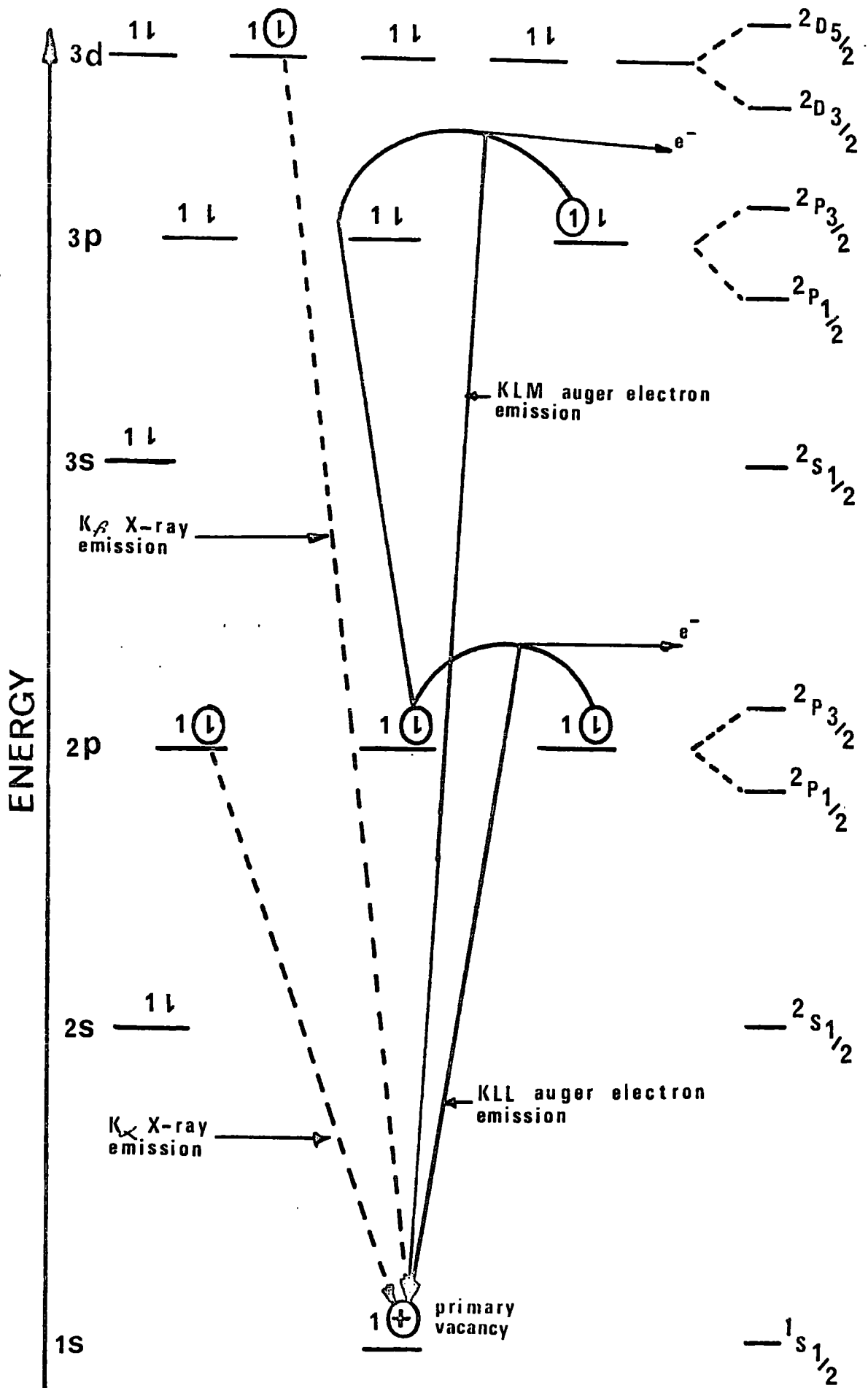


Fig. 7.3 Diagram for electron relaxation.



atom containing a  $1s$  vacancy. The normal  $K_{\alpha}$  and  $K_{\beta}$  X-ray emission lines are shown as transitions from the  $2p$  and  $3d$  orbitals to the  $1s$  orbital respectively. This represents X-ray fluorescence if photoionisation by X-rays has been used or X-ray emission for electron excitation. Auger electron emission is the other main process for electronic relaxation. Auger emission is a radiationless process in which an electron from a higher orbital undergoes a transition to a lower orbital while simultaneously a second electron is ejected from the atom. Figure 7.3 shows a KLL Auger electron emission. The term KLL means that the primary vacancy occurred in the K shell, an L electron underwent a transition to fill the primary vacancy, and a second L electron was ejected. The probability of Auger emission is high in light atoms (virtually unity for atoms of atomic number 11 or less), conversely X-ray emission has virtually zero probability for the same atoms. Auger electrons serve as a good internal standard since their energy is independent of energy of the exciting photon (photoejected electrons have energies depending on the energy of the exciting photon). Electron spectroscopy has two major advantages over X-ray fluorescence, firstly, in general, line widths are much narrower and can therefore be measured more precisely and secondly, all elements can be examined. X-ray fluorescence is in general only applicable to elements with  $Z$  greater than 20.

The photo ejection of an electron results in the electron having a kinetic energy  $E'_K$  and by the application of the conservation of energy we have

$$E'_K = h\nu - E_r - E'_B$$

where  $h\nu$  is the energy of the incident X-ray,  $E_r$  is the recoil energy.

For magnesium  $K_{\alpha}$  X-rays the maximum recoil energy is less than one electron

volt and becomes negligibly small for elements after helium (i.e.  $Z > 2$ ).  $E'_B$  is the energy required to promote the electron to the vacuum of the spectrometer.

The recoil energy term is necessary because in the photoejection of the electron the kinetic energy will be distributed between the electron and the atom. Since in all cases the electron has very much less mass than the atom almost all of the kinetic energy will be taken up by the electron in order that the momentum of the atom and the electron is zero.

In general a small electric field exists in the space between the source and the entrance slit of the spectrometer. This arises because grounding the source and the spectrometer material means that their Fermi levels are the same. Any difference in work function of the source material and the spectrometer material gives a difference in macro potential (120,121) i.e. a contact potential. The kinetic energy  $E_K$  of the electron when it enters the spectrometer is therefore different from the energy  $E'_K$  which it had on ejection from the source. The energy of the electron measured is  $E_K$ . The Fermi level is chosen as a reference level for electron binding energies and taken as zero binding energy. Application of the conservation of energy gives

$$E_B = h\nu - E_K - \phi_{sp}$$

where  $E_B$  is the binding energy of the electron,  $h\nu$  is the energy of the incident X-ray,  $E_K$  is the measured kinetic energy of the ejected electron and  $\phi_{sp}$  is the work function of the spectrometer. It should be noted that work function of the source material does not enter into the equation. It has been found that in insulators sufficient numbers of free charge carriers are formed during X-ray irradiation to enable the Fermi level to adjust to the thermodynamical equilibrium state thus allowing examination by XPS (118).

Examinations of materials using XPS can also be subject to errors arising from surface charges building up on the source. In ionic solids a term due to the Madelung Potential will need to be taken into account. In the XPS studies of the author the  $C_{1s}$  level of the  $\pi$ -cyclopentadienyl ligand was assumed to remain constant and all the other levels were measured with reference to the  $C_{1s}$  level of the  $\pi$ -cyclopentadienyl ligands. This type of technique overcomes the changes in Madelung Potential of the crystal and any charge build up at the surface, but of course the absolute values are only true if the assumption is correct. Since the studies are primarily concerned with changes in binding energy and the width of the lines it is not necessary to know the absolute values.

The photon source of an electron spectrometer ideally supplies a steady level of monochromatic radiation which can be focussed on the sample. X-ray tubes are used in XPS, a magnesium  $K\alpha$  tube being employed on the instrument used. The X-ray tube is often separated from the sample compartment by a thin window through which the exciting radiation passes. For PES an ultra violet source is used, a helium source being employed on the instrument used in the authors study. The main transition occurring in the helium lamp is an electron dropping from the singlet 2p level to the 1s level giving rise to light of wavelength  $584\overset{\circ}{\text{A}}$  which corresponds to an energy of  $21.21$  eV. This transition produces about 98% of the energy radiated by a Helium lamp.

PES is particularly useful for examining the valence shell electrons since better resolution is obtained than when using XPS. This is partly due to the fact that u.v. photons have a much narrower linewidth than X-ray photons. The Heisenberg Uncertainty Principle states that it is impossible to determine accurately by experimental means both the exact position and the exact energy content of a small particle such as an

electron

$$\Delta E \Delta T \geq h$$

where  $\Delta E$  represents the possible ranges of values which might be assigned to the energy of the electron and  $\Delta T$  represents the possible range of values for the time that the electron may exist with an energy  $E$ .

The linewidths of the photoejected electron are not only governed by the Heisenberg uncertainty principle but also by the linewidth of the incident radiation. In all spectra except those obtained on vapours, some broadening will occur due to the slightly differing sites of atoms in the lattice. If any change occurs on going from vapour to solid this also will introduce some broadening e.g. hydrogen bonding and polymerisation.

XPS can be obtained from samples which are solids, liquids or gases, provided that they do not decompose in high vacuum. PES is normally only carried out on gases or volatile liquids and solids, all spectra being recorded from sample molecules in the gaseous state.

For the majority of samples photoejection of electrons only occurs from a depth of about  $100\text{\AA}$ . Thus electron spectroscopy gives information about the surfaces of materials rather than dealing with bulk properties. This is a marked advantage when studying the surface properties of materials. Spectra can be obtained from as little as  $10^{-8}$  g. of sample. The sample should be adequately grounded to minimise the charging effects of the radiation on the sample.

Electron paths are influenced by magnetic fields hence it is important that the earth's field in the region of the spectrometer is reduced to zero. Ideally one should reduce the earth's field along the electron path to below  $10^{-4}$  g.

Three common types of electron monochrometer have been employed in electron spectroscopy namely retarding field, magnetic and electrostatic. The latter two use different means of focussing the electron whilst the former employs a completely different principle.

The detectors used in electron spectroscopy are GM counters, electron multipliers, photographic plates or charge cups.

Scan and readout systems commonly employed are continuous scan, incremental scan and multichannel analysers.

The chemical shifts measured in electron spectroscopy can be related to the atoms oxidation state provided a series of standard compounds containing the atom in question in a number of oxidation states have been measured. The magnitude of the chemical shifts observed vary from one element to another as well as from one oxidation state to another i.e. a change of oxidation state by unity will not have the same chemical shift for all values of the initial oxidation state.

Atomic core electrons are influenced by the attractive force of the nucleus and the repulsive force of the outer electrons. A change in the population of electrons in the valence shell therefore affects the binding energy of the core electrons. As valency shell electrons are removed the binding energy of the core electrons increases which results in a decrease in the kinetic energy of the electron when photoejected. In compounds which contain readily polarised electron clouds, such as  $\pi$  orbitals, a simple electrostatic approach can not be used, the most satisfactory approach being that of molecular orbital calculations.

Electron spectroscopy has however a great potential for chemical structure determination, since it not only enables the detection of an atom in different chemical environments but also the number of atoms in

each particular environment. For example the electron spectrum of sodium azide shows two peaks in the nitrogen 1s region with a ratio of 2:1 corresponding to the two identical end nitrogens and the centre nitrogen. PES enables ionisation potentials, particularly up to 21.21 eV limit of the helium ultra violet source, to be determined.

XPS spectra discussed in this chapter were kindly provided by Dr. D.T. Clark and Mr. D.B. Adams. PES spectra were kindly supplied by Messrs. Perkin Elmer Ltd.

#### 7.1.2. Results and Discussion

Photoelectron spectra of the  $\pi$ -cyclopentadienyl compounds examined are given in Table 7.1. Bis( $\pi$ -cyclopentadienyldicarbonyl iron(I)) was also examined but the spectra varied with temperature and it was thought that the spectrum was attributable mainly to decomposition products and was therefore unreliable. Tetrakis( $\pi$ -cyclopentadienylcarbonyl iron(I)) was the most readily ionised compound examined which was in agreement with the iron atom being in a formal oxidation state +1, all other compounds contained iron atoms in the (+2) oxidation state. Of the +2 iron compounds examined ferrocene was the most readily ionised and its spectrum has been interpreted on the basis of molecular orbital calculations. Ionisation became increasingly difficult as one of the  $\pi$ -cyclopentadienyl ligands was replaced by a dicarbonyl ligand grouping; a general increase in ionisation potentials was observed as the ligand changed along the series  $\sigma$ -methyl, iodine, bromine and chlorine. The results showed that the molecular orbitals varied very little although the electronegativity of the ligand varied over the range 2.65-3.15 (I to Cl). This is not too surprising since carbon monoxide acts as a

Table 7.1

Photo Electron Spectra of Some  $\pi$ -Cyclopentadienyl Iron Compounds

(energies in eV)						
$[(\pi-C_5H_5)_5Fe(CO)]_4$	$(\pi-C_5H_5)_2Fe$	$(\pi-C_5H_5)_2Fe(CO)_2CH_3$	$(\pi-C_5H_5)_2Fe(CO)_2I$	$(\pi-C_5H_5)_2Fe(CO)_2Br$	$(\pi-C_5H_5)_2Fe(CO)_2Cl$	$Fe(CO)_5^*$
6.45	7.15	7.90	7.81	7.95	8.0	
6.87	7.45	8.68	8.18	8.27	8.27	
8.58			8.8	8.91	8.95	
8.9	9.0	9.25	9.35	9.8	10.15	
9.15	9.65	10.02	10.12	10.45	10.65	
11.30	12.5	12.6	10.48			
11.90	13.15	13.44	12.89	12.79	12.70	
12.30	13.75		13.69	13.95	13.88	
15.4	16.7	16.35	16.81	16.95	16.72	8.60 9.50

\* D.R. Lloyd and E.W. Schlag, Inorg. Chem., 1969, 8, 2544.

particularly good source of electron density. An increase in electronegativity of the ligand would tend to reduce electron density at the iron atom which would reduce the amount of back donation from the iron atom to the carbon monoxide. Back donation lowers the frequency of the carbonyl stretch, hence the carbonyl stretch of  $(\pi\text{-C}_5\text{H}_5)\text{Fe}(\text{CO})_2\text{Cl}$  would be expected to be at higher frequency than that observed for  $(\pi\text{-C}_5\text{H}_5)\text{Fe}(\text{CO})_2\text{I}$  and this is indeed so.  $\pi$ -Cyclopentadienyldicarbonyl iron(II) $\sigma$  methyl has carbonyl stretching frequencies at lower values than does  $\pi$ -cyclopentadienyldicarbonyl iron(II) iodide suggesting, as does the photoelectron spectra, that the  $\sigma$ -methyl ligand is less electronegative than iodine.

The PES of iron pentacarbonyl has been examined by Lloyd and Schlag (122) who found two strong peaks in the 8-10 eV region but were unable to resolve the complex system of peaks of higher energy than 13.5 eV. The two peaks in the 8-10 eV range were assigned to non-bonding and anti-bonding d type orbitals. The iron atom is in a formal oxidation state of zero, but the ionisation potentials recorded were higher than the iron +1 and +2 compounds. The bonding scheme for iron pentacarbonyl must be different to that for the  $\pi$ -cyclopentadienyl complexes and no useful correlations can be obtained until more detailed information about the bonding schemes are known.

The results of the X-ray photoelectron spectral studies are given in Table 7.2. Although satisfactory elemental analyses were obtained for all compounds, examination by XPS showed the presence of sulphate and of silver in the samples prepared by the sulphuric acid and silver hexafluorophosphate techniques respectively. Reprecipitation of the compounds from acetone solution by the addition of hexane failed to eliminate these



Table 7.2 Continued

$[(\pi C_5H_5)Fe(CO)_2]_2 ClPF_6^+$	$[(\pi C_5H_5)Fe(CO)_2]_2 BrPF_6^+$	$[(\pi C_5H_5)Fe(CO)_2]_2 I^+PF_6^-$	$[(\pi C_5H_5)Fe(CO)]_4 PF_6^-$	$[(\pi C_5H_5)Fe(CO)]_4 Br_3^-$
C 1s 286.4 ( $\pi C_5H_5$ ) 288.7 (-C $\equiv$ O)	C 1s 286.4 ( $\pi C_5H_5$ ) 288.2 (-C $\equiv$ O)	C 1s 286.4 ( $\pi C_5H_5$ ) 287.3 (-C $\equiv$ O)	C 1s 286.4 ( $\pi C_5H_5$ ) 287.8 (-C-O)	C 1s 286.4 ( $\pi C_5H_5$ ) 287.5 (-C-O)
Fe 2p <sup>1/2</sup> 725.1 2p <sup>3/2</sup> 713.2	Fe 2p <sup>1/2</sup> 726.2 2p <sup>3/2</sup> 713.2	Fe 2p <sup>1/2</sup> 713.6 2p <sup>3/2</sup> 713.6	Fe 2p <sup>1/2</sup> 724.4 2p <sup>3/2</sup> 711.8	Fe 2p <sup>1/2</sup> 724.2 2p <sup>3/2</sup> 711.0
C 12p <sup>1/2</sup> 201.6 2p <sup>3/2</sup> 199.8	P 2p <sup>1/2</sup> 138 2p <sup>3/2</sup> 136.8	I 3d <sup>3/2</sup> 637.5 3d <sup>5/2</sup> 625.8	P 2p <sup>1/2</sup> 137.8 2p <sup>3/2</sup> 136.9	Br 3d 69.6
P 2p <sup>1/2</sup> 138.2 2p <sup>3/2</sup> 136.6	Br 3d 70.4	F 1s 689.1		

impurities. Any technique that examined bulk properties failed to show any appreciable amount of impurities and it was concluded that these compounds only contained impurities on the crystal surfaces.

The spectra of the compounds were recorded over narrow ranges which were so chosen to supply the information sought. The binding energy of the iron 2p levels, halogen p levels and carbon 1s level were recorded for all compounds. Phosphorus 2p levels and fluorine 1s levels were recorded for the hexafluorophosphate salts. The iron +1 compounds had Fe2p levels with lower binding energies than the iron +2 compounds. There was only a very marginal difference between the two iron +1 compounds but tetrakis( $\pi$ -cyclopentadienylcarbonyl iron(I)) had a lower binding energy than bis( $\pi$ -cyclopentadienyldicarbonyl iron(I)). If, however, the binding energy of the  $C_{1s}$  level of the  $\pi$ -cyclopentadienyl ligand was assumed to remain constant and all levels measured relative to the  $\pi$ -cyclopentadienyl  $C_{1s}$  level the order was reversed. Bis( $\pi$ -cyclopentadienyldicarbonyl iron(I)) would be expected to have lower Fe 2p binding energy than tetrakis( $\pi$ -cyclopentadienylcarbonyl iron(I)) since the former compound has two carbon monoxide ligands per iron atom whilst the latter only has one carbon monoxide ligand per iron atom. The assumption that the  $\pi$ -cyclopentadienyl ligand  $C_{1s}$  level remains constant also enables a satisfactory explanation for the observed  $C_{1s}$  levels of the carbon monoxide ligands. The binding energy of the carbon monoxide  $C_{1s}$  level would be expected to increase as the ligand progressed along the series, monodentate, bidentate and finally tridentate. There would also be a larger difference in binding energies between mono and bidentate than between bi and tridentate this follows the pattern observed for the frequency shifts of the carbonyl absorptions in the infrared spectra.

The spectra of the iron +2 compounds are reported in Table 7.2; the binding energy of the  $C_{1s}$  level of the  $\pi$ -cyclopentadienyl ligand has been assumed to remain constant and differences in the binding energies of the electron levels are not absolute. This is not important to chemists since they are usually primarily interested in shifts which can be interpreted as changes in electron distributions.

The  $2p^{3/2}$  level of the iron atom in the  $\pi$ -cyclopentadienyldicarbonyl iron(II) halides (chloride, bromide and iodide) had a binding energy of 712.5 eV ( $\pm 0.1V$ ) with a half-width of 1.4-1.5 eV. The  $C_{1s}$  level attributed to the carbon monoxide ligand was within 0.2eV for the three compounds, and had a half width of 1.4-1.5 eV. In the case of the  $\pi$ -cyclopentadienyldicarbonyl iron- $\mu$ -halogeno  $\pi$ -cyclopentadienyldicarbonyl iron hexafluorophosphates (halogeno = chloro, bromo and iodo) the iron  $2p^{3/2}$  level has a binding energy which increases as the halogens atomic weight increases. Arguments based on electronegativity would predict shifts which are in the opposite direction to those observed. The binding energy will reflect the amount of sigma donation from the halogen, the more sigma electron density donated to the iron atom the lower the binding energy. The ( $\pi$ -cyclopentadienyldicarbonyl iron(II)) monocation would be expected to be a soft acid i.e. one which has readily polarisable electron clouds. Soft acids interact more strongly with soft bases than with hard bases. Iodide would be classified as a softer base than bromide which in turn is a softer base than chloride. The product of two  $\pi$ -cyclopentadienyldicarbonyl iron(II) cations interacting with a halide would, therefore, be expected to give the most stable product when the halide was iodide. The thermal stabilities of these compounds show an increase with increasing atomic weight of the halide. The electron density at the iron atom in the

s levels would therefore be expected to increase on going from chloride to iodide, and this is confirmed by the  $^{57}\text{Fe}$  Mossbauer studies. The above argument would also suggest that the binding energies of the iron atom should decrease on going from chloride to iodide. The XPS of the iron 2p levels will also be altered by the amount of back donation to the halogen atom,  $^{57}\text{Fe}$  Mossbauer shifts however are only influenced very marginally by alterations in electron density in levels other than s orbitals. An increase in the binding energy of a level indicates removal of electron density from that level. Therefore an increase in the binding energy of the iron 2p levels observed for the  $[(\pi\text{-C}_5\text{H}_5)\text{Fe}(\text{CO})_2]_2\text{X}^+$  (X = Cl, Br and I) cations is consistent with iodide being the best pi acceptor, and chloride being the poorest pi acceptor. An alternative explanation for the observed iron 2p binding energies in these compounds is given below. Consider that the electron density at the iron atoms and halide atoms remain constant

$$\text{i.e.} \quad q_{\text{Fe}}^{\text{Cl}} = q_{\text{Fe}}^{\text{I}}$$

$$\text{and} \quad q'_{\text{hal}}^{\text{Cl}} = q'_{\text{hal}}^{\text{I}}$$

The observed binding energy  $B_{\text{Fe}}$  is given by equations (1) and (2)

$$B_{\text{Fe}}^{\text{Cl}} = kq_{\text{Fe}}^{\text{Cl}} - \frac{q_{\text{hal}}^{\text{Cl}}}{r_{\text{Fe-Cl}}} \quad (1)$$

$$B_{\text{Fe}}^{\text{I}} = kq_{\text{Fe}}^{\text{I}} - \frac{q_{\text{hal}}^{\text{I}}}{r_{\text{Fe-I}}} \quad (2)$$

where k is a constant and r is the internuclear distance

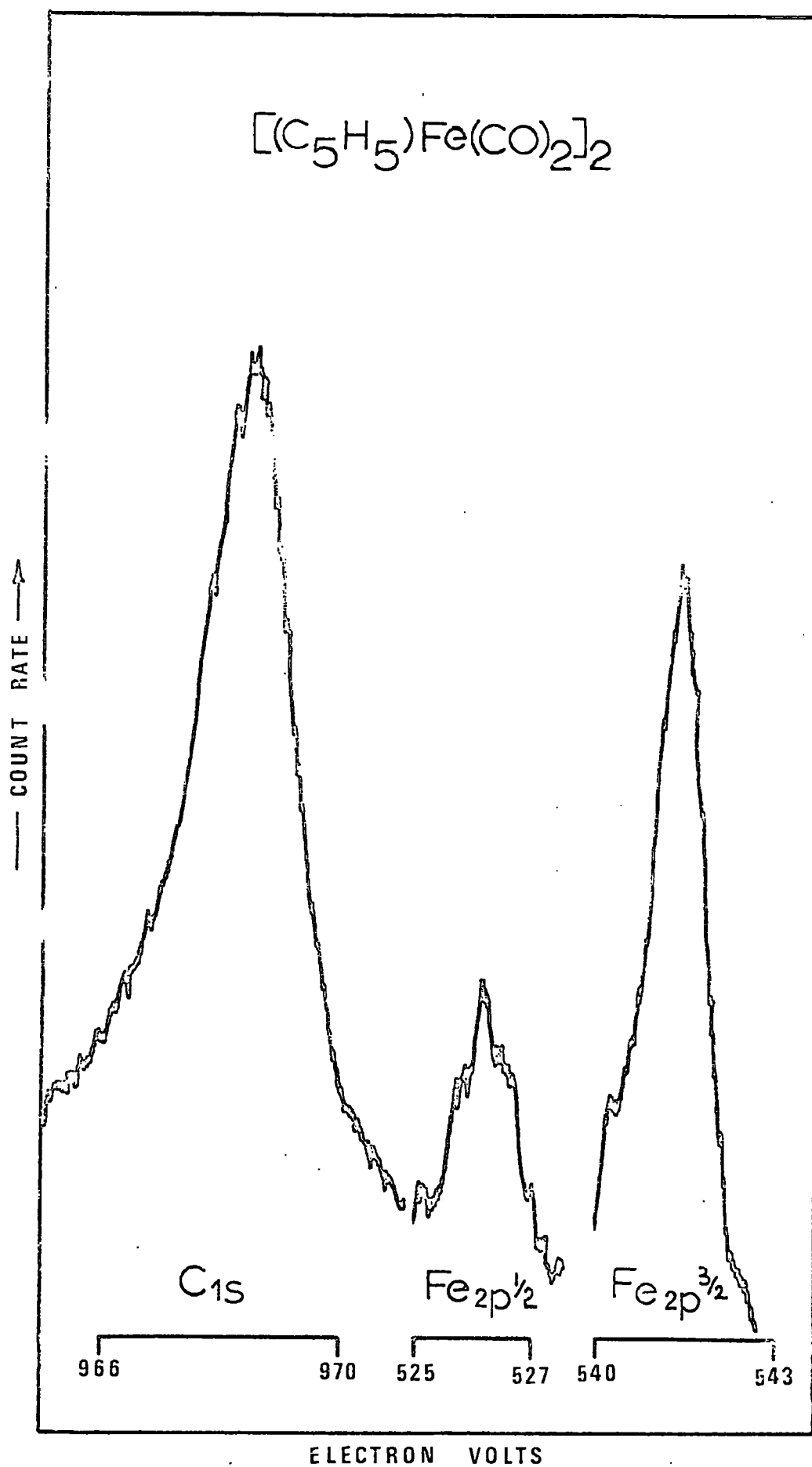
$$\therefore \Delta = B_{\text{Fe}}^{\text{Cl}} - B_{\text{Fe}}^{\text{I}} = -q_{\text{hal}}^{\text{Cl,I}} \left( \frac{1}{r_{\text{Fe-Cl}}} - \frac{1}{r_{\text{Fe-I}}} \right)$$

The internuclear distance would be largest for the iodide resulting in  $\Delta$  which is negative.

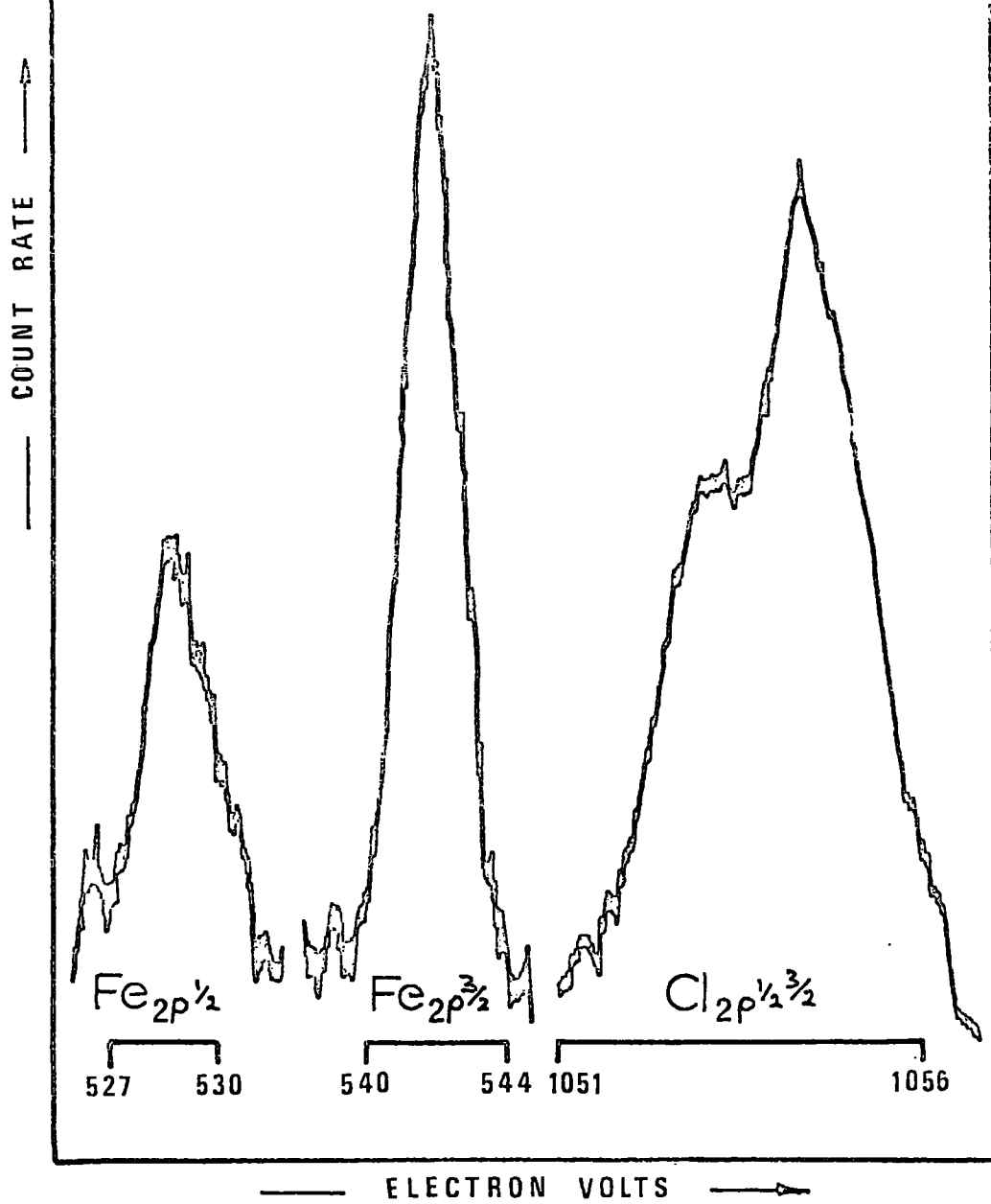
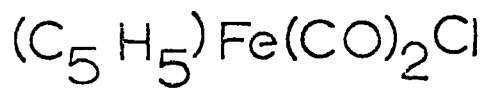
The binding energies of the halogen atoms are observed to increase on going from the  $\pi$ -cyclopentadienyldicarbonyl iron(II) halide to the corresponding  $\pi$ -cyclopentadienyldicarbonyl iron- $\mu$ -halogeno  $\pi$ -cyclopentadienyldicarbonyl iron hexafluorophosphate, which is consistent with the introduction of a positive charge. The binding energy of the chlorine atom in  $\pi$ -cyclopentadienyldicarbonyl iron- $\mu$ -chloro  $\pi$ -cyclopentadienyldicarbonyl iron hexafluorophosphate when compared with the chlorine atom in chlorinated methanes (123) is consistent with the chlorine carrying some overall negative charge, although somewhat reduced from that which the chlorine atom in  $\pi$ -cyclopentadienyldicarbonyl iron(II) chloride carries. An examination of the carbon 1s level of the carbon monoxide ligands of the  $\pi$ -cyclopentadienylcarbonyl iron- $\mu$ -halogeno  $\pi$ -cyclopentadienyldicarbonyl iron(II) cations shows decrease in binding energy with increasing atomic number of the halogen. This is consistent with the carbon monoxide donating more electron density when associated with the more electronegative halogen. The carbon monoxide ligands are most tightly bound in the  $\pi$ -cyclopentadienyldicarbonyl iron(II) chloride.

Examination of the tetrakis( $\pi$ -cyclopentadienylcarbonyl iron) compounds shows only marginal increases in binding energies on oxidation to the monocation. The increases observed are within experimental error ( $\pm 0.25$  eV) and are intermediate between the iron +1 and iron +2 compounds discussed previously. There would only be expected marginal changes since one electron is being removed from four iron atoms ( $^{57}\text{Fe}$  Mossbauer studies show that all the four iron atoms are equivalent). Typical spectra are given in Spectra 7.1-7.8.

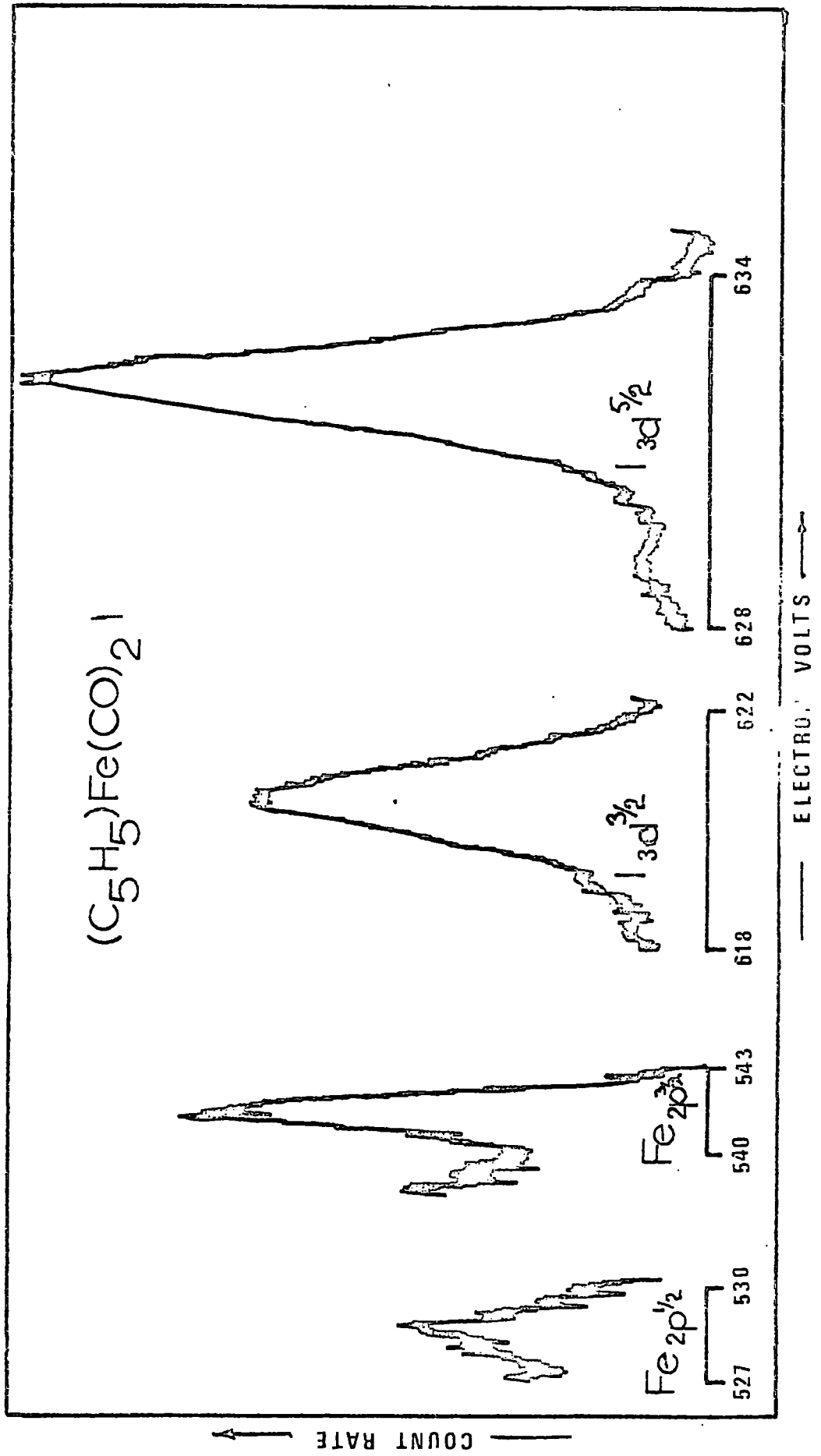
Spectrum number 7.1



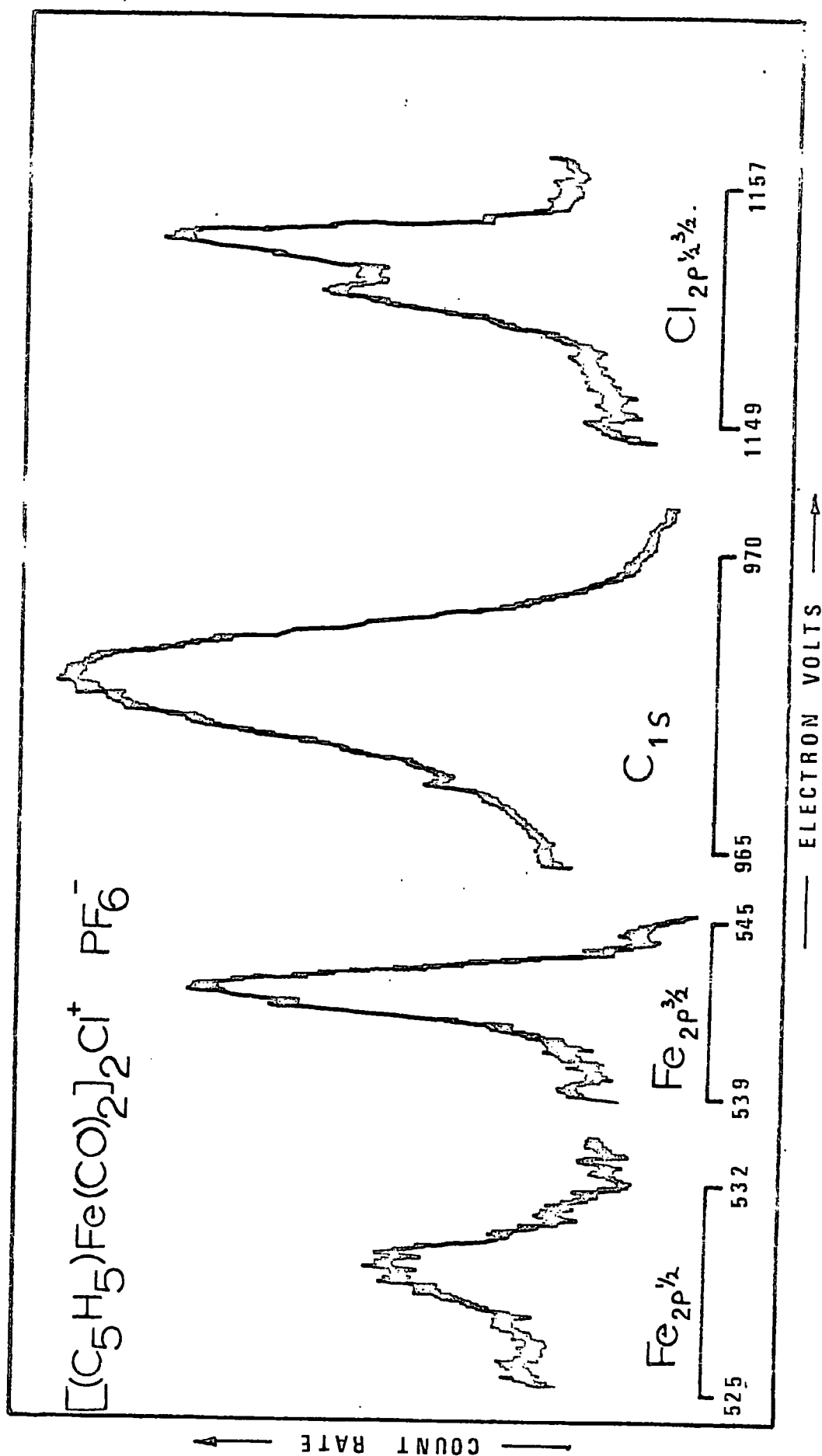
Spectrum number 7.2



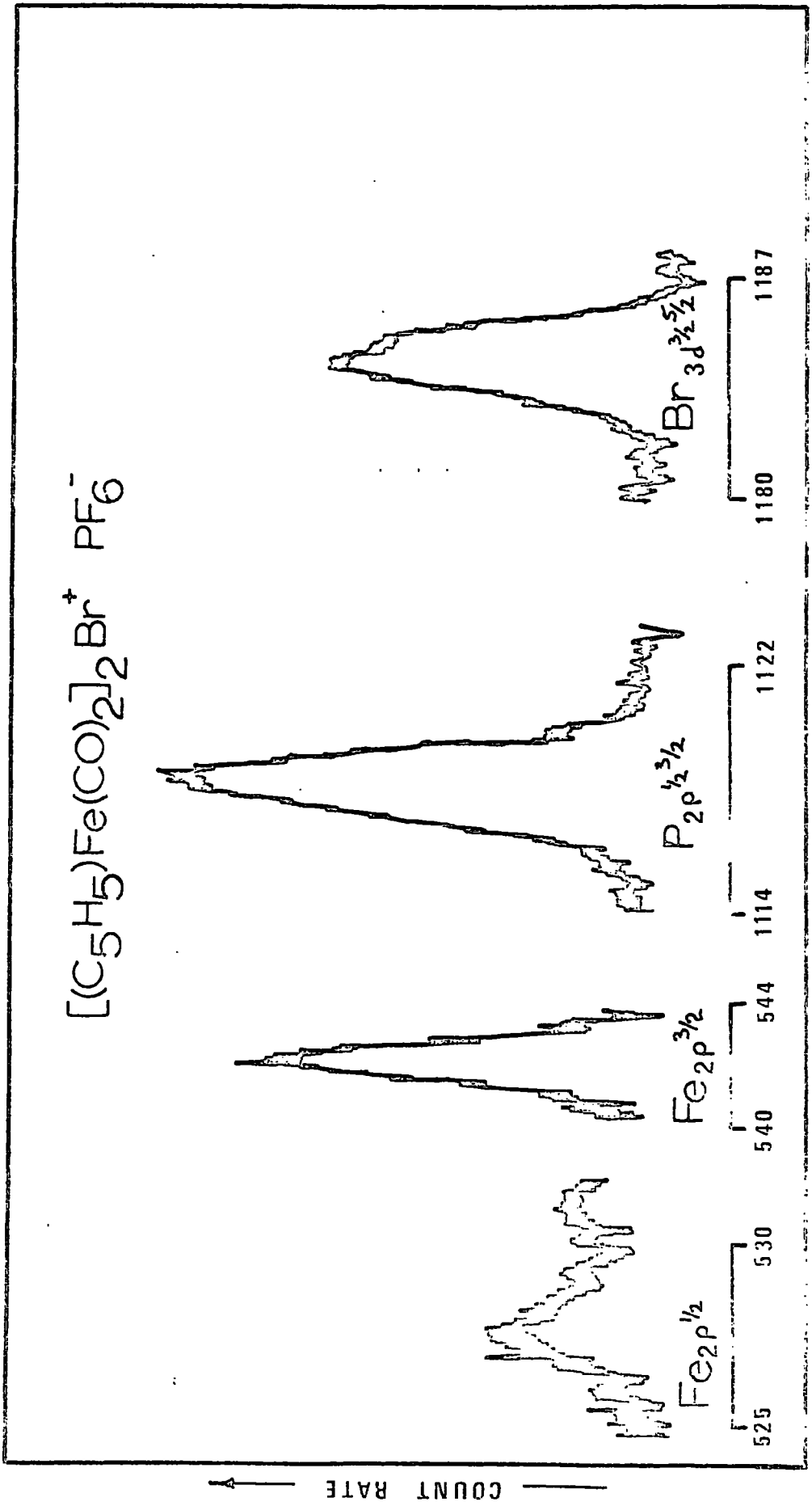
Spectrum number 7.3



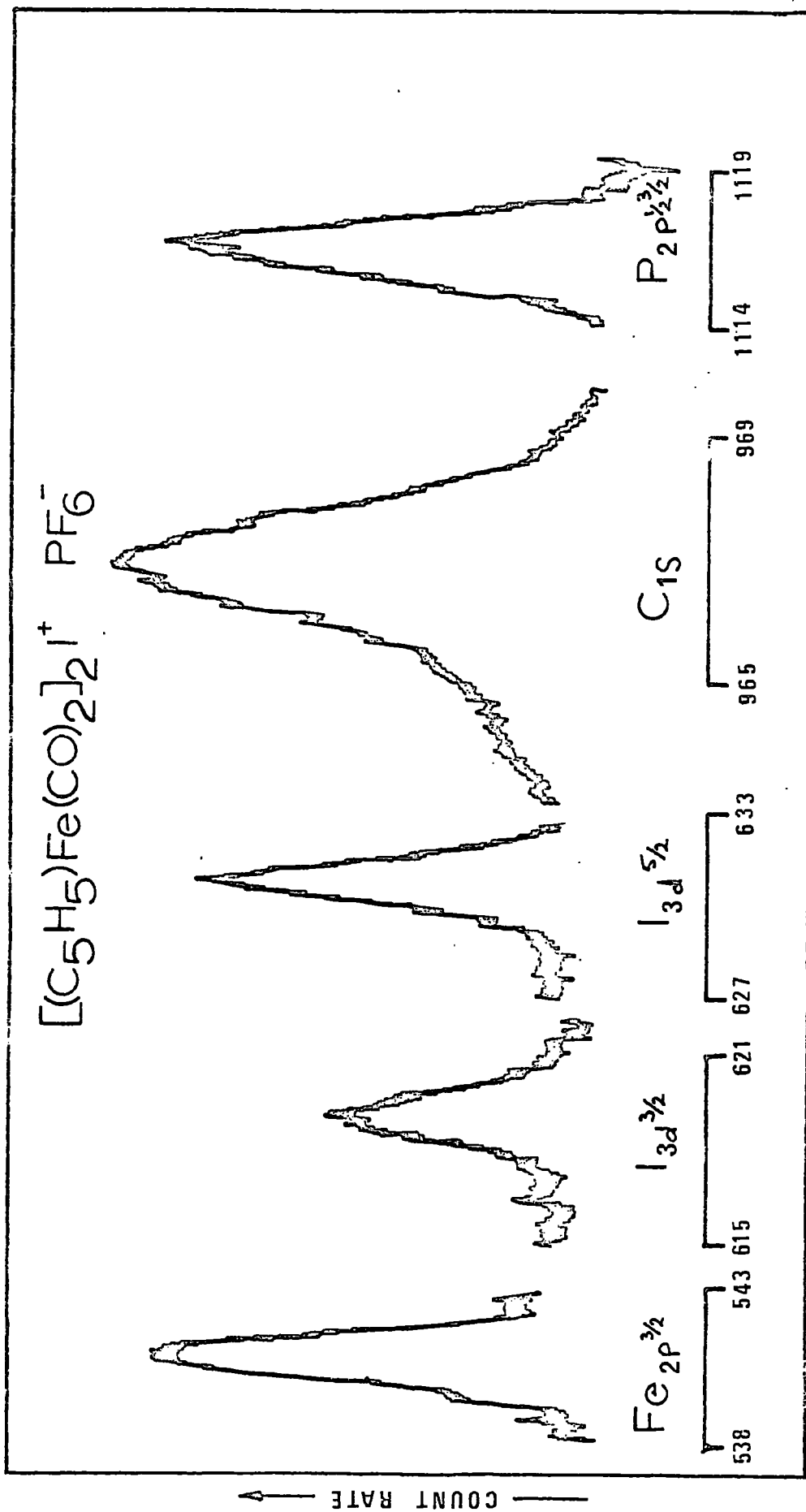
Spectrum number 7.4



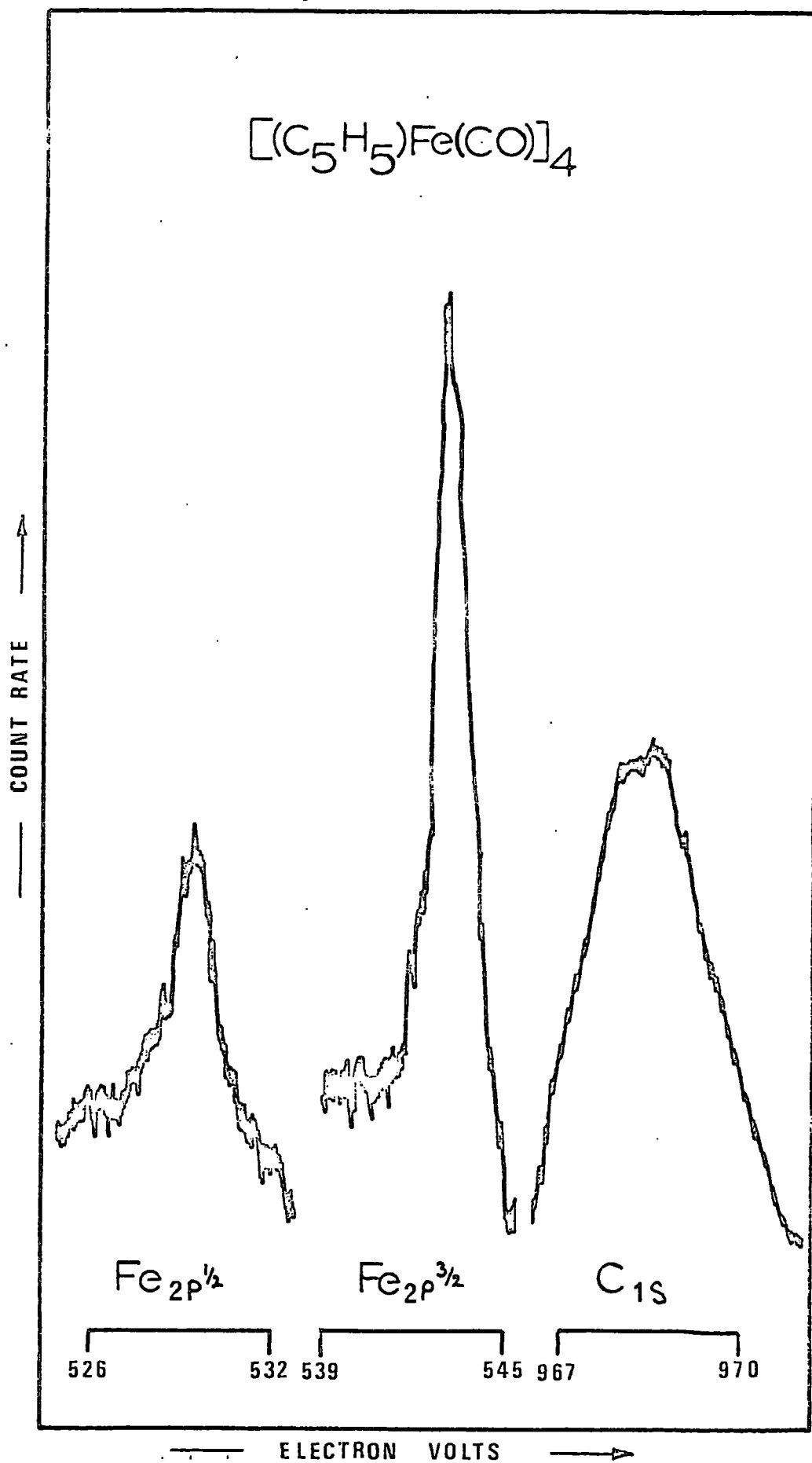
Spectrum number 7.5



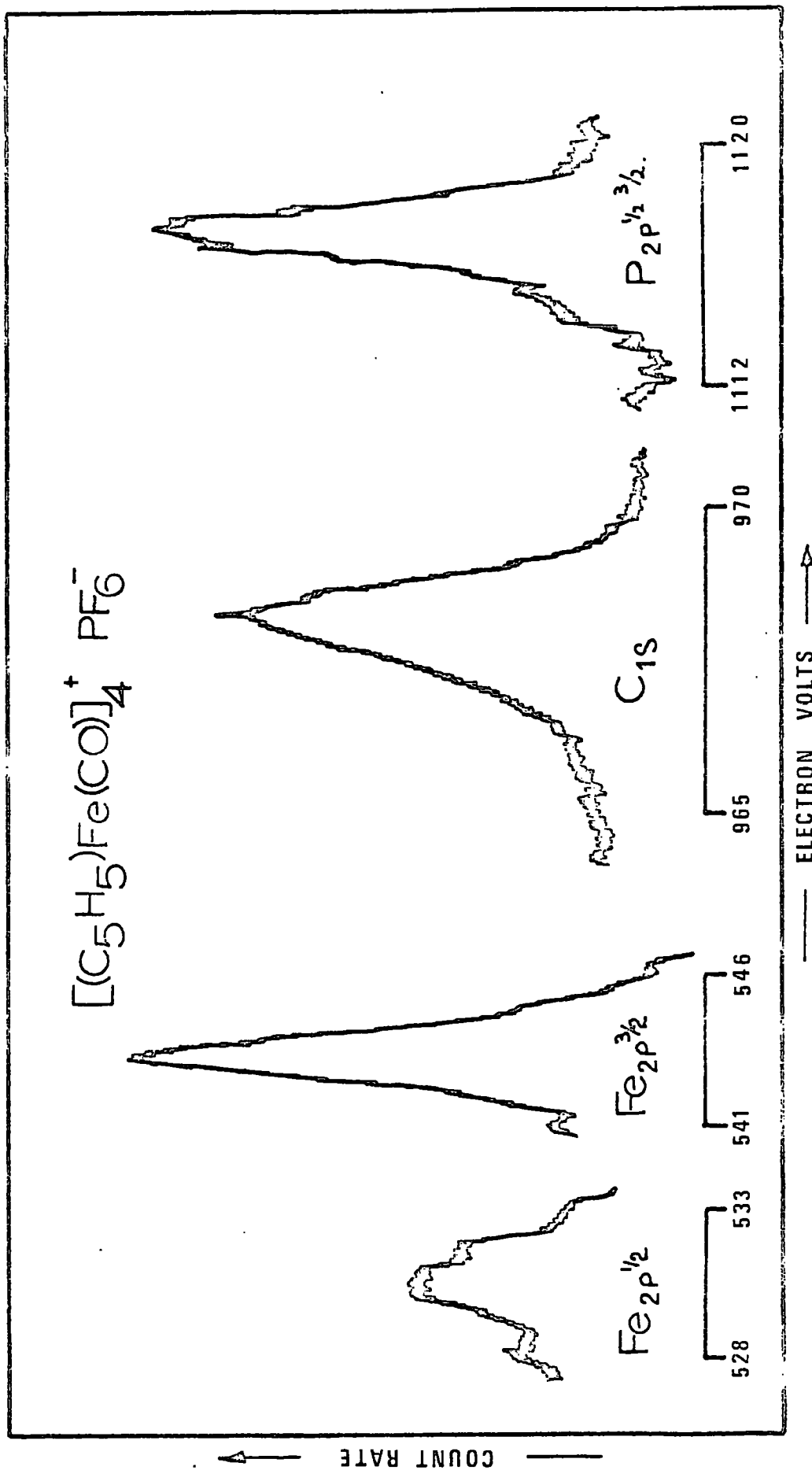
Spectrum number 7.6



Spectrum number 7.7



Spectrum number 7.8



## 7.2. <sup>57</sup>Fe Mossbauer Spectroscopy

### 7.2.1. Introduction

The Nobel prize in Physics for 1961 was awarded to R.L. Mossbauer for his discovery of the recoilless emission of  $\gamma$  rays and their resonant reabsorption. This technique is now universally known as Mossbauer Spectroscopy. During the past decade Mossbauer spectroscopy has played an increasingly important role in many diverse areas of chemistry. The Mossbauer effect has been observed for at least 32 elements and has been predicted for a further 17 elements. There is no Mossbauer effect in elements with atomic number less than 26 except for potassium, however, Mossbauer nuclei can be used as 'observers' of a chemical environment comprising non-active elements.

Information of chemical significance has been obtained from about twelve Mossbauer nuclei. Well over 1000 compounds have been investigated of which half have been compounds of iron and one third are compounds of tin.

The application of Mossbauer spectroscopy to chemistry depends on hyperfine interactions between the nuclear energy levels. These interactions give rise to chemical shifts,  $\delta$ , quadrupole splittings,  $\Delta$ , and magnetic hyperfine Zeeman splittings. These effects can be observed in Mossbauer spectroscopy since the energy quanta can be measured extremely precisely. The gamma ray has an energy precision determined solely by the Heisenberg Uncertainty Principle. If the excited state energy level has a lifetime of  $t$  and an energy  $E_{\gamma}$ , the uncertainty in the gamma ray energy  $\Delta E_{\gamma}$  is given by

$$t \cdot \Delta E_{\gamma} \geq h$$

Thus for  $^{57}\text{Fe}$  with a lifetime of  $10^{-7}$  sec and an energy of  $14.4$  KeV, the precision of the energy is  $E_{\gamma}/\Delta E_{\gamma} \approx 10^{12}$ . These Mossbauer lines are at least  $10^9$  times sharper than a typical infrared line in the gas phase. In practice it is impossible to measure the absolute energy of the gamma ray to better than 1 part in  $10^5$ , but relative energies can be measured to 1 part in  $10^{12}$ . This is achieved by modulating the energy of the  $\gamma$  rays by moving the source relative to the absorber by  $10^{-12}$  of the speed of light, i.e. by about 1 mm/sec. The experimental technique consists of moving the  $\gamma$  ray source relative to the absorber, the spectrum consisting of a plot of  $\gamma$  ray counts against relative velocity of source towards absorber. At some velocity there is a resonant absorption and the count rate decreases.

In order to use Mossbauer spectroscopy a knowledge of the electron-nuclear hyperfine interactions is necessary. The chemical shift,  $\delta$ , depends on the fact that nuclear energy levels depend minutely on the chemical environment of the nucleus. The radius of the nucleus is different in the excited and ground states and using First Order perturbation theory the chemical shift can be shown to be given by equation (1).

$$\delta = \text{constant} \cdot \frac{\delta r}{r} \cdot \delta/\psi_s 0/2^2 \quad - \quad (1)$$

where  $\delta$  is the chemical shift

$$\text{constant} = \frac{4\pi}{5} Z e^2 r^2$$

$\delta r$  = radius of excited - radius of ground state

$\delta/\psi_s 0/2^2$  is the change in S electron density at the nucleus in going from the source to the absorber. When  $\delta r/r$  is positive a positive chemical shift corresponds to an increase in s electron density at the nucleus conversely when  $\delta r/r$  is negative a positive chemical shift

correspond to a decrease in s electron density at the nucleus. Steady trends with electronegativity are frequently observed. Changes in valency also cause changes in the effective s electron density at the nucleus, this is shown very strongly by tin. Tin in the +2 and +4 oxidation states has an electronic structure  $5s^2$  and  $5s^0$ , respectively, and on going from a Sn(II) compound to a Sn(IV) compound a very remarked reduction in s electron density is observed. For  $^{57}\text{Fe}$   $\delta r/r$  is negative thus an increase in chemical shift signifies a decrease in s electron density. Although high spin iron compounds show chemical shifts dependent on its oxidation state low spin iron compounds have chemical shifts which tend to be independent of oxidation state from -2 to +2. This is due to the fact that in a low spin environment the central iron atom tends towards charge neutrality independently of its formal oxidation state. With complexes containing  $\pi$ -bonding ligands, the  $\pi$ -back-bonding de-shields the nucleus by removing d electrons, hence the strongest  $\pi$  bond has the highest s electron density at the nucleus and the smallest chemical shift.

If the nucleus is not spherical (as assumed previously) any nuclear state with a spin  $I > \frac{1}{2}$  has a quadrupole moment, Q, which can align itself either parallel or perpendicular to an electric field gradient. For  $^{57}\text{Fe}$  the excited state has  $I = \frac{3}{2}$ , and the ground state has  $I = \frac{1}{2}$  hence two lines are observed. Some spectra of  $^{57}\text{Fe}$  compounds do not show a quadrupole splitting, this is due to the fact that there is no electric field gradient at the  $^{57}\text{Fe}$  nucleus i.e. there is identical electron density in the x, y and z directions. The usual method of determining the direction of the electric field gradient is by the application of an external magnetic field, although the line due to  $m = \pm \frac{3}{2}$  is sometimes broadened by magnetic interactions thus enabling the determination of the line associated with this substate.

The third and last major type of electron-nuclear hyperfine interactions that can be studied by Mossbauer is hyperfine Zeeman splitting of the nuclear energy levels in a magnetic field. Each level of spin quantum number  $I$  will split into  $(2I + 1)$  sublevels and a change in quantum number of 0 or  $\pm 1$  is only allowed. For  $^{57}\text{Fe}$  the ground state has  $I = \frac{1}{2}$ , and the excited state has  $I = \frac{3}{2}$ , the energy level diagram is given in Figure 7.4. If in the magnetically perturbed spectrum the spacing of the highest velocity pair of lines is greater than the spacing of the lowest velocity pair of lines, the sign of the electric field gradient is such that it raises the  $\pm \frac{3}{2}$  levels.

$^{57}\text{Fe}$  Mossbauer studies were provided by the P.C.M.U., Harwell and the author would like to thank Dr. Johnson and Dr. Dale for their assistance. The computer programme for the calculation of parameters of the magnetically perturbed spectra was written by Dr. B. Dale and is to be published shortly.

### 7.2.2. Results and Discussion

$^{57}\text{Fe}$  Mossbauer studies of the  $\pi$ -cyclopentadienyl compounds are recorded in Table 7.3. All the compounds had quadrupole split spectra consistent with non-symmetrical octahedral symmetry about the iron atom.

An examination of bis( $\pi$ -cyclopentadienyldicarbonyl iron(I)) and its protonated salts shows that on protonation a positive chemical shift is observed which indicates a decrease in s electron density. The half-widths of the absorptions are about 0.25 mm/sec which is consistent with a singlet rather than an unresolved doublet, no increase in width occurred on cooling. Herber et al (124) studied the Mossbauer spectra of 51 organo-iron compounds and calculated the partial isomer shifts for various

ligands. They concluded that ligands which donate a lone pair of electrons to the iron atom make only a very minor contribution to the isomer shift. Hence substitution of one electron pair donor by another will not always significantly alter the resonance of the iron atom. This has been very clearly demonstrated by Carty et al (125) who examined the  $^{57}\text{Fe}$  Mossbauer spectra of the complex  $[(\pi\text{-C}_5\text{H}_5)_2\text{Fe}_2(\text{CO})_3]_2\text{Ph}_2\text{PCCPPH}_2$  and found that the two iron atoms were identical. However addition of a proton to carbonyl iron anions is normally accompanied by significant changes in the isomer shift and quadrupole splitting (126).  $^{57}\text{Fe}$  Mossbauer studies of numerous low spin iron(II) complexes were examined by Bancroft et al (127) who calculated the partial centre shift and partial quadrupole split of several of the more common ligands. A correlation between the partial centre shift and the ligand field strength was deduced and found to hold for all the cases examined. All these studies were carried out at  $295^\circ\text{K}$  but this technique could be applied to results obtained at any temperature provided a sufficient number of compounds have been examined.

In the  $\pi$ -cyclopentadienyldicarbonyl iron(II) halides (halide = chloride, bromide or iodide) the s electron density is less than in the bis( $\pi$ -cyclopentadienyldicarbonyl iron(I)) compounds mentioned previously and the s electron density increases as the electronegativity of the halide decreases as expected. The  $\pi$ -cyclopentadienyldicarbonyl iron- $\mu$ -halogeno  $\pi$ -cyclopentadienyldicarbonyl iron compounds (halogeno = chloro, bromo or iodo with the exception of the tetrachloroborate salt (which will be discussed later) show a further decrease in s electron density and a similar trend with electronegativity of the halogen as observed previously. The half width of the absorption bands are  $0.25 \text{ mm/sec}$  at room temperature but on cooling to  $1.3^\circ\text{K}$  some broadening has occurred. The

Table 7.3  
<sup>57</sup>Fe Mossbauer Data

Compound	Temp. (K)	Isomer Shift* (mm/s)	Quadrupole Splitting (mm/s)	Widths at half height (mm/s)
$[(\pi\text{-C}_5\text{H}_5)\text{Fe}(\text{CO})_2]_2$	78	0.47	1.91	
$[(\pi\text{-C}_5\text{H}_5)\text{Fe}(\text{CO})_2]_2$	78	0.46	1.89	
$[(\pi\text{-C}_5\text{H}_5)\text{Fe}(\text{CO})_2]_2\text{H}^+\text{BCl}_4^-$	300	0.49	1.87	0.25
	4.2	0.60	1.90	0.25
$[(\pi\text{-C}_5\text{H}_5)\text{Fe}(\text{CO})_2]_2\text{H}^+\text{PF}_6^-$	300	0.47	1.82	0.25
	4.2	0.55	1.83	0.25
$(\pi\text{-C}_5\text{H}_5)\text{Fe}(\text{CO})_2\text{Cl}$	300	0.51	1.86	0.29
$(\pi\text{-C}_5\text{H}_5)\text{Fe}(\text{CO})_2\text{Br}$	300	0.52	1.85	0.20
$(\pi\text{-C}_5\text{H}_5)\text{Fe}(\text{CO})_2\text{I}$	300	0.49	1.83	0.21
$[(\pi\text{-C}_5\text{H}_5)\text{Fe}(\text{CO})_2]_2\text{Cl}^+\text{BCl}_4^-$	300	0.50	1.86	0.25
	4.2	0.60	1.93	0.29
$[(\pi\text{-C}_5\text{H}_5)\text{Fe}(\text{CO})_2]_2\text{Cl}^+\text{PF}_6^-$	300	0.58	1.90	0.24
	1.3	0.67	1.97	0.29
$[(\pi\text{-C}_5\text{H}_5)\text{Fe}(\text{CO})_2]_2\text{Br}^+\text{PF}_6^-$	300	0.55	1.76	0.25
	1.3	0.63	1.96	0.29
$[(\pi\text{-C}_5\text{H}_5)\text{Fe}(\text{CO})_2]_2\text{I}^+\text{PF}_6^-$	300	0.53	1.64	0.27
	1.3	0.62	1.83	0.30
$[(\pi\text{-C}_5\text{H}_5)\text{Fe}(\text{CO})]_4$	78	0.52	1.71	-
	77	0.50	1.78	0.31
	1.4	0.52	1.80	0.48
$[(\pi\text{-C}_5\text{H}_5)\text{Fe}(\text{CO})]_4^+\text{PF}_6^-$	1.7	0.53	1.43	0.28
$[(\pi\text{-C}_5\text{H}_5)\text{Fe}(\text{CO})]_4$ in $\text{H}_2\text{SO}_4$	1.8	0.42	1.53	0.28
$[(\pi\text{-C}_5\text{H}_5)\text{Fe}(\text{CO})]_4$ in $\text{CH}_3\text{SO}_3\text{H}$	1.7	0.42	1.56	0.33
$[(\pi\text{-C}_5\text{H}_5)\text{Fe}(\text{CO})]_4$ in $\text{CF}_3\text{COOH}$	1.8	0.47	1.72	0.28

\* relative to sodium nitroprusside

broadening may be due to the fact that to obtain a temperature of  $1.3^{\circ}\text{K}$  liquid helium is boiled off under vacuo introducing pump vibrations and also reducing the time for collecting data. This interpretation would seem to be the most likely since the XPS technique failed to show any variation in the half-widths of the signals obtained. The  $^{57}\text{Fe}$  Mossbauer spectra of the samples were recorded at low temperatures in order to reduce the possibility of the situation where the bridging atom is oscillating between the two iron atoms i.e. structures V to VIII shown on page 72. The rate of a reaction was given by Arrhenius as

$$\log_{10} K = \log_{10} A - E/2.303RT$$

where K is the rate constant; A is the pre-exponential factor; E is the activation energy.

Since in the  $^{57}\text{Fe}$  Mossbauer spectra we do not see two different iron atoms at  $1.4^{\circ}\text{K}$ , the rate of exchange of the chlorine atom from one atom to the other must be at least  $10^7$  (i.e. reciprocal of time scale of  $^{57}\text{Fe}$  Mossbauer) or faster. At room temperature we do not see an absorption band characteristic of a iron chlorine terminal stretch, so that if exchange is occurring it must be slower than  $10^{12}$  (i.e. reciprocal of time scale of infrared). If we substitute these rates and temperatures into the Arrhenius Rate equation we calculate an activation energy E of 35 calories. Activation energies of similar types of reaction could not be found in the literature. In cases of electron transfer and ligand exchange all had activation energies of the order of several kilo calories. It is therefore a reasonable assumption that the transfer of the chlorine atom from one iron atom to the other would have an activation energy of greater than 35 calories. It is therefore most unlikely that the chlorine atom is not associated with both iron atoms.

The spectrum of the  $\pi$ -cyclopentadienyldicarbonyl iron- $\mu$ -chloro  $\pi$ -cyclopentadienyldicarbonyl iron tetrachloroborate is very similar to that recorded for the  $\pi$ -cyclopentadienyldicarbonyl iron(II) chloride and there is a strong possibility that by the time that the spectrum had been recorded the sample had decomposed according to the equation:



At room temperature boron trichloride is evolved slowly from the tetrachloroborate, and in vacuo  $\pi$ -cyclopentadienyldicarbonyl iron(II) chloride is readily formed.

Tetrakis( $\pi$ -cyclopentadienyl carbonyl iron(I)) has a chemical shift which indicates a lower s electron density at the iron nucleus than that observed for bis( $\pi$ -cyclopentadienyldicarbonyl iron(I)). The absorptions at 1.4<sup>o</sup>K are very broad and are almost certainly due to instrumental broadening. Instrumental broadening is shown by the line shape having a very large Gaussian component, instead of a predominantly Lorentzian shape. On forming the tetrakis( $\pi$ -cyclopentadienylcarbonyl iron) cation a slight reduction in s electron density was observed. In an attempt to determine if each of the iron sites in the tetrakis( $\pi$ -cyclopentadienylcarbonyl iron) cation were equivalent or if one iron atom was different from the other three iron atoms the <sup>57</sup>Fe Mossbauer spectrum was recorded in the presence of an external magnetic field. Theory predicts that six absorptions should be seen for each iron atom in a different environment. In the case of the tetrameric compound, therefore either a single sextuplet or a sextuplet of intensity three and sextuplet of intensity one superimposed on each other should be observed. The fact that the spectrum was recorded on a powder necessitates computation since all possible orientations of the crystals with respect to the applied magnetic field will be present. The

computer fit was carried out by Dr. B. Dale and the results are presented in Table 7.4. Both the heptaiodide and hexafluorophosphate salts exhibited lines of 0.305 and 0.287 mm sec<sup>-1</sup> half width respectively, slightly broader than the 0.27 mm sec<sup>-1</sup> normally observed for spectra of this type. Ax, Ay and Az are the three directions in space at the <sup>57</sup>Fe nucleus, a value of about 0.4 is expected for a diamagnetic material. The slight deviation from 0.4 observed is consistent with an internal magnetic field acting in opposition to the applied magnetic field. The fact that Az is different from Ax and Ay indicate a small asymmetric orbital component. The asymmetry parameter is very small indicating that the symmetry around the iron atom is three or four fold. The evidence supports all the iron atoms being equivalent or very nearly so.

The magnetically perturbed spectrum of tetrakis( $\pi$ -cyclopentadienyl-carbonyl iron(I)) in trifluoroacetic acid showed that all the iron atoms were diamagnetic and were equivalent. The half width of 0.25 mm sec<sup>-1</sup> was very narrow and values for Ax, Ay and Az were 0.404. The very small asymmetry parameter showed that the symmetry about the iron atom was either three or four fold.

For the solutions of tetrakis( $\pi$ -cyclopentadienylcarbonyl iron(I)) in sulphuric, methane sulphuric and trifluoroacetic acids (table 7.3) the most interesting feature was the isomer shift. The isomer shift indicated a greater S electron density at the <sup>57</sup>Fe nucleus than that observed in any of the other tetrakis( $\pi$ -cyclopentadienylcarbonyl iron) compounds.

The application of Group Theory to a tetrahedron of four atoms results in the generation of the following molecular orbitals.

4 face bonding symmetry	$A_1 + T_2$
6 edge bonding symmetry	$A_1 + E + T_2$
8 face anti-bonding symmetry	$E + T_1 + T_2$
6 edge anti-bonding symmetry	$T_1 + T_2$

Table 7.4

57Fe Mossbauer Data for Magnetically Perturbed Spectra

Compound	width at half height mm sec <sup>-1</sup>	Temperature °K	Ax	Ay	Az	Asymmetry Parameter
$[(\pi\text{-C}_5\text{H}_5)\text{Fe}(\text{CO})]_4^+ \text{I}_7^-$	0.305	1.6	0.346	0.377	0.235	-0.134
$[(\pi\text{-C}_5\text{H}_5)\text{Fe}(\text{CO})]_4^+ \text{PF}_6^-$	0.287	1.7	0.349	0.366	0.246	+0.101
$[(\pi\text{-C}_5\text{H}_5)\text{Fe}(\text{CO})]_4$ in $\text{CF}_3\text{COOH}$	0.25	1.7	0.404	0.404	0.404	+0.082

According to the theory of ascending symmetry the energy of the orbitals will be  $A_1 < E < T_1 < T_2$ . The detailed scheme of the position of orbitals in the overall bonding scheme is not known but in general the face bonding orbitals will have lower energy than the edge bonding orbitals which in turn have lower energy than the face anti-bonding orbitals. The edge anti-bonding orbitals will have the highest energy. If we consider only the four iron atoms in the +1 oxidation state and the four carbonyl ligands we have 36 electrons ( $4 \times 7 + 4 \times 2$ ) to fill the available molecular orbitals. This results in the face bonding orbitals, edge bonding orbitals and the face antibonding orbitals being filled leaving the edge antibonding orbitals empty.

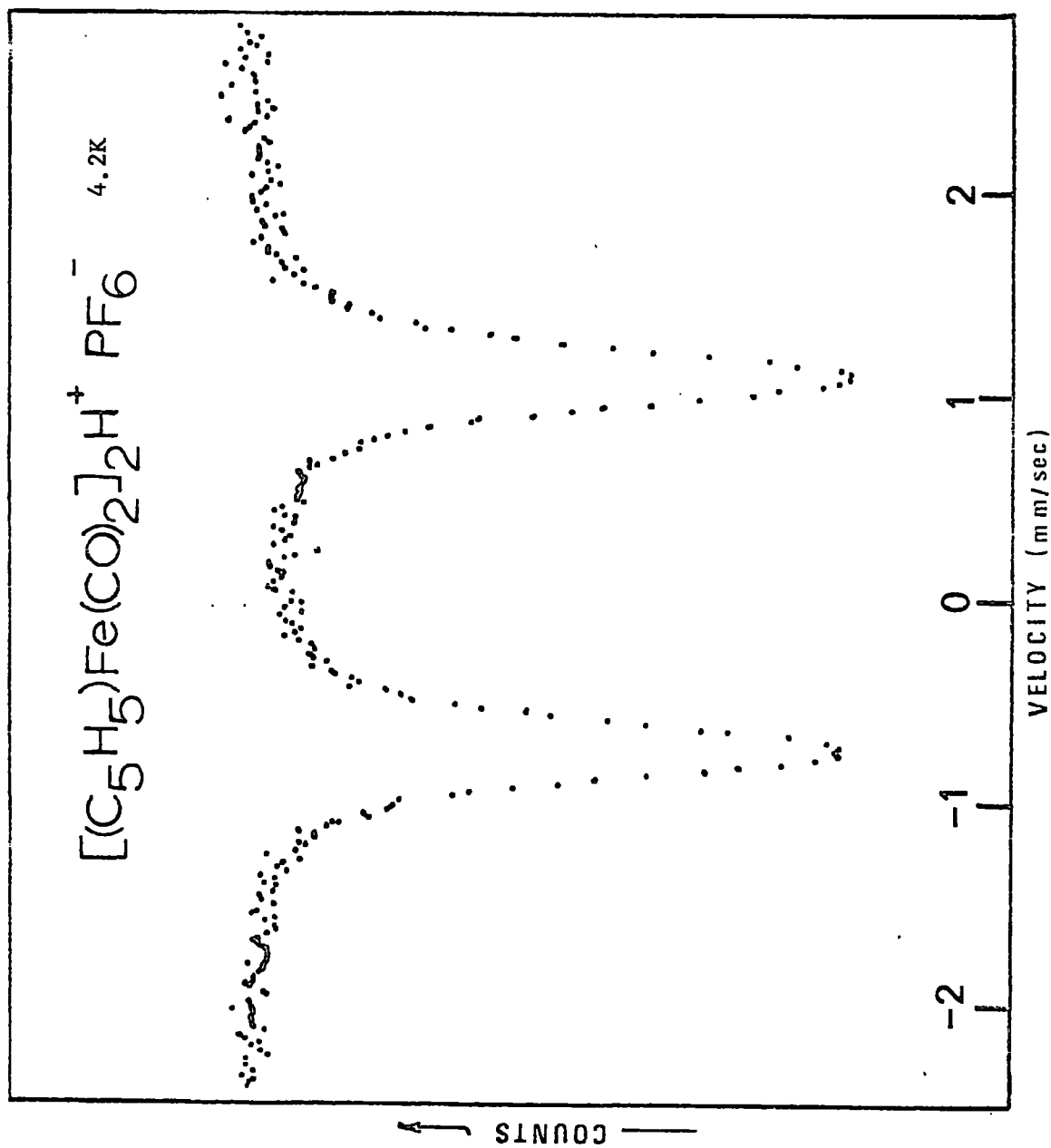
On oxidation of tetrakis( $\pi$ -cyclopentadienylcarbonyl iron(1)) to the monocation the electron will be removed from the highest filled orbital i.e. an antibonding orbital. It is worthy of recalling the symmetries of the various orbitals at this point and they are:

$$\begin{array}{ll} \text{S} & A_1 + T_2 \\ \text{P} & A_1 + E + T_1 + 2T_2 \\ \text{d} & A_1 + 2E + 2T_1 + 3T_2 \end{array}$$

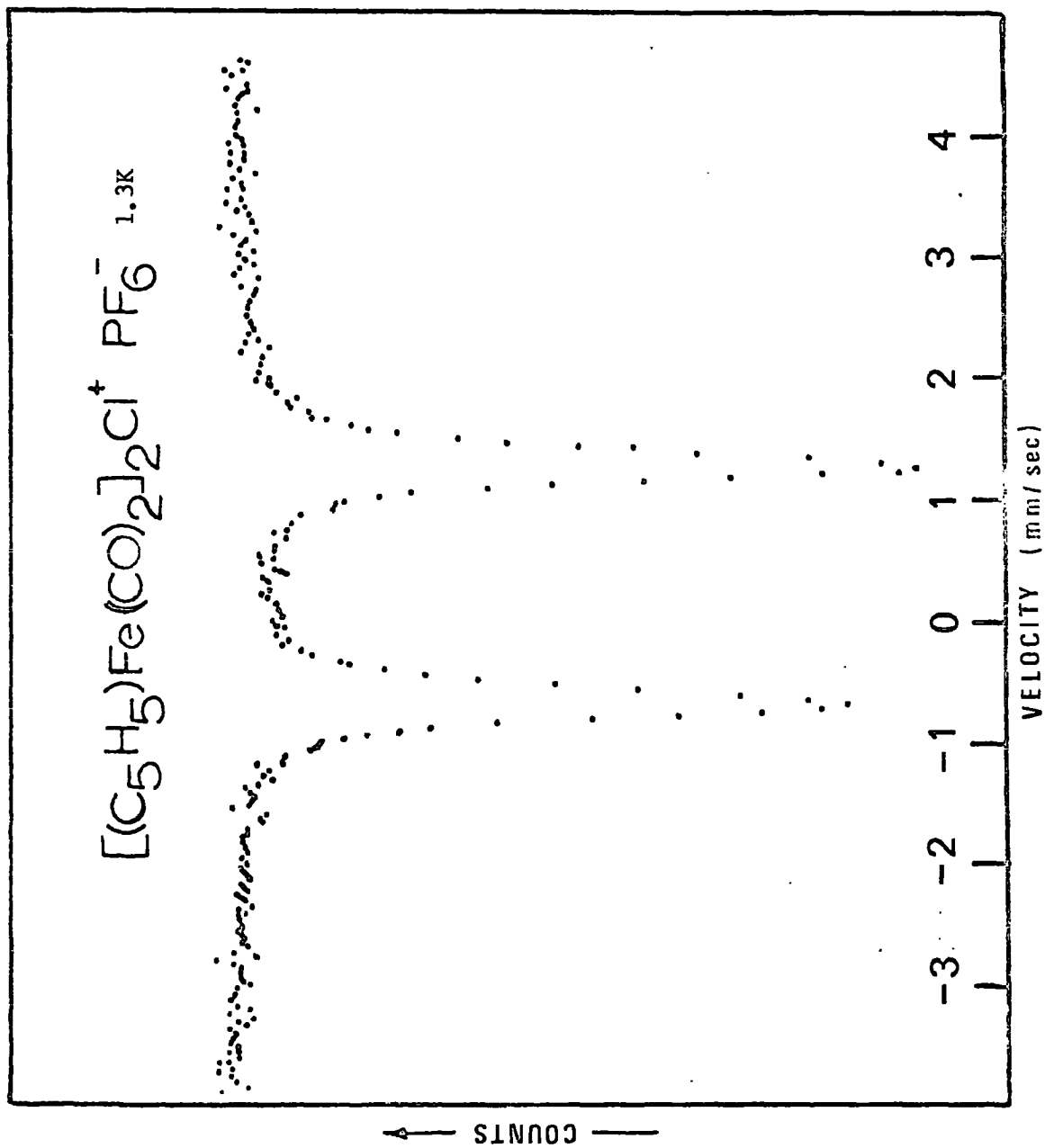
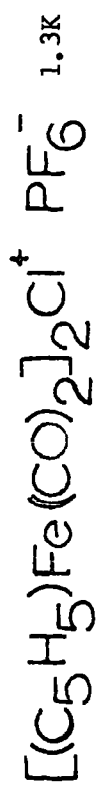
It is now clear that the face bonding and anti-bonding orbitals have an identical symmetry to the P orbitals and hence alterations in the electron density of these orbitals will not have much affect on the  $^{57}\text{Fe}$  mossbauer parameters since these parameters are primarily affected by changes in S electron density. Protonation however will be most likely to occur on the edges of the tetrahedron of iron atoms due to steric interactions restricting the availability of the faces. Protonation of two opposite edges will cause tetragonal distortion by the lengthening of the iron iron bonds involved in protonation and result in the complex having a  $D_{2d}$  symmetry.

Protonation causes a reduction of the back bonding into the carbonyl anti-bonding orbitals, the overall effect is one of causing an enlargement of the faces of the tetrahedron of iron atoms. This enlargement then allows the bonding orbitals of the face to repulse the filled S orbitals of the iron atom which results in the observation of an increase in S electron density at the  $^{57}\text{Fe}$  nucleus.

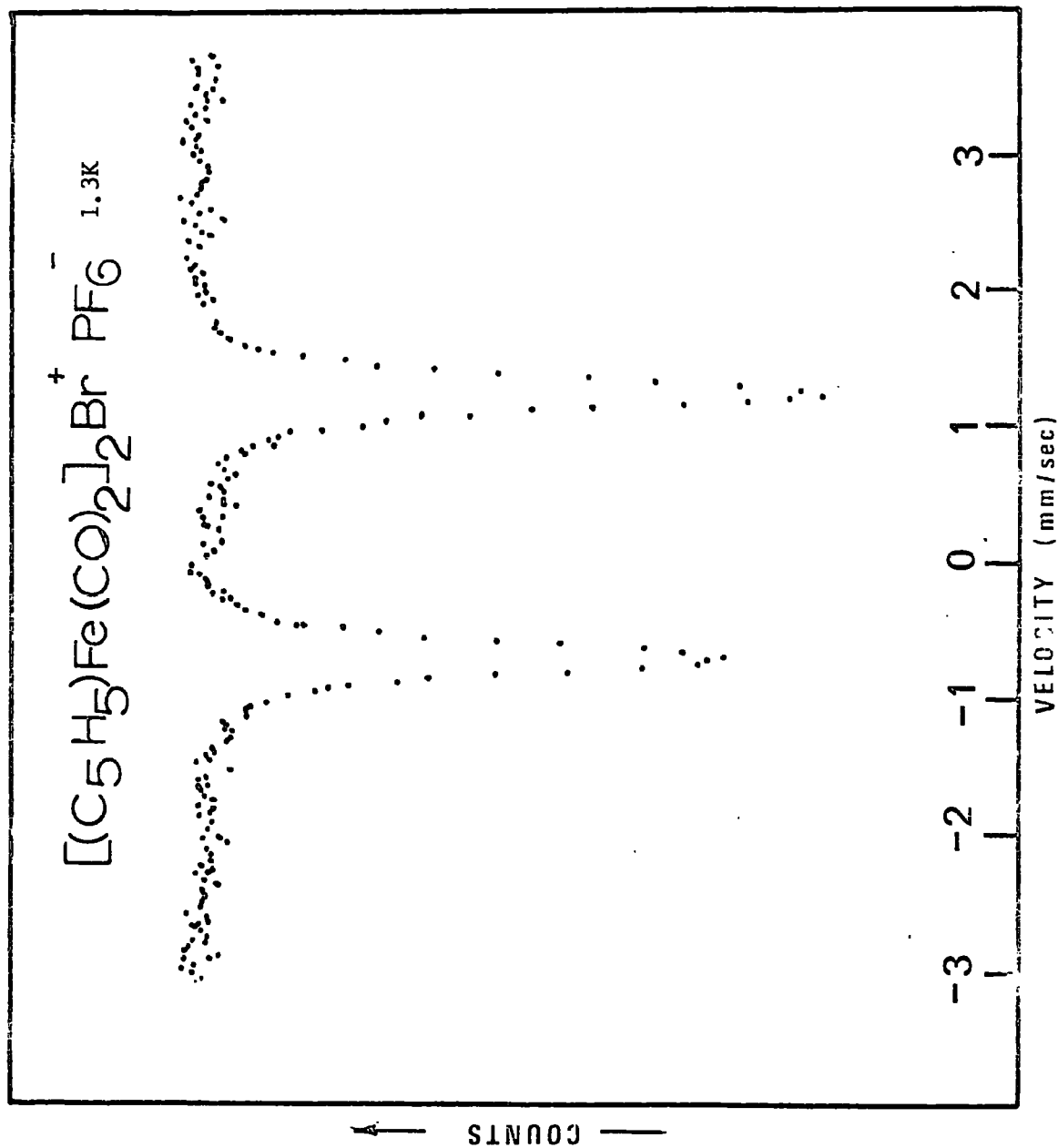
Spectrum number 7.9



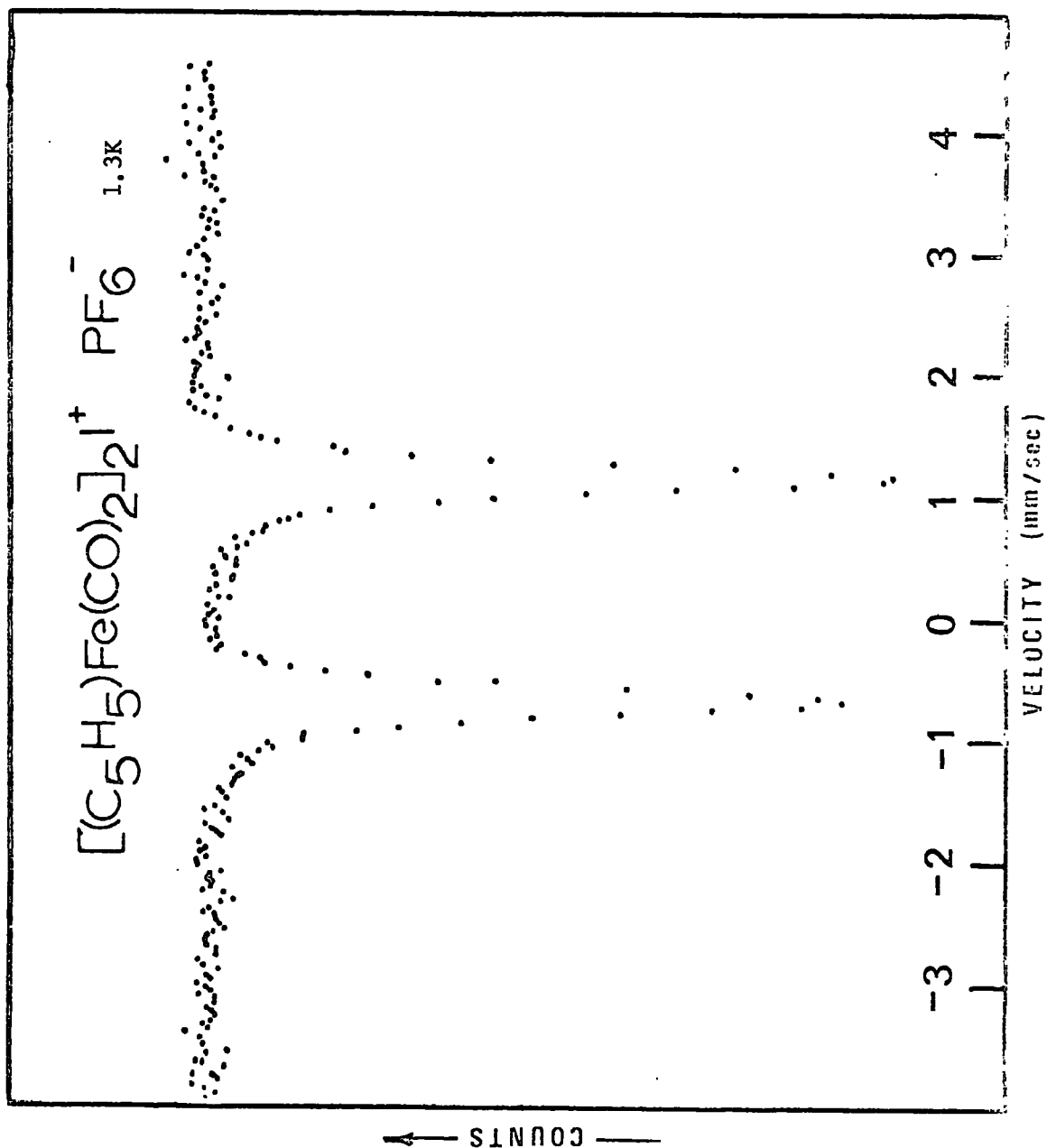
Spectrum number 7.10



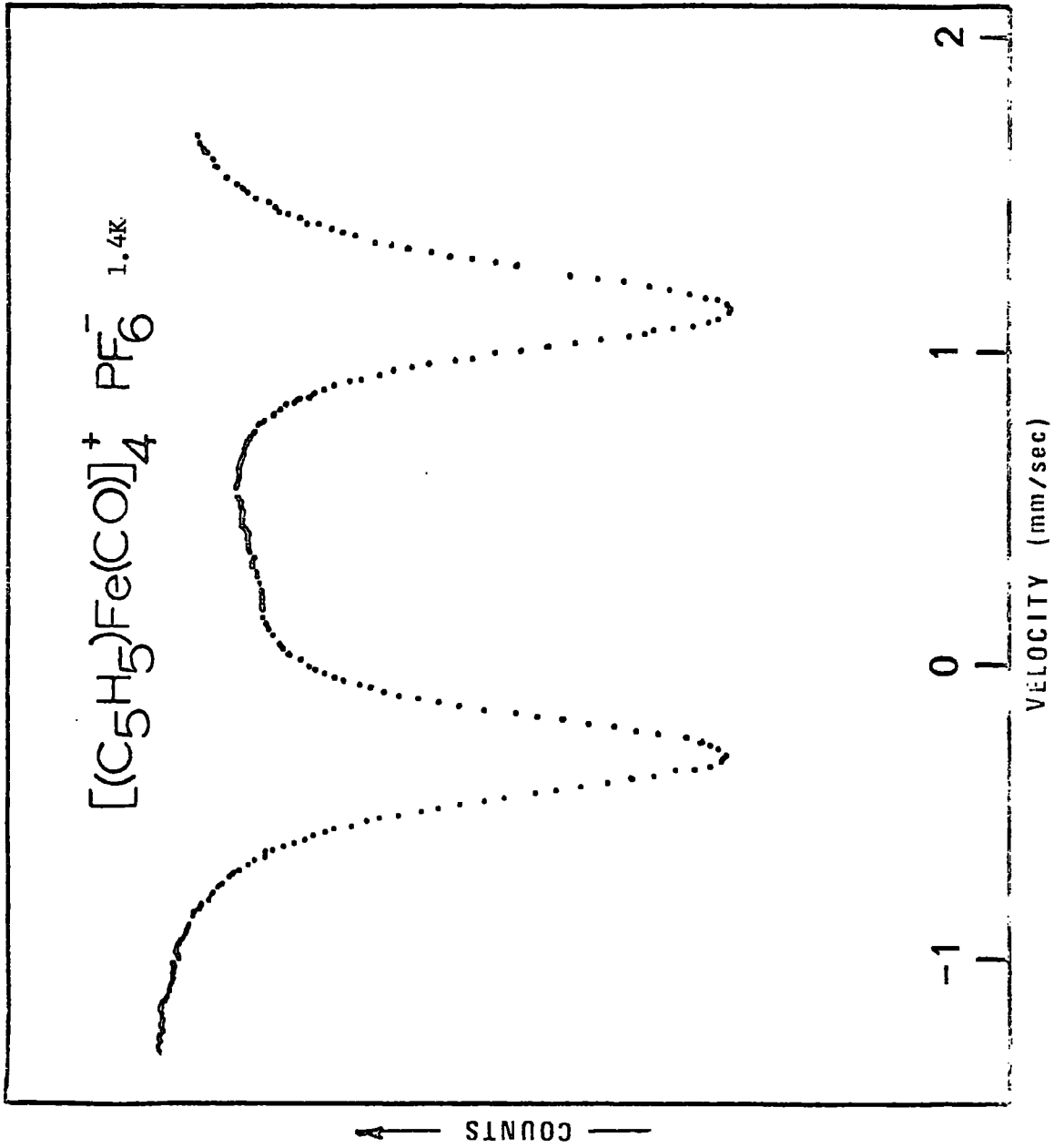
Spectrum Number 7.11



Spectrum Number 7.12



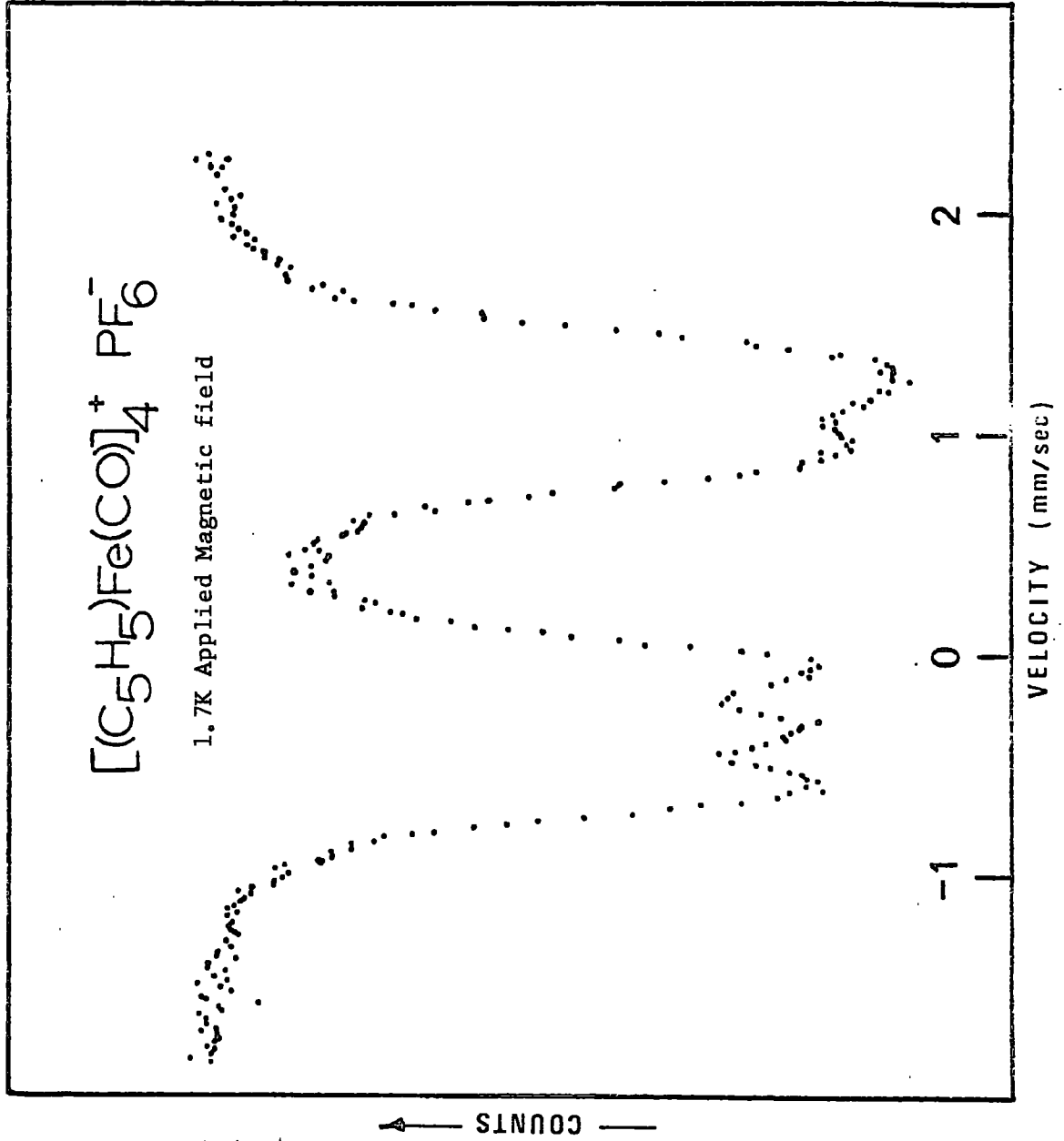
Spectrum Number 7.13



Spectrum number 7.14

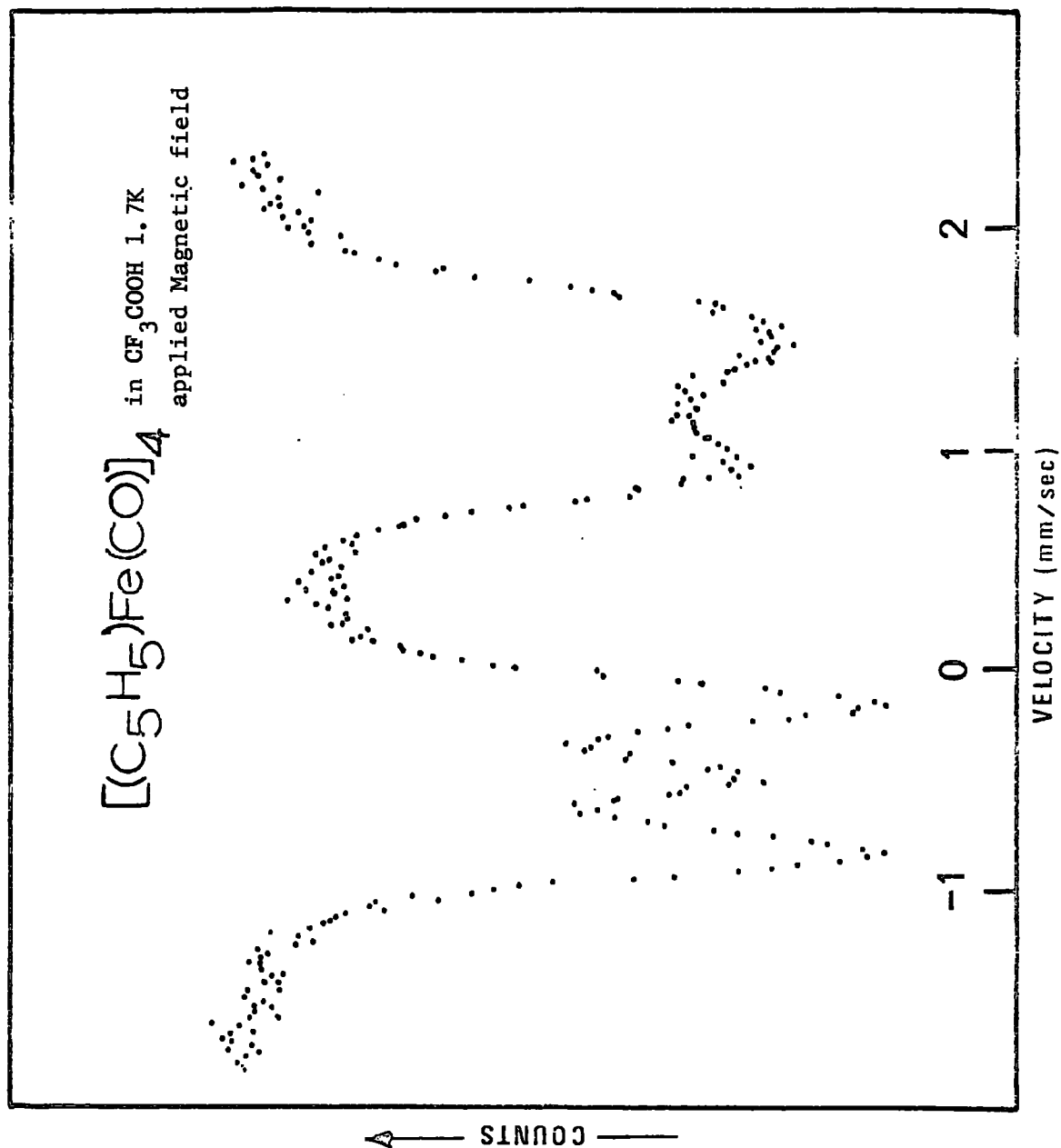


1.7K Applied Magnetic field



Spectrum Number 7.15

$[(C_5H_5)Fe(CO)]_4$   
in  $CF_3COOH$  1.7K  
applied Magnetic field



## CHAPTER 8

### FAR INFRARED SPECTRAL STUDIES

#### 8.1. Introduction

The far infrared spectra recorded over the region  $50\text{--}400\text{ cm}^{-1}$  were obtained using a Beckman-RIIC FS-720 Interferometer. The interferogram was recorded on eight track paper tape and then analysed using the computer program given in Appendix A. The computation was carried out using the IBM 360/67 computer jointly owned by the Universities of Durham and Newcastle upon Tyne. Graph plots of the processed data were performed exclusively using the IBM 1130 computer of Durham University using a program supplied by Mr. B.R. Lander of the Durham University Computer Unit. The author expresses his thanks to Mr. B.R. Lander for supplying the graph plotting procedures.

Fourier theory was developed by J.B.J. Fourier (129) when working on the theory of heat transmission, however this theory has found applications far beyond the boundaries of heat transmission. The application of Fourier theory to spectroscopy dates back to the pioneering work of Michelson (128). Michelson discovered that the interference pattern from a two beam interferometer, as a function of the path difference between the two beams, is the Fourier transform of the optical power spectrum of the source illuminating the interferometer. The development of optical detectors and electrical data recording techniques overcame Michelson's problems arising from the fact he had to observe the fringes visually and estimate the visibility of them. It is only since the advent of modern computer technology (i.e. over the last fifteen years) that Fourier transform spectroscopy has become a practical technique for complicated spectra.

There have been a number of excellent papers written on the application of Fourier theory to interferometric spectroscopy in the far infrared, for example by Strong and Vanasse (130), Jacquot (131), Connes (132) and Genzel (133). The detailed theory of Fourier transform spectroscopy is beyond the scope of this thesis and only a brief resume of it will be included here. It is not necessary for the chemist to understand the theory of Fourier transformations in order that the spectra obtained by that method can be interpreted.

#### 8.1.1. Advantages of interferometry over conventional spectroscopic techniques.

Studies of the absorption of light in the  $50\text{-}400\text{ cm}^{-1}$  region of the electromagnetic spectrum before the advent of interferometric techniques were very difficult. Sources of radiation in the far infrared region ( $400\text{ cm}^{-1}$  and less) are very weak. The source which is most commonly employed is a high pressure mercury discharge in a silica envelope. The silica envelope is opaque above about  $70\text{ cm}^{-1}$ , and at frequencies above  $100\text{ cm}^{-1}$  these sources function merely as hot silica rods.

Dispersion monochrometers for use in this region are inefficient and to cover the region several gratings will be required. These monochrometers also require a series of filters for removing unwanted orders of diffracted radiation. Only a single resolution width of radiation will fall on the detector at any instance. In techniques using a dispersion monochromator to double the resolution it is necessary to reduce the entrance and exit slits by a factor of two, resulting in the signal level being reduced by a factor of four. To obtain a spectrum with the same signal to noise ratio would take sixteen times as long, on the

assumption that the noise is random. Interferometric techniques allow the whole spectral range of interest to be incident on the detector at one time resulting in much higher signal to noise ratios. To obtain a spectrum with double the resolution the length of travel of the moving mirror has to be doubled (this will become clear from later discussions). The spectral region over which an interferometer can be used is governed by the efficiency of the beam splitter, and it is these beam splitters which are the weakest link in the far infrared Michelson interferometer. A membrane with a reflectance and transmittance of 50% would be an ideal beam splitter. In actual practice, the best results are achieved by using a dielectric reflection from a film, or a metallic reflection from a wire screen. The most commonly used film is Mylar or Melinex (polyethylene terephthalate) because it has a reasonably high dielectric constant, a refractive index of 1.85 in the far infrared (136) and is readily available. Plots of the efficiencies of various thicknesses of beam splitters are given in Figure 8.1.

The ideal efficiency of the beam splitter should be 25% (i.e. product of transmittance and reflectance values). Complications arise due to the fact that multiple reflections occur within the beam splitter (134,135) which give rise to the overall efficiency of the beam splitter being given by the equation

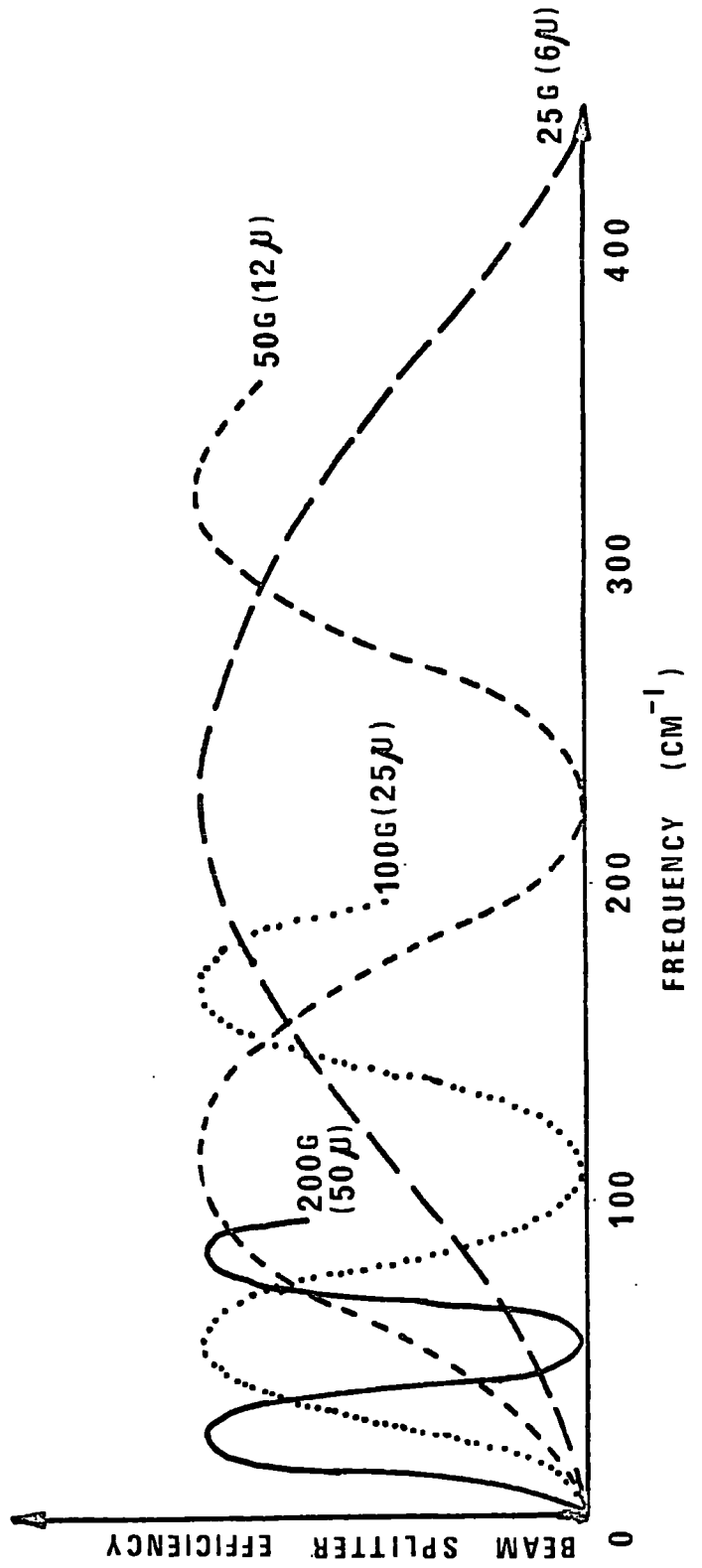
$$E\alpha(2\pi \nu d')$$

where E is the efficiency,  $\nu$  is the frequency of the incident radiation, and  $d'$  is the apparent thickness of the beam splitter material. For a beam splitter which is at  $45^\circ$  to the two Michelson mirrors, and has a true thickness of  $d$  and a refractive index of  $n$ , the relationship is

$$d' = d\sqrt{n^2 - \frac{1}{2}}$$

# RELATIVE BEAM SPLITTER EFFICIENCIES

Fig. 8.1



By using different thicknesses of beam splitter a wide range of frequencies can be covered very efficiently. To obtain the best results it is necessary to use optical filtering to remove any unwanted radiation.

Table 8.1 lists some useful beam splitter and optical filter combinations.

Table 8.1

Frequency Range of interest -1 cm	Beam Splitter thickness mm	Filters
40-400	0.006	Black Polythene
20-200	0.012	Black Polythene and 2 mm crystal quartz
10-90	0.025	Black Polythene and 1 mm crystal quartz
5-50	0.050	Black Polythene and 100 lines/cm cross-ruled polythene filter
5-35	0.050	Black Polythene and 60 lines/cm cross-ruled polythene filter

The detectors for use in the far infrared are the third and final problem area. Most commercial far infrared spectrophotometers employ a Golay cell, which is a pneumatic detector. The two big advantages of the Golay cell are that it operates at room temperature and it is readily available. Compared with the cooled bolometers and photoconductive detectors the Golay cell is up to two orders of magnitude less sensitive and its response is relatively slow. Noise-equivalent-power is the power input of the detector required to give an output voltage of the same

magnitude as the noise of the detector; and the responsivity is the output voltage of the detector per watt of power incident on the detector. Golay cells have a noise-equivalent-power of about  $10^{-10}$  watts and a responsivity of about  $10^5$  volts/watt. This enables a resolution of  $2 \text{ cm}^{-1}$  to be utilised in grating instruments with a signal to noise ratio of 30-50, but a signal to noise ratio in excess of 140 is achieved in a interferometer (both instruments covering the 30-400  $\text{cm}^{-1}$  region and requiring about two hours for the collection of data).

In all of the problems outlined above the technique of interferometry enables the best use of the limited output of far infrared sources. The only area where interferometry is at a disadvantage is that the interferogram requires computation before a spectrum can be obtained. The advent of small digital computers and the fact that most organisations have access to digital computers means that this disadvantage is not too serious.

#### 8.1.2. Theory

The theory of Fourier transforms given here will be restricted to the basic factors which directly affect the operational performance of a Michelson interferometer.

Fourier transform spectroscopy is based on the fact that in a two beam interferometer the intensity of the central light fringe (measured at the output of the device) is the Fourier transform of the incident optical power spectrum. The spectral intensity  $G(\nu)$  at any frequency  $\nu$  ( $\text{cm}^{-1}$ ) with the measured interferogram intensity  $I(x)$  is given by the equation

$$G(\nu) = \int_{x=0}^{x=\infty} [I(x) - \frac{1}{2} I(0)] \cdot \text{Cos}(2\pi \nu x) \cdot dx \quad (1)$$

where  $x$  is the optical path difference of the two beams and  $I(0)$  is the interferogram intensity at zero path difference (measured in arbitrary units). In the interferometer used for the authors studies the intensities of the interferogram are measured at discrete values of optical path difference  $n \cdot \Delta x$  up to some maximum value  $N \cdot \Delta x$ , where  $n$  is an integer equal to  $0, 1, 2, 3, 4, \dots, N$  and  $\Delta x$  is the interferogram sampling interval. In order to obtain unambiguous information, the value of  $\Delta x$  must be such that

$$\Delta x \leq \frac{1}{2(\nu_1 - \nu_2)} \quad (2)$$

where  $(\nu_1 - \nu_2)$  is the total band width of optical frequencies received by the detector. In far infrared interferometers low-pass filters are used to restrict the range of frequencies incident on the detector to  $0 - \nu_{\text{max}}$ . Where  $\nu_{\text{max}}$  is the high frequency cut off so that

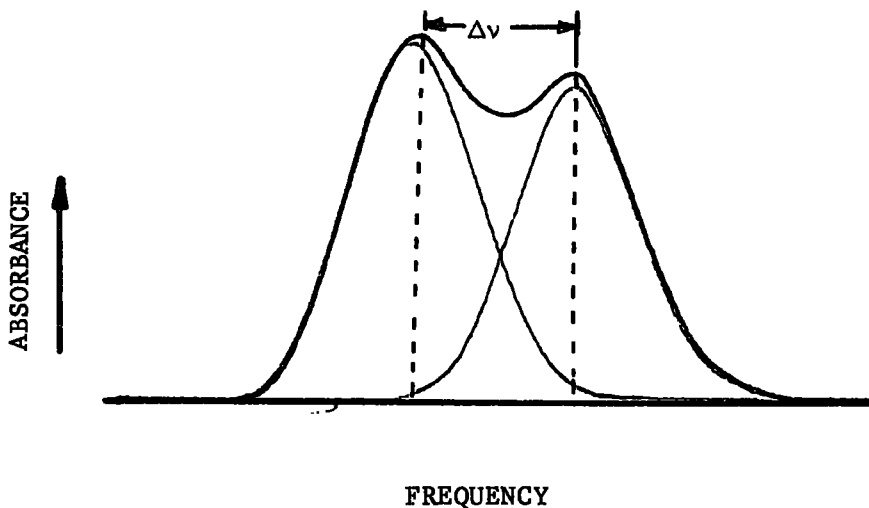
$$\Delta x \leq \frac{1}{2\nu_{\text{max}}} \quad (3)$$

This ensures that the amplitude of the highest frequency radiation is measured at least once every half cycle. Equation (1) then becomes approximated to the summation

$$G(\nu) = \sum_{n=0}^{n=N} [I(n \cdot \Delta x) - \frac{1}{2} I(0)] \cdot \text{Cos}(2\pi \nu n \Delta x) \cdot \Delta x \quad (4)$$

The output of the detector is amplified and digitised. The range of the digitiser is from 0 to 4095. A spectrum of intensity as a function of frequency is then computed digitally using equation (4). The value of  $\frac{1}{2}I(0)$  may be obtained taking the average value of the interferogram, and must be subtracted from all the values of  $I(x)$  before Fourier transform computations commence. It is important to note that the computed spectral intensities  $G(\nu)$  are directly proportional to the measured amplitudes of the oscillatory interferogram function  $[I(n, \Delta x) - \frac{1}{2}I(0)]$ , and that the first ( $n = 0$ ) value of the summation ( $\approx \frac{1}{2}I(0)$ ) makes a constant contribution to the whole spectrum of frequencies and is independent of  $\nu$ . Errors in measuring the true value of  $I(0)$  thus result in base line shifts in the computed spectra which reduces the accuracy of absolute transmittance or reflectance measurements. In practice interferograms rarely have a sampling point exactly at zero path position, then care must be taken to correct interferograms for these slight displacements which are known as 'phase errors'.

Two peaks are said to be just resolved when the absorption maximum of one peak just co-incides with the base of the adjacent peak as shown below



The optical resolution  $\Delta\nu$  of an interferometer is related to the maximum path difference  $D$  of the recorded interferogram by the instrumental scanning or 'slit' function and is of the form

$$\Delta\nu = 2D \left[ \frac{\sin 2\pi(\nu - \nu')D}{2\pi(\nu - \nu')D} \right] \quad (5)$$

where  $D$  is the path difference and is given by

$$D = N \cdot \Delta x \quad (6)$$

$\nu'$  is the frequency of the peak at its maxima and has a width at half height of  $(\nu - \nu')$ . Equation (5) reduces such that the smallest interval resolved is approximately given by:

$$\Delta\nu \approx 0.7/D \quad (7)$$

When the region of interest includes a large number of frequencies (as is usually the case) the subsidiary side lobes of the scanning function (5) cause oscillations to be seen near regions where rapid changes in spectral intensity are occurring. The oscillations can be mistaken for weak spectral lines and it is therefore, desirable to suppress these oscillations. This can be achieved mathematically by weighting or 'apodising' the recorded interferogram values  $[I(n \cdot \Delta x) - \frac{1}{2}I(0)]$  so that the modulation of the interferogram goes to zero at maximum path difference  $D$ ,  $(N \cdot \Delta x)$ . Common apodisation techniques is to modify the scanning function (5) so that it takes the form

$$\Delta\nu = 2D \left[ \frac{\sin^2(2\pi(\nu - \nu')D)}{(2\pi(\nu - \nu')D)^2} \right] \quad (8)$$

This scanning function takes no negative values and the side-lobes are considerably reduced, although the central band is made much broader.

The optical resolution now becomes

$$\Delta\nu \approx \frac{1}{D} \quad (9)$$

The resolving power  $R$  of an interferometer is also limited by the angular beam spread of off-axis rays brought about by imperfect collimation of the finite source aperture. If the source subtends a solid angle  $\phi$  at the collimating mirror, then the maximum value of  $R$  (131) is given by:

$$R = \nu/\Delta\nu \quad (10)$$

$$R = \frac{2\pi}{\phi} \approx 8 \left(\frac{f}{d}\right)^2 \quad (11)$$

where  $d$  is the source diameter and  $f$  is the focal length of the collimating mirror.

The FS-720 has source apertures of 10, 5 and 3 mm which result in resolving powers of  $10^3$ ,  $4 \times 10^3$  and  $10^4$  respectively.

The spread of off axis rays of light from the source also leads to an average ray path length which is slightly longer than that of an axial ray resulting in all frequencies in the computed spectrum being over-estimated by a factor of approximately  $(1 + \phi/4\pi)$ . The true frequencies  $\nu$  can be obtained from the computed frequencies  $\nu_{(obs)}$  by the formula:

$$\nu = \frac{\nu_{(obs)}}{\left(1 + \frac{\phi}{4\pi}\right)} \quad (12)$$

In practice this correction factor is very small (of the order of  $10^{-4} \nu_{obs}$ ) and only becomes significant for high resolution studies at high frequencies.

### 8.1.3. Instrumentation

The instrument used for these far infrared studies was a Beckman-RIIC model FS-720 spectrophotometer with a FS-200 series electronics.

The spectrophotometer consists of a Michelson interferometer which employs 8 cm diameter all reflecting optics of  $f/1.5$ - $f/2$  aperture. The sample optics give a 12 mm diameter image and  $f/2$  aperture enabling reasonably small solid or liquid samples to be studied. A high pressure mercury source which is water cooled is used to provide the radiant energy and mylar films of thicknesses of 0.0006-0.0050 cm are used as beam splitters (see Table 8.1). A Pye-Unicam Golay cell fitted with a 3 mm diameter diamond window is used as the detector. The entire instrument operates in a vacuum ( $2 \times 10^{-2}$  or less) to remove effects of atmospheric absorptions (primarily those of water vapour).

The interferograms are recorded by the continuous movement of one of the Michelson mirrors. The moveable mirror has a movement of 10 cm either side of zero path and the displacement of this mirror is monitored by a subsidiary Moire fringe system. The fixed Michelson mirror is adjusted by a system of levers and for best results should be adjusted with the thinnest beam splitter in position.

The radiation of the mercury arc source is chopped and the ac signal from the Golay is amplified, then rectified and smoothed to give a dc electrical voltage which is proportional to the intensity of the interferogram. The d.c. electrical output is then fed to a digitizer which converts the signal into 12 bit binary numbers, which are recorded on eight track paper tape.

Equation (1) shows that the intensities of the wavenumber computed spectrum are directly proportional to the amplitudes of the interferogram

function  $[I(x) - \frac{1}{2}I(0)]$ . In order to record accurate spectra it is necessary that the interferogram values close to  $I(0)$  are recorded with a very high precision. When strongly absorbing samples are being examined it is necessary to employ long time constants to maintain a high signal to noise ratio and therefore the scanning times must be increased to avoid distortions due to the inherent time constant of the electrical system.

The highest practical resolution that can be obtained with a far infrared interferometer is usually restricted by signal to noise considerations. No advantage is gained by scanning interferograms beyond a point where meaningful features containing spectral information are indistinguishable from the noise level. In general the interferogram signal to noise should be much higher than the total number of spectral elements to be resolved in a single scan, e.g. to achieve  $1 \text{ cm}^{-1}$  resolution over an optical band width of  $400 \text{ cm}^{-1}$ , the interferogram signal to noise ratio should be greater than 400:1.

#### 8.1.4. Computation

The program to compute the wavenumber spectrum from the interferogram is given in Appendix A. The program is based on the Cooley-Tukey algorithm (75). In the format presented in this thesis the maximum number of points to be transformed was 2048 and the core store requirements of the program was 143,000 bytes. On increasing the size of the arrays to enable 8,192 points to be transformed the core store requirements were 494,000 bytes. Core store was not an immediate problem on the computer used, (core store 1 megabyte and in certain modes this was backed up by a magnetic drum of 1 megabyte). Table 8.2

lists the number of points to be transformed, time required for computation and the maximum resolution obtainable under the working conditions used. These maximum resolution values were obtained by running the water vapour spectrum under as near identical conditions as possible to those used for solid state samples. The strong modulation of the water vapour interferogram and the lower value of amplifier gain both mean that the signal to noise value would be much higher in the case of the water vapour spectrum than in the solid state spectra.

Table 8.2

Central Processor Unit Times Required for  
Fourier Transform Programs

Number of Points to be transformed	Time required in seconds
256	36
512	55
1024	122
2048	378
4096	1367
8192	5263

The program (which was originally supplied by Dr. J. Yarwood of this University) was written in Fortran IV and was originally written to run under the IBM 360 Operating System, using a Fortran IV level G computer. The author carried out alterations to enable the program to be compatible with both the IBM 360 Operating System and the Michigan Terminal System currently used on the IBM 360/67 computer. Other alterations were introduced to enable the program to run using a Fortran

IV level H compiler, this increased the core store requirements by about 50 per cent but reduced the cpu time required by 50 per cent also.

A brief description of the program will now be given; explaining the main function of each section.

(i) Main

This section merely defines the sizes of the arrays required, reads in the control parameters to be used in the computation and calls each subprogram required in the correct order.

(ii) Subroutine TPREAD (tape read)

The interferogram which has been recorded as a 12 bit binary number on an eight track tape is read in and processed with the program DCL99SPY. This program translates the 12 bit binary numbers to I4 (4 digit integer) numbers and then stores these in blocks of 20 as magnetic records on magnetic discs. The TPREAD subprogram reads in these I4 numbers into array A. The end of a data set being marked by a -999 signal. Arrangement to read in a sample and background data set being provided.

(iii) Subroutine SUBDH (data handling)

This routine calls subroutine AMX (Array A maximum value) which then finds the maximum value in array A and then calculates the average value of the interferogram. The central portion of array A which is required for transformation is then selected and the average subtracted from each value in the array. The 'reduced interferogram' is then auto-correlated to remove any phase error. Autocorrelation is the process of displacement multiplication and integration of a function with itself. This process always results in a function which is symmetrical about the maximum value, hence phase errors are eliminated.

Subroutine AMX is then called and the maximum value of the autocorrelated interferogram found. The autocorrelated interferogram is then normalised by dividing each member in the array by the maximum value of the array, and is stored with largest number in element 1 of the array. The treated interferogram is then apodised using a cosine function.

(iv) Subroutine TM (transformation)

The autocorrelated and apodised interferogram then undergoes Fourier transformation using the Cooley Tukey Algorithm (75).

(v) Subroutine PT (plot)

The results of the transformation over the region of interest are selected, the square root of the intensities taken and then normalised in an absorbance mode. The subroutine calls the subroutine LP (line printer) which prints the scale on the absorbance axis prior to printing the spectrum on the line printer using subroutine GP (graph plot).

(vi) Subroutine GP

A plot of the spectrum on the line printer is produced together with either cards or a magnetic record of the card images in order that a graph plotted spectrum may be obtained.

The card output was then used in conjunction with the graph plotting procedure which is given in Appendix A, to give a plot of absorbance against frequency. The subprograms of the plotter program SCALF, FPLOT, FGRID, FCHAR, are standard subroutines of the disc monitor system of IBM for 1130 computers and is given a full description in 'IBM 1130/1800 Plotter subroutines' publication C26-3755.

## 8.2 Results and Discussions

The examination of the infrared spectra of compounds in the 400-50  $\text{cm}^{-1}$  region has only recently become feasible on a routine basis. There is a lack of reliable data in the above region and for this reason several compounds were re-examined in order to try and facilitate the assignments of the absorption bands.

### 8.2.1. Examination of the water vapour spectrum

One of the standard methods of calibrating a spectrophotometer in the 400-50  $\text{cm}^{-1}$  region is by the use of water vapour. By recording the interferogram of water vapour and then analysing the interferogram using the fourier transform program given in this thesis the following checks were made:

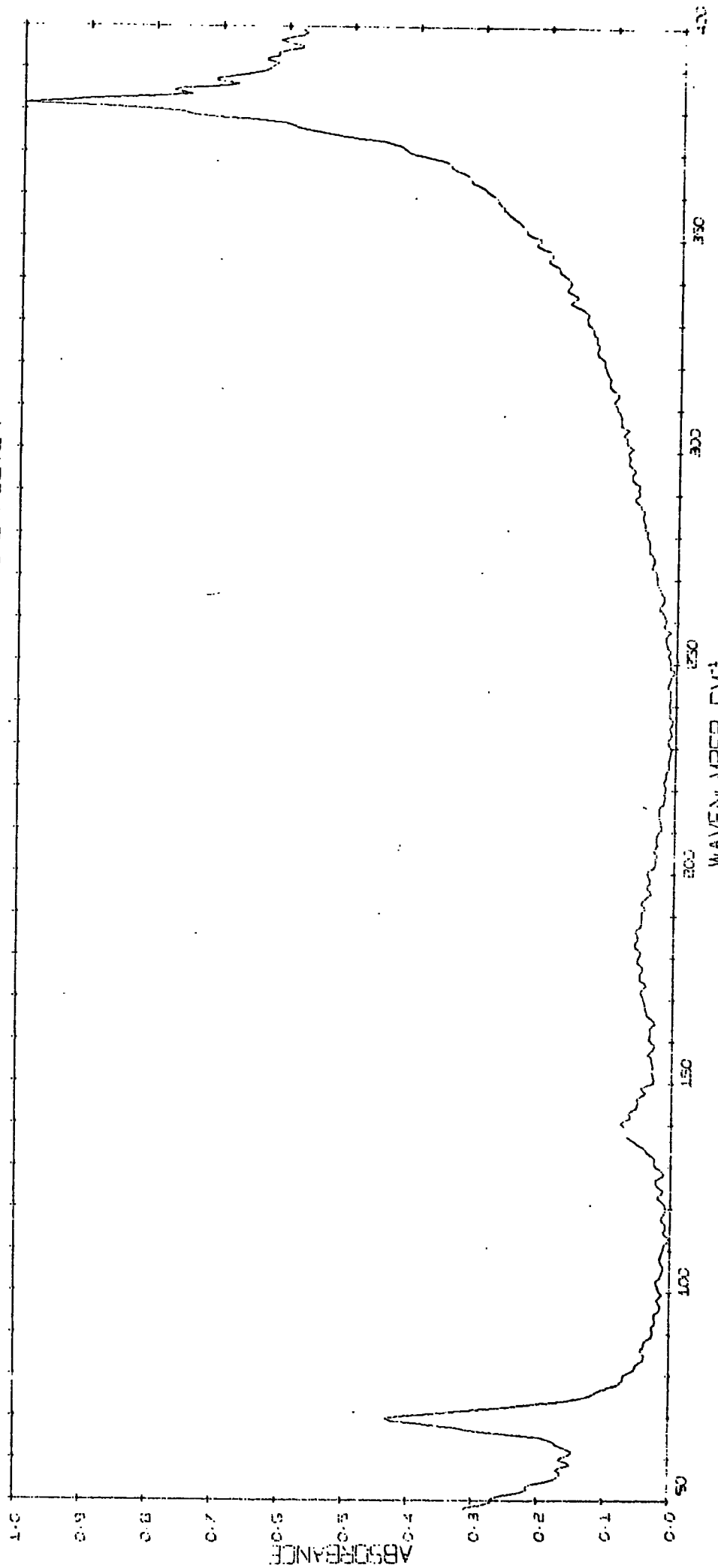
(a) That the power spectrum (plot of absorbance against frequency) gave absorbance values with correct frequency.

(b) That relative absorbance values were comparable with those obtained using a conventional infrared spectrophotometer.

(c) And calculation of the resolution obtained with different lengths of recorded interferogram.

It is important to point out at this stage that the resolution figures obtained (Table 8.3) refer to a gas (water vapour). The absorption bands are subject to pressure broadening (since the interferogram was recorded at atmospheric pressure), no attempt was made to obtain high resolution gas spectra but just to give an idea of the minimum length of run necessary to achieve the desired resolution. The conditions used were as near as possible to those used for the recording of the nujol mull spectra but it is probable that the resolution figures obtained are somewhat optimistic.

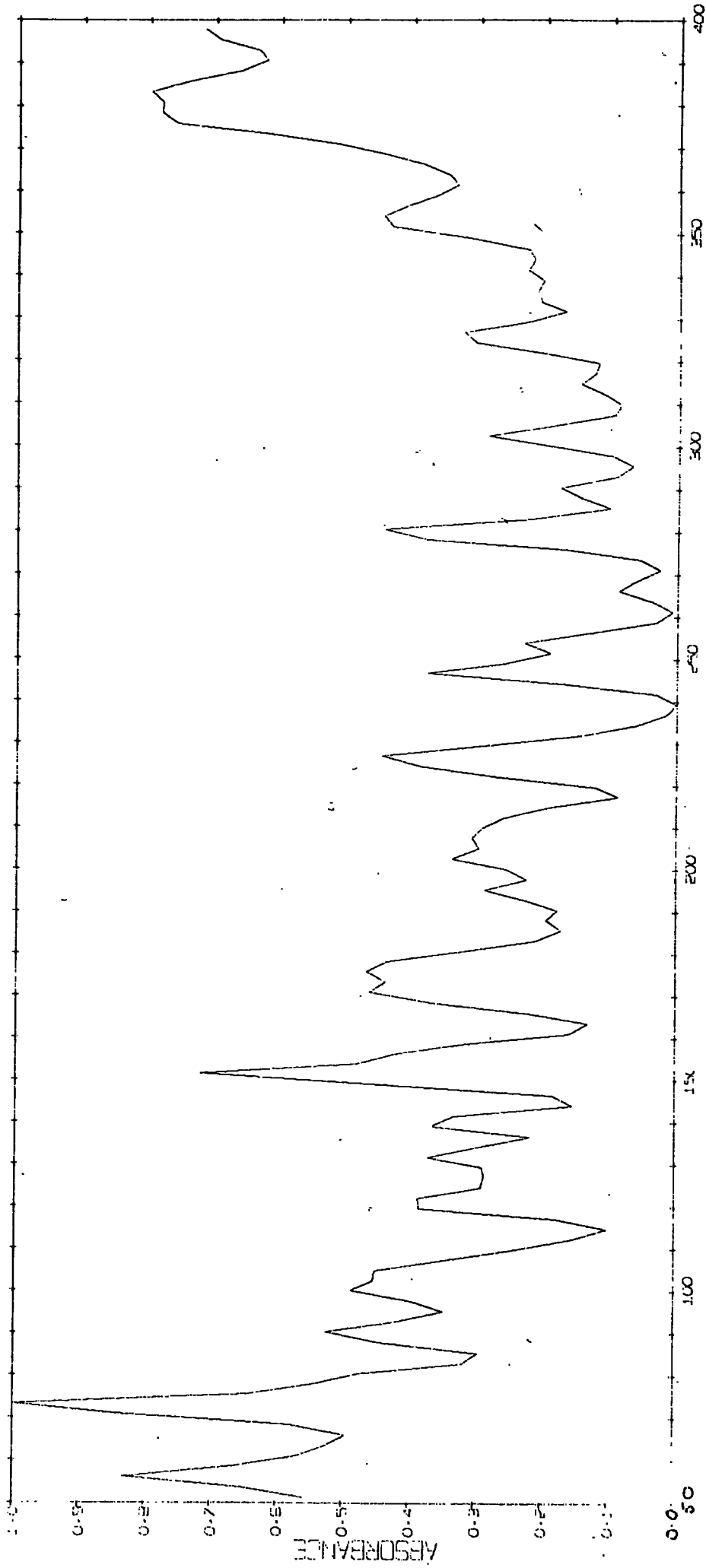
BACKGROUND WHITE LENS AND BLACK POLYTHENE FILTER



WAVENUMBER CM<sup>-1</sup>

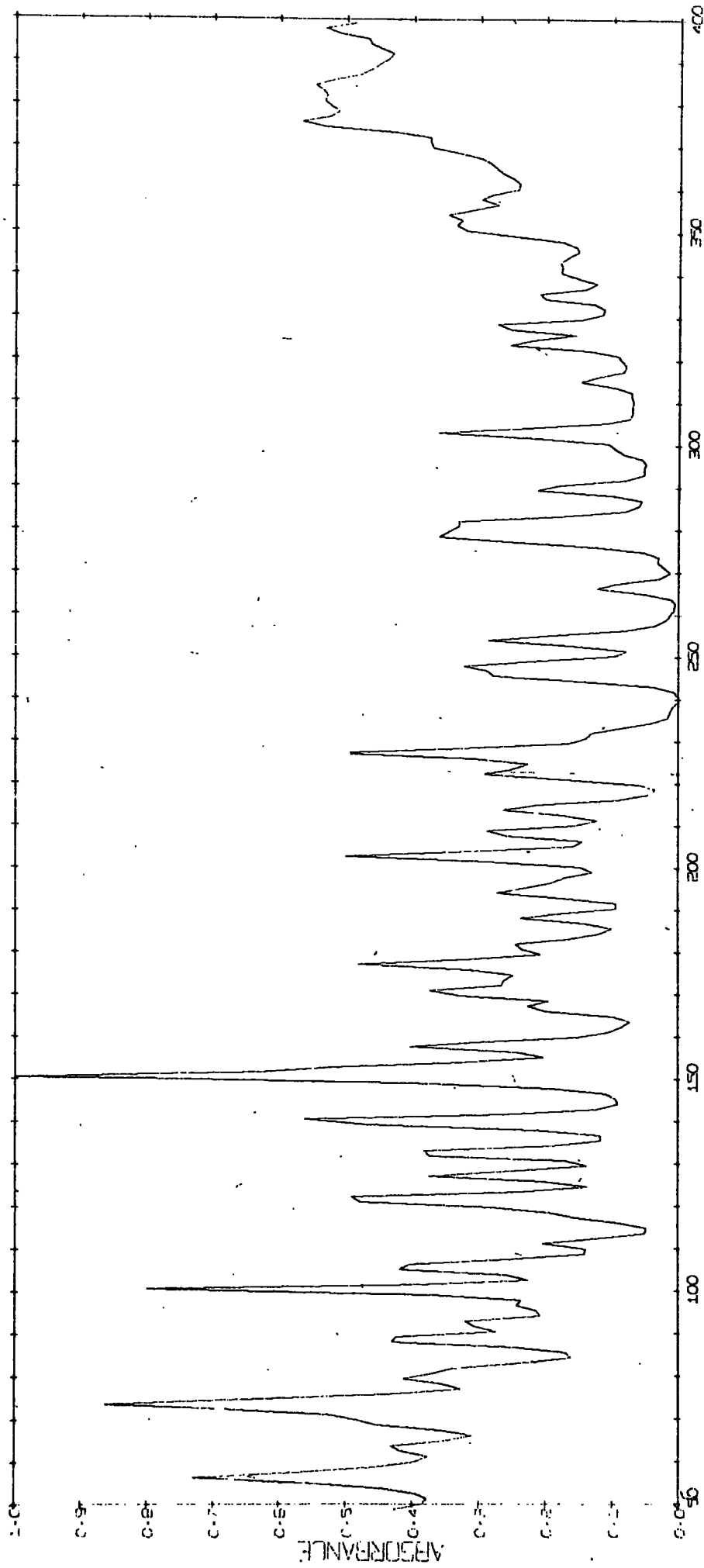
Spectrum 8.1

WATER VAPOUR 512 POINT ANALYSIS



WAVENUMBER (CM<sup>-1</sup>)  
Spectrum 8.2

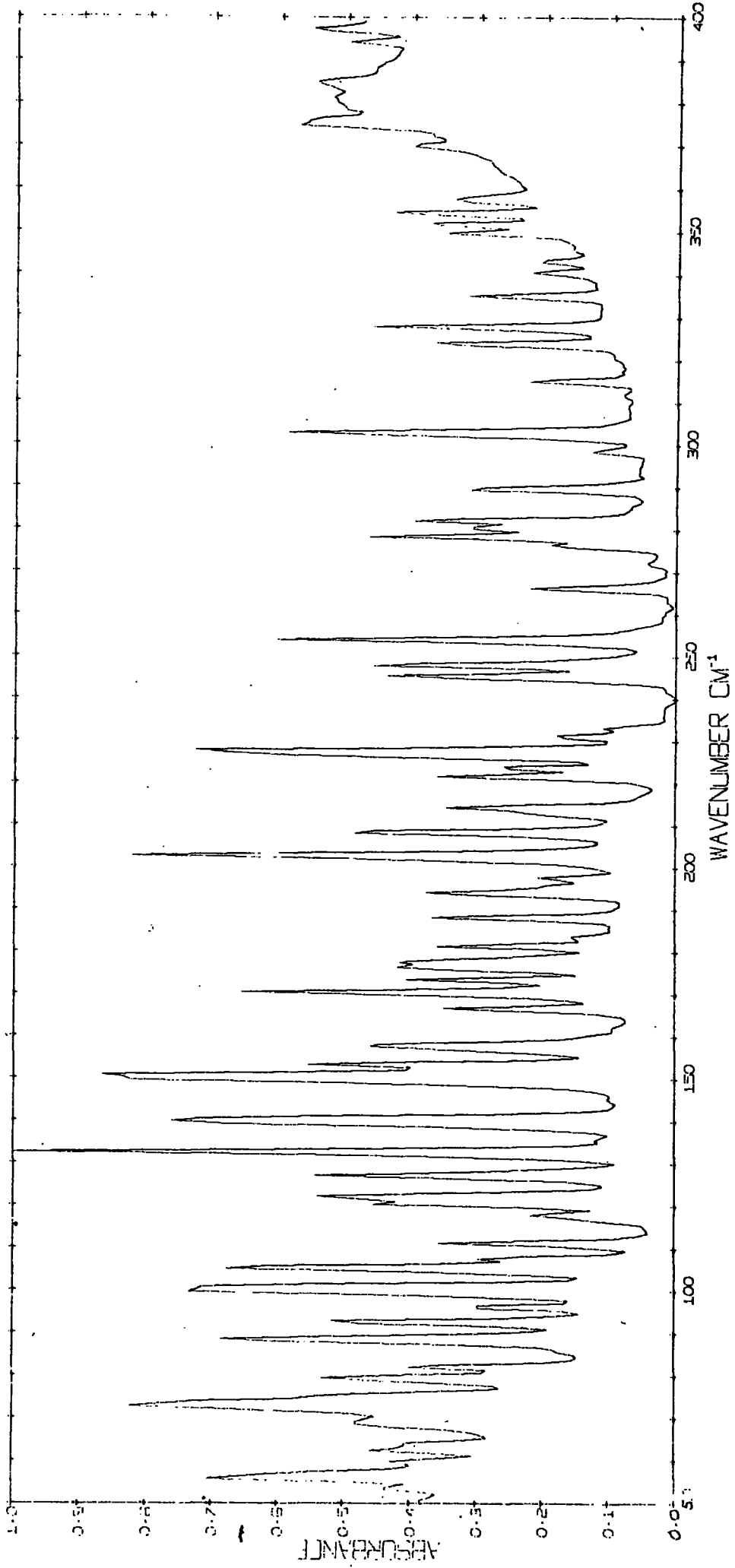
WATER VAPOUR 1024 POINT ANALYSIS



WAVENUMBER CM<sup>-1</sup>

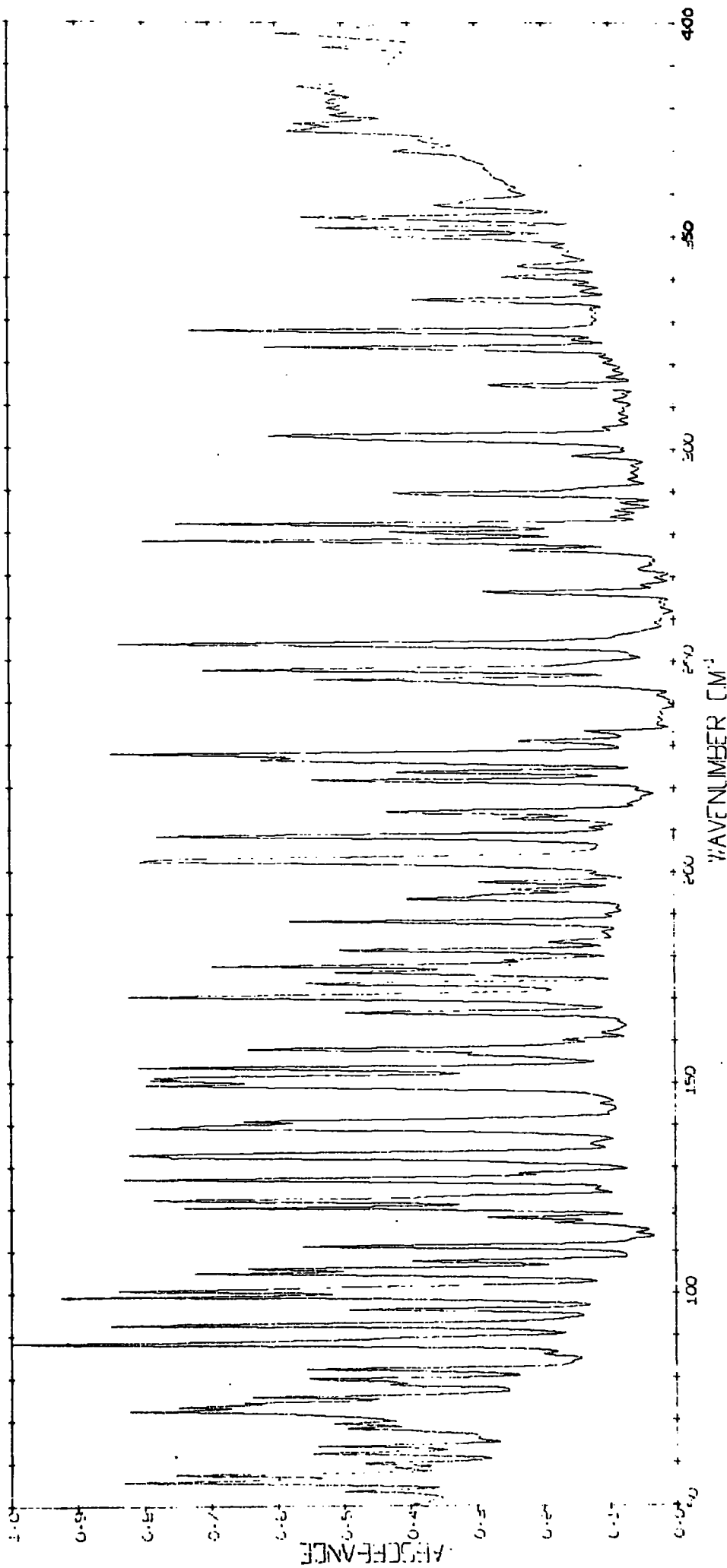
Spectrum 8.3

WATER VAPOUR 2048 POINT ANALYSIS



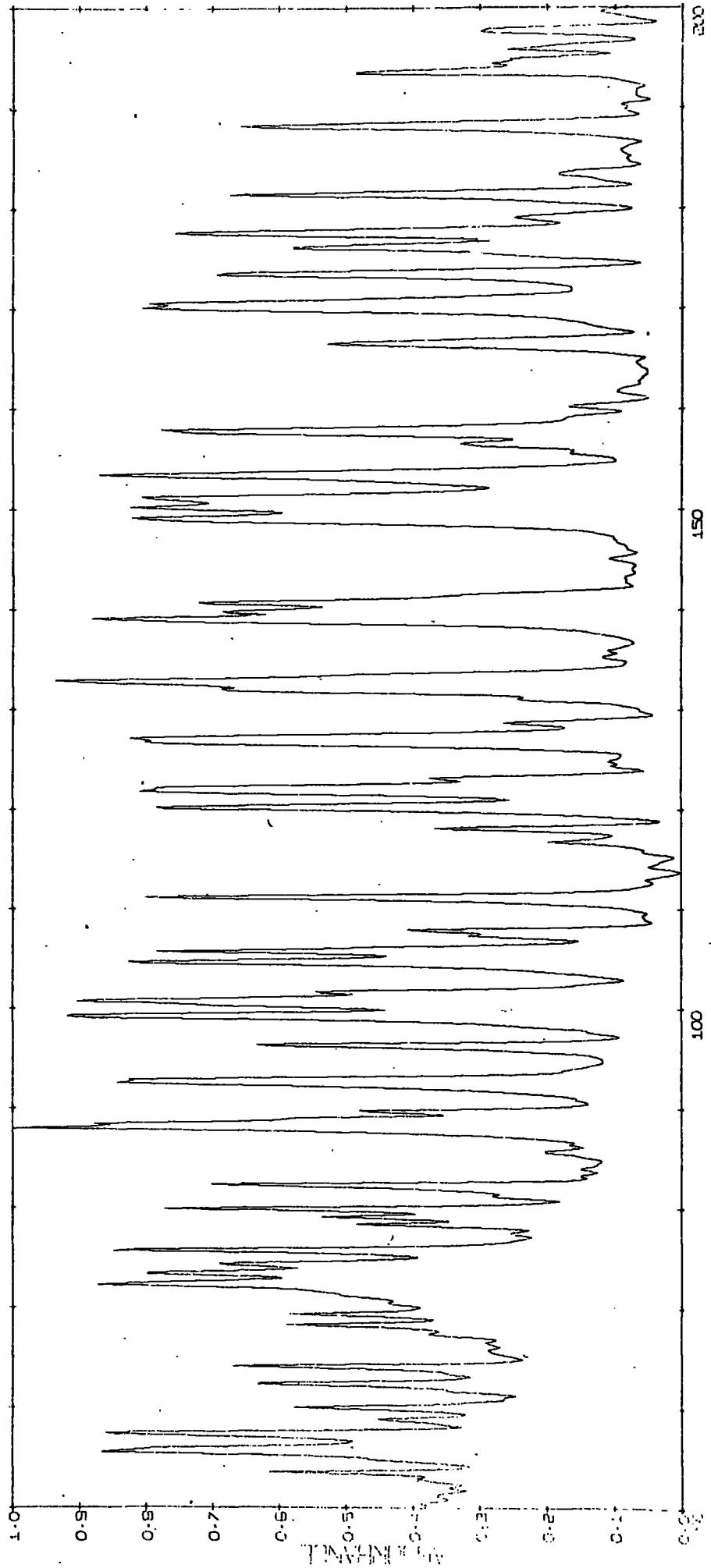
Spectrum 8.4

WATER VAPOUR 4096 POINT ANALYSIS



Spectrum 8.5

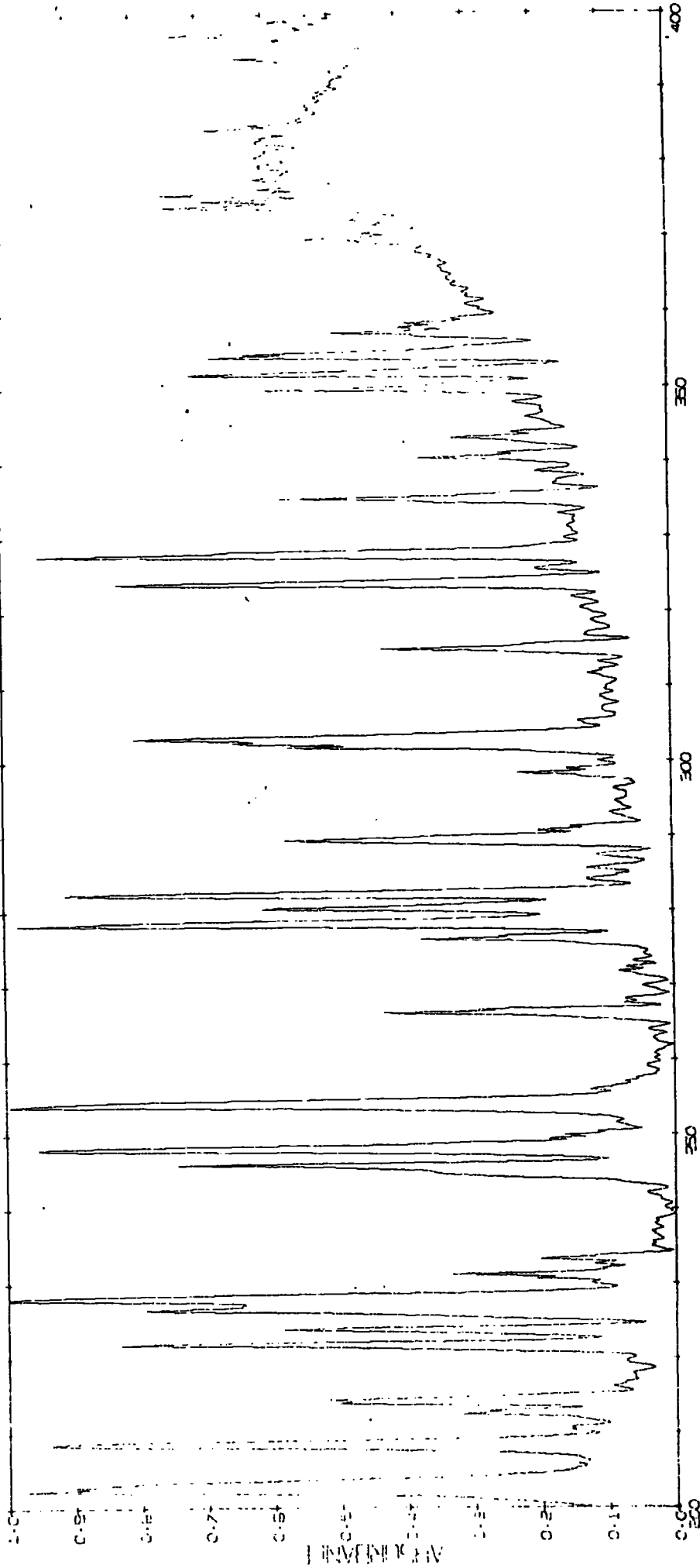
WATER VAPOUR, 8192 POINT ANALYSIS



WAVENUMBER CM<sup>-1</sup>

Spectrum 8.6A

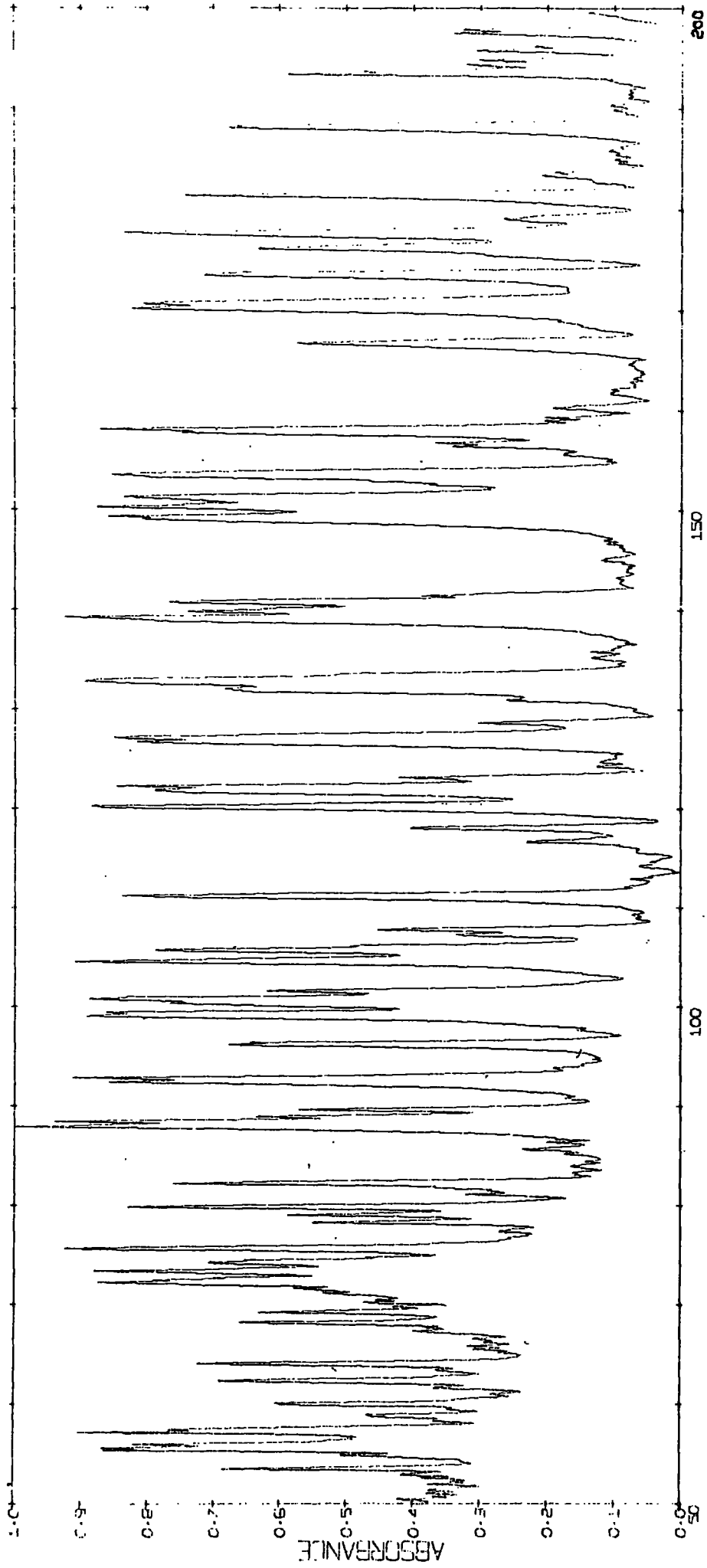
WATER VAPOUR, 8192 POINT ANALYSIS



WAVENUMBER CM<sup>-1</sup>

Spectrum 8.6B

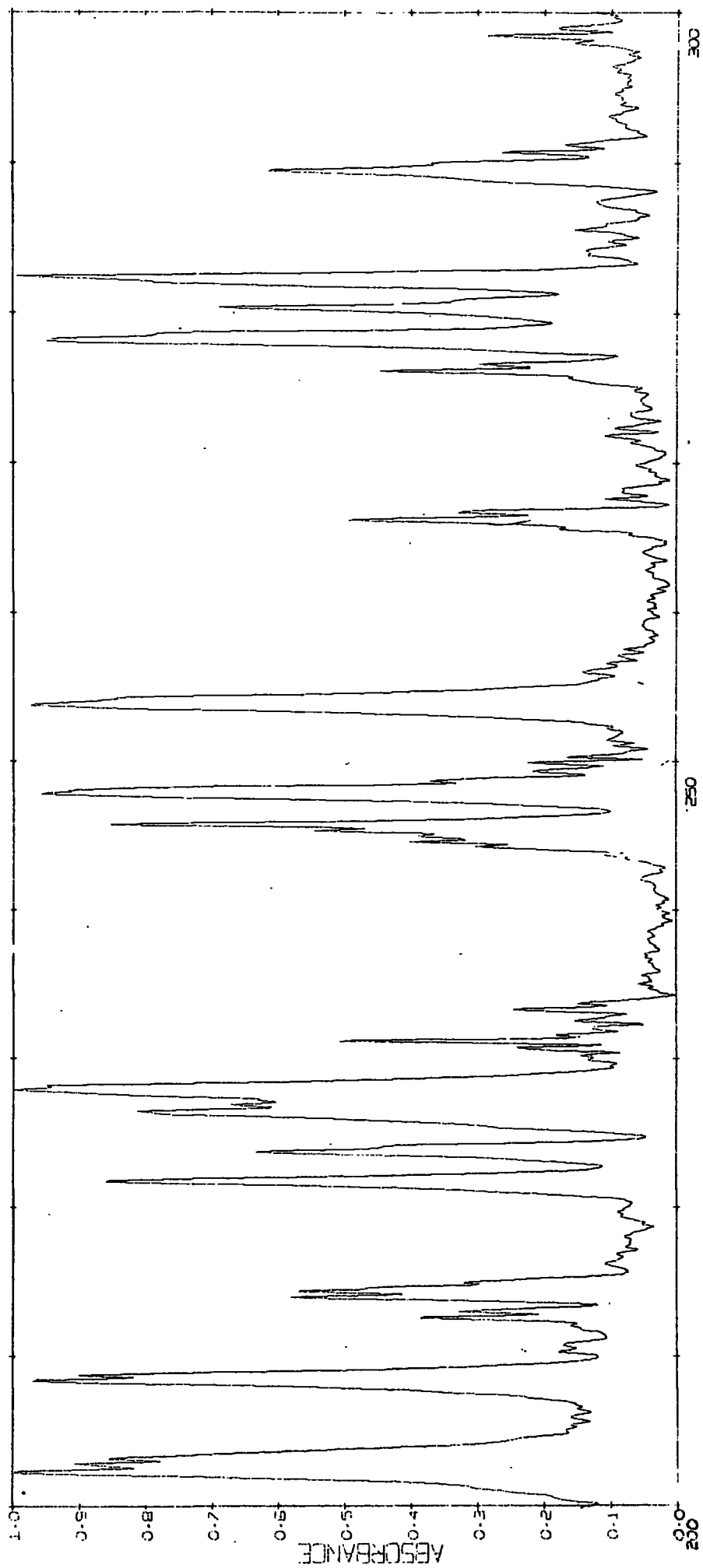
WATER VAPOUR 16384 POINT ANALYSIS



WAVENUMBER  $CM^{-1}$

Spectrum 8.7A

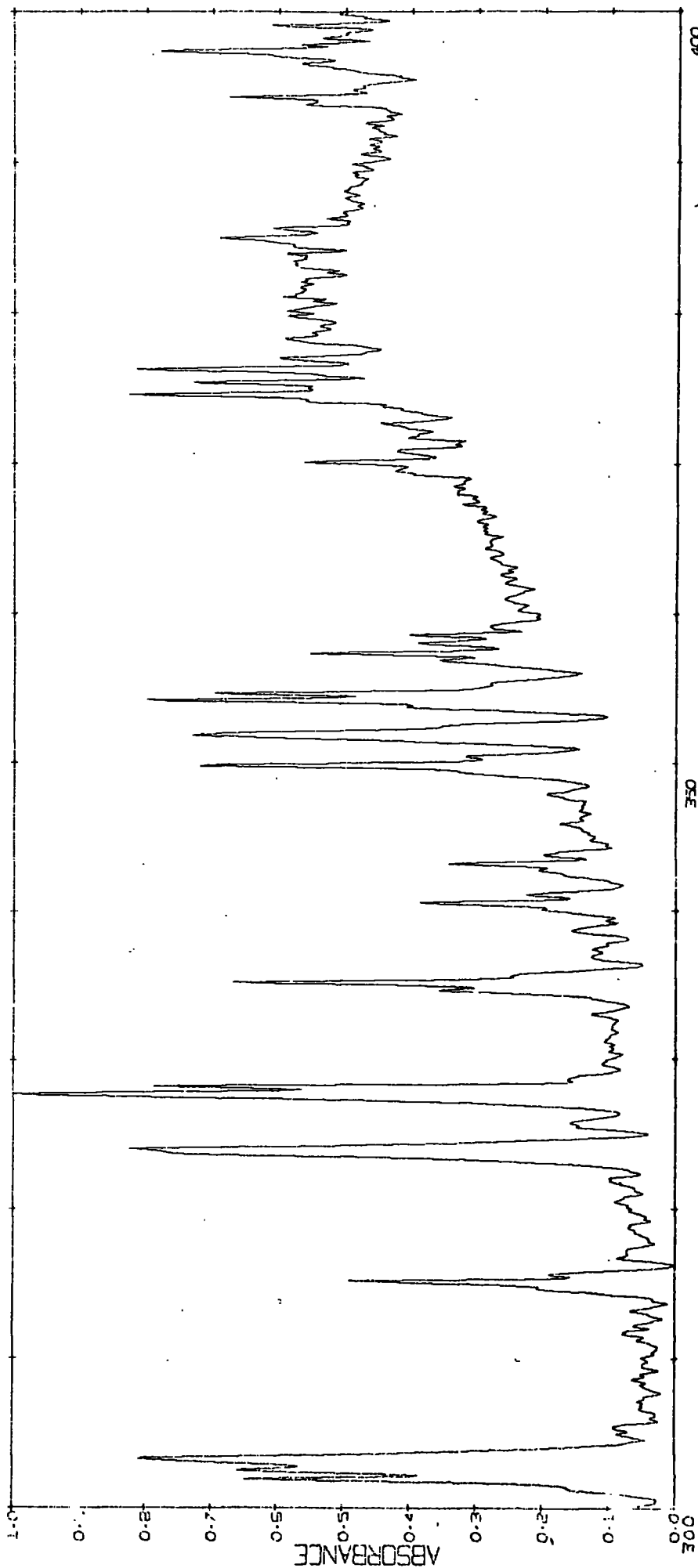
WATER VAPOUR 16384 POINT ANALYSIS



WAVENUMBER CM<sup>-1</sup>

Spectrum 8.7B

WATER VAPOUR 16384 POINT ANALYSIS



WAVENUMBER CM<sup>-1</sup>

Spectrum 8.7C

Table 8.3Observed Resolution Values for Water Vapour

Number of data sets	Resolution $\text{cm}^{-1}$
512	5.0
1024	3.0-4.0
2048	2.0
4096	1.5
8192	0.95
16384	0.55

Typical spectra recorded for the instrumental background and for water vapour are shown in spectra 8.1 and 8.2-8.7 respectively.

#### 8.2.2. Metal carbonyl halides

Tetracarbonyl iron(II) dibromide and tetracarbonyl iron(II) diiodide are known to have a cis configuration (138-141) when freshly prepared. In the presence of sunlight however the cis form of the compound is converted into the trans isomer (142-144). The infrared spectra of these compounds has been reported by Clark and Crosse (145) in the 205-70  $\text{cm}^{-1}$  region and these results have been confirmed. The Fe-Br stretching region showed a complex band which can be assigned as follows:

The bands at 242 and 239  $\text{cm}^{-1}$  are due to the asymmetric Fe-Br stretching mode and are split due to the two isotopes of bromine. Bands at 220 and 217  $\text{cm}^{-1}$  are due to the symmetrical Fe-Br stretching mode and again the splitting arises from the two isotopes of bromine present. Calculated splitting for the two isotopes are 2.4 and 2.2  $\text{cm}^{-1}$  respectively.

The bands at 206 and 198  $\text{cm}^{-1}$  are both too intense and too far apart to be due to isotopic effects and are probably due to solid state effects.

For the case of the tetracarbonyl iron di-iodide only two absorption bands are observed in the Fe-I stretching region and can be assigned to the asymmetric and symmetric Fe-I stretching modes (200 and 186  $\text{cm}^{-1}$  respectively). Absorption bands in the 100-120  $\text{cm}^{-1}$  region in these compounds are assigned as  $\delta(\text{CFeC})$  modes. An absorption at 87 and 60  $\text{cm}^{-1}$  has tentatively been assigned as a  $\delta(\text{CFeX})$  mode in the tetracarbonyl iron dibromide and tetracarbonyl iron di-iodide respectively. The  $\delta(\text{CReI})$  mode has previously been assigned to an absorption band at 42  $\text{cm}^{-1}$  observed in pentacarbonyl rhenium iodide (146). The infrared spectra of tetracarbonyl iron dibromide and tetracarbonyl iron di-iodide are shown in spectra 8.8 and 8.9 respectively and are tabulated together with other iron carbonyl halide spectra in Table 8.4.

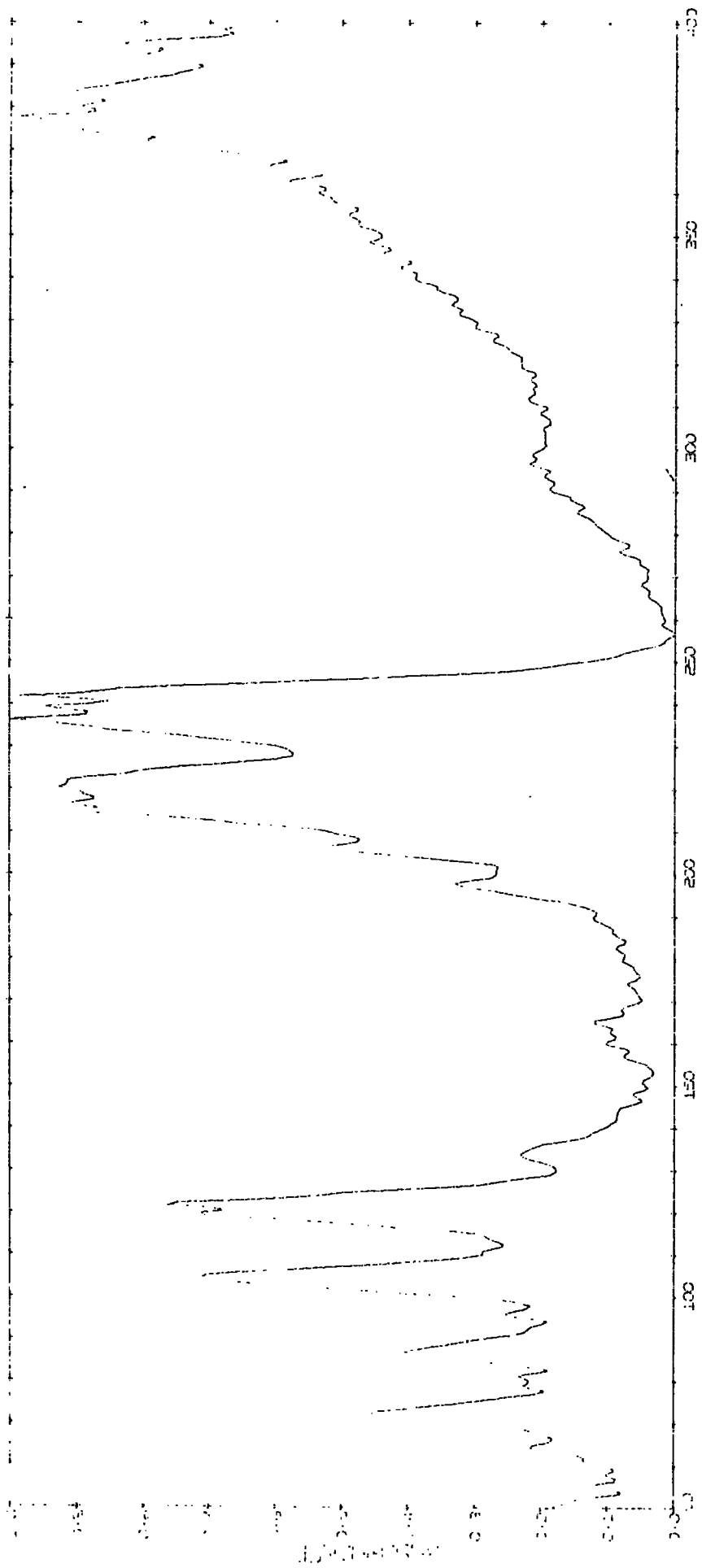
$\pi$ -cyclopentadienyldicarbonyl iron halides (halide = chloride, bromide and iodide) show absorption bands at 302, 233 and 203  $\text{cm}^{-1}$  respectively which are assigned to a Fe-X stretching mode. Confirmation of the assignments in the case of the chloride and bromide came from the observation of isotopic splitting of the  $\nu$  Fe-X modes due to the two isotopes of the halogens present ( $\text{Cl}^{35}$ ,  $\text{Cl}^{37}$  and  $\text{Br}^{79}$ ,  $\text{Br}^{81}$ ). The expected isotopic splittings for chlorine and bromine in these complexes were calculated to be 7.0  $\text{cm}^{-1}$  and 2.4  $\text{cm}^{-1}$  respectively. Any absorptions in the 100-120  $\text{cm}^{-1}$  were thought to be  $\delta(\text{CFeC})$  modes. No  $\delta(\text{ring FeC})$ ,  $\delta(\text{ring FeX})$  or  $\delta(\text{CFeX})$  modes could be assigned to any absorptions observed. The spectra of the  $\pi$ -cyclopentadienyldicarbonyl iron halides (halide = chloride, bromide and iodide) are shown in spectra 8.10-8.12 respectively.

Table 8.4

Infrared Spectra of some Halogen containing Iron Carbonyl Compounds in the 400-50  $\text{cm}^{-1}$  region

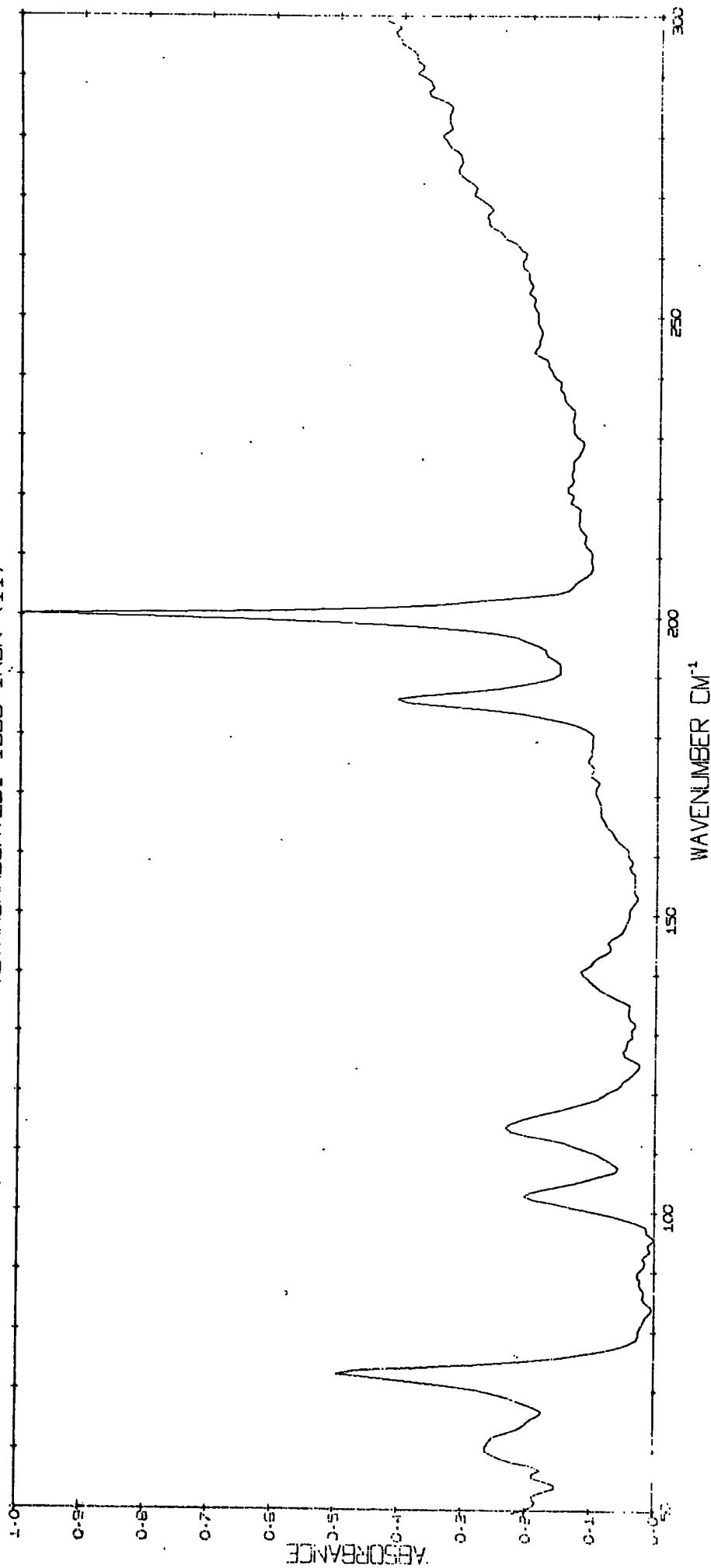
Assignment	$\text{Fe}(\text{CO})_4\text{Br}_2$	$\text{Fe}(\text{CO})_4\text{I}_2$	$(\pi\text{-C}_5\text{H}_5)\text{Fe}(\text{CO})_2\text{Cl}$	$(\pi\text{-C}_5\text{H}_5)\text{Fe}(\text{CO})_2\text{Br}$	$(\pi\text{-C}_5\text{H}_5)\text{Fe}(\text{CO})_2\text{I}$	$[(\pi\text{-C}_5\text{H}_5)\text{Fe}(\text{CO})_2\text{Cl}]_2\text{PF}_6^-$	$[(\pi\text{-C}_5\text{H}_5)\text{Fe}(\text{CO})_2\text{Br}]_2\text{PF}_6^-$	$[(\pi\text{-C}_5\text{H}_5)\text{Fe}(\text{CO})_2\text{I}]_2\text{PF}_6^-$
Fe-C	388m 380m	395m	375w 353m	378w 353m 300vw	365msh 360s	389m 382m 353ms	390w 380m 350ms 311vw	385s 363s 313w
Fe-X	242s 239s 220s 217sh 206m 198w	200s 186m	302s 298sh	233s 231sh	203s	319s 313sh	231s	206w
$\delta(\text{CFeC})$	120s 104s	114m 103m	162s	142s	152m 132ms	252m 183m 136w ?	207m 157m	195m 156m 146s 128m
$\delta(\text{CFeX}) ?$	87m	60w		118w	118s		115w	

TETRACARBONYLIRON IRON (II)



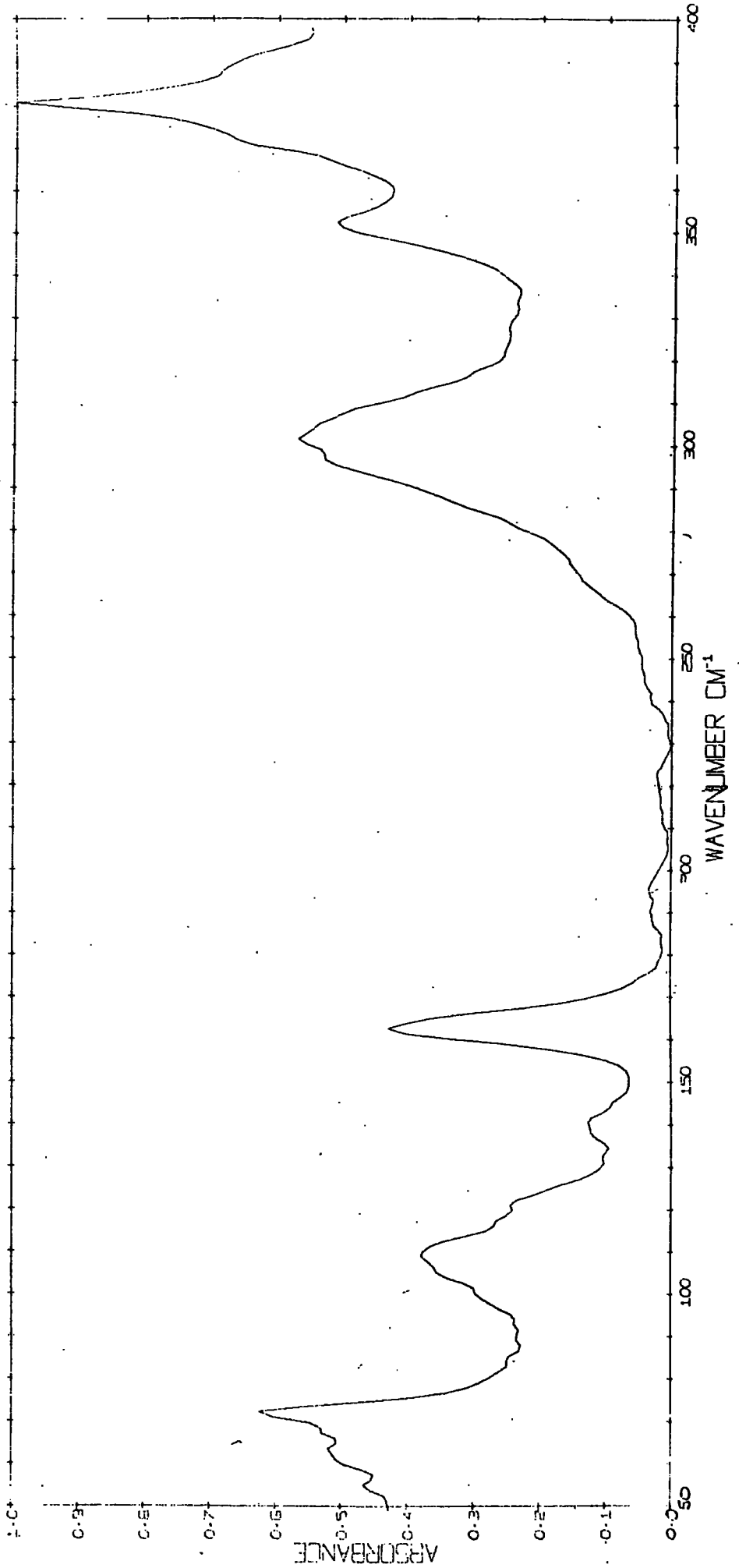
WAVENUMBER CM⁻¹  
Spectrum 8.8

TETRACARBONYLDI-1000 IRON (II)



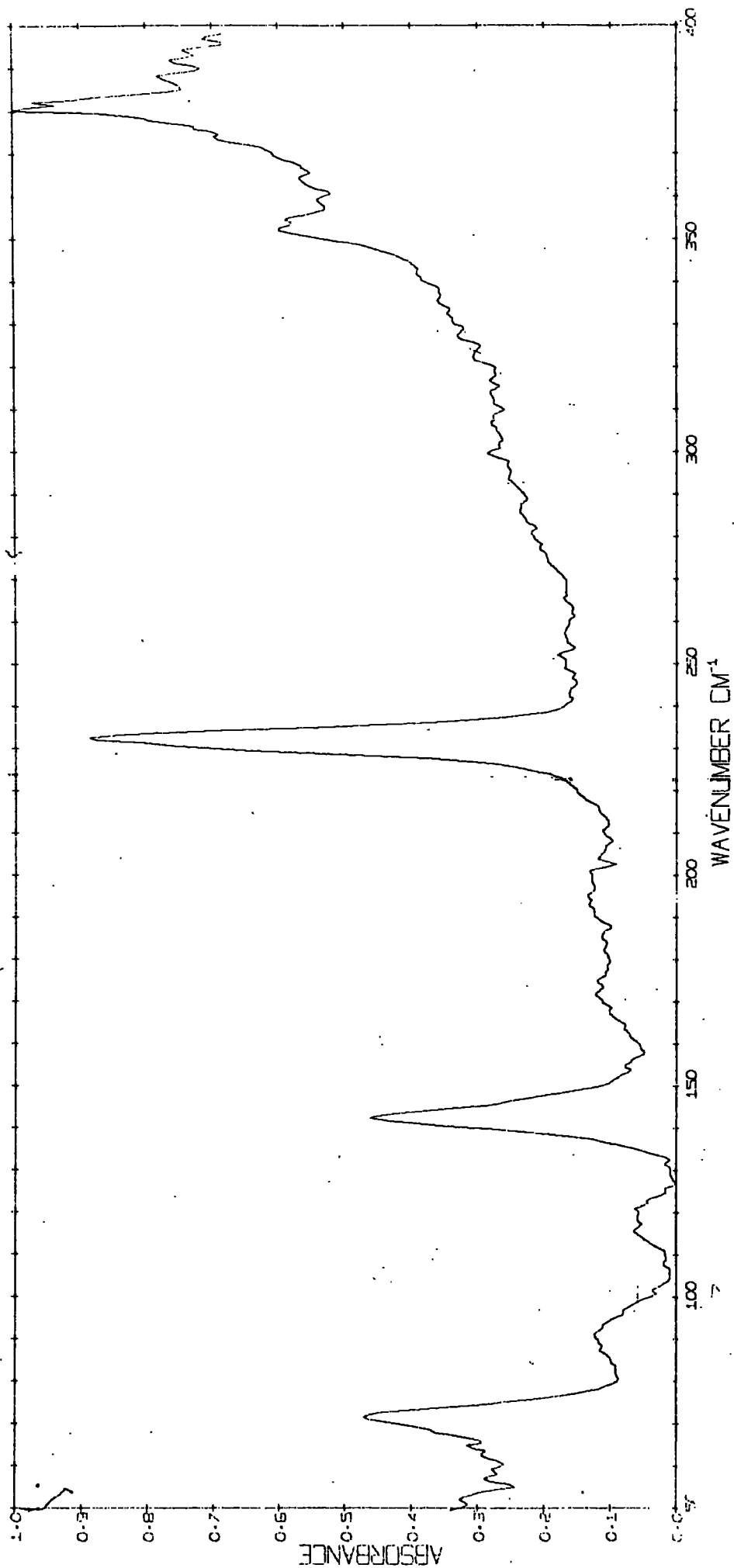
Spectrum 8.9

CYCLOPENTAADIENYL DICARBONYL IRON(II) CHLORIDE



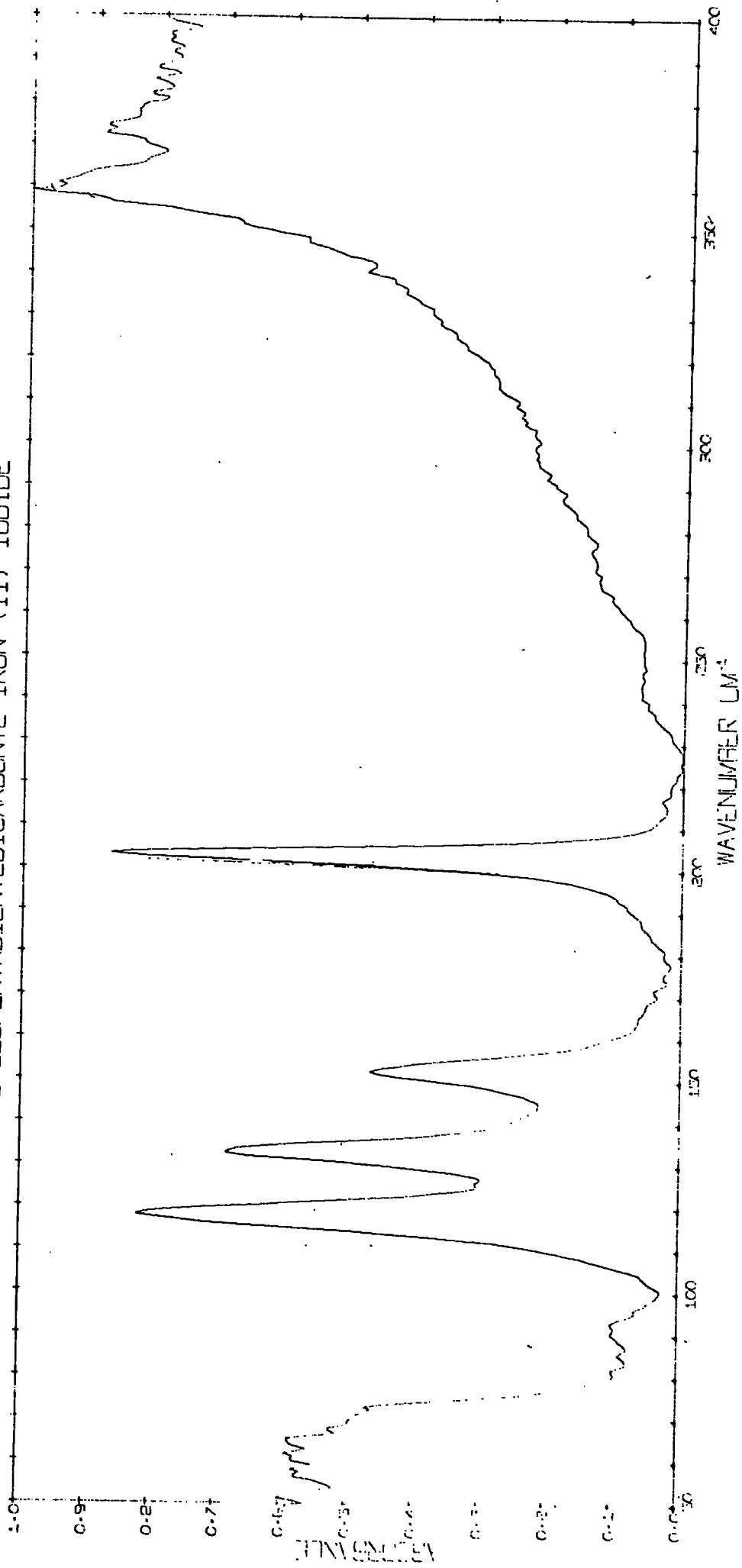
Spectrum 8.10

CYCLOPENTADIENYL DICARBONYL IRON (II) BROMIDE

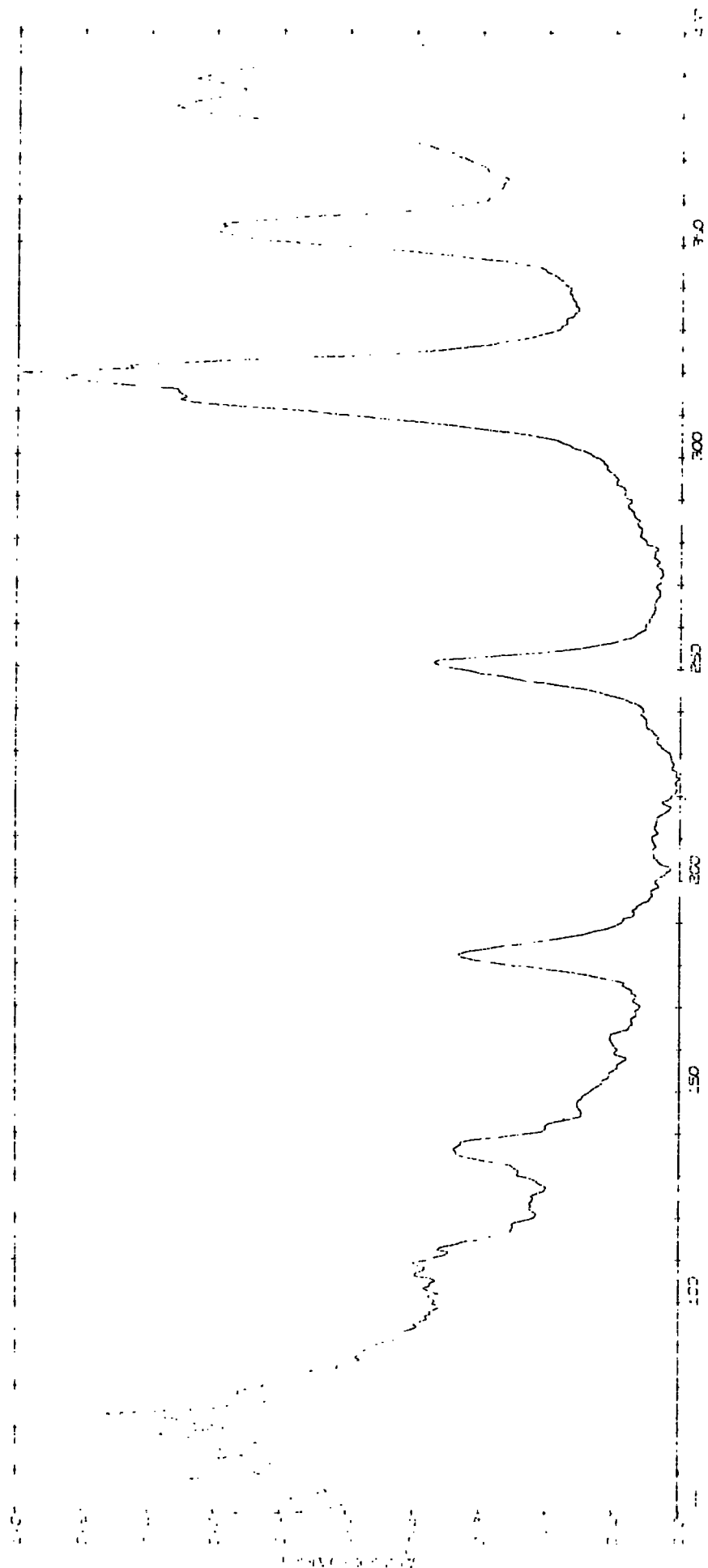


Spectra 8.11

CYCLOPENTADIENYL CARBONYL IRON (II) IODIDE



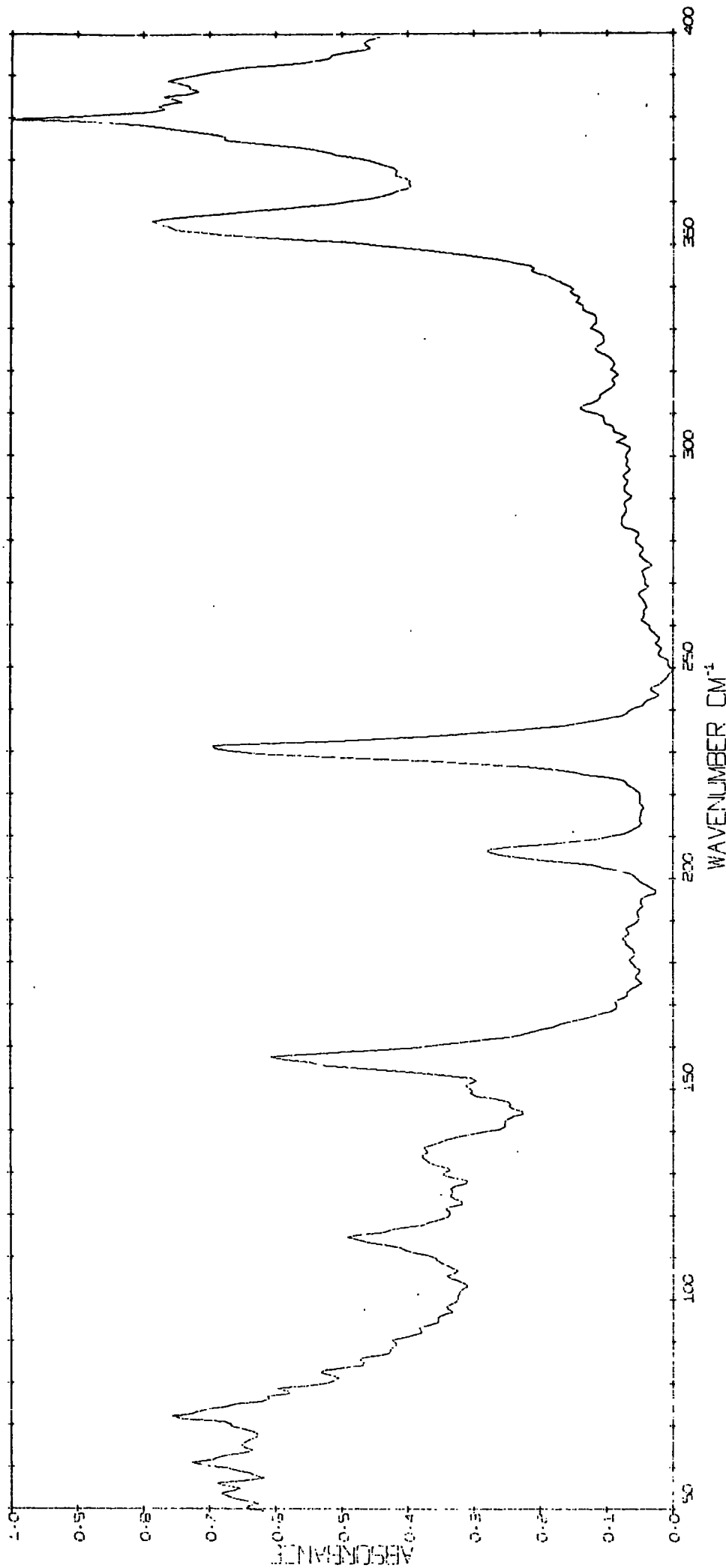
(CF<sub>3</sub>)<sub>2</sub>CO<sub>2</sub>Cl PFG



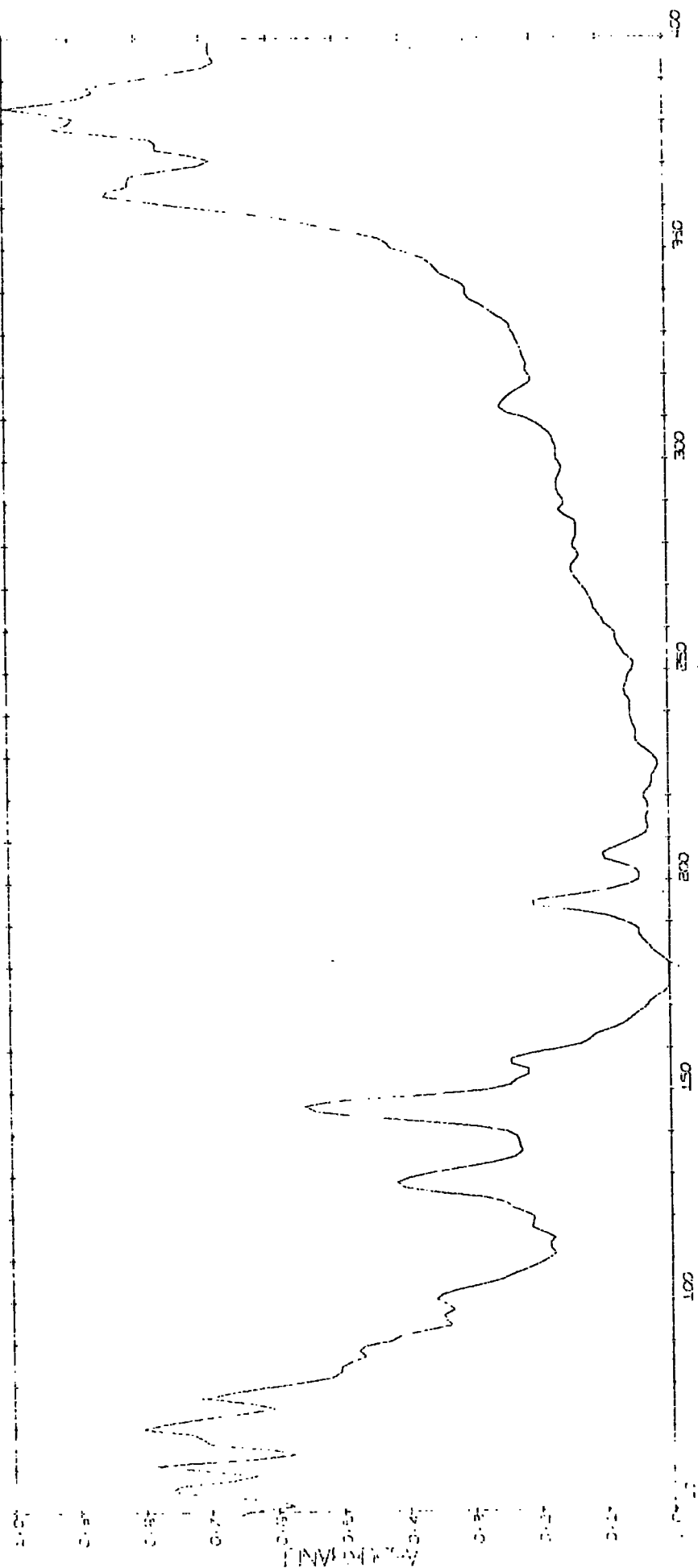
WAVENUMBER CM<sup>-1</sup>

Spectrum 8.13

( C P F E ( C O ) 2 ) 2 B R P F 6



(CPFE (CO)E )2 I PF6



WAVENUMBER CM<sup>-1</sup>

Spectrum 8.15

The infrared spectra of the  $\pi$ -cyclopentadienyldicarbonyl iron- $\mu$ -halogeno  $\pi$ -cyclopentadienyldicarbonyl iron hexafluorophosphates (halogeno = chloro, bromo and iodo) are shown in spectra 8.13-8.15 respectively.

The asymmetric stretching mode of the Fe-X-Fe (X = Cl, Br and I) has been assigned partly on the intensity of absorptions and partly on the expected change in frequency on going from chlorine to iodine. If the Fe-X-Fe is non linear both the asymmetric and symmetric vibrations would be infrared active. The infrared spectra below  $250\text{ cm}^{-1}$  of these bridged complexes was much more complicated than the parent  $\pi$ -cyclopentadienyldicarbonyl iron(II) halides (halide = chloride, bromide and iodide). The absorptions below  $120\text{ cm}^{-1}$  were much more intense in the hexafluorophosphate salts and this was thought to contain the lattice modes. Attempts to obtain high resolution spectra in order that the isotopic splitting of the absorption bands involving chlorine or bromine were unsuccessful. The bands which are expected to be observed below  $260\text{ cm}^{-1}$  are the symmetrical stretch of Fe-X-Fe (if it is infrared active) and such modes as  $\delta(\text{ring FeC})$ ,  $\delta(\text{CFeC})$ ,  $\delta(\text{ring FeX})$  and  $\delta(\text{CFeX})$ . The  $\delta(\text{ring Fe ring})$  mode of ferrocene has been assigned at  $170\text{ cm}^{-1}$  (147) but no modes clearly of the  $\delta(\text{ring FeC})$  type could be observed in bis( $\pi$ -cyclopentadienyldicarbonyl iron(I)).

### 8.2.3. $\pi$ -cyclopentadienylcarbonyl iron complexes

The infrared absorption bands of some  $\pi$ -cyclopentadienylcarbonyl iron complexes are given in Table 8.5. The absorption bands in the  $350\text{-}400\text{ cm}^{-1}$  region are almost certainly  $\nu\text{Fe-C}$  stretching modes. The absorption bands at  $155\text{-}137\text{ cm}^{-1}$  may be due to some form of wagging mode ( $\delta$ ) but it is not clear whether they are  $\delta(\text{CFeC})$  or  $\delta(\text{ring FeC})$  or both modes. A large number of rather broad absorptions occur in the

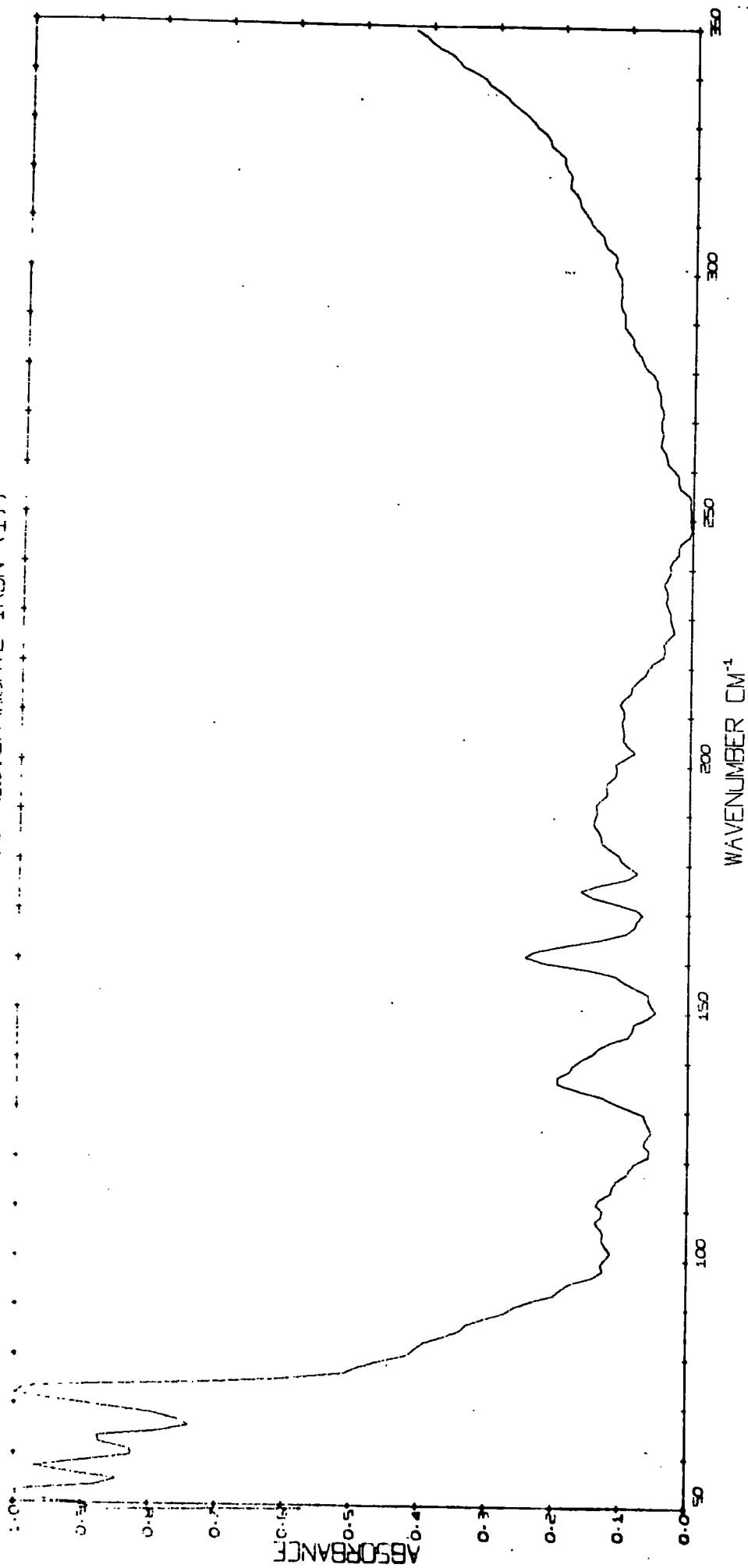
heptaiodide and tribromide salts of the tetrakis( $\pi$ -cyclopentadienylcarbonyl iron) cation which are assumed to be associated with the anion as no absorptions in these regions occur in the hexafluorophosphate salt. Spectra of the compounds are shown in spectra 8.16-8.20.

Table 8.5  
 Infrared Spectra of some  $\pi$ -Cyclopentadienylcarbonyl iron Complexes in the 50-400  $\text{cm}^{-1}$  region

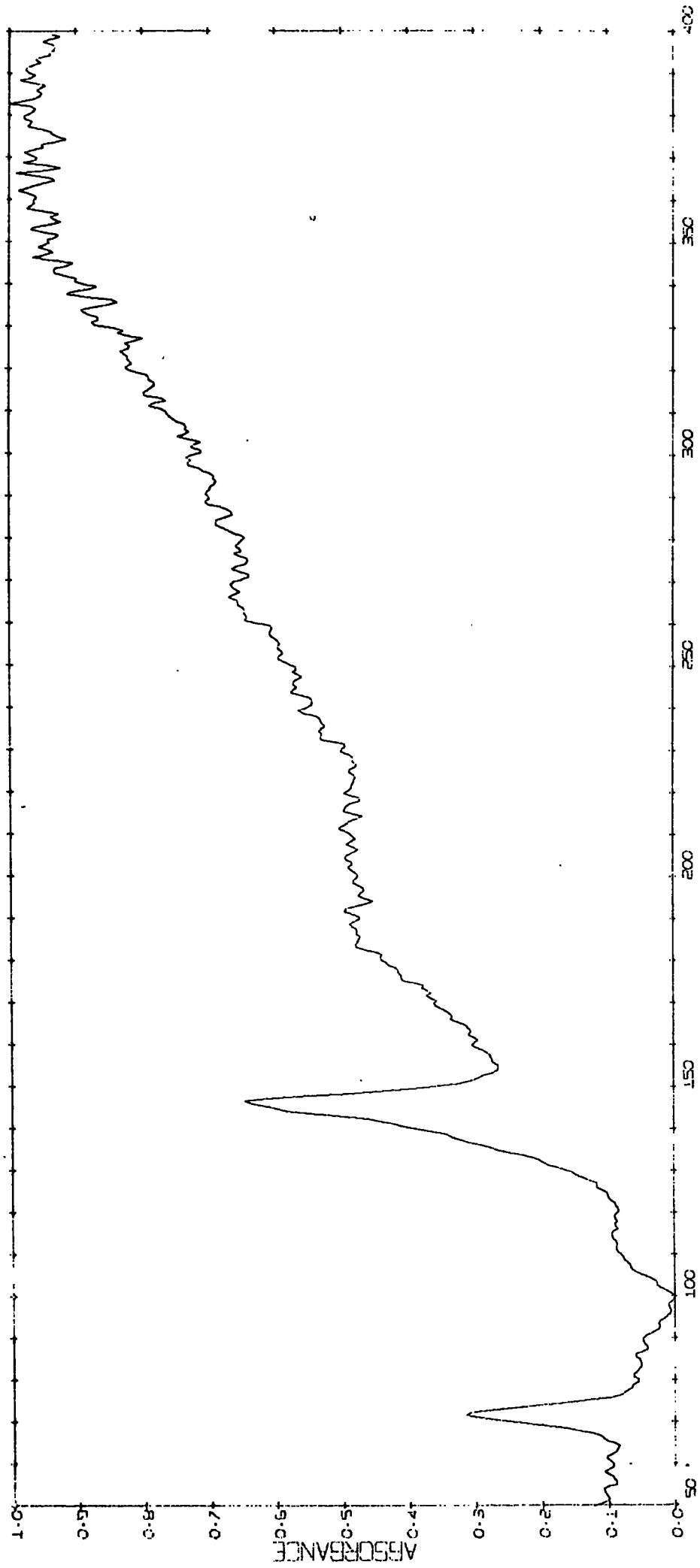
Assignment	$[\text{CpFe}(\text{CO})_2]_2$	$[\text{CpFe}(\text{CO})]_4$	$[\text{CpFe}(\text{CO})]_4^+ \text{PF}_6^-$	$[\text{CpFe}(\text{CO})]_4^+ \text{I}_7^-$	$[\text{CpFe}(\text{CO})]_4^+ \text{Br}_3^-$
Fe-C	389m 350s	356s	361s	358s	360s
$\text{I}_7^-$ modes ?				209bw 188bw 175w 161w	
$\text{Br}_3^-$ modes ?	154w 137w	146m 143sh	138m	136w	192wsh 170ssh 162s 153ssh 145sh 136msh

Spectrum Number 8.16

BIS(CYCLOPENTADIENYL)DICARBONYL IRON (1)

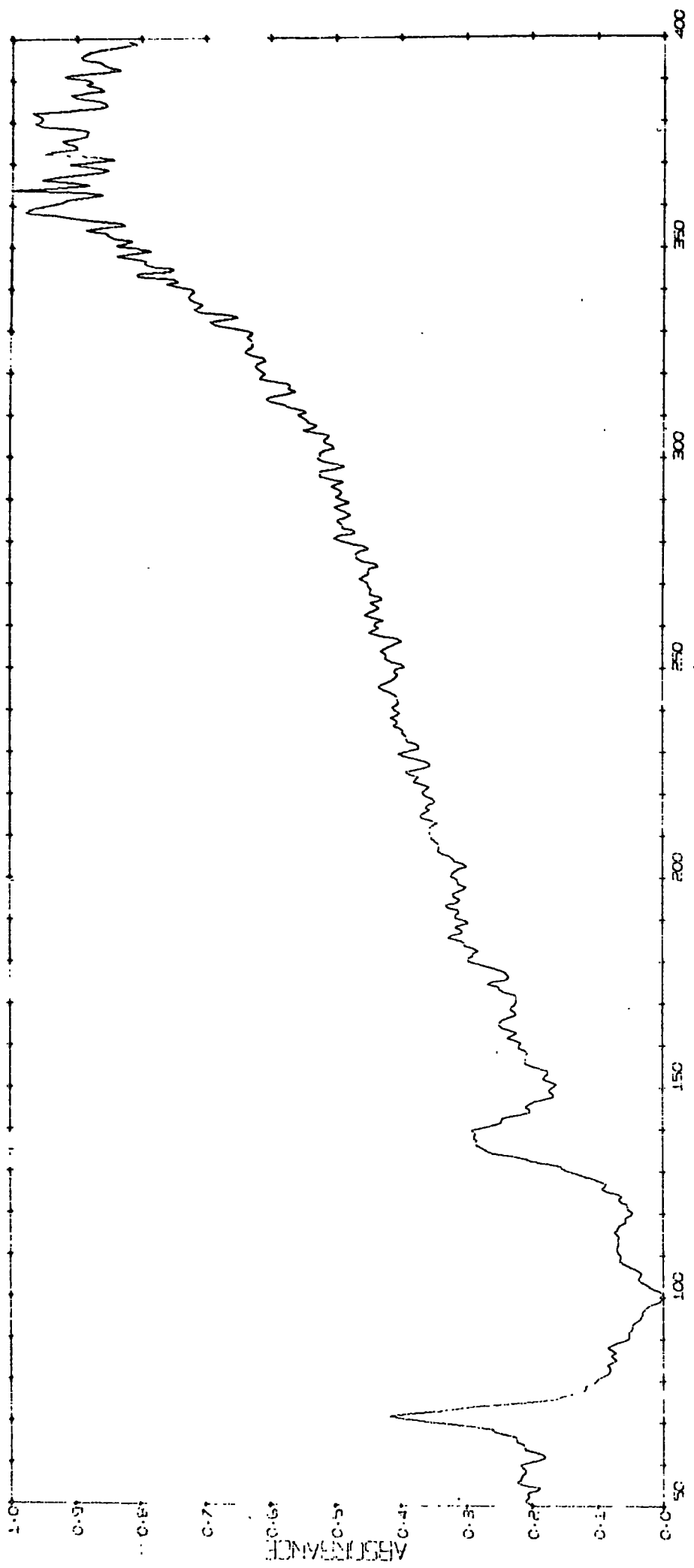


( CP FE (CO) ) 4



Spectrum 8.17

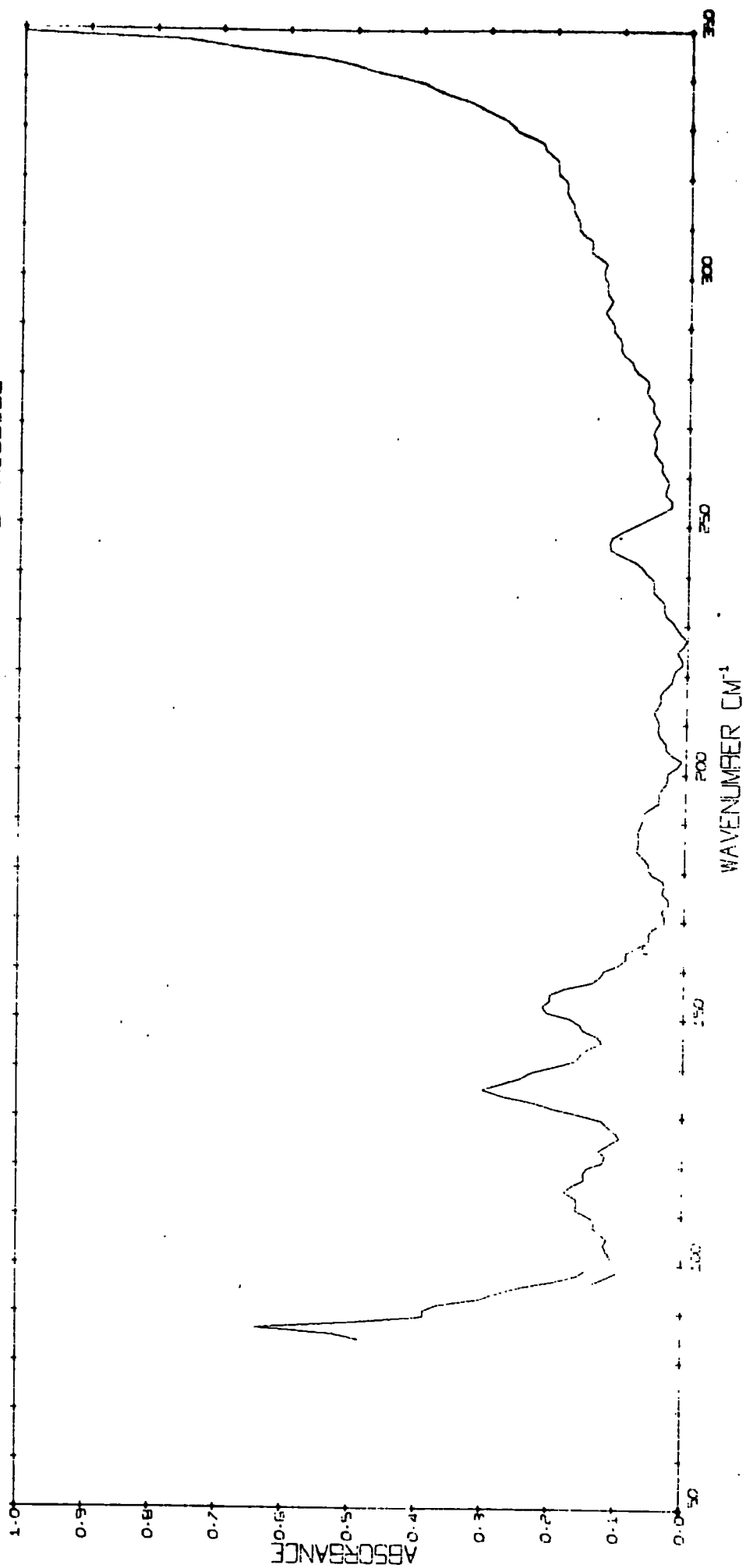
( CP FE (CO) ) 4 PF6



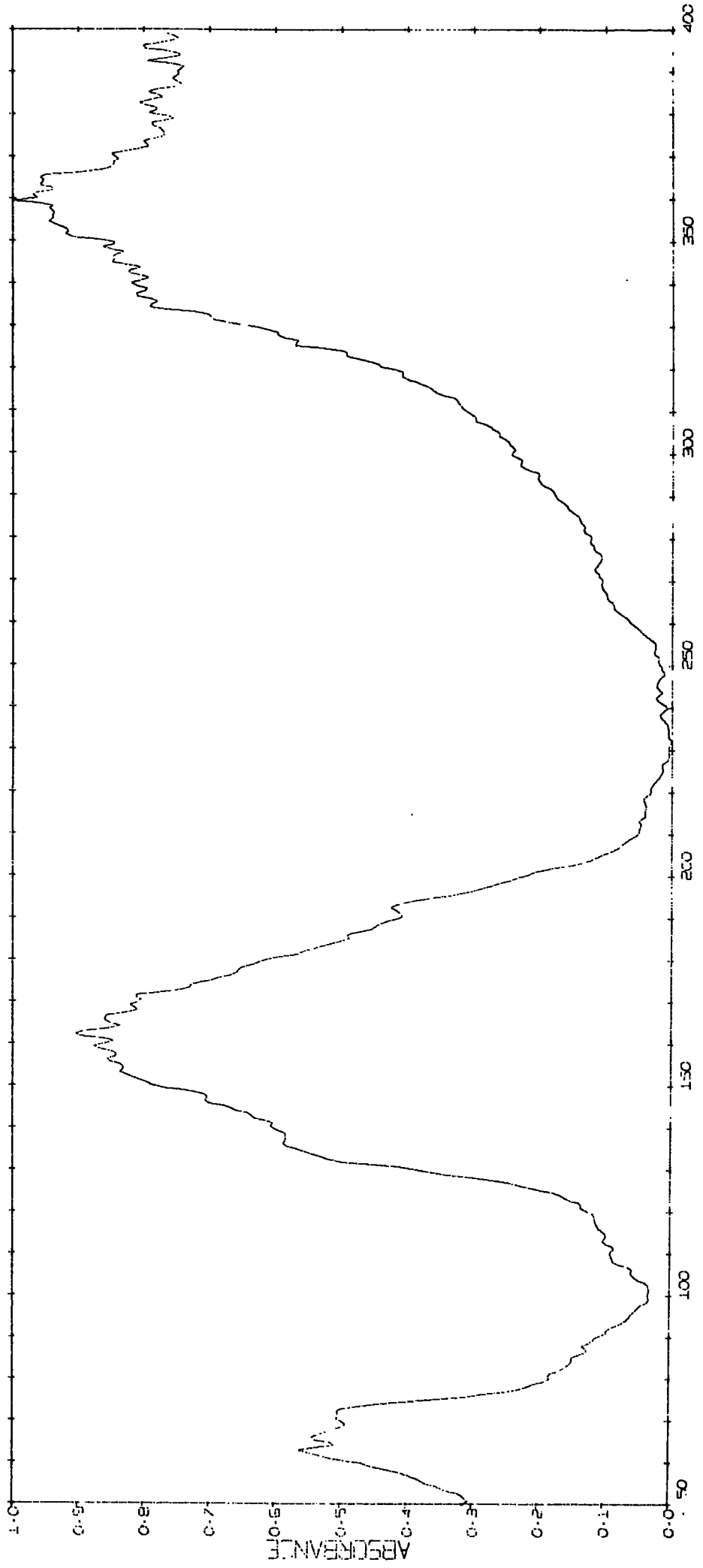
Spectrum 8.18

Spectrum Number 8.19

TETRAKIS(CYCLOPENTADIENYL CARBONYL IRON) HEPTAIOXIDE



( CP FE (CO) ) 4 BR3



WAVENUMBER CM⁻¹

Spectrum 8.20

## CHAPTER 9

### CONCLUSIONS AND FUTURE WORK

#### 9.1 Acid-Base Reactions

The work on the protonation reactions described in this thesis has shown that  $\pi$ -cyclopentadienylcarbonyl iron complexes can be protonated in hydrogen chloride at low temperatures. The course of the reaction could be followed conductimetrically when boron trichloride was used as the acid. Due to the low solubility of the materials at low solubility of the materials at low temperatures conductimetric techniques are limited.

The fact that solid products could be isolated showed that hydrogen chloride has a major advantage over sulphuric acid systems.

The range of compounds examined was very limited but many other complexes could be examined, especially using liquid hydrogen chloride at room temperature to enhance solubility.

If conductimetric techniques could be developed which enabled them to be carried out at room temperature, conductimetric techniques might be more useful. One inherent problem is that these materials tend to give side reactions which would probably be enhanced at room temperature. Techniques for the purification of reaction products are very limited and this may restrict the work somewhat.

The failure of  $\pi$ -cyclopentadienyldicarbonyl iron(II) bromide and  $\pi$ -cyclopentadienyldicarbonyl iron(II) iodide to act as bases in the solvent with boron trichloride may be overcome by using the corresponding hydrogen halide and boron trihalide.

The current trend for research in non-aqueous solvents is to exploit their preparative characteristics. The value of hydrogen chloride as an

acidic medium may be extended if a aprotic solvent (such as hexane, methylene chloride or sulphur dioxide) was used to dissolve the material under investigation and hydrogen chloride used as a reagent rather than the solvent. This might also limit side reactions and assist in obtaining pure products, and enable information to be obtained from conductimetric studies once more.

### 9.2. Oxidation Reactions

The majority of the oxidation studies in the solvent were carried out using chlorine. This proved to attack the rings and cause extensive decomposition of the complexes. A more gentle oxidant would be perhaps more useful when examining these materials.

A technique that has never been attempted but which may provide the answer is to use electrochemical techniques and control the applied potentials. If compounds were studied which did not contain a readily oxidised organic ligand information about oxidation of the metal complexes may be more readily available.

Very little work on oxidations has been carried out in the solvent and the field is little understood and warrants further investigation

### 9.3. Structure of the $\pi$ -cyclopentadienyldicarbonyl iron- $\mu$ halogeno- $\pi$ -cyclopentadienyldicarbonyl iron cations

All of the spectroscopic techniques used to examine the structure of these cations indicate a centrosymmetric structure with the halogen midway between the two iron atoms, and that each  $\pi$ -cyclopentadienyldicarbonyl iron unit is identical. Since a compound with a bridging atom placed nearer to one iron atom than the other iron atom was not available there is a possibility that the techniques are not sufficiently sensitive to slight changes in the position of the halogen atom.

To remove this element of doubt the structure of the  $\pi$ -cyclopentadienyl-dicarbonyl iron- $\mu$ -bromo  $\pi$ -cyclopentadienyldicarbonyl iron hexafluorophosphate is now being carried out in conjunction with Dr. N. Alcock at Warwick University, using X-ray crystallography. This technique will also in addition to giving the stereochemistry and dimensions of the Fe-Br-Fe system give information about whether the two  $\pi$ -cyclopentadienyldicarbonyl iron units are related by cis or trans isomerism. In solution there may be an equilibrium between the two forms but the most energetically favourable isomer probably crystallises out.

#### 9.4. Techniques Available

##### 9.4.1. Infrared Spectroscopy

This proved to be the most valuable spectroscopic technique available for the examination of the products obtained. With the advent of fourier transform spectrophotometers the range of routinely available instruments has been extended down to  $10\text{-}20\text{ cm}^{-1}$ . The time scale of infrared spectroscopy is about  $10^{-12}$  seconds so that if the bridging atom is vibrating at this sort of rate between the two iron atoms it will appear to be midway between the iron atoms. If the bridging atom is attached to one of the iron atoms longer than the time of a vibration then two different  $\pi$ -cyclopentadienyl-dicarbonyl iron units should be observable. The running of spectra at liquid nitrogen temperatures would help reduce hot bands and assist in the achievement of higher resolution spectra in the far infrared. The computation of the power spectrum from the interferogram is a fairly sophisticated piece of programming and at this stage is still fairly well in its infancy. The development of quicker, more accurate and satisfactory programs to overcome the problems of the instrument being a single beam spectrophotometer is still desirable.

#### 9.4.2. <sup>57</sup>Fe Mossbauer and Electron Spectroscopy

Both of these techniques are governed by the Heisenberg Uncertainty Principle, the time scales however are very different. <sup>57</sup>Fe Mossbauer has a time scale of about  $10^{-7}$  seconds whereas electron spectroscopy has a time scale of less than  $10^{-12}$  seconds. Mossbauer spectroscopy is limited to examining the small change in energy levels in a nucleus brought about by changes in the electron populations. Primarily it is changes in S electron density that have greatest effect on Mossbauer parameters. The advantage of Mossbauer studies is that the changes in nuclear energy levels can be measured extremely precisely (approximately to one part in  $10^{12}$ ). Electron spectroscopy has the advantages of a much faster time scale and it is applicable to all elements, however, the measurement of the energy levels are nowhere nearly so precise as those determined by Mossbauer spectroscopy. The application of XPS to low spin complexes is probably the most critical of the technique. This is partly due to the fact that the ligands tend to act as reservoirs of electron density and reduce any changes that occur by spreading the change over the whole molecule. In practice <sup>57</sup>Fe Mossbauer spectroscopy proved to be more sensitive to electron density changes than was XPS. Another problem with XPS is that it is primarily a surface technique and this can lead to results which are atypical from the bulk properties of the material under investigation.

#### 9.4.3. UV/Visible Spectroscopy

In many studies involving reactions of transition metal complexes ultra violet and visible spectroscopy have proved to be a very sensitive method of detecting these reactions. Many of the techniques that are applicable to use in the hydrogen chloride solvent system suffer from the fact that they are not sufficiently sensitive enough. There are practical

difficulties of recording spectra in liquid hydrogen chloride but the author feels that they are not insurmountable.



```

      LOC,CNT=0 ;
L01 : GET EDIT (CARD) (A(80)) ;
      IF SUBSTR(CARD,1,4)='//*P' THEN GO TO L02 ;
      GO TO L01 ;
L02 : GET EDIT (CH(1)) (A(1)) ;
      IF UNSPEC(CH(1))=NULL | CH(1)=BLANK THEN GO TO L02 ;
      ELSE GET EDIT ((CH(I) DO I=2 TO 3)) (2(A(1)));
      CARD=' ' ;
      GO TO L04 ;
L03 : GET EDIT (( CH(I) DO I=1 TO 3)) ( A(1)) ;
L04 : DO I=1 TO 3 ;
      IF UNSPEC(CH(I))=NULL | CH(I)=BLANK THEN GO TO E00 ;
      END ;
      ERR=0 ;
      DO I=1 TO 3 ;
      BT(I)=UNSPEC(CH(I)) ;
      SUBSTR(BT(I),1,2)='00'B ;
      LH(I)=SUBSTR(BT(I),1,4) ;
      RH(I)=SUBSTR(BT(I),5,4) ;
      IF LH(I)≠COMP(I) THEN ERR=1 ;
      END ;
      IF ERR THEN DO ;
      IF LH(3)=COMP(1) THEN DO ;
      CH(1)=CH(3) ;
      GET EDIT((CH(I) DO I=2 TO 3)) (2 A(1)) ;
      GO TO L04 ;

```

```
END ;
ELSE PUT EDIT('ERROR ',(BT(I) DO I=1 TO 3))
(SKIP,A,3 (X(3),B(8))) ;
GO TO L03 ;
END ;
R=RH(1) || RH(2) || RH(3) ;
LOC=LOC+1 ;
PUT STRING (DUM) EDIT (R) (F(4)) ;
SUBSTR(CARD,LOC,4)=DUM ;
LOC=LOC+3 ;
IF LOC=80 THEN DO ;
LOC=0 ; CNT=CNT+1 ;
PUT FILE(CARDS) EDIT(CARD) (A(80)) ;
CARD=' ' ;
END ;
GO TO L03 ;
EQ0 : LOC=LOC+1 ; SUBSTR(CARD,LOC,4)='-999' ;
PUT FILE(CARDS) EDIT(CARD) (A(80)) ;
LOC=0 ; CNT=CNT+1 ;
CARD=' ' ; GET SKIP ;
GO TO L01 ;
L999 : PUT EDIT (CNT,'CARD IMAGES TO FILE CARDS')
(SKIP(2),F(10),A) ;
END YBINDEC ;
```

Fourier Transform Program based on Cooley Tukey Algorithm.

```

C * * * * *
C * * * * *
C * *
C * *   THIS PROGRAM WAS ORIGINALLY SUPPLIED BY * *
C * * DR.J.YARWOOD,BUT HAS SINCE BEEN MODIFIED BY D.A. * *
C * * SYMON. PROGRAM WITH ABSORBANCE OUTPUT,USING A * *
C * * PROCEDURE TO ENSURE THAT THE ARRAYS ARE POSITIVE. * *
C * * SPECTRAL COMPUTATION IS DONE USING COMPLETE * *
C * * AUTOCORRELATION 'SUBDH3' WITH THE COOLEY-TUKEY * *
C * * TRANSFORMATION ROUTINE. * *
C * *
C * * * * *
C * * * * *
      IMPLICIT REAL*4(A-H,O,S,V-Z),INTEGER*4(J-N,P-R,T-U)
      DIMENSION A(8192),C(8192),B(4096),D(4096),F(1),G(1),
1H(50),O(1024),V(11),I(15),ZX(20)

      COMMON A,C,B,D

      COMMON/PUNCH/ NPAIR,XXQ(10)

140 FORMAT(20A4)

101 FORMAT(3I2,3XA4,1XA4)

103 FORMAT(I3,I6)

100 FORMAT(I4,2XF5.2,2XF7.2,2XF7.2,2XI1,2XI1,2XI1,2XI1)

      READ(8,103) NSETS,NEXIT

      IF(NEXIT.NE.081145) GO TO 98

11 IF(NSETS)13,13,12

12 I(7)=0

```

```

      I(9)=0
      NPAIR=0
      READ(8,100) N,FSINT,FREQL,FREQH,IOPUT,NSIG,NOUT,NCARD
C * * * * * * * * * * * * * * * * * * * * * * * * * * * *
C * * * * * * * * * * * * * * * * * * * * * * * * * * * *
C * *
C * * N/2 IS THE NUMBER OF POINTS TO BE TRANSFORMED * *
C * * FSINT IS THE SAMPLING INTERVAL IN MICRONS * *
C * * FREQL IS THE LOWER FREQUENCY LIMIT IN WAVE * *
C * * NUMBERS, FREQH IS THE UPPER FREQUENCY LIMIT IN * *
C * * WAVE NUMBERS. * *
C * * IOPUT IS THE NUMBER OF POINTS PER RESOLUTION, * *
C * * WHICH CAN ONLY BE 1,2,3,4 OR 5. * *
C * * NSIG=2(DOUBLE BEAM),NSIG=1(SINGLE BEAM), * *
C * * NOUT=0(NO LINE PRINTER OUTPUT),NOUT=1(SPECTRUM), * *
C * * NOUT=2(SPECTRUM AND INTERMEDIATE ARRAYS). * *
C * * NCARD=0(NO CARDS),NCARD=1(CARDS SINGLE BEAM), * *
C * * NCARD=2(CARDS DOUBLE BEAM). * *
C * * READS IN DATE (I11 TO I13) AND TAPE REFERENCE * *
C * * NUMBER,ZX IS THE TITLE FOR EACH SPECTRUM. * *
C * *
C * * * * * * * * * * * * * * * * * * * * * * * * * * * *
C * * * * * * * * * * * * * * * * * * * * * * * * * * * *
      READ(8,101) I(11),I(12),I(13),I(14),I(15)
      READ(8,140) ZX
      WRITE(6,200) N,FSINT,FREQL,FREQH,IOPUT,NSIG,NOUT,

```

```

      INCARD,I(14)
200  FORMAT('1',I4,2X,F5.2,2X,F7.2,4(2X,I1),
           140X,'SAMPLE TAPE REFERENCE NUMBER=',A4)
28  I(7)=I(7)+1
      Z=FLOAT(N)
      HI=3.14159265
C * * * * *
C * * * * *
C * *
C * *   CALLS SUBROUTINE WHICH READS IN BINARY DATA   * *
C * *   FROM SOURCE TAPE.                               * *
C * *
C * * * * *
C * * * * *
      IF(NSIG.EQ.2) GO TO 33
      IF(I(7).EQ.1) GO TO 32
      GO TO 33
22  CALL TPREAD(M,NOUT,9)
C * * * * *
C * * * * *
C * *
C * *           READS BACKGROUND TAPE.                 * *
C * *
C * * * * *
C * * * * *
      GO TO 34

```

```

33 CALL TPREAD(M,NOUT,5)
C * * * * *
C * * * * *
C * *
C * *          READS SAMPLE TAPE.
C * *
C * * * * *
C * * * * *
34 WRITE(6,141) ZX
141 FORMAT(1H ,80X10A4)
WRITE(6,142)
142 FORMAT(/1H ,80X,'SPECTRUM NO =  ')
CALL SUBDH(N,Z,M,NOUT)
J=N/2
L=J
K=N/4
Z=Z/2.0
C * * * * *
C * * * * *
C * *
C * * J IS EQUAL TO N/2 TO START WITH,L IS HALVED AT
C * * EACH SUCCESSIVE STAGE IN THE TRANSFORM.THE MAX-
C * * IMUM VALUE FOR J IS 4096.
C * *
C * * * * *
C * * * * *

```



```

C * * * * *
C * * * * *
C * *
C * * THIS SECTION NORMALLY CONTAINS THE DOUBLE BEAM * *
C * * SECTION, HOWEVER AT THE PRESENT MOMENT IT HAS * *
C * * BEEN OMITTED AS A SATISFACTORY TECHNIQUE HAS * *
C * * NOT YET BEEN DEVELOPED. * *
C * *
C * * * * *
C * * * * *
CALL SUBPT(I(9),I(7),Z,FSINT,FREQI,FREQH,IOPUT,I(14),I
1I(11),I(12),I(13),ZX,NOUT,NCARD,NSIG)
113 NSETS=NSETS-1
99 CALL SUBGP(V(7),X,F(1),I(9),NCARD,NOUT,NSIG,ZX)
IF(NCARD-1)11,1001,1001
1001 IF(NPAIR)11,11,1002
1002 WRITE(7,1003)(XXQ(M),M=1,NPAIR)
1003 FORMAT(5(F7.2,2XF6.4))
GO TO 13
98 WRITE(6,105)
105 FORMAT('YOU ARE AN UNAUTHORISED USER,HENCE THE JOB',
1' HAS BEEN TERMINATED,PLEASE SEEK THE PERMISSION OF',
2' MR. DAVID A. SYMON')
13 CALL EXIT
STOP
END

```

```
SUBROUTINE SUBDH(N,Z,M,NOUT)
  IMPLICIT REAL*4(A-H,O,S,V-Z),INTEGER*4(J-N,P-R,T-U)
  COMMON A(8192),C(8192),B(4096),D(4096)
111 FORMAT(1X,10F12.6)
101 FORMAT(1X,10F12.3)
  MM=1
  CALL AMX(MM,M,J,AMAX,AVE)
  T=N/2
  IF(M-N) 12,29,14
12 DO 9 K=M,N
  A(K)=A(M)
  9 CONTINUE
  GO TO 29
14 L=J-T
  IF(L.LE.0) L=1
  DO 15 K=1,N
  A(K)=A(L+K-1)
15 CONTINUE
29 IF(NOUT-1) 13,13,20
20 WRITE(6,106)
106 FORMAT(/' COPIED INTERFEROGRAM ')
  WRITE(6,101) (A(K),K=1,N)
13 DO 3 K=1,N
  C(K)=A(K)-AVE
  3 CONTINUE
  IF(NOUT-1) 21,21,22
```

```
22 WRITE(6,102)
102 FORMAT(/' REDUCED INTERFEROGRAM ')
      WRITE(6,101)(C(K),K=1,N)
21 DO 4 K=1,N
      ASUM=0.0
      DO 5 KK=1,N
          K1=KK+K-1
          IF(K1-N) 6,6,7
7      K1=K1-N
6      ASUM=ASUM+C(KK)*C(K1)
5      CONTINUE
      A(K)=ASUM
4      CONTINUE
      IF(NOUT-1) 23,23,24
24 WRITE(6,103)
103 FORMAT(/' AUTOCORRELATED INTERFEROGRAM ')
      WRITE(6,101)(A(K),K=1,N)
23 CALL AMX(MM,M,J,AMAX,AVE)
      DO 8 K=1,N
          A(K)=A(K)/AMAX
8      CONTINUE
      IF(NOUT-1) 25,25,26
26 WRITE(6,107)
107 FORMAT(/' NORMALISED INTERFEROGRAM ')
      WRITE(6,111)(A(K),K=1,N)
25 DO 10 K=1,T
```

```
APOD=COS(3.141593*(K-1)/(N-2))**2
A(K)=A(K)*APOD
A(N-K+2)=A(N-K+2)*APOD
10 CONTINUE
  A(1+T)=0.0
  DO 11 K=1,N
    C(K)=0.0
11 CONTINUE
  IF(NOUT-1) 27,27,28
28 WRITE(6,104)
104 FORMAT(/'  FINAL DATA SET LENGTH = N AFTER ',
  1' ADPODISATION ')
  WRITE(6,101)(A(K),K=1,N)
27 CONTINUE
  RETURN
  END
  SUBROUTINE AMX(MM,M,J,AMAX,AVE)
  COMMON A(8192),C(8192),B(4096),D(4096)
  AMAX=0
  AVE=0
  DO 1 K=1,M
    AVE=AVE+A(K)
    IF(A(K)-AMAX) 1,1,2
2  AMAX=A(K)
  J=K
1 CONTINUE
```

```

WRITE(6,200) J
200 FORMAT(3H J=,I4)
L=-3
DO 3 IQ=1,7
KK=J+L
C(IQ)=A(KK)
L=L+1
3 CONTINUE
AVE=AVE/(M-MM+1)
WRITE(6,201) AVE
201 FORMAT(/1H ,8HAVERAGE=F6.0)
RETURN
END
SUBROUTINE SUBTM(NMAX,NOUT)
C * * * * *
C * * * * *
C * *
C * * SUBROUTINE TO TRANSFORM DATA INTO A SPECTRAL * *
C * * OUTPUT.THIS MAKES USE OF A TECHNIQUE DUE TO * *
C * * J.W.COOLEY AND J.W.TUKEY (MATHEMATICS OF COMPU- * *
C * * TATION VOLUME 19,PAGE 195,1965).MODIFICATIONS * *
C * * TO THIS TECHNIQUE HAVE BEEN MADE SO THAT THE * *
C * * FOURIER ELEMENTS COME OUT IN A NORMAL ORDER. * *
C * *
C * * * * *
C * * * * *

```



```

DIMENSION TR1(4096),TI1(4096),TR2(2048),TI2(2048)
COMMON TR1,TI1,TR2,TI2
JHALF=NMAX/2
IHALF=NMAX/2
KHALF=NMAX/4
PI=3.14159265
C * * * * *
C * * * * *
C * *
C * *      CLEARS ARRAY TI1 READY FOR COM-      * *
C * *      PUTATION,AND CHECKS TO SEE IF N      * *
C * *      PASSFS HAVE BEEN MADE.THE SETTING      * *
C * *      OF THE CONSTANTS FOR EACH PASS      * *
C * *      ARE WR AND WI,WHICH ARE THE REAL      * *
C * *      AND IMAGINARY PARTS OF EXP(2*PI*      * *
C * *      J*K/NMAX) RESPECTIVELY AND THEY      * *
C * *      ARE AT 1 AND 0 AT THE START OF      * *
C * *      EACH PASS.      * *
C * *
C * * * * *
C * * * * *
      DO 10 I=1,NMAX
10  TI1(I)=0.0
34  IF(IHALF)999,65,37
37  JP=0
      WR=1.0

```

WI=0.0

```

C * * * * *
C * * * * *
C * *
C * * I AND L ARE THE INDICIES OF THE LOCATIONS OF
C * * WHERE THE PARTIAL SUMS WOULD BE TRANSFERRED TO
C * * IF TR1,TI1,TR2,TI2 WHERE OF EQUAL LENGTH.TR2
C * * AND TI2 ARE NEEDED FOR AUXILLARY STORAGE.
C * * JK=J*K AND DETERMINES THE PROPER FREQUENCIES
C * * DURING THE PASS.
C * *
C * * * * *
C * * * * *
DO 81 I=1,JHALF
L=I+JHALF
IF(IHALF-1)38,38,39
38 JK=I-1
ANG= PI*FLOAT(JK)/FLOAT(JHALF)
WR=COS(ANG)
WI=SIN(ANG)
GO TO 48
39 IMOD=I-(I/IHALF)*IHALF
IF(IMOD)999,48,41
41 JK=I-IMOD
IF(JK-JP)999,48,43
43 ANG= PI*FLOAT(JK)/FLOAT(JHALF)

```

JP=JK

WR=COS(ANG)

WI=SIN(ANG)

```

C * * * * *
C * * * * *
C * *
C * * IP AND IQ ARE THE LOCATIONS OF THE PREVIOUSLY
C * * CALCULATED PARTIAL SUMS ARE STORED IN THE
C * * LOCATIONS TRI AND TI2.THE RESULTS ARE STORED
C * * TEMPORARILY IN THE LOCATIONS TR1,TI1,TR2,OR TI2
C * * DEPENDING ON THE RELATION BETWEEN I AND KHALF.
C * * I AND U ARE THE INDICIES OF THE LOCATIONS TR2
C * * AND TI2,WHERE THE RESULTS OF THE PARTIAL SUMS
C * * ARE TO BE STORED AND CORRESPOND TO I AND L
C * * RESPECTIVELY FOR I LESS THAN OR EQUAL TO KHALF.
C * *
C * * * * *
C * * * * *

```

48 IP=JK+I

IQ=IP+IHALF

IF(I-KHALF)51,51,53

51 IU=I+KHALF

AR=TR1(IP)

AI=TI1(IP)

BR=TR1(IQ)\*WR-TI1(IQ)\*WI

BI=TR1(IQ)\*WI+TI1(IQ)\*WR



TI1(IU)=AI-BI

81 CONTINUE

```

C * * * * *
C * * * * *
C * *
C * *
C * * STORES THE PARTIAL SUMS JUST CALCULATED (TR1,
C * * TI1,TR2,TI2) IN TR1 AND TI1 IN THE PROPER
C * * ORDER PRIOR TO THE NEXT PASS.
C * *
C * *
C * * * * *
C * * * * *

```

JJJ=KHALF+1

DO 83 IK=JJJ,JHALF

JJMK=IK-KHALF

JJPK=IK+KHALF

JJPJ=IK+JHALF

TR1(IK)=TR1(JJMK)

TI1(IK)=TI1(JJMK)

TR1(JJPJ)=TR1(JJPK)

TI1(JJPJ)=TI1(JJPK)

TR1(JJMK)=TR2(JJMK)

TI1(JJMK)=TI2(JJMK)

TR1(JJPK)=TR2(IK)

83 TI1(JJPK)=TI2(IK)



```

SUBROUTINE TPREAD(M,NOUT,MM)
  DIMENSION A(8192)
  COMMON A
  I=1
  10 K=I+19
  READ(MM,100)(A(J),J=I,K)
  C * * * * *
  C * * * * *
  C * *
  C * * READS IN SAMPLE TAPE ON FILE 5 AND BACKGROUND * *
  C * * TAPE ON FILE 9. * *
  C * *
  C * * * * *
  C * * * * *
  DO 50 J=I,K
  IF(A(J)) 20,50,50
  50 CONTINUE
  I=I+20
  GO TO 10
  20 M=J-1
  IF(NOUT-1) 21,21,22
  22 WRITE(6,101)(A(J),J=1,M)
  21 WRITE(6,102) M
  100 FORMAT(20F4.0)
  101 FORMAT(/10F6.0)
  102 FORMAT(19H NO OF DATA POINTS=,I6)

```

```

      IF(MM.EQ.5) GO TO 11
      REWIND 9
11  RETURN
      END

      SUBROUTINE SUBLP
C * * * * *
C * * * * *
C * *
C * * SUBROUTINE USED TO SET UP LINE PRINTER SO THAT * *
C * * THE DATA CAN BE OBTAINED IN A SPECTRAL FORM. * *
C * *
C * * * * *
C * * * * *
      DIMENSION CHAR(101),XNUM(11)
      DATA DOT,DIV/1H.,1H+/
      DATA XNUM/0.0,0.1,0.2,0.3,0.4,0.5,0.6,0.7,0.8,0.9,1.0/
      WRITE(6,101) XNUM
101 FORMAT(17X,F3.1,10(7X,F3.1))
      DO 90 K=1,101
90 CHAR(K)=DOT
      DO 91 IZ=1,21
      IK=1
      IK=IK+5*(IZ-1)
91 CHAR(IK)=DIV
      WRITE(6,100) CHAR
100 FORMAT(1H ,16X,101A1)

```

RETURN

END

SUBROUTINE SUBPT(I9,I7,Z,FSINT,FREQL,FREQH,IOPUT,I14,  
I115,I11,I12,I13,ZX,NOOUT,NCARD,NSIG)

C \* \* \* \* \*  
C \* \* \* \* \*  
C \* \* \* \* \*  
C \* \* SUBROUTINE USED FOR PLOTTING OUT THE DATA OBTAI \* \*  
C \* \* -NED FROM THE TRANSFORMATION, IN A FORM WHICH \* \*  
C \* \* CAN BE RECOGNISED AS A SPECTRUM. \* \*  
C \* \* \* \* \*  
C \* \* \* \* \*  
C \* \* \* \* \*

IMPLICIT REAL\*4(A-H,O,S,V-Z),INTEGER\*4(J-N,P-R,T-U)

DIMENSION H(50),I(15),G(1),F(1),V(11),ZX(20)

COMMON A(8192),C(8192)

3 I9=1+I9

WRITE(6,200) I9

200 FORMAT(/6H I9 = ,I3)

V(7)=1.0000

IF(I9.EQ.4) GO TO 26

DATA H/1.0,2\*9.0,1.0,5.0,60.0,30.0,2\*4.0,30.0,60.0,  
15.0,7.0,105.0,35.0,5.0,1.0,2\*9.0,1.0,5.0,35.0,105.0,  
27.0,6.0,108.0,27.0,4.0,8.0,84.0,56.0,2\*7.0,56.0,84.0,  
38.0,4.0,27.0,108.0,6.0,16.0,2\*81.0,128.0,16.0,128.0,  
416.0,128.0,4\*125.0/





```
600 FORMAT(16H LARGEST NO Y = ,F9.6)
```

```
C * * * * *
C * * * * *
C * *
C * * FINDS THE LARGEST NUMBER IN THE ARRAY Q,K
C * *
C * * * * *
C * * * * *
```

```
DO 13 M=IK,L
```

```
IF (A(M).GT.YY) GO TO 13
```

```
YY=A(M)
```

```
13 CONTINUE
```

```
WRITE(6,601) YY
```

```
601 FORMAT(18H SMALLEST NO YY = ,F9.6)
```

```
C * * * * *
C * * * * *
C * *
C * * FINDS THE SMALLEST NUMBER IN THE ARRAY Q,K
C * *
C * * * * *
C * * * * *
```

```
IF(I9.EQ.3) GO TO 9999
```

```
CC=9.0000/SQRT(Y-YY)
```

```
DO 11 M=IK,L
```

```
A(M)=A(M)-YY
```

```
A(M)=SQRT(A(M))
```

```

      A(M)=CC*A(M) + 1.0000
      A(M)=10.0000/A(M)
      A(M)=ALOG10(A(M))
11  CONTINUE
      GO TO 9998
9999 CC=1.000/(Y-YY)
      DO 500 M=IK,L
      A(M)=A(M)-YY
      A(M)=CC*A(M)
500  CONTINUE
C * * * * *
C * * * * *
C * *
C * *   CARRIES OUT A NORMILISATION PROCEDURE BY PROD-
C * *   UCING AN ARRAY BETWEEN 1.0 AND 0.0 .
C * *   IT THEN PRODUCES A SPECTRUM IN ABSORBANCE MODE,
C * *   AND IF I(9) EQUALS 1,IT WRITES THE CURRENT DATE
C * *
C * * * * *
C * * * * *
9998 IF(I9.NE.1) GO TO 26
      12 WRITE(6,107) I11,I12,I13
      107 FORMAT(/8H DATE = ,I2,1X I2,1X I2)
      140 FORMAT(1H ,20A4)
      26 GO TO (44,2,5,6),I9
      44 IF(NSIG.EQ.2) GO TO 2

```

```
GO TO 4
2 WRITE(6,140) ZX
WRITE(6,112)
112 FORMAT(' NORMALISED SAMPLE SPECTRUM ')
GO TO 300
4 WRITE(6,113)
113 FORMAT(' NORMALISED BACKGROUND SPECTRUM ')
GO TO 300
5 WRITE(6,140) ZX
WRITE(6,114)
114 FORMAT(' ABSOLUTE ABSORBANCE SPECTRUM OF ',
1' SAMPLE-BACKGROUND ')
GO TO 300
6 WRITE(6,115)
115 FORMAT(' I(9)=4,AN ERROR HAS OCCURRED')
300 GO TO (99,8),I9
99 IF(NSIG.EQ.2) GO TO 8
GO TO 9
8 WRITE(6,116) I14
116 FORMAT(' SAMPLE TAPE REF.NO. =',A4)
GO TO 48
9 WRITE(6,117) I15
117 FORMAT(' BACKGROUND TAPE REF.NO. =',A4)
48 CONTINUE
V(7)=1.0000
WRITE(6,124)
```

```

124 FORMAT(' FREQ. ABSORBANCE')
50 CALL SUBLP
34 P=10*IOPUT
    R=30*IOPUT
    G(1)=FLOAT(IOPUT)
    G(1)=G1/G(1)
C * * * * *
C * * * * *
C * *
C * * G1 IS THE FREQUENCY INCREMENT WHICH RESULTS IF * *
C * * IOPUT IS GREATER THAN ONE, FI IS THE ALIAS * *
C * * FREQUENCY. * *
C * *
C * * * * *
C * * * * *
    DO 61 MI=K,Q
    DO 62 IK=1,IOPUT
    X=FLOAT(MI)
    X=X*G1
    IF(X.GT.FI) GO TO 35
    IF(IK.GT.1) GO TO 27
    F(1)=A(1+MI)
    GO TO 25
27 Y=FLOAT(IK)
    Y=Y-1
    Y=Y*G(1)

```

X=X+Y

IF(MI.EQ.Q) GO TO 35

```
C * * * * *
C * * * * *
C * *
C * * CHECKS FOR THE END OF ARRAY Q,K
C * *
C * * * * *
C * * * * *
```

Y=A(MI)\*C(P+IK)

E=A(1+MI)\*C(P-1K)

Y=Y+E

E=A(2+MI)\*C(R+IK)

Y=Y+F

E=A(3+MI)\*C(R-1K)

F(1)=Y+E

```
C * * * * *
C * * * * *
C * *
C * * USES INTERPOLATING COEFFICIENT C TO GIVE CORR-
C * * ECTED AMPLITUDES F(1) AT THE NEW FREQUENCY
C * * INTERVAL G(1). THE FREQUENCY CORRESPONDING TO
C * * THE AMPLITUDE F(1) IS X.
C * *
C * * * * *
C * * * * *
```

```
25 CALL SUBGP(V(7),X,F(1),I9,NCARD,NOOUT,NSIG,ZX)
62 CONTINUE
61 CONTINUE
35 RETURN
    END
    SUBROUTINE SUBGP(V7,X,F1,I9,NCARD,NOOUT,NSIG,ZX)
    DIMENSION CHAR(101),ZX(20)
    COMMON/PUNCH/ NPAIR,XXQ(10)
    DATA BLANK,PLOT,PLUS/1H ,1H*,1H+/
    Y=F1
    IF(NOOUT-1) 105,99,99
99 DO 92 K=2,101
92 CHAR(K)=BLANK
    CHAR(1)=PLUS
    I=(Y*100)+0.5
    IF(I.GT.100) GO TO 3
    IF(I.LT.1) GO TO 5
    GO TO 4
3 I=101
    GO TO 4
5 I=2
4 CHAR(I)=PLOT
    WRITE(6,103) X,Y, CHAR
103 FORMAT(1X,F6.2,3X,F6.4,2X,101A1)
105 IF(I9-2+NSIG-NCARD) 11,8,11
8 IF(NCARD-1) 11,10,10
```

```
10 IF(NPAIR-10)200,201,200
201 WRITE(7,250) XXQ
250 FORMAT(5(F7.2,2XF6.4))
      NPAIR=0
200 NPAIR=NPAIR+1
      XXQ(NPAIR)=X
      NPAIR=NPAIR+1
      XXQ(NPAIR)=Y
11 RETURN
      END
```

```

C * * * * *
C * * * * *
C * *
C * *
C * *      THIS GRAPH PLOTTER PROGRAM WAS SUPPLIED BY      * *
C * *      MR.B.R.LANDER THE OPERATIONS SUPERVISOR OF      * *
C * *      THE UNIVERSITY OF DURHAM COMPUTER UNIT.          * *
C * *      IT IS DESIGNED TO READ SPECTRAL OUTPUT           * *
C * *      DATA PRODUCED FROM THE FOURIER TRANSFORM        * *
C * *      PROGRAM (PRESENTED IN THIS THESIS) AND PLOT      * *
C * *      IT IN A PRE-DEFINED GRID BOX.THIS IS DONE       * *
C * *      USING AN I.B.M. 1130 COMPUTER AND ITS            * *
C * *      RELEVANT SUPPORT PROGRAMS FOR GRAPH PLOTTING.    * *
C * *
C * *
C * * * * *
C * * * * *

```

```

DIMENSION TITLE(20)

```

```

DIMENSION DUM(5,2)

```

```

DEFINE FILE 3 (3000,4,U,K)

```

```

IW=5

```

```

IP=7

```

```

IR=8

```

```

PI=3.14159

```

```

READ (IR,100) TITLE

```

```

READ(IR,110) NP,IS,IF,SCALE

```



```

C * * * * *
C * * * * *
C * *
C * * THE FOLLOWING SECTION DRAWS THE BOX FOR THE PLOT * *
C * * THE TOTAL LENGTH OF THE X-AXIS IS CONVERTED * *
C * * FROM AN INTEGER NUMBER TO A FLOATING POINT * *
C * * NUMBER.IT THEN SETS UP THE VARIABLES USED IN * *
C * * POSITIONING THE TITLE CENTRALLY ALONG THE UPPER * *
C * * X-AXIS.AFTER THAT IT CALCULATES THE NUMBER OF * *
C * * MARKERS ALONG THE X-AXIS,AND SETS UP THE SCALE * *
C * * ( 0.05 INCHES PER UNIT MULTIPLIED BY THE FACTOR * *
C * * 'SCALE' PREVIOUSLY READ IN).THE PEN IS LOWERED * *
C * * AND THE BOX IS DRAWN IN THE FOLLOWING DIRECTIONS * *
C * * NORTH,WEST,SOUTH,AND EAST.THE LOWER X-AXIS IS * *
C * * THEN MARKED AT FIFTY WAVE-NUMBER INTERVALS. * *
C * *
C * * * * *
C * * * * *

```

```
IX = IF-IS
```

```
YIX = IX
```

```
YIA=(YIX-(320.*(1./SCALE)))/2.
```

```
YIB=(YIX-(52.*(1./SCALE)))/2.
```

```
IX = IX / 10
```

```
SCALO=SCALE*0.05
```

```
CALL SCALF(SCALO,9.0,0.,0.)
```

```
CALL FPLOTT(2,0.,0.)
```

```

CALL FGRID(0,0.,0.,10.,IX)
CALL FGRID(1,YIX,0.,0.1,10)
CALL FGRID(2,YIX,1.,10.,IX)
CALL FGRID(3,0.,1.,0.1,10)
YJ = 0.0
DO 30 J=IS,IF,50
CALL FCHAR (YJ-3.,-.03,.13,.13,0.)
WRITE (IP,141) J
YJ = YJ + 50.0

```

```
30 CONTINUE
```

```

C * * * * *
C * * * * *
C * *
C * * THE LOWER X-AXIS LABEL IS WRITTEN WITH A CENTRAL * *
C * * DISPOSITION,THE SCALE IS THEN CHANGED AND THE * *
C * * LOWER ORDINATE CALIBRATIONS ARE WRITTEN.THE * *
C * * THE LEFT HAND Y-AXIS LABEL IS WRITTEN,AGAIN * *
C * * WITH A CENTRAL DISPOSITION.THE PREVIOUSLY READ * *
C * * IN TITLE IS NOW WRITTEN ALONG THE TOP X-AXIS * *
C * * WITH A CENTRAL DISPOSITION.THE PEN IS THEN * *
C * * RETURNED TO THE ORIGIN READY TO START PLOTTING. * *
C * *
C * * * * *
C * * * * *

```

```

CALL FCHAR (YIB,-0.08,.2,.25,0.)
WRITE (IP,140)

```



```

C * * * * *
C * * * * *
C * *
C * * THIS SECTION READS ONE DATA CARD INTO THE DUMMY * *
C * * ARRAY,PICKING OFF EACH PAIR OF COORDINATES IN * *
C * * TURN.THE NUMBER OF COORDINATES READ IN IS TESTED * *
C * * AGAINST NP THE NUMBER OF COORDINATES TO BE * *
C * * READ AND IF THIS IS GREATER THAN THE NUMBER * *
C * * OF COORDINATES ALREADY READ IN,THEN THE READING * *
C * * PROCESS IS CONTINUED,AS ABOVE. * *
C * * THE MINIMUM AND MAXIMUM Y-COORDINATE VALUES ARE * *
C * * FOUND AND EACH PAIR OF COORDINATES ARE STORED * *
C * * IN THE DUMMY ARRAY. * *
C * *
C * * * * *
C * * * * *
XMAX=0.0
XMIN=1.0
II=0
NR=(NP/5)+1
DO 345 I=1,NR
READ (IR,392) ((DUM(N,J),J=1,2),N=1,5)
DO 345 L=1,5
II=II+1
IF (NP-II) 345,309,309
309 IF (XMIN-DUM(L,2)) 320,320,321

```

```

321 XMIN=DUM(L,2)
320 IF (XMAX-DUM(L,2)) 322,325,325
322 XMAX=DUM(L,2)
325 WRITE (3'K) (DUM(L,M),M=1,2)
345 CONTINUE
C * * * * *
C * * * * *
C * *
C * * THE FACTOR FOR NORMALISING THE DATA BETWEEN THE * *
C * * VALUES 0.0 AND 1.0 IS CALCULATED. * *
C * * THE STARTING POINT FOR THE X-AXIS IS CONVERTED * *
C * * TO A FLOATING POINT NUMBER. * *
C * * THE FILE POINTER IS RESET TO THE BEGINNING OF * *
C * * THE DATA FILE AND THE X AND Y COORDINATES ARE * *
C * * READ FROM THE DATA FILE IN TURN.THE Y COORDINATE * *
C * * VALUE IS ADJUSTED AND THE COORDINATES ARE * *
C * * PLOTTED.THE FINAL PROCEDURE IS TO RESET THE PEN * *
C * * READY FOR THE NEXT PLOT. * *
C * *
C * * * * *
C * * * * *
RECIP=1.0/(XMAX-XMIN)
ST=IS
K=1
DO 370 I=1,NP
READ(3'K) X,Y

```

```
Y=(Y-XMIN)*RECIP
CALL FPLOT (-2,X-ST,Y)
370 CONTINUE
CALL FPLOT(1,YIX+(99.*(1/SCALE)),0.)
CALL EXIT
100 FORMAT(20A4)
110 FORMAT (3I6,F4.2)
130 FORMAT (' ABSORBANCE ')
135 FORMAT (F3.1)
140 FORMAT (' WAVENUMBER CM ')
141 FORMAT(I4)
142 FORMAT ('-1')
392 FORMAT (5(F7.2,F8.4))
END
```

## APPENDIX B

### Estimation of Phosphorus

#### Introduction

The method is based on the reaction of an acidified solution containing orthophosphate with a solution of ammonium metavanadate and ammonium molybdate in nitric acid which gives a vanadomolybdophosphoric acid. The vanadomolybdophosphoric acid is yellow in colour and has an unknown structure. The measurement of the absorbancy of the vanadomolybdophosphoric acid thus enables an estimation of the orthophosphate content of the original solution. The maximum absorption of the vanadomolybdophosphoric acid occurs in the region of about  $31,750 \text{ cm}^{-1}$  (315 nm), however at this frequency the reagent absorbs strongly, the absorption of which is very sensitive to nitric acid concentration. To overcome these disadvantages the absorbance measurements are carried out on the slope of the absorption curve at about  $23,810 \text{ cm}^{-1}$  (420 nm). To eliminate any errors in the setting of the monochrometer a standard solution of orthophosphate should be estimated at the same time as the unknown estimation is carried out.

#### Range

The test solution should contain between 0.2 and 1.25 mg. of phosphorus in  $100 \text{ cm}^3$  solution, preferably in the 0.4-0.9 mg range for best accuracy.

#### Reagents

##### Ammonium molybdate/ammonium metavanadate solution

A.R. ammonium molybdate tetrahydrate (20 g.) was dissolved in water ( $250 \text{ cm}^3$ ). A.R. ammonium metavanadate (1.000 g.) was dissolved in water

(200 cm<sup>3</sup>) containing nitric acid (40 cm<sup>3</sup> sp.gr. 1.42). After mixing the two solutions nitric acid (100 cm<sup>3</sup>, sp.gr. 1.42) was added, then the solution was diluted to 1000 cm<sup>3</sup> in a standard flask.

#### Standard orthophosphate solution (1)

Monopotassiumdihydrogenorthophosphate (2.1968 g.) which had previously been dried at 105° for at least one hour was dissolved in water and diluted to one litre in a standard flask at 20°C.

#### Standard orthophosphate solution (2)

25.0 cm<sup>3</sup> of standard orthophosphate solution (1) was measured by pipette into a 250 cm<sup>3</sup> standard flask and diluted to the mark with distilled water at 20°C.

$$1.00 \text{ cm}^3 \equiv 0.05 \text{ mg.P}$$

#### Procedure

The sample was fused in a Parr bomb with sodium peroxide (about 1 g.). After extraction of the melt with water and neutralisation with hydrochloric acid the solution was boiled for about one hour to hydrolyse any condensed phosphates to orthophosphate. The test solution (which should contain 0.4-0.9 mg.P) was then transferred to a 100 cm<sup>3</sup> flask and ammonia added dropwise until just alkaline to litmus. The solution was then made just acid by the addition of nitric acid. 25.0 cm<sup>3</sup> of ammonium molybdate/ammonium vanadate reagent was added by pipette into the 100 cm<sup>3</sup> flask and the solution diluted to the mark with distilled water. Into a second 100 cm<sup>3</sup> standard flask was added by pipette 10.0 cm<sup>3</sup> of the standard orthophosphate solution (2) and 25.0 cm<sup>3</sup> of the ammonium molybdate/ammonium vanadate reagent. The solution was then diluted to the mark with distilled water. 25.0 cm<sup>3</sup> of the ammonium

molybdate/ammonium vanadate reagent was added by pipette into a third 100 cm<sup>3</sup> standard flask and diluted to the mark with distilled water. This solution was to be used as the blank in the spectrophotometric determination.

The absorbancy of the test and standard solutions were then measured at 23,810 cm<sup>-1</sup> (420 nm) using 10 mm glass cells against the reagent blank.

The phosphorus content of the test solution is then given by the expression:

$$\frac{\text{absorbancy of test solution}}{\text{absorbancy of standard solution}} \times 0.5 = \text{mg. of P in test solution}$$

#### Note

A calibration graph over the range 0.2-1.25 mg. P is linear, but it is advisable to prepare a calibration graph using the spectrophotometer used in the determinations to ensure that the calibration is linear over the range used.

The colour of the complex forms immediately and is stable for long periods.

The acidity of the test solution must not be greater than 0.3N prior to the addition of the ammonium molybdate/ammonium metavanadate reagent.

APPENDIX C

Magnetochemistry of the tetrakis( $\pi$ -cyclopentadienyl carbonyl  
iron cation)

This work was carried out in conjunction with Mr. J. Cope and Dr. J.J. Cox of Wolverhampton Polytechnic. Measurements were carried out on a Newport Instruments variable temperature Gouy balance fitted with an electromagnetic which has 4 inch poles. Measurements were carried out at temperatures over the range +25 to  $-180^{\circ}\text{C}$  with magnetic fields of 1,2,3 and 7 Kgauss and are given in Table C.1.

The results obtained with the lower magnetic fields are much more likely to be inaccurate than those obtained with the 7 Kgauss magnetic field. The general trends of the magnetic moments however are clear and thought to be reliable.

The simplest theory of magnetic moments is based on the assumption that only unpaired electrons give rise to paramagnetism and that no spin-orbit coupling occurs. The effective magnetic moment,  $\mu_{\text{eff}}$ , is given by the equation

$$\mu_{\text{eff}} = \sqrt{n(n + 2)}$$

where  $n$  is the number of unpaired electrons. Hence values of  $\mu_{\text{eff}}$  of 1.73, 2.83 and 3.88 are expected for 1, 2 and 3 unpaired electrons respectively. However for atoms with more than a half filled  $d$  shell spin orbit coupling can not be ignored and increases the magnetic moments above the spin only value.

The magnetic moments observed for the tetrakis( $\pi$ -cyclopentadienyl carbonyl iron) cation are much greater than that predicted by the spin only formula. Indeed the values are much larger than expected even allowing for

Table C.1.  
Magnetic Moments of the Tetrakis( $\pi$ -cyclopentadienylcarbonyl iron) cation

Temp. °C	$[\text{CpFe}(\text{CO})]_4^+ \text{PF}_6^-$							$[\text{CpFe}(\text{CO})]_4^+ \text{I}_7^-$								
	$\mu_{\text{eff}}$							$\mu_{\text{eff}}$								
25	2.52	1.80	2.47	2.30	2.20	2.00	2.05	2.03	3.49	3.47	3.29	3.40	2.93	2.97	2.52	2.53
0	2.41	2.40	2.22	2.20	2.11	2.10	2.04	2.03	3.82	3.32	3.28	3.13	2.91	2.84	2.49	2.48
-20	2.32	2.31	1.98	2.12	2.03	2.08	2.03	2.04	3.68	3.66	3.15	3.14	2.85	2.84	2.46	2.46
-40	2.23	2.70	2.18	2.17	2.05	2.04	2.05	2.04	3.53	3.51	3.03	3.12	2.79	2.77	2.44	2.44
-60	2.13	2.58	2.09	2.08	2.01	2.05	2.04	2.03	3.37	3.73	3.00	3.09	2.71	2.78	2.41	2.41
-80	2.03	2.02	2.10	2.09	2.05	2.04	2.03	2.02	3.57	3.55	3.06	2.94	2.74	2.73	2.38	2.38
-100	2.34	1.91	1.99	1.98	2.10	2.09	2.03	2.02	3.38	3.36	2.80	2.88	2.63	2.66	2.34	2.34
-120	1.80	2.19	2.07	2.15	2.04	2.07	2.04	2.04	3.18	2.84	2.81	2.71	2.61	2.56	2.31	2.31
-140	1.68	1.67	2.09	2.00	2.06	2.05	2.04	2.03	2.67	2.95	2.69	2.68	2.50	2.54	2.27	2.27
-160	2.18	2.17	2.07	2.06	2.08	2.07	2.05	2.04	2.73	2.72	2.55	2.47	2.46	2.42	2.23	2.22
-180	1.97	1.96	2.05	2.04	2.08	2.07	2.03	2.01	2.71	2.69	2.49	2.48	2.37	2.40	2.17	2.19
Run	1	2	1	2	1	2	1	2	1	2	1	2	1	2	1	2
Magnetic Field (Gauss)	1K	1K	2K	2K	3K	3K	7K	7K	1K	1K	2K	2K	3K	3K	7K	7K

spin orbit coupling. Another assumption in the magnetic theory used is that the compounds are magnetically dilute, i.e. that neighbouring molecules have no effect on one another. For non-magnetically dilute materials there are two basic types of interactions, ferromagnetism where adjacent magnetic dipoles tend to align themselves in the same direction and antiferromagnetism where adjacent magnetic dipoles tend to align themselves in opposite directions. The magnetic susceptibilities of the hexafluorophosphate and hepta-iodide salts of the tetrakis( $\pi$ -cyclopentadienylcarbonyl iron) cation show identical trends although the values themselves are markedly different. This is probably due to the differing degree of magnetic dilution in the two salts. The structure of the hexafluorophosphate salt is probably based on a system of closely packed spheres whereas the structure of the hepta-iodide salt is probably based on packing of spheres and rods. There is therefore a much more likely case of magnetic interaction in the hepta-iodide salt than in the hexafluorophosphate salt. The data presented are not reliable enough to calculate a theoretical Curie-Weiss law plot and observe a clear break in the curve showing the compound to be ferromagnetic. Over the temperature range examined the compounds do not show a Néel point which would indicate the materials to be antiferromagnetic. To solve these problems would require a more detailed and thorough study to be carried out and was beyond the scope of this thesis and the techniques available. The aim of the studies were to confirm that only one electron had been removed from the tetrakis( $\pi$ -cyclopentadienylcarbonyl iron(I)) in the formation of the cation.



REFERENCES

1. C.C. Addison, Roy. Inst. Chem. Lectures, Monographs, reports 1960, No.2
2. L.F. Audrieth and J. Kleinberg, 'Non-Aqueous Solvents', Wiley, New York, 1953.
3. R.S. Drago and K.F. Purcell, 'Progress in Inorg. Chem.', 6, Interscience, 1964.
4. H.J. Emeléus and J.S. Anderson, 'Modern Aspects of Inorganic Chemistry' Routledge and Kegan Paul, 1959.
5. V. Gutmann, Quart. Revs., 1956, 10, 451.
6. R. Drago, Chem. In Brit., 1967, 3, 516.
7. V. Gutmann, Chem. In Britain, 1971, 7, 102.
8. T.C. Waddington, 'Non-Aqueous Solvents', Nelson, 1969.
9. J. Jander and C. Lafrenz, 'Ionizing Solvents', Wiley, 1970.
10. T.C. Waddington, 'Non-Aqueous Solvent Systems', Academic Press, 1965.
11. G. Gore, Phil. Mag.(4), 1865, 29, 541.
12. E.H. Archibald, D. McIntosh and B.D. Steele, Phil. Trans., 1905, 205, 99.
13. F. Klanberg and T.C. Waddington, Naturwiss, 1959, 46, 578.
14. F. Klanberg and T.C. Waddington, Z. anorg. Chem., 1960, 304, 185.
15. F. Klanberg and T.C. Waddington, J. Chem. Soc., 1960, 2329.
16. F. Klanberg and T.C. Waddington, J. Chem. Soc., 1960, 2332.
17. F. Klanberg and T.C. Waddington, J. Chem. Soc., 1960, 2339.
18. J.A. White, Ph.D. Thesis, Cambridge, 1961.
19. T.C. Waddington and J.A. White, J. Chem. Soc., 1963, 2701.
20. M.E. Peach and T.C. Waddington, J. Chem. Soc., 1961, 1238.
21. M.E. Peach and T.C. Waddington, (a) J. Chem. Soc., 1962, 600; (b) J. Chem. Soc., 1962, 2680.
22. M.E. Peach, Can. J. Chem., 1969, 47, 1675.

23. R.M. Fuoss and C.A. Krauss, J. Amer. Chem. Soc., 1933, 55, 2387.
24. M.E. Peach and T.C. Waddington, J. Chem. Soc., 1963, 69.
25. M.E. Peach and T.C. Waddington, J. Chem. Soc., 1963, 799.
26. J.A. Salthouse and T.C. Waddington, J. Chem. Soc.(A), 1966, 1188.
27. J.A. Salthouse and T.C. Waddington, J. Chem. Soc.(A), 1967, 1096.
28. M.E. Peach and T.C. Waddington, J. Chem. Soc.(A), 1968, 180.
29. A. Davison, W. McFarlane, L. Pratt, and G. Wilkinson, J. Chem. Soc., 1962, 3653.
30. Z. Iqbal and T.C. Waddington, J. Chem. Soc.(A), 1968, 2958.
31. Z. Iqbal and T.C. Waddington, J. Chem. Soc.(A), 1969, 1092.
32. G. Glocker and R.E. Peck, J. Chem. Phys., 1936, 4, 658.
33. S. Glasstone, 'Textbook of Physical Chemistry', Macmillan and Co. London, 1956.
34. D.O. Schissler and D.P. Stevenson, J. Chem. Phys., 1956, 24, 926.
35. A. Hantzsch, Chem. Ber., 1930, 63B, 1789.
36. H.H. Hyman, L.A. Quarterman, M. Kilpatrick and J.J. Katz, J. Phys. Chem., 1961, 65, 123.
37. F. Kaufler and E. Kunz, Chem. Ber., 1909, 42, 2482.
38. H.F. Herbrandson, R.T. Dickerson and J. Weinstein, J. Amer. Chem. Soc., 1954, 76, 4046.
39. T.C. Waddington, J. Chem. Soc., 1958, 1708.
40. D.G. Tuck and E.J. Woodhouse, Proc. Chem. Soc., 1963, 53.
41. R.E. Vallée and D.H. McDaniel, Inorg. Chem., 1963, 2, 997.
42. K.M. Harmon and S. Davis, J. Amer. Chem. Soc., 1962, 84, 4359.
43. K.M. Harmon and P.A. Gebauer, Inorg. Chem., 1963, 2, 1319.
44. J.A. Salthouse, Ph.D. Thesis, Cambridge, 1965.
45. A.G. Davies and E.C. Baughan, J. Chem. Soc., 1961, 1711.
46. N.N. Greenwood and H.J. Emeléus, J. Chem. Soc., 1950, 987.
47. R.J. Gillespie and J.A. Leisten, Quart. Revs., 1954, 8, 40.

48. R.J. Gillespie and E.A. Robinson, 'Adv. in Inorg. and Radiochem.', 1959, 1, 385.
49. G. Gore, J. Chem. Soc., 1869, 22, 368.
50. K. Fredenhagen, Z. Phys. Chem., 1933, A164, 176.
51. J.H. Simons, Chem. Revs., 1931, 8, 213.
52. W. Klatt, Z. Phys. Chem., 1936, A185, 306.
53. G. Jander, 'Die Chemie in Wasseranlichen Losungsmitteln', Springer-Verlag, Berlin, 1949.
54. G. Wilkinson and J.M. Birmingham, J. Amer. Chem. Soc., 1955, 77, 3421.
55. M. Rosenblum and J.O. Santer, J. Amer. Chem. Soc., 1959, 81, 5517.
56. T.J. Curphey, J.O. Santer, M. Rosenblum and J.H. Richards, J. Amer. Chem. Soc., 1960, 82, 5249.
57. M.L.H. Green, J.A. McCleverty, L. Pratt and G. Wilkinson, J. Chem. Soc., 1961, 4854.
58. A. Davison, W. McFarlane, L. Pratt and G. Wilkinson, J. Chem. Soc., 1962, 4821.
59. D.R. Falkowski, D.F. Hunt, G.P. Lillya and M.D. Rausch, J. Amer. Soc., 1967, 89, 6387.
60. I. Pavtik and J. Šubrt, Coll. Czech. Chem. Comms., 1967, 32, 76.
61. K.R. Laing and W.R. Roper, J. Chem. Soc.(A), 1969, 1889.
62. G.M. Bancraft, M.J. Mays, B.E. Prater and F.P. Stefanini, J. Chem. Soc.(A), 1970, 2146.
63. A.J. Deeming, B.F.G. Johnson and J. Lewis, J. Chem. Soc.(A), 1970, 2967.
64. J.C. Katz and D.G. Pedrotty, J. Organomet. Chem., 1970, 22, 425.
65. J. Knight and M.J. Mays, J. Chem. Soc.(A), 1970, 711.
66. K.Kudo, M. Hidai, T. Murayama and Y. Uchida, J. Chem. Soc.(D), 1970, 1701.
67. P. Legzdins, R.W. Mitchell, G.L. Rempel, J.D. Ruddick and G. Wilkinson, J. Chem. Soc.(A), 1970, 3322.
68. M.L.H. Green, L. Pratt and G. Wilkinson, J. Chem. Soc., 1958, 3916.
69. A.J. Deeming and B.L. Shaw, J. Chem. Soc.(A), 1969, 1802.

70. M.E. Peach, Ph.D. Thesis, Cambridge, 1962.
71. J.D. Cotton, Ph.D. Thesis, Cambridge, 1964.
72. J.A. Salthouse, Ph.D. Thesis, Cambridge, 1965.
73. R.E. Dodd and P.L. Robinson, 'Experimental Inorganic Chemistry', Elsevier, 1954.
74. 'Handbook of Chemistry and Physics', 46th Edn. Chemical Rubber Publishing Co., Cleveland, Ohio.
75. J.W. Cooley and J.W. Tukey, Mathematics of Computation, 1965, 19, 195.
76. A.I. Vogel, 'A Text-Book of Quantitative Inorganic Analysis', Longmans, London, 3rd Edn., 1961.
77. K. Nakamoto, 'Infrared Spectra of Inorganic and Co-ordination Compounds', Wiley-Interscience, New York, 2nd Edn., 1970.
78. W. Lange and E. Muller, Chem. Ber., 1930, 63, 1058.
79. H.S. Gulowsky and A.D. Liehr, J. Chem. Phys., 1952, 20, 1652.
80. L. Landau and W.H. Fletcher, J. Mol. Spect., 1960, 4, 276.
81. R.H. Pierson, A.N. Fletcher and E. St. C. Gantz, Anal. Chem., 1956, 28, 1218.
82. K. Noack, J. Inorg. Nuclear Chem., 1963, 25, 1383.
83. F.A. Cotton and G. Yagupsky, Inorg. Chem., 1967, 6, 15.
84. R.D. Fischer, A. Vogler and K. Noack, J. Organometallic Chem., 1967, 7, 135.
85. T.S. Piper, F.A. Cotton and G. Wilkinson, J. Inorg. Nuclear Chem., 1955, 1, 165.
86. A.R. Manning, J. Chem. Soc.(A), 1971, 106.
87. B.F. Hallam and P.L. Pauson, J. Chem. Soc., 1956, 3030.
88. R.B. King and F.G.A. Stone, Inorg. Synth., 1963, 7, 99.
89. L. Busetto and R.J. Angelici, Inorg. Chem. Acta., 1968, 2, 391.
90. T.S. Piper and G. Wilkinson, J. Inorg. Nuclear Chem., 1956, 3, 104.
91. R.B. King, Inorg. Chem., 1966, 5, 2227.
92. I.A. Cohen and F. Basolo, J. Inorg. Nuclear Chem., 1966, 28, 511.
93. A. Davison, M.L.H. Green and G. Wilkinson, J. Chem. Soc., 1961, 3172.

94. R.D. Peacock and D.W.A. Sharp, *J. Chem. Soc.*, 1959, 2762.
95. L.M. Haines and M.H.B. Stiddard, *Adv. Inorg. Chem. Radiochem.*, 1970, 12, 53.
96. E.O. Fischer and E. Moser, *J. Organometallic Chem.*, 1965, 3, 16.
97. E.O. Fischer and E. Moser, *Z. Anorg. Chem.*, 1966, 342, 156.
98. R.D. Fischer, A. Vogler and K. Noack, *J. Organometallic Chem.*, 1967., 7, 135.
99. D.A. Brown, A.R. Manning and D.J. Thornhill, *J. Chem. Soc.(D)*, 1969, 338.
100. R.J. Haines and A.L. du Preez, *J. Amer. Chem. Soc.*, 1969, 91, 769.
101. R.J. Haines and A.L. du Preez, *J. Chem. Soc.*, 1970, 2341.
102. A. Davison, J.A. McCleverty and G. Wilkinson, *J. Chem. Soc.*, 1963, 1133.
103. R.G. Hayter, *J. Amer. Chem. Soc.*, 1966, 88, 4376.
104. J.A. Ferguson and T.J. Meyer, *J. Chem. Soc.(D)*, 1971, 623.
105. J. Knight and M.J. Mays, *J. Chem. Soc.(A)*, 1970, 711.
106. N.J. Nelson, N.E. Kime, and D.F. Shriver, *J. Amer. Chem. Soc.*, 1969, 91, 5173.
- 107.K.D. Bartle, D.W. Jones, and (in part) S. Maričić, *Croat. Chem. Acta*, 1968, 40, 227.
108. L.F. Farnell, E.W. Randall and E. Rosenbury, *J. Chem. Soc.(D)*, 1971, 1078.
109. P.M. Treichel, R.L. Shubkin, K.W. Barnett and D. Reichard, *Inorg. Chem.*, 1966, 5, 1177.
110. R.D. Feltham, H.G. Metzger and W. Silverthorn, *Inorg. Chem.*, 1968, 7, 2003.
111. H. Kuroda, *J. Mol. Spectroscopy*, 1969, 30, 355.
112. J.J. Smith and B. Meyer, *J. Chem. Phys.*, 1968, 48, 5436.
113. N. Svartholm and K. Siegbahn, *Arkiv. Mat. Astron. Fys.*, 1946, 33A, 21.
114. K. Siegbahn and K. Edvarson, *Nucl. Phys.*, 1956, 1, 137.
115. C. Nordling, E. Sokolowski and K. Siegbahn, *Arkiv. Fys.*, 1958, 13, 483.
116. S. Hagstrom, C. Nordling and K. Siegbahn, *Phys. Lett.*, 1964, 9, 235.

117. C. Nordling, S. Hagstrom and K. Siegbahn, *Z. Physik*, 1964, 178, 433, 439.
118. K. Siegbahn, C. Nordling, A. Fahlman, R. Nordberg, K. Hamrin, J. Hedman, G. Johansson, T. Bergmark, S.E. Karlsson, I. Lindgren and B. Lindberg, 'ESCA; Atomic Molecular and Solid State Structure Studied by means of Electron Spectroscopy', Almquist and Wiksells, Upsala, 1967.
119. D.W. Turner and M.I. Al-Joboury, *J. Chem. Phys.*, 1962, 37, 3007.
120. E. Sokalowski, *Arkiv Fysik*, 1959, 15, 1.
121. C. Nordling, *Arkiv Fysik*, 1959, 15, 397.
122. D.R. Lloyd and E.W. Schlag, *Inorg. Chem.*, 1969, 8, 2544.
123. D.T. Clark and D. Kilcast, *J. Chem. Soc.(A)*, 1971, 3286.
124. R.H. Herber, R.B. King and G.K. Wertheim, *Inorg. Chem.*, 1964, 3, 101.
125. A.J. Carty, T.W. Ng, W. Carter, G.J. Palenik and T. Birchall, *J. Chem. Soc.(D)*, 1969, 1101.
126. K. Farmery, M. Kilner, R. Greatrex and N.N. Greenwood, *J. Chem. Soc.(A)*, 1969, 2339.
127. G.M. Bancroft, M.J. Mays and B.E. Prater, *J. Chem. Soc.(A)*, 1970, 956.
128. A.A. Michelson, 'Light Waves and their Uses', University of Chicago Press, 1902.
129. J.B.J. Fourier, 'Theorie Analytique da la Chaleur,' 1822.
130. J.D. Strong and G.A. Vanesse, *J. Opt. Soc. Amer.*, 1959, 49, 844.
131. P. Jacqunot, *Rep. Prog. Phys.*, 1960, 23, 267.
132. J. Connes, *Rev. Optique*, 1961, 40, 45, 116, 171 and 231.
133. L. Genzel, *J. Mol. Spectroscopy*, 1960, 4, 241.
134. D.J. James and J. Ring, 'Methodes Nouvelles de Spectroscopie Instrumentale' Supplement of *J. de Physique*, 1967, 28, CZ.
135. J.E. Chamberlain, G.W. Chantry, F.D. Findlay, H.A. Gebbie, J.E. Gibbs, N.W.B. Stone and A.J. Wright, *Infrared Phys.*, 1966, 6, 195.
136. H.A. Gebbie and N.B. Stone, *Infrared Physics*, 1964, 4, 85.
137. J.W. Mellor, 'Comprehensive Treatise on Inorganic and Theoretical Chemistry', Longmans and Co. London.

138. R.C. Taylor and W.D. Horrocks, *Inorg. Chem.*, 1964, 3, 584.
139. E.W. Abel and I.S. Butler, *Trans. Faraday Soc.*, 1967, 63, 45.
140. L.A.W. Hales and R.J. Irving, *J. Chem. Soc.(A)*, 1967, 1389.
141. E.R. Corey, M.V. Evans, and L.F. Dahl, *J. Inorg. Nucl. Chem.*, 1962, 24, 926.
142. K. Noack, *Helv. Chim. Acta*, 1962, 45, 1847.
143. B.F.G. Johnson, J. Lewis, P.W. Robinson, and J.R. Miller, *J. Chem. Soc.(A)*, 1968, 1043.
144. M. Pańkowski and M. Bigorgne, *J. Organometallic Chem.*, 1969, 19, 393.
145. R.J.H. Clark and B.C. Crosse, *Chem. and Ind.*, 1969, 1593.
146. I.J. Hyams, D. Jones and E.R. Lippincott, *J. Chem. Soc.(A)*, 1967, 1987.
147. E.R. Lippincott and R.D. Nelson, *Spectrochim. Acta*, 1958, 10, 307; *J. Chem. Phys.*, 1953, 21, 1307; *J. Amer. Chem. Soc.*, 1955, 77, 4990.

## NOTE ADDED IN PROOF:

Preliminary results from the X-ray crystal structure being carried out by Dr N. Alcock at Warwick University shows that the unit cell contains 2 molecules and has a symmetry of  $P_{\bar{1}}$ . The analysis carried out so far shows that for  $\pi$ cyclopentadienyldicarbonyl iron- $\mu$ -bromo  $\pi$  cyclopentadienyldicarbonyl iron hexafluorophosphate that the iron bromine distances are 2.38 and 2.42Å ( $\pm 0.02$ Å) and that the iron bromine iron angle is  $116^\circ$  ( $\pm 2^\circ$ ). The iron bromine distances are identical within the experimental error and confirms the evidence obtained from examination by other physical techniques.



**The Liquid Hydrogen Chloride Solvent System. Part XIV.<sup>1</sup> Reactions of  $\pi$ -Cyclopentadienyldicarbonyliron Dimer, of  $\pi$ -Cyclopentadienyliron dicarbonyl Chloride, Bromide, and Iodide, and of  $\pi$ -Cyclopentadienyltricarbonyliron Chloride in the Solvent**

By D. A. Symon and T. C. Waddington, Chemistry Department, The University of Durham, Durham City

Reprinted from

JOURNAL  
OF  
THE CHEMICAL SOCIETY

SECTION A  
Inorganic, Physical, and Theoretical Chemistry

1971



## The Liquid Hydrogen Chloride Solvent System. Part XIV.<sup>1</sup> Reactions of $\pi$ -Cyclopentadienyldicarbonyliron Dimer, of $\pi$ -Cyclopentadienylirondicarbonyl Chloride, Bromide, and Iodide, and of $\pi$ -Cyclopentadienyltricarbonyliron Chloride in the Solvent

By D. A. Symon and T. C. Waddington, Chemistry Department, The University of Durham, Durham City

$\pi$ -Cyclopentadienyldicarbonyliron dimer is monobasic in liquid hydrogen chloride, giving the  $[(\pi\text{-C}_5\text{H}_5)\text{Fe}(\text{CO})_2]_2\text{H}^+$  ion. Spectroscopic evidence (Mössbauer,  $^1\text{H}$  n.m.r., and i.r.) shows that this ion contains two  $(\pi\text{-C}_5\text{H}_5)\text{Fe}(\text{CO})_2$  units linked by a symmetric Fe-H-Fe bridge. Reaction of a solution of the dimer with nitrosyl chloride or chlorine gives mixtures containing  $\pi$ -cyclopentadienyldicarbonyliron chloride.  $\pi$ -Cyclopentadienyldicarbonyliron chloride is a base in the solvent forming  $[(\pi\text{-C}_5\text{H}_5)\text{Fe}(\text{CO})_2]_2\text{Cl}^+\text{BCl}_4^-$  on treatment with boron trichloride.  $\pi$ -Cyclopentadienyltricarbonyliron chloride also acts as a base in the solvent giving  $(\pi\text{-C}_5\text{H}_5)\text{Fe}(\text{CO})_3^+\text{BCl}_4^-$  with boron trichloride.

$\pi$ -CYCLOPENTADIENYLDICARBONYLIRON dimer appears to be monobasic in several anhydrous acids,<sup>2</sup> but the structure of the  $[(\pi\text{-C}_5\text{H}_5)\text{Fe}(\text{CO})_2]_2\text{H}^+$  ion has not been clearly established. The i.r. data reported is difficult to understand, particularly the occurrence of three

carbonyl bands in the i.r. region and the lack of agreement between the spectrum in the carbonyl region of a solution in sulphuric acid and of the solid hexafluorophosphate. We have examined the behaviour of pure<sup>3,4</sup>

<sup>2</sup> A. Davison, W. McFarlane, L. Pratt, and G. Wilkinson, *J. Chem. Soc.*, 1962, 3653.

<sup>3</sup> K. Noak, *J. Inorg. Nuclear Chem.*, 1963, 25, 1383.

<sup>4</sup> A. R. Manning, *J. Chem. Soc. (A)*, 1968, 1319.

<sup>1</sup> Part XIII. Z. Iqbal and T. C. Waddington, *J. Chem. Soc. A*, 1969, 1092.

TABLE 2

I.r. spectra of  $\pi$ -cyclopentadienyldicarbonyliron dimer in anhydrous acids in the region 2200—1700  $\text{cm}^{-1}$  (mulls between polythene plates)

Mulling agent	$\nu_{\text{CO}}$ frequencies ( $\text{cm}^{-1}$ )			
$\text{H}_2\text{SO}_4^a$	2122 *	2066 *	2035 †	2012 †
$\text{H}_2\text{SO}_4/(20\% \text{SO}_3)$	2124 *	2068 *	2039 †	2013 †
$\text{CH}_3\text{SO}_3\text{H}$	2122 *	2062 *	2040 †	2010 †
$\text{HSO}_3\text{Cl}$	2123 *	2068 *	2034 †	2012 †
$\text{CF}_3\text{CO}_2\text{H}^\dagger$	2125	2063		2012
$\text{H}_2\text{PO}_3\text{F}^\ddagger$	2124	2070	2037	2015
$\text{HPO}_3\text{F}_2^\ddagger$	2123	2068	2040	2019

\* Bands increasing in intensity with time. † Bands decreasing in intensity with time. ‡ Effect of time not studied.

<sup>a</sup> Ref. 2 2068ms, 2045vs, 2022vs. <sup>b</sup> Poor mull, solvent evaporated, 2063 band very broad.

of potassium hexafluorophosphate gave  $(\pi\text{-C}_5\text{H}_5)\text{Fe}(\text{CO})_3^+\text{PF}_6^-$ , identical with the material described by Busetto and Angelici.<sup>8</sup> With the salt  $(\pi\text{-C}_5\text{H}_5)\text{Fe}(\text{CO})_2]_2\text{H}^+\text{PF}_6^-$  in KCl discs, in addition to the carbonyl bands due to the protonated species, carbonyl bands which can be assigned to  $[(\pi\text{-C}_5\text{H}_5)\text{Fe}(\text{CO})_2]_2$  itself and to  $(\pi\text{-C}_5\text{H}_5)\text{Fe}(\text{CO})_3^+$  appear, increasing in intensity with time (Figure 2). Similar results are found with  $[(\pi\text{-C}_5\text{H}_5)\text{Fe}(\text{CO})_2]_2\text{H}^+\text{BCl}_4^-$ . From the i.r. data on the tetrachloroborate and hexafluorophosphate salts of the  $[(\pi\text{-C}_5\text{H}_5)\text{Fe}(\text{CO})_2]_2\text{H}^+$  ion (Table 3), we conclude that the carbonyl frequencies in these salts are two in number and occur at 2031s and 2001s  $\text{cm}^{-1}$ ; slight shifts occur in the acid mulls to 2037s and 2012s  $\text{cm}^{-1}$ . Davison *et al.*<sup>2</sup> report carbonyl bands of  $[(\pi\text{-C}_5\text{H}_5)\text{Fe}(\text{CO})_2]_2\text{H}^+\text{PF}_6^-$  at 2138s, 2068sh, 2050vs, and 2018vs  $\text{cm}^{-1}$ ; the bands at 2138s and 2068sh are probably due to  $(\pi\text{-C}_5\text{H}_5)\text{Fe}(\text{CO})_3^+$ . Similarly the band at 2068ms  $\text{cm}^{-1}$  which they report in

an Fe-H stretch; we failed to observe an Fe-D stretch in our deuterium compound and no evidence of a

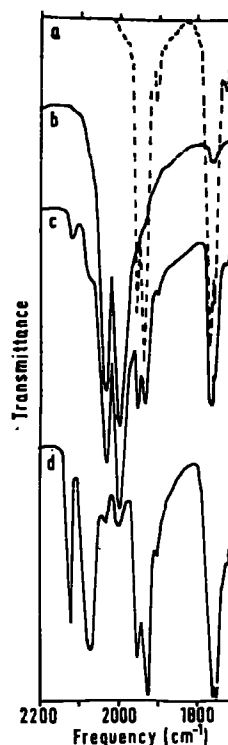


FIGURE 2 The i.r. spectrum of  $[(\pi\text{-C}_5\text{H}_5)\text{Fe}(\text{CO})_2]_2\text{H}^+\text{PF}_6^-$  in the carbonyl region as a function of time. a,  $[(\pi\text{-C}_5\text{H}_5)\text{Fe}(\text{CO})_2]_2$ , b,  $[(\pi\text{-C}_5\text{H}_5)\text{Fe}(\text{CO})_2]_2\text{H}^+\text{PF}_6^-$  initially, c, the same after 2 h in the i.r. beam, and d, the same after 18 h in the i.r. beam

band in this region could be observed in any of the acid mulls. The band at 1767  $\text{cm}^{-1}$  is probably due to traces

TABLE 3

Bands in the i.r. spectra region 4000—100  $\text{cm}^{-1}$

Assignments	$[(\pi\text{-C}_5\text{H}_5)\text{Fe}(\text{CO})_2]_2\text{H}^+\text{BCl}_4^-$	$[(\pi\text{-C}_5\text{H}_5)\text{Fe}(\text{CO})_2]_2\text{H}^+\text{PF}_6^-$	$[(\pi\text{-C}_5\text{H}_5)\text{Fe}(\text{CO})_2]_2\text{H}^+\text{ClBCl}_4^-$	$[(\pi\text{-C}_5\text{H}_5)\text{Fe}(\text{CO})_2]_2\text{H}^+\text{ClBF}_4^-$ *	$(\pi\text{-C}_5\text{H}_5)\text{Fe}(\text{CO})_3\text{BCl}_4^\dagger$
Sym C-H	3110w	3110w	3110w		3107w
CO stretch				2083ssh	2117s <sup>2</sup>
CO stretch	2030s	2032s	2055sh 2049s 2019sh	2053s	2066vs
CO stretch			2002s	2016s	
C-C stretch	1420m	1420m	1420m	1423s 1075vs 1049vs 1037vs	
$\text{BF}_4^-$ {					
$\nu_3 \text{PF}_6^-$		845vs			
$\nu_3 \text{BCl}_4^-$	691ms		691ms		606ms
$\nu_1 + \nu_4 \text{BCl}_4^-$	659ms		661ms		666ms
$\nu_4 \text{PF}_6^-$		555			

\* Ref. 6.

† Recorded on a Grubb-Parsons Spectromaster.

their sulphuric acid mull spectra is probably attributable to  $(\pi\text{-C}_5\text{H}_5)\text{Fe}(\text{CO})_3^+$ , (the band at 2122  $\text{cm}^{-1}$  is much weaker than the one at 2068  $\text{cm}^{-1}$ , probably explaining why no band at 2122  $\text{cm}^{-1}$  was observed). Davison *et al.*<sup>2</sup> also report a weak band at 1767  $\text{cm}^{-1}$  as possibly

of  $[(\pi\text{-C}_5\text{H}_5)\text{Fe}(\text{CO})_2]_2$  itself;  $\nu_{\text{CO}}$  at 1954s, 1937s, 1767s, 1755s. The existence of only two carbonyl frequencies in the protonated species strongly suggests that the two

<sup>8</sup> L. Busetto and R. J. Angelici, *Inorg. Chim. Acta*, 1968, 2, 391.

## EXPERIMENTAL

**Handling Techniques.**—The apparatus and general techniques have been described previously.<sup>7</sup> Large-scale preparations (*ca.* 3–5 mmol) were carried out in glass ampoules fitted with Teflon valves (ROTAFLOR TR6/24) at solid CO<sub>2</sub> temperatures. All hygroscopic materials were handled in a dry box flushed with dry nitrogen.

**Chemicals.**—Hydrogen chloride, nitrosyl chloride, boron trichloride, chlorine, and cyclopentadienyldicarbonyliron dimer were obtained commercially. Phosphorus pentafluoride was prepared by the decomposition of Phosphorogen A. All volatile chemicals were purified by trap-to-trap distillation. Cyclopentadienyldicarbonyliron halides (chloride,<sup>16</sup> bromide,<sup>17</sup> and iodide<sup>18</sup>) and cyclopentadienyldicarbonyliron chloride<sup>9</sup> were prepared by literature methods and purified by recrystallisation. Deuterium chloride was prepared by the addition of deuterium oxide to phosphorus pentachloride.

**Analyses and Physical Measurements.**—Weight analyses were carried out as described previously.<sup>7</sup> Conductivities were measured on a Wayne Kerr Bridge type B221. Carbon, hydrogen, and nitrogen were determined by micro-combustion. Iron was determined by atomic absorptiometry. Chloride was determined potentiometrically and phosphorus by visible spectroscopy as the vanadophosphomolybdate complex. I.r. spectra were recorded on a Perkin-Elmer 621 double-beam spectrophotometer in the region 4000–300 cm<sup>-1</sup> and on a RIIC FS720 interferometric spectrometer in the region 50–350 cm<sup>-1</sup>. <sup>1</sup>H N.m.r. spectra were recorded on Perkin-Elmer R10 and Varian A56/60D spectrometers. Mössbauer spectra were provided by Dr. Johnson of the Physico-Chemical Measurements Unit, Harwell.

**Preparation of the Compounds.**—(i) *π-Cyclopentadienyldicarbonyliron dimer hydrogen tetrachloroborate*, [(π-C<sub>5</sub>H<sub>5</sub>)Fe(CO)<sub>2</sub>]<sub>2</sub>HBCl<sub>4</sub>. Cyclopentadienyldicarbonyliron dimer (0.7 g, 2 mmol) was weighed into an ampoule and degassed under high vacuum overnight. After the sample had been cooled to -196° (liquid-nitrogen bath) hydrogen chloride (*ca.* 7 ml, 0.25 mol) was distilled in. Dissolution was effected by warming the mixture to -95° (toluene slush bath). The solution was cooled to -196° and boron trichloride (4 mmol) was distilled into the ampoule. The mixture was allowed to react at -84° (solid CO<sub>2</sub>-acetone bath), and an immediate red-brown precipitate was observed. All volatiles were removed *in vacuo*. The solid obtained at room temperature was washed with methylene chloride (freshly distilled from phosphorus pentoxide) to yield a red-brown solid which decomposed slowly (Found: % increase in weight on the dimer, 43.4; C, 31.8; H, 2.1; Cl, 27.0; Fe, 20.9. C<sub>14</sub>H<sub>11</sub>BCl<sub>4</sub>Fe<sub>2</sub>O<sub>4</sub> requires % increase in weight on the dimer, 41.4; C, 33.1; H, 2.2; Cl, 27.9; Fe, 22.0%).

(ii) *π-Cyclopentadienyldicarbonyliron dimer hydrogen hexafluorophosphate*, [(π-C<sub>5</sub>H<sub>5</sub>)Fe(CO)<sub>2</sub>]<sub>2</sub>HPF<sub>6</sub>. *π-Cyclopentadienyldicarbonyliron dimer* (0.7 g, 2 mmol) was weighed into an ampoule and degassed under high vacuum overnight. The sample was cooled to -196°, hydrogen chloride (*ca.* 7 ml, 0.25 mol) was distilled in, and dissolution was effected by warming the mixture to -95°. The solution was cooled to -196° and phosphorus pentafluoride (6 mmoles) was distilled into the ampoule. The mixture was allowed to react at -84° overnight. The volatiles were removed *in vacuo*.

The resulting solid at room temperature was washed with methylene chloride (freshly distilled from phosphorus pentoxide) to give a red-brown solid (Found: C, 33.4; H, 2.15; Fe, 22.1; P, 6.05. C<sub>14</sub>H<sub>11</sub>F<sub>6</sub>Fe<sub>2</sub>O<sub>4</sub>P requires C, 33.65; H, 2.2; Fe, 22.35; P, 6.2%).

(iii) *π-Cyclopentadienyldicarbonyliron dimer deuterium hexafluorophosphate*, [(π-C<sub>5</sub>H<sub>5</sub>)Fe(CO)<sub>2</sub>]<sub>2</sub>DPF<sub>6</sub>.—The procedure described above was employed, except that deuterium chloride was used instead of hydrogen chloride.

(iv) *π-Cyclopentadienyldicarbonyliron dimer chlorotetrachloroborate*, [(π-C<sub>5</sub>H<sub>5</sub>)Fe(CO)<sub>2</sub>]<sub>2</sub>ClBCl<sub>4</sub>.—*π-Cyclopentadienyldicarbonyliron chloride* (0.42 g, 2 mmol) was weighed into an ampoule and degassed overnight under high vacuum. The sample was cooled to -196° and hydrogen chloride (*ca.* 12 ml, 0.43 mol) was distilled in. Dissolution was effected by warming the mixture to -95°; the solution was cooled to -196°, boron trichloride (5 mmol) was added, and the mixture was allowed to react at -84°. Removal of all the volatiles *in vacuo* left a red-brown solid (Found: % increase in weight on chloride, 29.9; C, 30.1; H, 1.82; Cl, 31.7. C<sub>14</sub>H<sub>10</sub>BCl<sub>5</sub>Fe<sub>2</sub>O<sub>4</sub> requires % increase in weight on chloride, 27.6; C, 31.0; H, 1.86; Cl, 32.7%).

(v) *π-Cyclopentadienyldicarbonyliron tetrachloroborate*, (π-C<sub>5</sub>H<sub>5</sub>)Fe(CO)<sub>2</sub>BCl<sub>4</sub>. *π-Cyclopentadienyldicarbonyliron chloride* (0.38 g, 1.60 mmol) was cooled to -196° and then hydrogen chloride (*ca.* 12 ml, 0.43 mol) was distilled into the sample. Boron trichloride (4 mmol) was then added and the mixture was warmed to -84°; a pale yellow solid was precipitated from solution. After removal of all the volatiles, a yellow solid remained at room temperature (Found: C, 26.1; H, 1.7; Cl, 38.2. C<sub>8</sub>H<sub>5</sub>BCl<sub>4</sub>FeO<sub>3</sub> requires C, 26.9; H, 1.4; Cl, 39.7%).

(vi) *Reaction of π-cyclopentadienyldicarbonyl dimer with chlorine*. *π-Cyclopentadienyldicarbonyliron dimer* (0.7 g, 2 mmol) was weighed into an ampoule; the sample was cooled to -196°, hydrogen chloride (*ca.* 10 ml, 0.38 mol) was distilled in, and dissolution was effected by warming the mixture to -95°. The solution was then frozen to -196° and chlorine (1 mmol) was distilled into the ampoule. After 4 h at -84° all volatile components were removed. I.r. spectroscopy showed evolution of carbon monoxide; further, it showed the solid obtained at room temperature to be a mixture of *π-cyclopentadienyldicarbonyliron chloride* and other decomposition products.

(vii) *Reaction of π-cyclopentadienyldicarbonyliron dimer with nitrosyl chloride*. *π-Cyclopentadienyldicarbonyliron dimer* (0.7 g, 2 mmol) was weighed into an ampoule; the sample was cooled to -196°, hydrogen chloride (*ca.* 7 ml, 2 mmol) was distilled in and dissolution effected by warming to -95°, and nitrosyl chloride (2 mmol) was distilled into the ampoule. Reaction was allowed to proceed at -84° for 18 h, before removal of all volatiles. I.r. spectroscopy showed the presence of nitric oxide and carbon monoxide. The solid obtained at room temperature was washed with methylene chloride, which on evaporation to low volume yielded crystals of *π-cyclopentadienyldicarbonyliron chloride* (Found: C, 40.4; H, 2.25; Cl, 17.1. C<sub>7</sub>H<sub>5</sub>ClFeO<sub>2</sub> requires C, 39.6; H, 2.4; Cl, 16.7%).

[0/1449 Received, August 21st, 1970]

<sup>20</sup> B. F. Hallam and P. L. Pauson, *J. Chem. Soc.*, 1956, 3030.

<sup>19</sup> T. S. Piper, F. A. Cotton, and G. Wilkinson, *J. Inorg. Nuclear Chem.*, 1955, 1, 165.

<sup>21</sup> T. S. Piper and G. Wilkinson, *J. Inorg. and Nuclear Chem.*, 1965, 2, 38.

# Apparatus and techniques

## A press for the infrared spectroscopic examination of air sensitive compounds

D A Symon† and J McClurg‡

† Department of Chemistry

‡ Central Science Site Workshops

University of Durham, South Road, Durham City

MS received 4 October 1971, in revised form 1 November 1971

**Abstract** We describe a design of a press for the preparation of air sensitive materials for examination by infrared spectroscopy. The materials can be dispersed in a matrix of alkali metal halide or polythene. The design allows preparation of the pressed disc to be carried out in a controlled environment, for example inert atmosphere such as dry nitrogen, without the use of hydraulic presses.

Examination by infrared spectroscopy of air sensitive compounds by the pressed disc technique is usually unsatisfactory owing to the limitations of hydraulic and mechanical presses available. We describe a press which is compact and can be used instead of a hydraulic press assembly and/or in a controlled atmosphere.

The design described below requires two spanners, a locking plate and the die. Preparation of a disc can be readily carried out in a work space 60 cm long, 30 cm high and 25 cm wide, for example in a glove box of modest proportions. The sectional diagram of the press (figure 1) shows the main body of the die 1 which is tapped to receive the inner die 2. This inner die houses the screw 3 that applies the pressure to the plates 4 and 5 which sandwich the sample to be pressed. When assembled the die can be evacuated before applying full pressure. The whole apparatus is made of stainless steel, except for the plates 4 and 5 which were purchased from Beckman-RHIC (Sunley House, 4 Bedford Park, Croydon) for use in their KBr press.

The preparation of the disc follows the normal procedure of grinding the sample and matrix in an agate pestle and mortar prior to loading between the plates 4 and 5 whilst the inner die was held upside down. After ensuring a uniform layer by rotating the plate 4 the main body 1 of the die was screwed down on the inner die 2 ensuring the inner die seats on to the nylon sealing washer. The screw 3 was then tightened fingertight before inverting. The entire assembly was then stood in the locking plate and the body tightened with a C spanner before evacuation. The screw 3 was then tightened to a torque of 5–8 kg m. After disconnecting the vacuum, the

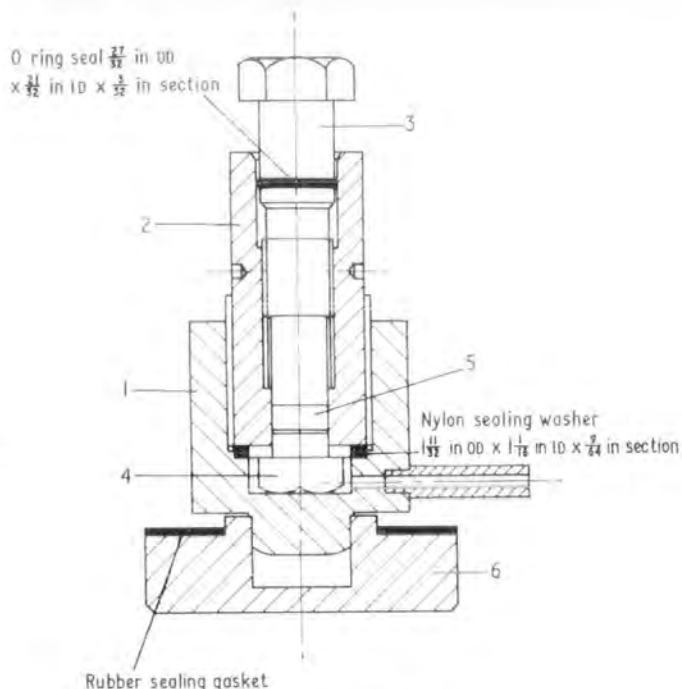


Figure 1 Sectional diagram of KBr press

screw 3 was slackened prior to removing the inner die 2 from the main body 1 whilst being held upside down. The head of the screw 3 was then inserted into the base plate and the inner die 2 screwed down until the disc was proud of the assembly.

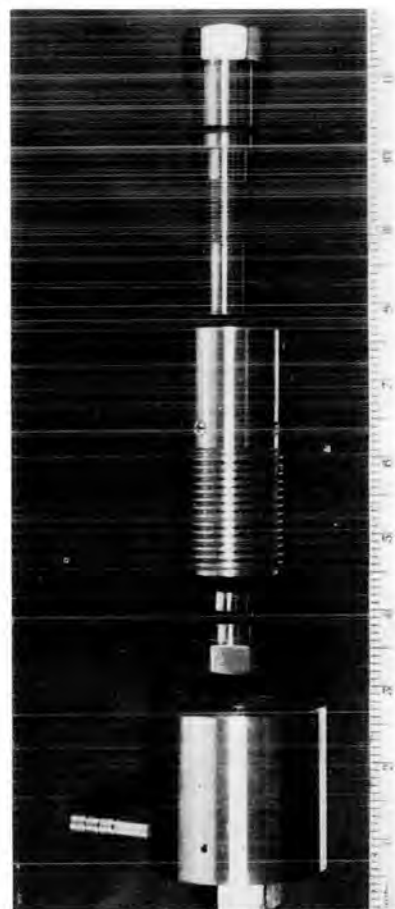


Figure 2 Exploded view of KBr press